THE UNIVERSITY
of EDINBURGH

Mechanisms of GH action on the skeleton: role of SOCS2

Ross Dobie

This thesis is presented for the degree of Doctor of Philosophy at The University of Edinburgh

2014

Declaration

I declare that his thesis has been composed entirely by the candidate, Ross Dobie. This work has not previously been submitted for a Doctor of Philosophy, a degree or any professional qualification. I have done all the work, unless acknowledged otherwise. All sources of information have been acknowledged.

Ross Dobie

Acknowledgements

I have received outstanding supervision throughout my PhD. I would like to thank my supervisors Colin Farquharson, Faisal Ahmed and Vicky MacRae for their guidance and support.

Thank you to everyone in the Bone Biology group, not only for their advice and assistance, but also for making the Roslin Institute an enjoyable place to work. In particular I would like to give thanks to Katherine Staines and Carmen Huesa for their help throughout my PhD.

I would also like to thank Rob van't Hof and Elspeth Milne for their technical support. Thanks also to Elaine Seawright for her continued technical assistance throughout my PhD.

Thanks to the BRF staff, in particular Darren Smith and Alex Robertson who have been outstanding at organising the mice and keeping me up to date.

I would also like to give gratitude to the BBSRC and Ipsen UK for funding this project.

My family and friends have supported me throughout my studies and I am extremely grateful to them for this. Finally, a special thank you to Nicola Holden, whose support and patience throughout has been much appreciated.

Abstract

Determining the mechanisms by which growth hormone (GH) enhances bone growth and development has proven difficult. GH can act either systemically via the stimulation of liver insulin like growth factor (IGF)-1, or locally via activation of the GH receptor (GHR). Furthermore, the local actions of GH may be IGF-1 dependent (indirect) or independent (direct). Suppressor of cytokine signalling 2 (SOCS2) has been identified as an important regulator of GH signalling via the JAK/STAT pathway. The SOCS2 knockout (*Socs2*$^{-/-}$) mouse is characterised by its overgrowth phenotype despite no elevation in systemic GH and IGF-1 levels. It therefore offers a valid and novel model to investigate the local effects of enhanced GH signalling on the skeleton.

The work presented in this thesis investigates the *Socs2*$^{-/-}$ mouse model to better understand the actions of local GH on longitudinal bone growth and bone accrual. *Ex vivo* metatarsal organ cultures, osteoblast cultures, and *in vivo* approaches are used to unravel the mechanisms of GH action on the skeleton. This thesis also explores the potential of SOCS2 as primary mediator of inflammatory induced bone loss through the utilisation of the dextran sulphate sodium (DSS) model of colitis.

Embryonic and postnatal *ex vivo* metatarsal organ cultures are used to study the mechanism of GH action on longitudinal bone growth. Specifically, the present work highlights that enhanced linear growth in the absence of SOCS2 is associated with an increase in the GH regulated proteins, IGF-2 and IGF binding protein 3 (IGFBP3), but not IGF-1. This indicates that IGF-1 may not be essential for mediating GH action on bone growth.

Completion of an in depth analysis of the bone phenotype of juvenile and adult, male and female *Socs2*$^{-/-}$ mice reveals an anabolic phenotype consistent with increased GH signalling. Male *Socs2*$^{-/-}$ mice are shown to have a greater enhancement of cortical parameters compared to females, resulting in increased bone strength. Investigation of the mechanisms behind the enhanced bone accrual in *Socs2*$^{-/-}$ mice identifies SOCS2

as the primary SOCS protein regulating GH signalling in primary osteoblasts. The JAK/STAT pathway is confirmed as the key signalling pathway targeted by SOCS2. Despite this enhanced signalling there is little evidence presented in this thesis to suggest that GH actions on osteoblasts and ultimately bone mass are mediated through increased *Igf1* expression.

GH treatment is shown to be anabolic to bone of young juvenile *Socs2*$^{-/-}$ mice, but not WT mice. This increase in bone mass is associated with increase bone p-STAT5 signalling, but no increase in *Igf1* levels indicating that GH may have IGF-1 independent effects in the *Socs2*$^{-/-}$ mouse model. GH treatment of young mice also reveals an age and sex specific effect of GH action where GH does not stimulate growth until approximately 3 weeks of age. From 3 weeks of age, WT female mice show increased growth in response to GH, but males do not. The increased growth is associated with increased p-STAT5 signalling and increased bone area.

This thesis also confirms SOCS2 a critical mediator of bone loss associated with inflammation. The present results show that deteriorated trabecular bone health in colitic mice is associated with elevated *Socs2* expression in bone. Furthermore, despite similar levels of gut inflammation observed in *Socs2*$^{-/-}$ mice with DSS induced colitis these mice are partly protected from poor bone health.

The work described herein has used the *Socs2*$^{-/-}$ mouse model to strengthen our understanding of the actions of local GH on skeletal growth and development. It also provides compelling evidence for the importance of SOCS2 as a mediator of bone loss in cases of inflammatory bowel disease.

Publications

Original peer reviewed papers

Dobie R., MacRae VE., Huesa C., Van't Hof R., Ahmed SF., Farquharson C. 2014 Direct stimulation of bone mass by increased GH signalling in osteoblasts of *Socs2*$^{-/-}$ mice. Journal of Endocrinology Oct;223(1):93-106. Doi: 10.1530/JOE-14-0292.

Published abstracts

Dobie R., MacRae VE., Pass C., Jasim S., Ahmed SF., Farquharson C. 2013 GH signalling independent of IGF-1 induces increased linear bone growth in SOCS2 knockout mice. Hormine Research in Paediatrics 80 (suppl. 1) FC7-156. Doi: 10.1159/000354131.

Dobie R., Huesa C., Van't Hof R., MacRae V., Ahmed SF., Farquharson C. 2012 Increased GH signalling independent of IGF-1 is associated with increased bone strength in the SOCS2 knockout mouse. Growth Hormone and IGF Research 22 pp. i-vi, S1-S94 OR01-2.

Dobie R., Huesa C., Van't Hof R., MacRae V., Ahmed SF., Farquharson C. 2011 Discordance between cortical and trabecular bone phenotype highlights the role of local versus circulating IGF-1 in the OSCS2 null mouse. Frontiers in Endocrinology. Doi: 10.3389/conf.fendo.2011.02.0015

Dobie R., Huesa C., Van't Hof R., MacRae V., Ahmed SF., Farquharson C. 2011 The SOCS2 KO mouse – a valid model for studying the local effects of GH on bone. Hormone Research in Paediarics 76 (Suppl. 2) FC-119. Doi:10.1159/000334325

Dobie R., MacRae VE., Huesa C., Van't Hof R., Ahmed SF., Farquharson C. 2013 Contribution to bone mass and strength of osteoblast GH action that are independent of local IGF1 production: lessons from the SOCS2 knockout mouse. Endocrine Abstracts 31 P4. doi: 10.1530/endoabs.31.P4

Dobie R., MacRae VE., Pass C., Jasim S., Huesa C., Ahmed SF., Farquharson C. 2013 Increased linear bone growth in SOCS2 knockout mice in response to GH is independent of systemic or local IGF1. Endocrine Abstracts 31 P2. doi: 10.1530/endoabs.31.P2

Dobie R., Ahmed S., Staines KA., Pass C., Jasim S., Huesa C., MacRae VE., Farquharson C. 2013 GH induced linear bone growth in SOCS2 knockout mice is IGF-1 independent. Journal of bone and mineral research 28 (Suppl. 1)

Dobie R., MacRae VE., Huesa C., Van't Hof R., Ahmed SF., Farquharson C. 2013 Osteoblast GH actions promote bone mass and strength through mechanisms that are independent of local IGF-1 production: Lessons from the SOCS2 knockout mouse. Journal of bone and mineral Research 28 (Suppl.1)

Abbreviations

AKT	Protein kinase B
ALP	Alkaline phosphatase
ALS	Acid labile subunit
ALSKO	Acid labile subunit knockout
BP3KO	Insulin like growth factor binding protein 3 knockout
CD	Chron's disease
cDNA	Complementary DNA
CO2	Carbon dioxide
DMP-1	Dentin matrix protein 1
DMSO	Dimethyl suloxide
DNA	Deoxyribonucleic acid
dNTP	Deoxyribonucleotide triphosphate
DSS	Dextran sulphate sodium
DTT	Dithiothreitol
ECD	Extracellular domain
ECM	Extracellular matrix
EDTA	Ethylenediaminetetraacetic acid
ER-α	Oestrogen receptor α
ER-β	Oestrogen receptor β
FGF-21	Fibroblast growth factor 21
FRF-23	Fibroblast growth factor 23
GH	Growth hormone
GHBP	Growth hormone binding protein
GHR	Growth hormone receptor
GHRH	Growth hormone releasing hormone
H^+	Hydron
HBSS	Hank's buffered salt solution
IBD	Inflammatory bowel disease
ICD	Intracellular domain
IGF	Insulin like growth factor
IGF-1	Insulin like growth factor 1
IGF-2	Insulin like growth factor 2
IGFBP	Insulin like growth factor binding protein
IGFBP-1	Insulin like growth factor binding protein 1
IGFBP-2	Insulin like growth factor binding protein 2
IGFBP-3	Insulin like growth factor binding protein 3
IGFBP-4	Insulin like growth factor binding protein 4
IGFBP-5	Insulin like growth factor binding protein 5
IGFBP-6	Insulin like growth factor binding protein 6
IGF-1R	Insulin like growth factor 1 receptor
IL-1β	Interleukin 1β
IL-6	Interleukin 6

IRS-1	Insulin receptor substrate 1
IRS-2	Insulin receptor substrate 2
JAK2	Janus kinase 2
KIR	Kinase inhibitory region
LB-Broth	Lysogeny broth
LIF	Leukemia inhibitory factor
LID	Liver specific IGF-1 deficient
MAPK	Mitogen-activated protein kinase
MEA	Methoxyethyl acetate
MMA	Methylmethacylate
mRNA	messenger RNA
MSC	Mesenchymal stem cell
MUP	Major urinary protein
$NaHCO_3$	Sodium bicarbonate solution
NFW	Nuclease-free water
NVP	NVP-AEW541 IGF-1R inhibitor
OSX	Osterix
PBS	Phosphate buffered saline
PHEX	Phosphate-regulating gene with homologies to endopeptidase on the X chromosome
PI3K	Phosphatidylinositol 3-kinase
PRL	Prolactin
PTP	Protein tyrosine phosphatases
RANKL	Receptor activator of nuclear factor kappa-B ligand
RA	Rheumatoid arthritis
rhGH	recombinant human growth hormone
rhIGF-1	recombinant human insulin like growth hormone 1
rhIGF-2	recombinant human insulin like growth hormone 2
RNA	Ribonucleic acid
RUNX2	Runt related transcription factor 2
SH2	Src homology domain
$^{35}SO_4$	Sulphate
SOCS	Suppressor of cytokine signalling
SOCS1	Suppressor of cytokine signalling 1
SOCS2	Suppressor of cytokine signalling 2
SOCS3	Suppressor of cytokine signalling 3
STAT	Signal transducer and activator of transcription
STAT1	Signal transducer and activator of transcription 1
STAT3	Signal transducer and activator of transcription 3
STAT5	Signal transducer and activator of transcription 5
TBS/T	Tris-buffered saline twee-20
TNFα	Tumour necrosis factor α
UC	Ulcerative colitis
WT	Wild-type

Table of Contents

Chapter 1: Introduction

Chapter 2: Materials and Methods

Chapter 3: SOCS2 regulation of longitudinal bone growth

Chapter 4: The *Socs2*$^{-/-}$ bone phenotype: actions of local GH signalling

List of Figures

List of Tables

Chapter 1

Introduction

Preface

Growth Hormone (GH) is anabolic, regulating both longitudinal bone growth and bone accrual. The mode of action of GH however is complex, and the development of novel mouse models aid in the investigation of its specific actions. This thesis will focus on the use of the suppressor of cytokine signalling (SOCS) 2 knockout mouse (*Socs2*$^{-/-}$) model to investigate the mechanisms of GH action on bone development.

1.1 Bone

Classically considered as an inert substance, bone is in fact a dynamic and complex connective tissue with many well established functions. It provides supports and protection to vital organs, while providing a scaffold to transmit muscular contractions. Aside from a mechanical role, bone also acts as storage for ions such as calcium and phosphorus, and contains an inner reservoir of bone marrow which is the site of haematopoiesis. Bone has also recently been shown to act as an endocrine organ through the production of bone specific endocrine factors such as osteocalcin and fibroblast growth factor (FGF)-23 (Lee *et al.* 2007; Guntur & Rosen 2012). As research progresses it is inevitable that our understanding of bone's function will continue to evolve.

1.1.1 Bone structure

Calcified bone is made up of a crystalline complex of calcium and phosphate (hydroxyapatite [$Ca_{10}(PO_4)_6(OH_2]$) embedded in a collagen matrix. Although most apatite crystals contain calcium and phosphate, there is a level of substitution with other cations (e.g. magnesium and sodium) and anions (e.g. fluoride) (Omelon *et al.* 2009). There are two major types of bone architecture – cortical and trabecular. The relative proportion of each of these within a bone is varied throughout the body. A bone from the axial skeleton comprises mainly of trabecular bone, whereas a bone from the appendicular skeleton is comprised of mainly cortical bone.

1.1.1.1 Cortical bone

Cortical bone accounts for 80% of the skeletal mass of an adult human. The majority of this is located in the shaft of long bones (diaphysis) surrounding the medullary cavity. The building block of cortical bone is the osteon. Osteon comprises of concentric circles of compact bone that surround an inner Haversian canal containing blood vessels and nerves (Fig 1.1). Consequently, cortical bone is dense with little porosity. This is important as its primary functions are to resist the tensile forces produced by the contraction of muscle, and to resist bending (Sommerfeldt & Rubin 2001).

1.1.1.2 Trabecular bone

The remaining 20% of skeletal mass comprises of trabecular bone. This is a less dense osseous tissue found primarily at the ends of long bones (epiphyses). The functional units of trabecular bone are trabeculae, which unlike cortical bone are highly porous. These trabeculae form a three dimensional network of bony processes arranged along lines of stress (Fig. 1.1). This arrangement makes trabecular bone less stiff and more elastic than cortical bone. As a result, it is therefore able to resist the compressive forces experienced during weight bearing (Sommerfeldt & Rubin 2001).

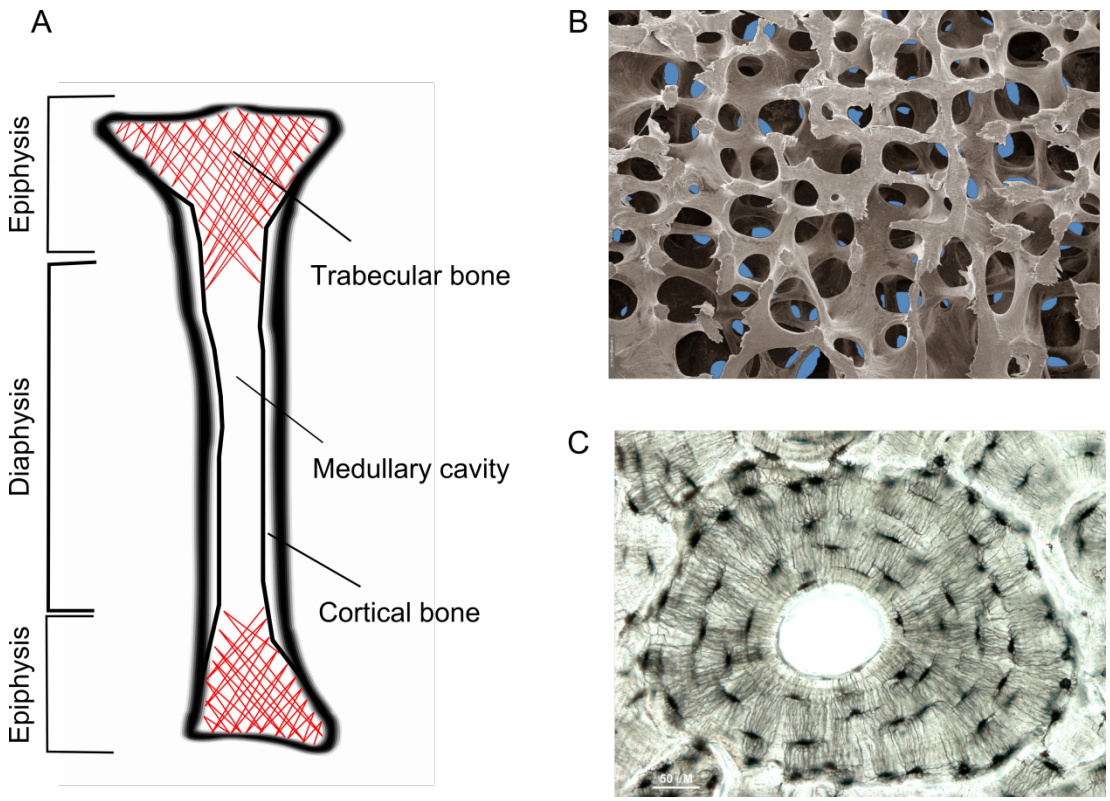

Figure 1.1 Structure of trabecular and cortical bone

A. Trabecular bone (red hatched) is located primarily at the epiphysis of long bones, whereas cortical bone is located primarily in the diaphysis **B.** Electron microscope image highlighting the 3D trabecular network within the lumbar spine of a 41 year old male. **C.** Image of a single osteon concentric circles of compact bone that surround an inner Haversian canal. Images kindly provided by Professor Tim Arnett, University College London.

1.2 Embryonic bone formation

During foetal development, there are two distinct modes of bone formation. Although both result in the synthesis of bone from pre-existing mesenchymal tissue, intramembranous ossification does this directly, whereas endochondral ossification forms an intermediate hyaline cartilage scaffold (Horton 2003).

1.2.1 Intramembranous ossification

Intramembranous ossification is important in the formation of flat bones such as the skull, mandible and clavicle. During embryogenesis, neural crest-derived mesenchymal cells condense into compact nodules. These cells differentiate into osteoblasts and start to secrete matrix. Mineralisation of this matrix results in a haphazard arrangement of weak bone known as 'woven bone.' This is eventually replaced by a stronger, more structured organisation known as 'lamellar bone'.

1.2.2 Endochondral ossification

The majority of bones, including all long bones, develop through the process of endochondral ossification (Fig 1.2). This is also an essential process during postnatal longitudinal bone growth and fracture healing. Mesenchymal cells, derived from somites (give rise to axial skeleton) and somatopleure (give rise to the appendicular skeleton), proliferate and condense into compact aggregates that produce an extracellular matrix (ECM). The ECM is initially rich in fibronectin and type I collagen, aiding the condensing process (Dessau *et al.* 1980; Olsen *et al.* 2000). This initial process is mediated by the adhesion molecules N-cadherin and neural cell adhesion molecule (N-CAM) which regulate cell-cell and cell-ECM interactions (Delise & Tuan 2002). The transcription factor Sox9 also has a vital role in this process and in the absence of Sox9 mesenchymal cells fail to condense (Akiyama *et al.* 2002). Within the newly formed aggregates, cells undergo differentiation into chondrocytes forming a cartilage template consisting of primarily type II collagen and the proteoglycan aggrecan (Dessau *et al.* 1980; Goldring *et al.* 2006). Again, Sox9

has been identified as being important in this process and along with Sox5 and Sox6, these transcription factors play a key role in chondrocyte differentiation (Lefebvre *et al.* 1998; Akiyama *et al.* 2002). Chondrocyte proliferation then causes the template to expand. Coinciding with this, perichondrial cells on the periphery of the template differentiate into osteoblasts. These cells produce osteoid that mineralises to form a bony collar (periosteum), supporting new bone growth. Chondrocytes in the centre of the template begin to hypertrophy and the primary ossification centre forms, with blood vessels containing osteoclasts, (section 1.4.1), osteoblast precursors (section 1.4.2), and bone marrow penetrating the bony collar, accessing the cartilage template. The primary ossification centre expands as a result of osteoclastic resorption of cartilage ECM, and osteoblastic formation of bone (Mackie *et al.* 2011). Similar mechanisms are responsible for the formation of a secondary ossification centre within the epiphyseal region. Between the primary and secondary ossification centres a cartilaginous region remains. This forms the epiphyseal growth plate, responsible for postnatal endochondral bone growth.

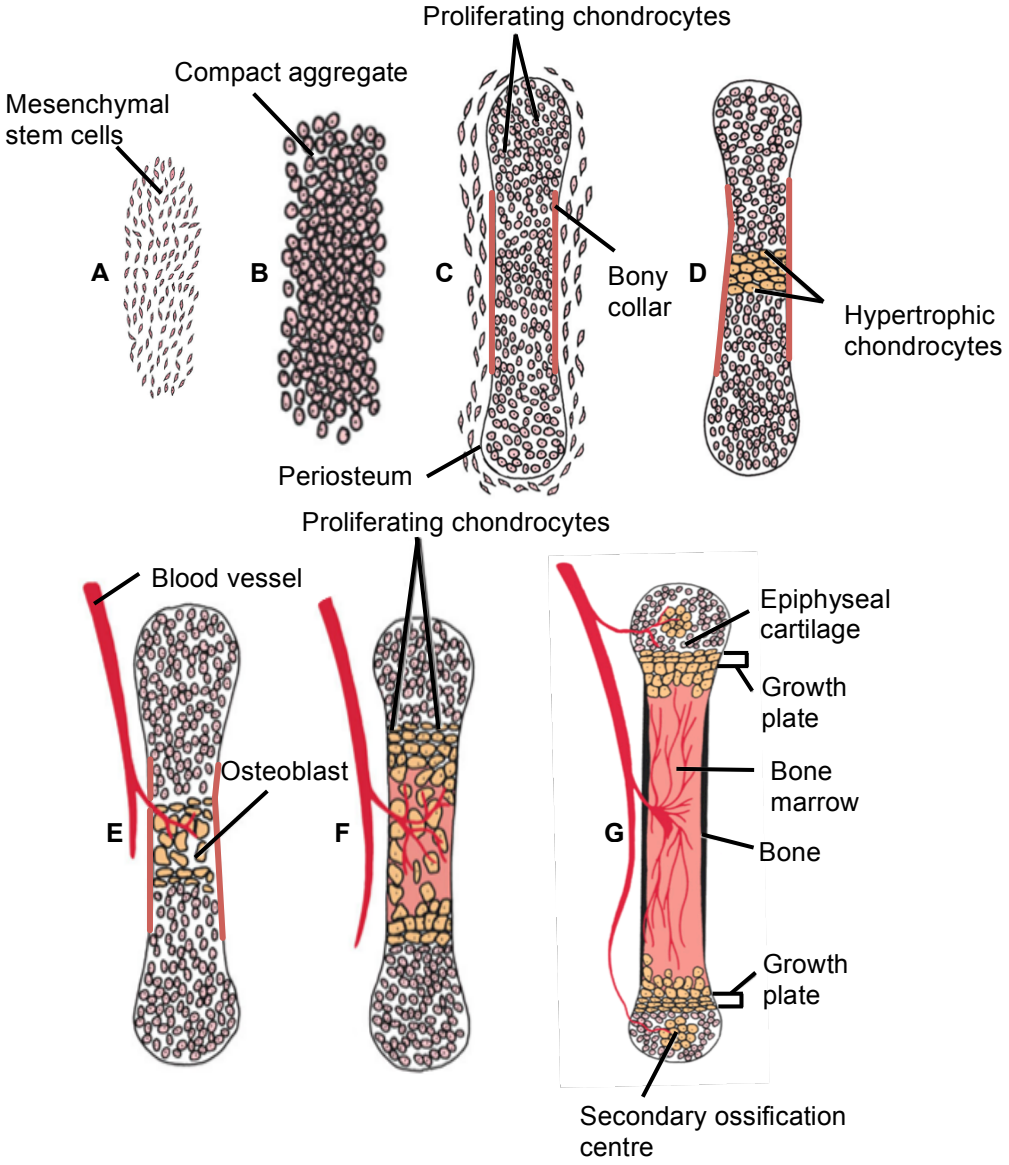

Figure 1.2 Endochondral ossification

Schematic representation of endochondral ossification. Mesenchymal stem cells (**A)** condense to form the cartilage anlagen comprising of pre-chondrocytes **(B)**. These cells differentiate and secrete ECM. At this point, a bony collar is formed by osteoblasts to support growth **(C)**. Chondrocytes in the centre hypertrophy **(D)**. Invasion of blood vessels allows infiltration of osteoblasts and osteoclasts leading to formation of the primary ossification centre **(E)**. The primary ossification centre expands throughout the diaphysis to the epiphyses **(F)**. A secondary ossification centre emerges at the epiphyses **(G)**. The epiphyseal growth plate remains between the ossification centres. Adapted from (SF Gilbert 2006).

1.3 The growth plate

The epiphyseal growth plate is situated between the metaphysis and epiphysis of all long bones. It consists of chondrocytes embedded in a proteoglycan and collagen type II rich ECM (Mackie *et al.* 2011). These cells are arranged into vertical columns that run parallel to the direction of growth. The growth plate can be divided into different anatomic zones, representing different stages of chondrocyte maturation (Fig 1.3). A chondrocyte will "move through" each stage while being held in a spatially fixed location by longitudinal and transverse septa (Hunziker 1994; Farquharson & Jefferies 2000). The growth plate of mammals is structurally and functionally similar (Zoetis *et al.* 2003). Therefore analysis of animal models such as mice and rats has translational benefits to human conditions. Care however must be taken as differences in growth plate physiology exist between species. An example of this is growth plate fusion which takes place in humans, but not mice or rats.

1.3.1 The resting zone

The resting zone, situated closest to the epiphysis, contains a pool of unorganised chondrocytes embedded in large volumes of ECM (Hunziker 1994) (Fig. 1.3). These cells are derived from chondrocyte progenitor cells residing in the groove of Ranvier, adjacent to the resting zone (Melrose *et al.* 2008). Chondrocytes within the resting zone contain high lipid levels, many cytoplasmic vacuoles and synthesise only low levels of proteoglycans and collagen type II (Burdan *et al.* 2009). These chondrocytes remain in a relatively quiescent state and share many characteristics with stem cells. This precursor pool of cells acts to supply the proliferative zone for future expansion (Kember 1972; Abad *et al.* 2002).

1.3.2 The proliferative zone

Chondrocytes within the proliferative zone adopt a flattened, oblate appearance, and begin to undergo rapid division (Hunziker 1994; Ballock & O'Keefe 2003). In mammalian growth plates these cell rearrange to form columns that run along the axis of growth (Hunziker 1994; Burdan *et al.* 2009) (Fig. 1.3). Synthesis and secretion

of ECM (consisting mainly of collagen type II and proteoglycans) within the transverse and longitudinal septa aid in separating the newly divided cells into columns (Ballock & O'Keefe 2003).

1.3.3 The hypertrophic zone

Chondrocytes within the hypertrophic zone cease proliferation and undergo hypertrophy (Fig. 1.3). Compared to cells within the proliferative zone, hypertrophic cells have a 5-10 times larger intracellular volume, and a 5 fold increase in cell height (Hunziker *et al.* 1987; Farnum *et al.* 2002). Some of this increase (~20%) can be attributed to an increase in organelle size, including mitochondria and endoplasmic reticulum. The remaining increase is a result of an osmotic gradient causing nuclear and cytoplasmic swelling (Buckwalter *et al.* 1986; Bush *et al.* 2008; Burdan *et al.* 2009).

The subsequent terminal differentiation of these cells is accompanied by an increase in secretion of matrix proteins including collagen type X (Sommer *et al.* 1996). Budding of the plasma membrane causes release of matrix vesicles into the surrounding ECM. These vesicles possess a number of proteins responsible for mediating mineralisation, including both intravesicular (orphan phosphatase 1) and extravesicular phosphatases (ALP and ectonucleotide pyrophosphatase/phosphodiesterase 1), and calcium channelling and binding proteins (annexins) (Harmey *et al.* 2004; Yadav *et al.* 2011; Millan 2013). These specialised proteins lead to the accumulation of calcium and inorganic phosphate, resulting in the nucleation of mineral within the matrix vesicle. The mineral, upon rupture of the matrix vesicle, is then released into the extracellular environment where it expands along the collagen fibrils primarily through the actions of ALP (Millan 2013). Mineralisation occurs within the longitudinal septa, but not the transverse septa by mechanisms that are as yet unclear (Ballock & O'Keefe 2003).

This mineralised tissue acts as a scaffold for vascular invasion which brings with it osteoclasts (section 1.4.1) and osteoblast precursors (section 1.4.2). During hypertrophy, chondrocytes release a number of factors which promote vascular invasion (vascular endothelial growth factor) and influx of osteoblasts and osteoclasts (high-mobility group box 1 protein and receptor activator of NFκB ligand (RANKL) (Zelzer *et al.* 2002; Kishimoto *et al.* 2006; Taniguchi *et al.* 2007).

1.3.4 Regulation of longitudinal bone growth

The rate of longitudinal bone growth differs between species, with mammals considered to have a comparatively slow growth rate. Indeed, growth rate of the proximal tibia in humans (0.04mm/day), rabbits (0.39mm/day), and rats (0.22mm/day) is considerably less than that observed in chickens (0.86mm/day) (Kember 1972; Kember & Sissons 1976; Kember 1985; Kirkwood *et al.* 1989). The growth rate is dependent on a number of factors including cellular proliferation within the proliferative zone, cellular enlargement within the hypertrophic zone, and ECM synthesis (Wilsman *et al.* 1996).. Increased width of the proliferative zone and increased rate of proliferation both enhance longitudinal growth rate (Farnum & Wilsman 1993; Wilsman *et al.* 1996). Changes within the hypertrophic zone, including rate of hypertrophy and final cell volume, is the primary determinant of bone growth. Hypertrophic cell size accounts for approximately 60% of endochondral bone growth (Wilsman *et al.* 1996).

Endochondral bone growth is a tightly regulated process (Hunziker *et al.* 1994; Farnum *et al.* 2002). Endocrine factors such as thyroid hormone, oestrogens/androgens, glucocorticoids, vitamin D, and leptin have all been shown to regulate chondrocyte maturation, and subsequently longitudinal bone growth. Aside from endocrine factors, there is also autocrine and paracrine (local) regulation from factors such as Indian HH, bone morphogenic protein, fibroblast growth factor, and vascular endothelial growth factor. The precise actions of these are beyond the remit of this thesis. Further information outlining the specific action can

be found in the following reviews (Van Der Eerden *et al.* 2003; Kronenberg 2003; Nilsson *et al.* 2005). Longitudinal growth is also governed by the surrounding mechanical environment. Longitudinal growth is governed by the Hueter-Volkmann law (Villemure & Stokes 2009). This law states that bone growth is inhibited by mechanical compression on the growth plate and accelerated by growth plate tension. This plays a key role in the determination of bone size and partly explains why some bones are longer than others. Without exception, the most potent stimulator of longitudinal bone growth is the GH/insulin-like growth factor 1 (IGF-1) axis. The importance of this axis is evident as numerous conditions (e.g genetic abnormalities, pituitary abnormalities, inflammation) which cause GH deficiency or resistance result in severe growth retardation (Robson *et al.* 2002). The GH/IGF-1 axis is discussed in greater detail in section 1.5.

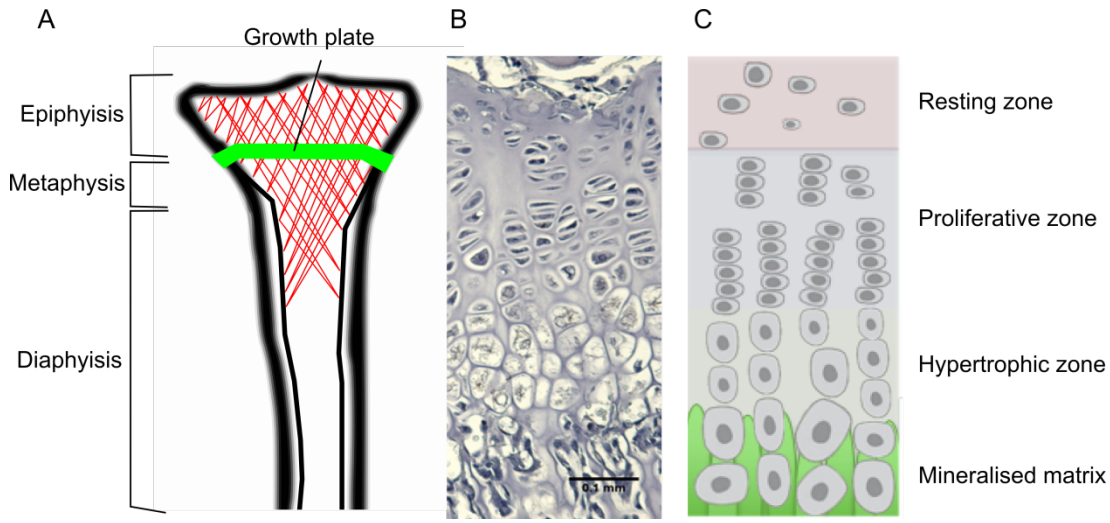

Figure 1.3 The epiphyseal growth plate

A. The epiphyseal growth plate (green line) is located between the epiphysis and metaphysis of long bones. **B.** Morphology of the proximal growth plate from a 3 week old mouse tibia. Image kindly provided by Dr Katherine Staines, University of Edinburgh). Scale bar = 0.1mm. **C.** Schematic representation of the distinct zones of the growth plate; the resting, proliferating and hypertrophic zone.

1.4 Bone modelling and remodelling

Aside from longitudinal growth, bone is constantly renewing and remodelling in response to mechanical and hormonal stimuli. During skeletal development, the process of modelling transforms bone shape. In response to physiological and mechanical stresses, bone architecture is remodelled to endure the forces that it encounters (Clarke 2008). The process of bone remodelling serves to maintain bone strength by removing micro-damaged bone and replacing it with new healthy tissue. The process also acts to maintain mineral homeostasis, as the removal of old bone results in a release of calcium (Hadjidakis & Androulakis 2006). Bone modelling is a result of bone resorption and formation working independently. Conversely, in bone remodelling, bone resorption and formation take place as a coupled process within a basic multicellular unit (BMU). The remodelling cycle consists of four successive phases – activation, resorption, reversal and formation (Fig. 1.4). An imbalance between formation and resorption can lead to a number of debilitating conditions. When the imbalance favours resorption, conditions such as osteopenia and osteoporosis are common. Conversely, a bias towards formation can result in osteopetrosis (Kular *et al.* 2012). Within bone there are three main cell types; osteoclasts (section 1.4.1), osteoblasts (1.4.2) and osteocytes (1.4.3). Although each cell has its own distinct function within bone, there is significant cross-talk to ensure homeostasis is maintained.

1.4.1 Osteoclasts

Osteoclasts account for less than 1% of bone cells. They are giant multinucleated cells responsible for bone resorption. These cells are derived from the monocyte-macrophage lineage, originating from hematopoietic stem cells (Sommerfeldt & Rubin 2001). During the initiation phase of bone remodelling, osteoclast precursors are recruited from the bone morrow via the circulating blood stream. Once at the resorption site, these cells differentiate into mature osteoclasts (Hill 1998). Mature

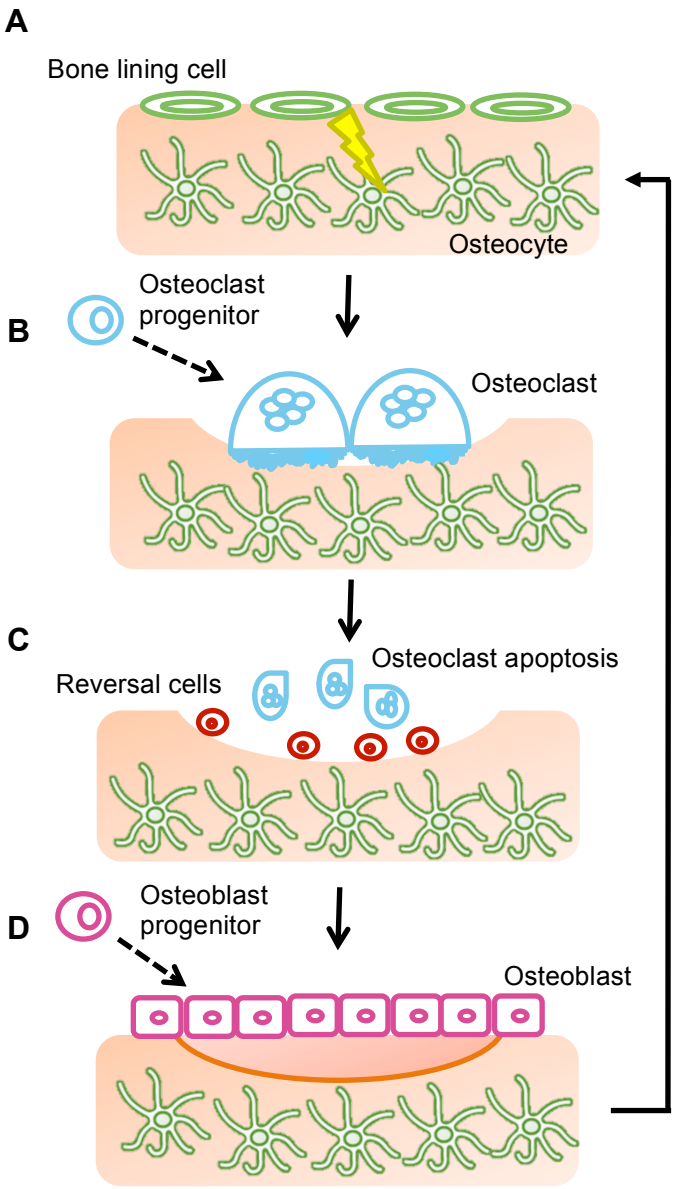

Figure 1.4 Bone remodelling cycle

Schematic representation of the bone remodelling process. **(A)** Activation – mechanical stimulation (yellow lightening) results in upregulation of RANKL by bone lining cells. **(B)** Resorption - osteoclast precursors differentiate and begin to resorb bone. **(C)** Reversal - osteoclasts die by apoptosis, while mononuclear cells (reversal cells) prepare the surface for osteoblasts to commence bone formation (Hadjidakis & Androulakis 2006). **(D)** Formation - osteoblast progenitors differentiate into mature osteoblasts and begin to form new bone. Image adapted from (Crockett *et al.* 2011).

osteoclasts are highly migratory, polarised cells that produce lysosomal enzymes (Sommerfeldt & Rubin 2001). Two key cytokines responsible for regulating osteoclast differentiation and function are RANKL, and macrophage colony stimulating factor (M-CSF). These factors drive proliferation of osteoclast precursors and differentiation and survival of mature osteoclasts. Osteoclast function is inhibited by osteoprotegrin (OPG) which is produced by osteoblasts and acts as a decoy receptor for RANKL (Crockett *et al.* 2011). A tight balance between these factors is required to control osteoclast action.

During the resorption phase, osteoclasts bind to the bone surface and polarise. This process is responsible for the formation of the sealing zone, an actin rich osteoclast specific structure which anchors the cell to bone, creating a resorption site sealed from the extracellular space (Vaananen & Horton 1995). Within this newly formed resorption lacuna, the bone resorbing surface of the osteoclast forms a 'ruffled border' of microvilli. The 'ruffled border' secretes H^+ ions which acidify the resorption lacunae, dissolving the mineral component of bone. This results in the release of calcium and phosphorus into the bloodstream. Decreased pH also allows secretion of enzymes responsible for degradation of the organic component of bone. These include the lysosomal enzymes, cathepsin K and tartrate-resistant acid phosphatase (Hill 1998 Hadjidakis & Androulakis 2006; Clarke 2008). Matrix metalloproteinases (MMPs); produced by osteoclasts; also play an important role in the digestion of collagen (Delaisse *et al.* 2003). Osteoblasts are recruited to these newly formed lacunae (known as Howship lacunae).

1.4.2 Osteoblasts

Osteoblasts are 'bone building' cells which make up approximately 5% of all bone cells. They are cuboidal in shape, and possess a well-developed endoplasmic reticulum, and a large Golgi complex which is characteristic of secretory cells (Dudley & Spiro 1961).

1.4.2.1 Osteoblast differentiation

Osteoblasts originate from the mesenchymal stem cell (MSC) linage, which also give rise to adipocytes, chondrocytes and myoblasts (Aubin *et al.* 1995). The commitment of MSCs to the osteoblast lineage involves a number of key transcription factors, including runt-related transcription factor 2 (Runx2, also referred to as Cbfa1), Osterix (Osx) and β-catenin (Komori 2006). Both *Runx2*$^{-/-}$ and *Osx*$^{-/-}$ mice display a complete lack of ossification, producing only a cartilaginous skeleton (Komori *et al.* 1997; Nakashima *et al.* 2002). During late stage differentiation, Runx2 acts to inhibit maturation thus maintaining an immature osteoblast supply (Komori 2006). Osx expression is lost in *Runx2*$^{-/-}$ mice, but Runx2 is not lost in *Osx*$^{-/-}$ mice. This indicates that Osx works downstream of Runx2 (Nakashima *et al.* 2002; Nishio *et al.* 2006). β-catenin (via the Wnt pathway) is essential for osteoblast lineage differentiation. In cases of β-catenin deficiency mesenchymal cells are unable to differentiate into osteoblasts, but can still differentiate in chondrocytes, indicating that a common precursor exists between both (Day *et al.* 2005; Hill *et al.* 2005).

1.4.2.2 Osteoblast function

During the formation phase of remodelling, osteoblasts are located at the bone surface where their primary function is to lay down ECM, composed mainly of type I collagen (osteoid). Type I collagen accounts for around 90% of the organic component of bone. Aside from the production of collagen, osteoblasts synthesise and secrete proteoglycans and non-collagenous proteins (Sommerfeldt & Rubin 2001; Long 2012). These non-collagenous proteins including osteocalcin, ALP and osteopontin, regulate the formation and propagation of mineral (Kornak 2011; Millan 2013). The mineralisation of bone through the accumulation of calcium phosphate, in the form of hydroxyapatite, produces a hard but lightweight composite material. Recently, osteocalcin has also been shown to act as a hormone in the body, regulating insulin release by the pancreas. As osteocalcin is produced solely by osteoblasts, it is now understood that bone can act as an endocrine organ (Lee *et al.* 2007; Fukumoto & Martin 2009). Following matrix deposition and

mineralisation, the osteoblast undergoes one of three fates. It becomes an inactive bone lining cell, undergoes apoptosis, or becomes encased in osteoid and differentiates into an osteocyte (Dallas & Bonewald 2010). Bone lining cells are involved in the activation of bone remodelling. Typically, mechanical loading or micro-fracture leads to the stimulation of quiescent bone lining cells to increase surface expression of RANKL. Expression of RANKL is however also regulated by host of factors present within the bone. Binding of RANKL to RANK (present on preosteoclasts) initiates osteoclast differentiation (Proff & Romer 2009; Crockett *et al.* 2011).

1.4.2.3 Regulation of osteoblast differentiation

Osteoblast differentiation is under tight regulation at both a hormonal (endocrine) and local (autocrine/paracrine) level. Although beyond the scope of this thesis, the main regulators of osteoblast differentiation are outlined in a number of elegant reviews (Yamaguchi *et al.* 2000; Hughes *et al.* 2006). The regulation of osteoblasts, and ultimately bone mass by the GH/IGF-1 axis is of particular relevance to the focus of this thesis and will be discussed in detail in section 1.5.

1.4.3 Osteocytes

Osteocytes are terminally differentiated osteoblasts embedded in the bone. They make up approximately 90% of cells in adult bone. Osteocytes are smaller than osteoblasts due to loss of a number of cytoplasmic organelles. They reside in lacunae within the mineralised bone matrix (Aubin 1998). These cells form long dendritic processes which travel through the canaliculi of bone connecting osteocytes to other osteocytes as well as osteoblasts, osteoclasts and bone lining cells (Bonewald 2007 Seeman 2008). Dendritic processes are constantly extending and retracting in response to mechanical loading, possibly under the regulation of the protein E11/podoplanin which is the earliest osteocyte marker (Bonewald 2007).

The recognised function of osteocytes is to convert mechanical stimuli into a biological response. Micro-damage to bone results in the apoptosis of closely lying osteocytes. This results in the release of RANKL, stimulating osteoclast formation and activity (Bonewald 2011; Kular *et al.* 2012). Mice lacking RANKL in osteocytes have an osteopetrotic bone phenotype due to deficiencies in bone resorption (Nakashima *et al.* 2011). Osteocytes also produce sclerostin (a late osteocyte marker) which is an inhibitor of Wnt signalling and bone formation. Through inhibition of Wnt/β-catenin signalling, sclerostin inhibits osteoblast proliferation and mineralisation (Li *et al.* 2005; Moester *et al.* 2010).

Osteocytes have also been implicated in the regulation phosphate homeostasis. This is mediated through the synthesis of molecules such as phosphate-regulating gene with homologies to endopeptidase on the X chromosome (PHEX), dentin matrix protein 1 (DMP-1), matrix extracellular phosphoglycoprotein (MEPE), and FGF-23 (Bonewald 2011). Expressed highly in osteocytes, DMP-1 and PHEX regulate FGF-23 expression, in turn regulating phosphate absorption and excretion by the kidneys (Bonewald 2011).

1.5 GH and IGF-1

GH is a peptide hormone produced by somatotrophic cells within the anterior pituitary. GH regulates a host of physiological processes, including somatic growth and development, and carbohydrate and lipid metabolism (Giustina *et al.* 2008; Perrini *et al.* 2010; Vijayakumar *et al.* 2010). GH releases from the pituitary is not continuously, but pulsatile. In humans these pulses occur every 3-5 hours. Studies on mice have shown that there is a sexual dimorphism in GH release with peak GH concentrations recorded every 2.5 hours in male and every 1.4 hour in females (Macleod *et al,* 1991). To ensure optimal GH secretion, somatotrophic cells are regulated by a number of factors. The synthesis and release of GH is primarily controlled by the positive regulator - growth hormone releasing hormone (GHRH), and the negative regulator - somatostatin (Frohman *et al.* 1992). In circulation, GH

binds to a GH-binding (GHBP) protein, comprising of the extracellular domain of the GH receptor (GHR) (Baumann 2001). Although the function of GHBP remains unclear, it is suggested that it may increase GH half-life, and reduce GH availability to the GHR (Baumann *et al.* 1987; Giustina *et al.* 2008). GH exerts its effects on target tissues via two modes of action. At a systemic level, GH acts indirectly through IGF-1 production in the liver (Melmed 1999). At a local level, GH acts directly through binding to the GHR. Functional GHRs are present on numerous cell types, including chondrocytes and osteoblasts (Barnard *et al.* 1988; Barnard *et al.* 1991; Werther *et al.* 1993; Nilsson *et al.* 1995).

1.5.1 GHR signalling

The GHR is a single membrane spanning receptor. It comprises of two fibronectin type III β sandwich domains (extracellular domain (ECD)) which are joined via a helical transmembrane domain to the intracellular domain (ICD). The ICD contains box 1 & 2 motifs which bind the tyrosine kinase, Janus kinase (JAK) 2 (Brooks *et al.* 2008). GH binding to the ECD results in the formation of a ligand-receptor complex comprising of one GH and two GHRs (Frank 2001; Brooks *et al.* 2008). The subsequent events that lead to receptor activation are still a matter of debate. It is widely accepted that GH binding leads to dimerisation of the ECD, and in turn activation of JAK2 through its transphosphorylation. A number of studies however shown the ECD to be present as a dimer independent of GH binding (Brooks *et al.* 2008). Subsequent GH binding results in conformational changes and rotation of the ICD, aligning JAK2 kinases (Zhu *et al.* 2001; Flores-Morales *et al.* 2006; Waters *et al.* 2006). JAK2 activation leads to phosphorylation of specific tyrosine residues on the ICD. These act as binding sites for proteins containing a Src homology 2 (SH2) domain, and initiate downstream signalling (Waters *et al.* 2006; Brooks *et al.* 2008). There are several pathways responsible for mediating GH action. These include the signal transducer and activator of transcription (STAT) pathway, the mitogen-activated protein kinase/extracellular signal-regulated kinases (MAPK/ERK) pathway, and the phosphatidylinositol 3-kinase (PI3K) pathway (Frank 2001). The

STAT pathway is central to the work presented in this thesis and is therefore described in detail (section 1.5.1.1).

1.5.1.1 STAT signalling

STAT1, 3, and 5 proteins are activated by GH (Ram *et al.* 1996; Herrington *et al.* 2000). These proteins reside in the cell cytoplasm until they bind to JAK2 proteins, through their SH2 domain. Phosphorylation of specific tyrosine/serine residues present on the C-terminus on the STAT proteins, results in homo- or hetero-dimerisation, and migration into the nucleus, activating gene transcription (Fig. 1.5) (Han *et al.* 1996; Smit *et al.* 1996; Herrington *et al.* 2000). STAT1 and 3 can form homodimers and/or heterodimers which bind to the sis inducible unit of the *c-fos* gene (Herrington *et al.* 2000; Zhu *et al.* 2001). Whereas *Stat1*$^{-/-}$ mice show few abnormalities in relation to growth, *Stat3*$^{-/-}$ mice are embryonic lethal, and it is therefore not possible to assess STAT3's role in mediating GH action (Meraz *et al.* 1996; Durbin *et al.* 1996; Takeda *et al.* 1997). STAT5 exists as two isoforms (STAT5a and STAT5b) sharing ~90% identity in the coding sequence. They have overlapping and distinct functions in mediating GH action (Herrington *et al.* 2000). High affinity binding of STAT5 to the GHR takes place through specific tyrosine residues: Y534, Y566, and Y627; and low affinity binding at Y487 and Y595 (Uyttendaele *et al.* 2007). STAT5 signalling is crucial in mediating GH action. *Stat5ab*$^{-/-}$ mice show similar growth retardation to *Ghr*$^{-/-}$ mice. *STAT5b* mutations in humans result in severe growth deficiency, similar to *GHR* mutations (Kofoed *et al.* 2003). As *Stat5b*$^{-/-}$ mice show no elevation in IGF-1 levels following GH stimulation, it is likely that the GH induced JAK/STAT pathway is important in regulating IGF-1 levels. The exact mechanisms involved in this are still being elucidated (Davey *et al.* 2001; Woelfle *et al.* 2003).

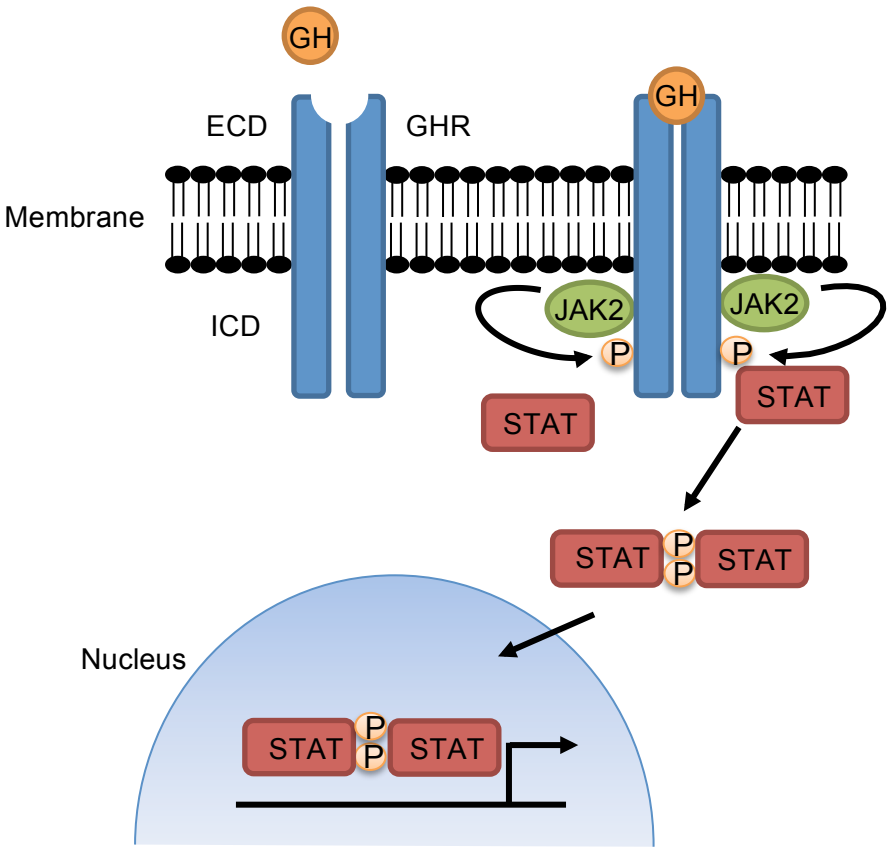

Figure 1.5 GH induced JAK/STAT signalling

Schematic representation of GH signalling via the JAK/STAT pathway. GH binding to the GHR results in JAK2 activation and the phosphorylation of tyrosine residue binding sites. STAT proteins bind to these specific sites and through phosphorylation dimerise and translocate into the nucleus where they initiate gene transcription.

1.5.2 GH and gender

In mice, it is generally understood that GH is the primary regulator of longitudinal growth and determinant of peak bone mass during puberty (Venken *et al.* 2007; Callewaert *et al.* 2010). Initially, postnatal growth is considered GH independent (Liu & LeRoith 1999). Consequently, growth of *Ghr*$^{-/-}$ and GHRH receptor (GHRHR) (*lit*/*lit*) mice are comparable to WT mice until ~2 weeks of age (Eicher & Beamer 1976; Lupu *et al.* 2001). The onset of the GH deficiency phenotypes coincide with a period of rapid growth during which male and female growth rates diverge (as measured by weight gain), with exaggerated growth in males (Liu & LeRoith 1999; Lupu *et al.* 2001). The anabolic changes in skeletal morphology are also greater in males at this stage (Lupu *et al.* 2001; Seeman 2001). This sexually dimorphic process is thought to be largely mediated by STAT5b signalling. *Stat5b*$^{-/-}$ male mice are growth retarded, whereas females are not (Udy *et al.* 1997; Teglund *et al.* 1998). This sex specific action is not shared with the STAT5a isoform, which alone has little effects on growth. In addition, growth divergence between male WT and *Stat5b*$^{-/-}$ male mice takes place at the same age as rapid GH dependent sexually dimorphic growth (Udy *et al.* 1997; Teglund *et al.* 1998; Lupu *et al.* 2001).

1.5.3 Regulation of GH signalling

There are a number of proteins responsible for the regulation of the GH induced JAK/STAT signalling. These include protein tyrosine phosphatases (PTPs), and suppressor of cytokine signalling proteins (SOCS) (Zhu *et al.* 2001; Greenhalgh & Hilton 2001; Flores-Morales *et al.* 2006). There are four PTP proteins associated with GH regulation. SH2 domain- containing protein-tyrosine phosphatase 1 (SHP-1) is a key PTP protein in the regulation of GH induced JAK/STAT signalling. Activated by GH, SHP-1 binds to and inhibits phosphorylated STAT5b and JAK2 (Ram & Waxman 1997). Like SHP-1, PTP-1b associates directly with JAK2, but can also bind directly to the phosphorylated intracellular domain of the GHR, leading to dephosphorylation. PTP-H1 also binds to the phosphorylated GHR (Pasquali *et al.* 2003). An additional PTP, SHP-2 has been shown to have both inhibitory and

stimulatory effects on GH signalling (Kim *et al.* 1998). The regulation of GH signalling by SOCS proteins is central to the work of this thesis and is discussed in full in section 1.6.

1.5.4 The IGF system

GH exerts its actions primarily through the secondary messenger IGF-1 (Herrington *et al.* 2000; Le Roith *et al.* 2001). Aside from exerting it anabolic effects on tissue, IGF-1 negatively regulates GH secretion directly, or through the stimulation of somatostatin (Giustina & Veldhuis 1998). Unlike IGF-1, IGF-2 (another member of the IGF system) is widely considered not to be under regulation from GH (Giustina *et al.* 2008; Annunziata *et al.* 2011).

1.5.4.1 IGFs in circulation

Systemic IGF-1 is synthesised primarily in the liver under the regulation of GH (Melmed 1999; Yakar *et al.* 1999; Sjogren *et al.* 1999). In circulation, the majority of IGFs form part of a 150-kDa ternary complex. This is composed of IGF (IGF-1 or IGF-2), an IGF binding protein (IGFBP) and an acid labile subunit (ALS). Together, these act to stabilise IGF, prolong its circulating half-life, and regulate its availability to target tissues (Jones & Clemmons 1995; Boisclair *et al.* 2001; Giustina *et al.* 2008). Although there are six IGFBPs (IGFBP1-6), only IGFBP3 and 5 form part of the ternary complex (Twigg & Baxter 1998; Boisclair *et al.* 2001; Le Roith *et al.* 2001). IGFBP3 is highly abundant in circulation, with the majority of IGF-1 forming a ternary complex with this protein. Only ~1% of IGF-1 circulates as a free hormone (Giustina *et al.* 2008). Similar to IGF-1, hepatic IGFBP3 and ALS synthesis are regulated by GH (Clemmons 1998; Boisclair *et al.* 2001). *Als*$^{-/-}$ and *Igfbp3*$^{-/-}$ mice have decreased serum IGF-1 levels, highlighting the importance of the ternary complex in increasing IGF-1 half-life (Yakar *et al.* 2009). IGFBP1, 2, 4, and 6 also bind to IGFs, but do not form a ternary complex (Holly & Perks 2006). In addition to their systemic roles, IGFBP's are also expressed in a number of extra-hepatic tissues.

Here, they regulate the local actions of IGF's, as well as eliciting IGF independent actions (Clemmons 1998; Spagnoli *et al.* 2002; Mohan & Baylink 2002).

1.5.4.2. IGF signalling

IGF-1 and IGF-2 binds to the IGF-1 receptor (IGF-1R), a transmembrane tyrosine kinase receptor (Liu *et al.* 1993). The IGF-1R comprises of a tetramer containing two extracellular α-subunits and two membrane spanning β units. The binding of IGF to the α-subunits results in conformational changes that stimulate intrinsic tyrosine kinase activity on the intramembranous β subunits. This leads to the activation of various intracellular substrates, including insulin receptor substrate (IRS)-1 and -2 and Shc proteins. These substrates mediate the effects of the IGFs (Adams *et al.* 2000) (Fig. 1.6). In relation to bone and the growth plate, IRS-1 is expressed in chondrocytes and osteoblasts, whereas IRS-2 is expressed in osteoblasts and osteoclasts, but not chondrocytes. *Irs2*$^{-/-}$ mice show an uncoupling of bone remodelling with decreased bone formation and increased resorption, with no changes to the growth plate (Akune *et al.* 2002). *Irs1*$^{-/-}$ mice also have decreased bone formation due to a reduction in osteoblast proliferation and differentiation. Osteoclasts however remain unaffected. Unlike *Irs2*$^{-/-}$ mice, *Irs1*$^{-/-}$ mice have decreased growth plate width and chondrocyte number (Ogata *et al.* 2000). IGF-1 binding to the IGF-1R initiates a number of signalling pathways, including the IRS-1 mediated PI3K/AKT pathway, and the Shc mediated MAPK/ERK pathway (Laviola *et al.* 2007). AKT signalling has important roles in cell proliferation, growth, and differentiation in numerous cells throughout the body (Peng *et al.* 2003). Specifically, inhibition of the PI3K/AKT pathway hinders longitudinal growth of mouse metatarsals, highlighting an important role for this pathway in endochondral bone growth (MacRae *et al.* 2007). The AKT signalling pathway can also block apoptosis, through activation of Sos which in turn activates Ras (a GPTase). This initiates a kinase cascade leading to the inactivation of the pro-apoptotic protein Bcl-2-associated death promoter (Datta *et al.* 1997). An additional receptor exists which binds IGF-2: IGF-2/mannose 6 phosphate receptor. This acts as an antagonist,

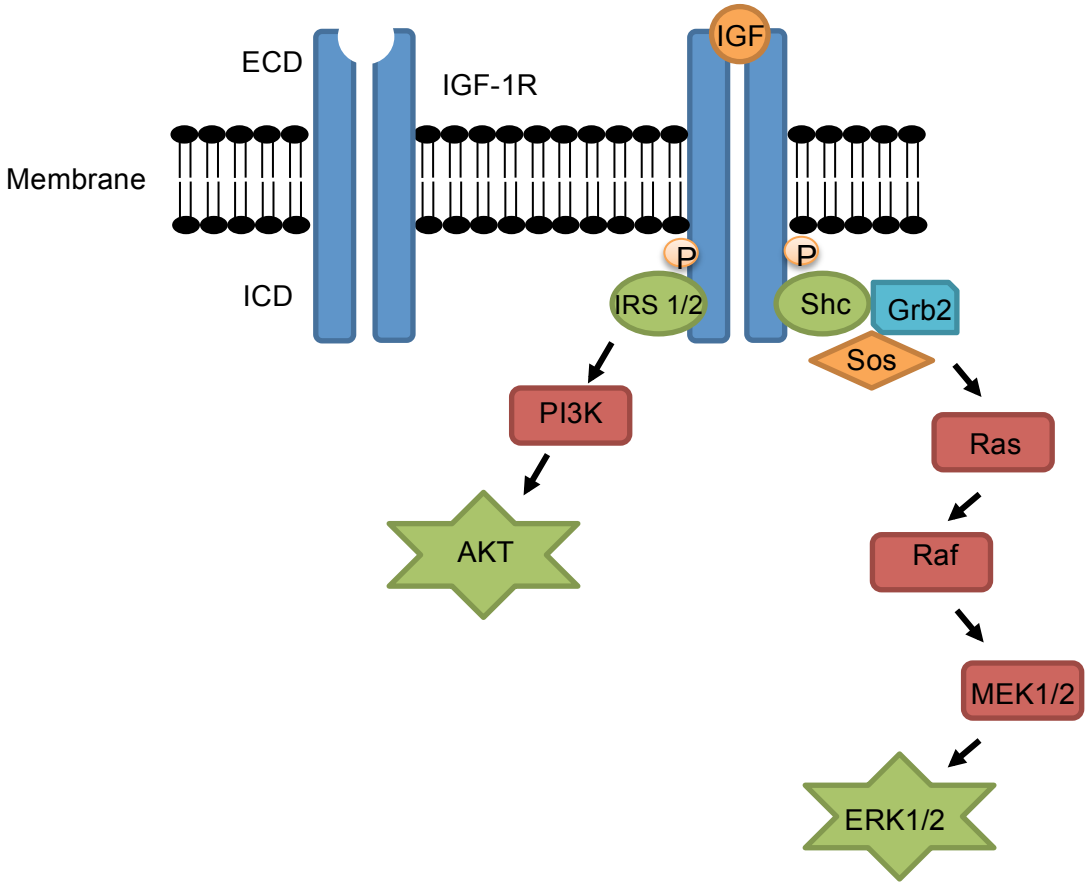

Figure 1.6 IGF-1 signalling

IGF-1 binding to the IGF-1R creates multiple docking sites (P) for intracellular substrates, including Shc and IRS1/2 proteins. Shc binds to the ICD of the IGF-1R. Grb2 binding to Shc forms a complex with Sos (a guanine nucleotide exchange factor). The formation of this complex initiates a signalling cascade involving Ras, Raf, MEK1/2 and finally ERK1/2. IRS1/2 binding to the ICD of the IGF-1R leads to activation of PI3K, which in turn activates the AKT pathway.

binding IGF-2 during foetal development and therefore reducing IGF-2 availability to other receptors (Baker *et al.* 1993; Gluckman & Pinal 2003).

1.5.5 GH and IGF-1 regulation of endochondral bone growth and bone turnover

GH is an important regulator of postnatal development, but has no apparent embryonic role. *Ghr*$^{-/-}$ mouse growth is indistinguishable from WT until approximately 2 weeks of age, at which point the mice start to show signs of growth retardation (Lupu *et al.* 2001). GHR deficiency results in reduced bone growth as a result of decreased growth plate chondrocyte proliferation, and decreased cortical expansion (Sims *et al.* 2000; Sjogren *et al.* 2000; Lupu *et al.* 2001). Conversely, overexpression of GH results in increased longitudinal growth and increased cortical cross-sectional area (Oberbauer *et al.* 1992; Eckstein *et al.* 2004). The effects of GH may however be mediated through IGF-1, as postnatal *Ghr*$^{-/-}$ mice have decreased systemic IGF-1 levels. GH transgenic mice on the other hand have elevated systemic IGF-1 levels (Zhou *et al.* 1997; Eckstein *et al.* 2004).

IGF-1 and IGF-2 have important roles in prenatal development. Both *Igf1*$^{-/-}$ and *Igf2*$^{-/-}$ mice have a 40% reduction in body weight compared to WT mice at birth (Baker *et al.* 1993; Liu *et al.* 1993). IGF-1 continues to play a crucial role in postnatal development as is evident from the growth retardation observed in *Igf1*$^{-/-}$ mice (Liu *et al.* 1993; Wang *et al.* 1999b; Lupu *et al.* 2001). At the level of the growth plate, *Igf1r* deletion results in disorganisation of the growth plate and reduced chondrocyte proliferation and maturation in both prenatal and postnatal mice, highlighting the importance of IGF signalling in mediating chondrocyte growth and differentiation (Wang *et al.* 2011). The effects of IGF-1 on prepubertal longitudinal bone growth and accretion are mediated predominantly via GH-independent mechanisms (Mohan *et al.* 2003). The onset of puberty, and post pubertal development however, appear to be predominantly GH dependent (Mohan *et al.* 2003). IGF-1 signalling also has important roles in mediating osteoblasts. *Igf1r*$^{-/-}$ mice have reduced bone volume and rate of mineralisation (Zhang *et al.* 2002). Alteration of IGF-2 levels has little effect

on postnatal growth and bone development suggesting that IGF-2 functions predominatly as a regulator of prenatal development (Dechiara *et al.* 1990; Wolf *et al.* 1994; Moerth *et al.* 2007).

1.5.5.1 The somatomedin hypothesis

The somatomedin hypothesis was originally created to explain the actions of GH on somatic growth. It was based on early experiments aimed at determining the mode of GH action by measuring $^{35}SO_4$ incorporation into chondroitin sulphate and DNA synthesis in cartilage. It was established that GH was unable to exert its effects directly, and instead functioned through a secondary messenger. Originally termed somatomedin, this intermediary was later identified as IGF-1 (Daughada & Reeder 1966; Daughada *et al.* 1972; Garland *et al.* 1972; Klapper *et al.* 1983). As a result, it became widely accepted that GH acts by stimulating production of hepatic IGF-1, subsequently acting as an endocrine factor to stimulate target tissues including the growth plate and bone (Fig. 1.7A). IGF-1 has since been found to be expressed in numerous tissues throughout the body, indicating that it may not only have an endocrine role, but also an autocrine/paracrine role (Dercole *et al.* 1984; Murphy *et al.* 1987). Furthermore, the GHR is expressed in numerous cells types, and GH has been shown to regulate IGF-1 expression in a number of tissues (Nilsson *et al.* 1986; Lowe *et al.* 1988; Isgaard *et al.* 1989; Ballesteros *et al.* 2000). Direct injections of GH into cartilage of hypophysectomised rats increases longitudinal growth, whereas the untreated contralateral limbs show no increase. Therefore, GH appears to function at a local level, independent of systemic IGF-1 (Isaksson *et al.* 1982) (Fig. 1.7B).

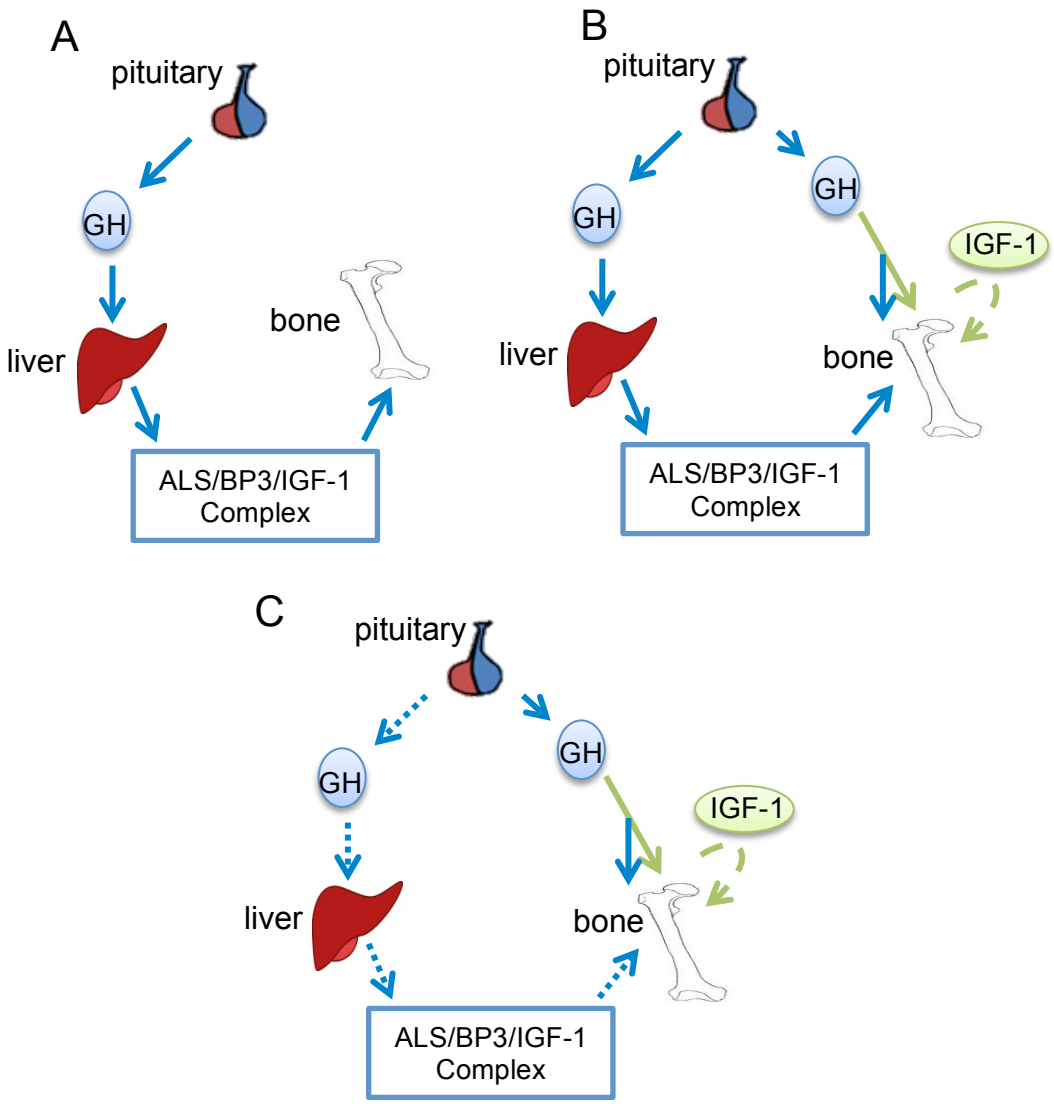

Figure 1.7 The evolution of the somatomedin hypothesis

Schematic representation of the evolving concepts in the actions of GH. **A.** Originally, GH was thought to illicit all of its effects through the up regulation of IGF-1 in liver, acting as an endocrine factor. **B.** GH has since been shown to function also at a local level (bone) either directly, or through the up regulation of IGF-1. **C.** The importance of the endocrine actions of IGF-1 have been questioned (dotted blue lines).

1.5.5.2 The dual effector theory

The evolution of an improved understanding of GH action led to the creation of the 'dual effector theory'. Originally proposed to describe the action of GH on adipocytes, the dual effector theory proposes that GH acts to recruit progenitor cells within the resting zone into a proliferative state, as well as stimulating IGF-1, promoting clonal expansion (Green *et al.* 1985; Nilsson *et al.* 1986; Isaksson *et al.* 1987; Ohlsson *et al.* 1992). Initially, GH was shown to stimulate multiplication of cells within the resting zone of the growth plate, whereas IGF-1 did not (Ohlsson *et al.* 1992). IGF-1 has since been shown to stimulate proliferation of resting zone chondrocytes, but to a lesser extent than GH (Hunziker *et al.* 1994). Resting zone size is increased in states of *Igf1* deficiency, yet decreased in $Ghr^{-/-}$ mouse. This indicates a possible IGF-1 independent role for GH on germinal cells (Wang *et al.* 2004). In support of this, tibial growth is retarded in both $Ghr^{-/-}$ and $Igf1^{-/-}$ mice. A reduction that is more pronounced in the double *Ghr*/*Igf1* knockout (Lupu *et al.* 2001). Studies on $Igf1^{-/-}$ mice suggest that IGF-1 acts predominantly to increase hypertrophic cell size, with minimal effects on cell proliferation (Wang *et al.* 1999). The importance of IGF-1 in mediating GH action on hypertrophic chondrocytes is further suggested by the reduction in chondrocyte hypertrophy observed in $Igf1^{-/-}$ mice despite elevated GH levels (Wang *et al.* 2004)

Interestingly, more recent studies found that *Igf1* mRNA expression is predominantly located in the surrounding perichondrium and bone, with comparatively low expression in any of the growth plate zone. This suggests that the perichondrium and bone may be the source of local IGF-1 which elicits a response in the growth plate via paracrine routes (Parker *et al.* 2007).

1.5.5.3 The evolving somatomedin hypothesis

The original somatomedin hypothesis was further questioned by findings that liver specific IGF-1 deficient (LID) mice, characterised by a significant reduction in systemic IGF-1 levels, had no defects in linear growth or development (Yakar *et al.*

1999; Sjogren *et al.* 1999). This cast doubt on the importance of systemic IGF-1 in regulating bone growth. Furthermore, reductions in systemic IGF-1 levels, achieved by disruption of the IGF-1 serum complex, produced similar results (Yakar *et al.* 2009). These murine models have however been called into question due to incomplete and progressive deletion (via albumin-*Cre* method of gene deletion) of liver *Igf1,* long after the critical post weaning growth spurt (Stratikopoulos *et al.* 2008). Hepatic IGF-1 has been shown to significantly contribute to growth (Stratikopoulos *et al.* 2008; Wu *et al.* 2009; Elis *et al.* 2010). Therefore the importance of systemic IGF-1 in regulating bone growth remains a matter of debate (Fig. 1.7C). The importance of local IGF-1 is well established; targeted deletion of *Igf1* in epiphyseal growth plate chondrocytes results in growth retardation (Govoni *et al.* 2007a).

Alterations in systemic IGF-1, through the use of various transgenic mouse models, also give an insight into the endocrine actions of IGF-1 on bone turnover. Decreased systemic IGF-1 levels results in a catabolic cortical bone phenotype, with minimal effects on trabecular bone (Sjogren *et al.* 2002; Yakar *et al.* 2002). Conversely, overexpression of IGF-1 in hepatocytes is anabolic to cortical bone (Elis *et al.* 2010). The effects of locally derived IGF-1 are clear from the targeted overexpression of *Igf1* to osteoblasts where it has anabolic effects on trabecular bone, with minimal alteration to cortical bone (Zhao *et al.* 2000). Taken together, these findings suggest that systemic IGF-1 is important for the maintenance of cortical bone structure, whereas local IGF-1 serves to maintain trabecular bone structure.

1.6 SOCS proteins

Suppressor of cytokine signalling (SOCS) proteins are a family of intracellular regulators. At present, eight SOCS proteins have been identified: SOCS1-7 and CIS. While SOCS1-3 are well defined, CIS and SOCS 4-7 are less so (Krebs & Hilton 2001; Rico-Bautista *et al.* 2006; Croker *et al.* 2008). All SOCS proteins are characterised by a

central SH2 domain, sandwiched between a conserved C-terminal domain named the SOCS box, and a variable N-terminal domain. SOCS1 and 3 contain an additional kinase inhibitory region in the N-terminal domain (Rico-Bautista *et al.* 2006; Croker *et al.* 2008) (Fig. 1.8). There are a number of mechanisms by which SOCS proteins regulate cytokine signalling. SOCS1 and 3, unlike other SOCS proteins are able to act as kinase inhibitors, inhibiting JAK activity (Krebs & Hilton 2001; Greenhalgh & Hilton 2001; Rico-Bautista *et al.* 2006) Through the SH2 domain, SOCS proteins are able to competitively bind to the tyrosine residue recruitment sites in the cytoplasmic domain of the cytokine receptor. This inhibits STAT attachment and signalling (Ram & Waxman 1999; Krebs & Hilton 2001; Pass *et al.* 2012). There is also evidence to suggest that SOCS proteins; through the SOCS box; act as adapter molecules, linking signalling proteins to the proteasome (Zhang *et al.* 1999) (Fig. 1.9). SOCS1-3 and CIS proteins are expressed in numerous tissues throughout the body. These proteins form a negative feedback loop, regulating the cytokines that induce their expression, including GH (Starr *et al.* 1997; Tollet-Egnell *et al.* 1999). Following GH stimulation, expression of these proteins either rapidly increases over a short period of time (SOCS1, SOCS3 and CIS), or gradually over a longer period of time (SOCS2). The different expression patterns may be a result of differences in the mechanism of action of specific SOCS proteins (Adams *et al.* 1998; Tollet-Egnell *et al.* 1999; Greenhalgh & Hilton 2001). Each of these proteins can be activated by a plethora of cytokines, as is reviewed by Krebs and Hilton 2001 (Krebs & Hilton 2001).

1.6.1 SOCS1

The generation of transgenic mice with deletions to the *Socs* genes has provided crucial insight into the physiological role played by each. The deletion of *Socs1* has helped identify it as a key regulator of IFN-γ induced STAT1 signalling (Alexander *et al.* 1999). These mice appear normal at birth, however exhibit stunted growth and die around 3 weeks of age. At this point they are found to have fatty degeneration and necrosis of the liver, and immune cell infiltration into the organs, causing severe

lymphopenia (Starr *et al.* 1998; Naka *et al.* 1998). Treatment of anti-IFN-γ antibodies to *Socs1*$^{-/-}$ mice prevents premature death (Alexander *et al.* 1999). SOCS1 overexpression results in a reduction in the T cell precursor (thymocyte) population, indicating a key role for SOCS1 in T-cell development and homeostasis (Starr *et al.* 1998; Naka *et al.* 1998; Marine *et al.* 1999b; Fujimoto *et al.* 2000).

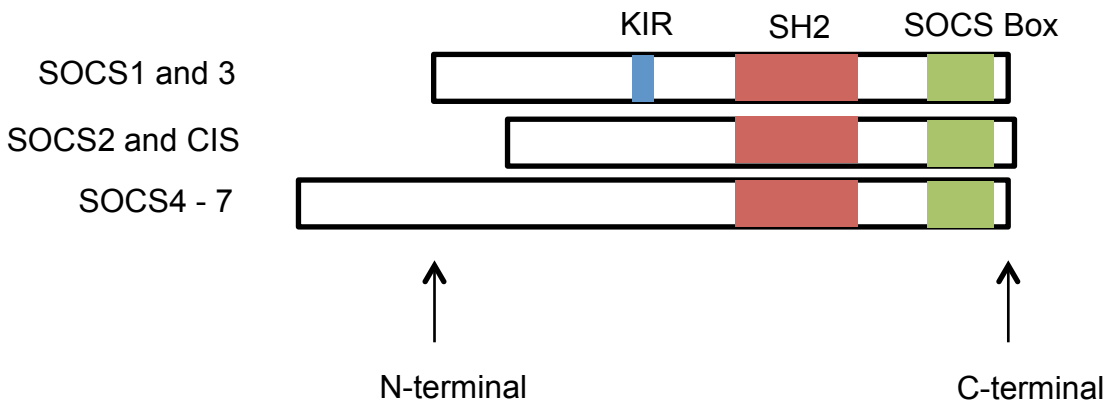

Figure 1.8 SOCS protein structure

Schematic representation of the structure of SOCS proteins. All SOCS proteins contain a central SH2 domain and a C-terminal domain named the SOCS box. The N-terminal region is of variable length in SOCS proteins. SOCS1 and 3 contain an additional kinase inhibitory region (KIR) within this region. Image adapted from (Rico-Bautista *et al.* 2006).

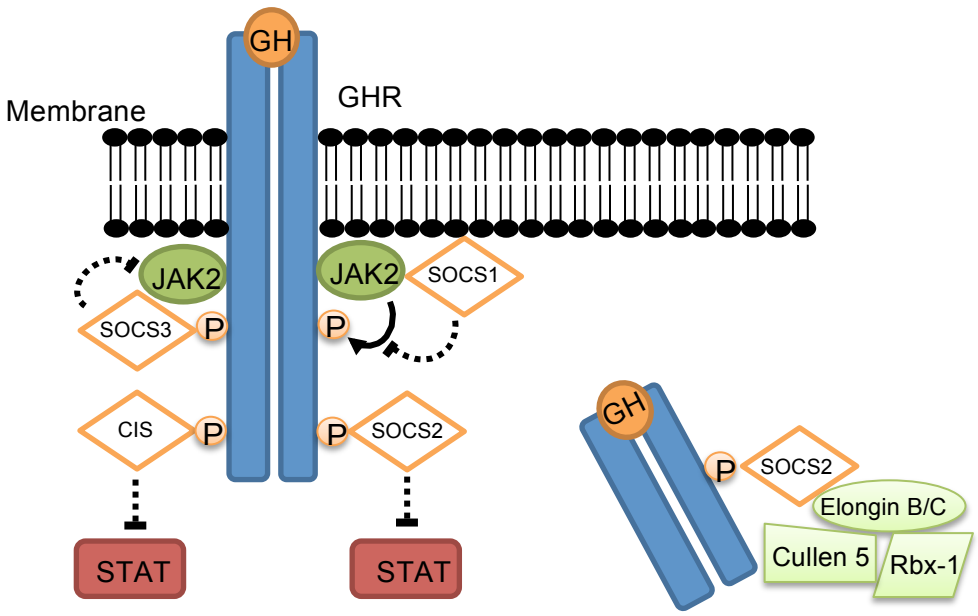

Figure 1.9 SOCS regulation of GH signalling

Schematic representation of the mechanisms by which SOCS proteins regulate GH signalling. SOCS1 binds to JAK2, inhibiting its phosphorylation. SOCS3 binds to the membrane adjacent to JAK2 and inhibits JAK2 activity. SOCS2 has two possible modes of actions. SOCS2 binds to specific tryrosine residues on the GHR, blocking STAT5 binding. Via the SOCS-Box, SOCS2 has also been shown to target signalling complexes for ubiquitination and proteasomal degradation. Image adapted from (Turnley 2005).

1.6.2 SOCS3

Both *Socs3*$^{-/-}$ and *Socs3* overexpressing mice are embryonic lethal. While the former show no anatomical abnormalities, they die between gestation days 11 and 13 due to placental defects and poor circulatory network in the developing embryo (Roberts *et al.* 2001). SOCS3 levels are low in adult tissues, but expression is high in foetal livers which coincides with an EPO-dependent stage of erythropoiesis (Marine *et al.* 1999a; Krebs & Hilton 2001). Hematopoietic progenitors from *Socs3*$^{-/-}$ mice have enhanced responsiveness to a number of cytokines. SOCS3 deficient mice display marked erythrocytosis, while SOCS3 overexpression results in a complete lack of erythropoiesis (Marine *et al.* 1999a).

1.6.3 CIS

Unlike SOCS1, 2, and 3, CIS knockout mice have no reported phenotype abnormalities (Marine *et al.* 1999a). Overexpression of CIS however results in a 20-30% decrease in weight, a reduction in major urinary protein (MUP) levels, and a reduction in STAT5 activation (Matsumoto *et al.* 1999). This phenotype has been likened to that observed in *Stat5b*$^{-/-}$ mice, which leads to feminisation of male mice (Udy *et al.* 1997; Teglund *et al.* 1998).

1.6.4 SOCS2

SOCS2 expression is found in a number of tissues, with high levels found in the liver and heart (Starr *et al.* 1997; Tollet-Egnell *et al.* 1999). It has been implicated in the regulation of a number of factors including GH, tumor necrosis factor (TNF) -α, prolactin (PRL), leukaemia inhibitory factor (LIF), and IGF-1 (Minamoto *et al.* 1997; Dey *et al.* 1998; Greenhalgh *et al.* 2005; MacRae *et al.* 2009). SOCS2 regulates PRL induced STAT5 signalling in the mammary gland (Harris *et al.* 2006), EGFR signalling in a PC12 (adrenal gland) cell line (Goldshmit *et al.* 2004), and LIF induced STAT3 signalling in a myeloid leukaemia cell line (Minamoto *et al.* 1997).

SOCS2 is best recognised for its inhibition of GH signalling. *In vitro*, SOCS1 and 3 cause complete inhibition of GH induced STAT5b signalling whereas SOCS2 is only

a partial inhibitor (Ram & Waxman 1999). The role of SOCS1 in the regulation of GH *in vivo* however is negligible, and prevention of premature lethality of the *Socs1*$^{-/-}$ mice does not result in an overgrowth phenotype (Alexander *et al.* 1999). Prenatal lethality in *Socs3*$^{-/-}$ mice makes it difficult to deduce a potential role for SOCS3 in regulating GH action *in vivo* (Horvat & Medrano 1998; Roberts *et al.* 2001). The ablation of SOCS2 results in an overgrowth phenotype due to de-regulated GH signalling (Greenhalgh *et al.* 2005; Metcalf *et al.* 2000; MacRae *et al.* 2009). At birth, the mice are indistinguishable from WT littermates. From 3 weeks of age *Socs2*$^{-/-}$ mice show increased growth. By 12 weeks, male mice are approximately 40% larger than male WT. SOCS2 null females also show increased growth, although this is not to the same extent as males (Metcalf *et al.* 2000). The overgrowth phenotype is characterised by an increase in body weight due to an increase in skeletal size and a proportional increase in size of most organs. Increased local production of *Igf1* in a number of tissues including lung, heart and spleen, as well as increased collagen deposition in the dermis, and decreased MUP levels, are indicative of de-regulated GH signalling. GH levels themselves are unaltered (Metcalf *et al.* 2000; Greenhalgh *et al.* 2002a). In addition, the onset of the phenotype coincides with a period of peak GH activity, occurring between postnatal days 20-40 (Wang *et al.* 2004). The *Socs2*$^{-/-}$ phenotype is lost when crossed with *Ghrhr* (*lit*/*lit*) deficient mice. This infers that the *Socs2*$^{-/-}$ phenotype is dependent on endogenous GH. Furthermore, the gigantism phenotype is rescued with the addition of exogenous GH (Greenhalgh *et al.* 2005). The phenotype observed with the ablation of SOCS2 is similar to that observed in high growth (hg) mice. These mice develop an overgrowth phenotype due to a spontaneous 500kb deletion in mouse chromosome 10, containing the SOCS2 allele (Horvat & Medrano 2001). A noticeable difference between the two models is that hg mice show increased levels of systemic IGF-1, whereas SOCS2 null mice do not (Metcalf *et al.* 2000; Horvat & Medrano 2001; Lorentzon *et al.* 2005; MacRae *et al.* 2009). This suggests that the overgrowth phenotype observed in *Socs2*$^{-/-}$ mice is a result of increased local GH signalling. Interestingly, SOCS2 overexpression also

results in a 13-15% increase in body weight (Greenhalgh *et al.* 2002b). There is however no evidence that these SOCS2 levels are physiologically achievable.

1.6.4.1 SOCS2 regulation of the GH/IGF-1 axis

GH induced STAT5b signalling has been identified as a key pathway in regulating the overgrowth phenotype of *Socs2*$^{-/-}$ mice. This phenotype is lost when crossed with a *Stat5b*$^{-/-}$ mouse (Greenhalgh *et al.* 2002a). Furthermore, in the absence of SOCS2, STAT5 signalling is enhanced in response to GH in a number of tissues (Greenhalgh *et al.* 2002a; Pass *et al.* 2012). Similar to results obtained *in vivo*, overexpression of SOCS2 *in vitro* leads to an increase in GH induced STAT5 dependent gene transcription. It has been proposed that this is due to the ability of SOCS2 to block SOCS1 and 3, the more potent GH inhibitor (Favre *et al.* 1999; Piessevaux *et al.* 2006). The mechanism by which SOCS2 regulates GH signalling remains unclear. Deleting tyrosine residues present on the GH receptor (Y487 and Y595) results in cessation of the inhibitory action of SOCS2 on GH signalling (Greenhalgh *et al.* 2005; Uyttendaele *et al.* 2007). As Y595 is also a binding site for STAT5, SOCS2 may act to block STAT5 attachment, and therefore GH signalling (Smit *et al.* 1996). Other studies have however shown Y487 and Y595 bind STAT5 with a low affinity compared to other tyrosine motifs, Y534, Y566 and Y627 (Uyttendaele *et al.* 2007). SOCS2 may alternatively act as an ubiquitin ligase, promoting the ubiquitination and degradation of the GHR (Rico-Bautista *et al.* 2006; Vesterlund *et al.* 2011). The conserved SOCS2 box motif binds Elongins B and C. This forms a complex with Cullin5 and Rbx-I and creates an ubiquitin ligase (Greenhalgh & Alexander 2004; Bullock *et al.* 2006) (Fig. 1.9). SOCS2 has also been shown to interact with the IGF-1R, inhibiting IGF-1 induced STAT3 signalling. This suggests a regulatory function for SOCS2 in IGF-1 signalling (Dey *et al.* 1998; Zong *et al.* 2000).

1.6.4.2 The *Socs2*$^{-/-}$ skeletal phenotype

The *Socs2*$^{-/-}$ mouse is characterised by its overgrowth phenotype. This increase in weight is the result of a significant increase in long bone length and a proportional increase in size of most of the organs. No increase in fatty tissue is reported in male or female *Socs2*$^{-/-}$ mice (Metcalf *et al.* 2000). As this thesis centres around the effects of GH on bone growth this section will focus on the effects of SOCS2 ablation on the bone phenotype

At 3 weeks of age, longitudinal bone growth of *Socs2*$^{-/-}$ mice is comparable to WT. At 6 weeks of age, *Socs2*$^{-/-}$ mice show increased growth plate width, bone growth rate, and chondrocyte proliferation within the growth plate (Pass *et al.* 2012). Examination of older mice reveals increased long bone length at 7 and 12 weeks (Metcalf *et al.* 2000; MacRae *et al.* 2009). The increase in growth plate width observed in *Socs2*$^{-/-}$ mice is the result of an increase in size of both the proliferative and hypertrophic zones (MacRae *et al.* 2009; Pass *et al.* 2012). It is unknown if this is the result of an increase in chondrocyte cell size or number. However, analysis of the liver and muscle suggest that increased organ size in *Socs2*$^{-/-}$ mice is the result of increased cell number and not an increase in cell size (Metcalf *et al.* 2000). This increase in longitudinal growth is likely mediated by STAT5 signalling, which is increased in growth plate chondrocytes from *Socs2*$^{-/-}$ mice (Pass *et al.* 2012).

The bone phenotype of *Socs2*$^{-/-}$ mice is less definite. Two independent studies have highlighted increased bone turnover in Socs2$^{-/-}$ mice (Lorentzon *et al.* 2005; MacRae *et al.* 2009). Nevertheless, the analysis of bone in these studies has produced opposing results. Male *Socs2*$^{-/-}$ mice have decreased cortical parameters and BMD, whereas female *Socs2*$^{-/-}$ mice have increased cortical area and trabecular volume, with no changes to BMD (Lorentzon *et al.* 2005; MacRae *et al.* 2009). The latter observations are consistent with the known anabolic effects of GH on bone (discussed in section 1.5.5) while the decreased cortical bone is less easy to explain. The signalling pathways involved in mediating the bone phenotype in *Socs2*$^{-/-}$ mice

remain undefined. STAT5 has been implicated as an important mediator of *Socs2*$^{-/-}$ growth. It's specific role in longitudinal growth and bone turnover has however been questioned. Bone length is reduced in *Stat5ab*$^{-/-}$ mice. Despite this, there is no decrease in growth plate width. Similar results are found in relation to bone remodelling. Cortical bone width is decreased, but a number of other parameters remain unaffected (Sims *et al.* 2000). This suggests that GH may mediate bone growth and the growth plate, via pathways independent of STAT5.

1.7 The central role for SOCS2 in regulating GH signalling

As described in section 1.6.4 SOCS2 is an important regulator of GH signalling forming part of a negative feedback loop. There is now also emerging evidence that SOCS2 may be a key mediator regulating GH signalling in response to a number of factors including sex steroids, fibroblast growth factor 21 (FGF-21), and inflammatory cytokines.

1.7.1 SOCS2 mediation of sex steroid action.

Sex steroids can mediate the local actions of GH at the level of GHR expression and signalling. It is well established that osteoblasts, as well as growth plate chondrocytes express the oestrogen receptors (ER-α, and ER-β) and androgen receptor (AR) (Van Der Eerden *et al.* 2002; Nilsson *et al.* 2003; Borjesson *et al.* 2010; Almeida *et al.* 2013). Although it is recognised that both androgen and oestrogen exert effects on these cells via GH/IGF-1 independent mechanisms, this is beyond the scope of this thesis and have been extensively reviewed elsewhere (Nilsson *et al.* 2005; Compston 2001; Vanderschueren *et al.* 2008; Khosla *et al.* 2012). One such mechanism for the local regulation of GH signalling by sex steroid steroids is the up regulation of SOCS proteins.

The ER-α is vital in mediating oestrogen's up regulation of SOCS2. This was identified in WT and ER-β deficient mice, where oestrogen stimulated *Socs2*

expression in the kidney (Jelinsky *et al.* 2003). Oestrogen induced hepatic *Socs2* and *Socs3* expression is dependent on an intact ER-α (Leong *et al.* 2004). Increased *Socs2* expression in response to oestrogen stimulation is associated with decreased GH induced STAT signalling. This response is abrogated in the absence of SOCS2, but not SOCS1 or 3 (Leung *et al.* 2003). Interestingly, oestrogen has also been shown to increase SOCS2 ubiquitination and degradation in human osteoblast cells. This resulted in an upregulation of GH-induced STAT5 signalling and gene expression (Bolamperti *et al.* 2013). Androgens stimulate SOCS2 expression in prostate cancer cells, with a resulting decrease in GH induced STAT5 signalling, cell proliferation and IGF-1 production (Iglesias-Gato *et al.* 2014).

1.7.2 SOCS2 mediation of FGF-21 action.

During starvation and malnutrition FGF-21 levels are increased. FGF-21 is required to induce the synthesis of ketone bodies; the principal source of energy during starvation (Inagaki *et al.* 2007). These conditions are also associated with GH resistance and growth inhibition. STAT5 activation is reduced in response to GH in a fasted state (Beauloye *et al.* 2002). It has been proposed that this inhibition may be due to the actions of FGF-21 working through SOCS2. FGF-21 transgenic mice have increased hepatic SOCS2 levels with an associated decrease in STAT5 activation and serum IGF-1 levels (Inagaki *et al.* 2008). Recently, FGF-21 has also been shown to inhibit GH action in human chondrocytes. Again SOCS2 is identified and the key regulatory protein up regulated during reduced caloric intake (Guasti *et al.* 2013).

1.8 Inflammation and bone

There is a growing body of evidence that factors involved in inflammation are linked with those critical for bone turnover (Lorenzo 2000). A number of inflammatory disorders such as inflammatory bowel disease (IBD), coeliac disease, uremia, and rheumatoid arthritis (RA), are associated with osteoporosis (Jensen *et al.* 2004; Ludvigsson *et al.* 2007; Reinshagen 2008; Ali *et al.* 2009; Kazama *et al.* 2013).

The aetiology of bone loss is multifactorial, and includes vitamin D and calcium deficiency, prolonged glucocorticoid use, decreased gonadal function, and inflammatory activity (Tilg *et al.* 2008; Ali *et al.* 2009). During inflammation, there is an increase in levels of pro-inflammatory cytokines, including interleukin (IL)-1β, IL-6, and TNFα (Rogler & Andus 1998; Mak *et al.* 2006; Sanchez-Munoz *et al.* 2008). IL-6 and TNFα transgenic mice have severe alterations in cortical and trabecular bone. This is associated with decreased osteoblast and increased osteoclast function (Schett *et al.* 2003; De Benedetti *et al.* 2006). Conversely, treatment with a TNFα antagonist (infliximab), increases bone formation in IBD and RA patients (Abreu *et al.* 2006; Seriolo *et al.* 2006).

1.8.1 GH resistance during inflammation

IL-1β, IL-6 and TNFα are recognised to have direct effects on regulating bone turnover (Thomson *et al.* 1986; Taichman & Hauschka 1992; Kuroki *et al.* 1994; Gilbert *et al.* 2000; Zhang *et al.* 2001). One of the factors governing bone loss in inflammatory conditions however is the interference of the systemic and tissue-levels of GH/IGF-1 signalling. An increase in pro-inflammatory cytokines observed in inflammatory conditions is often associated with GH resistance. This is characterised by normal GH secretion with decreased systemic IGF-1 levels (Tenore *et al.* 1977; Lang *et al.* 1997; Denko & Malemud 2004). IL-6, TNFα, and IL-1β have all been implicated in altering systemic IGF-1 levels. IL-6 overexpression reduces systemic IGF-1 levels, but GH levels remain unchanged (Kitamura *et al.* 1995; DeBenedetti *et al.* 1997). In these mice IGF-1 levels are rescued by IL-6 neutralisation (De Benedetti *et al.* 2001). TNFα and IL-1β treatment *in vitro* decreases GHR synthesis and subsequently IGF-1 production in hepatocytes (Wolf *et al.* 1996). Conversely, treatment with infliximab (a chimeric monoclonal antibody against TNFα) to people with IBD increases serum IGF-1 and IGFBP3 levels (Eivindson *et al.* 2007).

1.8.2 Local GH signalling during inflammation

The use of various murine models of inflammation has allowed the investigation of the specific mechanisms driving GH resistance. These also provide an insight into tissue levels of GH resistance in states of inflammation. A number of studies have shown the STAT5 pathway to be central in GH resistance associated with inflammation. Lipopolysaccharide (an inducer for systemic inflammation) decreases GH induced STAT5 phosphorylation and IGF-1 expression in liver and skeletal muscle of rats. Altered SOCS expression in these animals indicate that SOCS proteins may be responsible for mediating the GH resistance observed (Lang *et al.* 2003; Chen *et al.* 2007; Chen *et al.* 2009). Similar results were reported in the *IL10*$^{-/-}$ model of colitis. These mice are characterised as having decreased BMD and IGF-1 levels, associated with the down regulation of hepatic GHR and reduced STAT5b activation. TNFα treatment down regulates GHR abundance preventing GH induced STAT5 activation in hepatocytes from colitic mice. TNFα neutralisation restores GH activation of STAT5 and serum IGF-1 levels (Difedele *et al.* 2005). IL-1β also reduces GH induced STAT5 activation in rat hepatocytes through the up regulation of SOCS3 (Boisclair *et al.* 2000). Although STAT signalling was not measured, an inverse relationship exists between *Socs2* (a well-established regulator of GH induced STAT signalling) and *Igf1* expression in skeletal muscle from uremic mice (Greenhalgh *et al.* 2002a; Cheung *et al.* 2008). Taken together these results implicate SOCS proteins (including SOCS2) in the inhibition of GH signalling during inflammation.

1.9 Clinical Relevance

Recombinant human GH (rhGH) is currently used to treat a number of conditions that result in growth retardation including growth hormone deficiency (GHD), Turner syndrome, and Prader-Willi syndrome (Bang *et al.* 2012). Recombinant hGH therapy has also been used to treat growth retardation associated with chronic inflammatory diseases (Slonim *et al.*, 2000; Mauras *et al.*, 2002; Wong *et al.*, 2007). GH

treatment however is not always successful and a recent case focussing on GHD in children found that approximately 28% of participants do not respond to GH therapy (Bang *et al.* 2011). There is therefore the need to investigate possible alternatives that may increase the efficacy of GH treatment or acts as an alternative therapy. To achieve this there is need first to fully understand the mechanism of GH action. Much can be gained by studying murine models of growth deficiency to better understand how to treat clinical conditions.

There are many similarities in growth defects observed in GH deficient or resistant mouse models, and human conditions. A comprehensive review by Yakar and colleagues outlines a number of mouse models for GH and IGF-1 deficiency and their human counterparts (Yakar *et al.* 2010). An example of this is the defects observed in Snell and Ames dwarf mice which have blunted GHR activity are similar to the clinical characteristics of Laron syndrome in humans (Smeets & van Buul-Offers 1983; Heiman *et al.* 2003; Laron 2004). Similarities between mouse models of inflammation and human cases highlight the importance of the GH/IGF-1 axis in regulating growth during chronic inflammation. Both humans are murine models are characterised by increased GH resistance during inflammation (Tenore *et al.* 1977, Katsanos *et al* 2001, Harris *et al.* 2009). More recently, at the Endo conference in Boston (2011) a presentation was made regarding a patient with increased weight and height as the result of a heterozygous mutation in the SOCS2 gene (Suda *et al.* 2011). These are exciting results that highlight the potential clinical importance of SOCS2.

1.10 Aims

The *Socs2*$^{-/-}$ mouse has been identified as a valid model of studying the local effects for GH on bone, however the mechanisms involved remain largely undefined. Therefore, the aim of this studentship was to establish the local mechanisms of enhanced GH action in the absence of SOCS2 on bone. Furthermore, the project aimed to establish the importance of SOCS2 as a mediator of inflammatory induced bone loss. For this, the following aims have been completed:

1. Establish the importance of IGF-1 in mediating the effects of GH action in longitudinal bone growth in the absence of SOCS2.

2. Determine the bone phenotype of *Socs2*$^{-/-}$ mice and establish the underlying local mechanism of GH action on osteoblasts.

3. Investigate the mechanisms of SOCS2 regulation of GH induced bone growth *in vivo*.

4. Assess the importance of SOCS2 as a mediator of inflammatory associated bone loss.

Chapter 2

Materials and Methods

2.1 Reagents and solutions

All chemicals were purchased from Sigma-Aldrich (Dorset, UK), and tissue culture media and buffers from Invitrogen (Paisley, UK) unless stated otherwise. All culture medium and buffer recipes are shown in Appendix I. Primers, antibodies, and restriction enzymes used are shown in Appendix II.

2.2 Cell and organ culture

2.2.1 MC3T3 cells

MC3T3–E1 osteoblast like cells (RIKEN cell bank) (Quarles *et al.* 1992) were cultured in osteoblast medium in a humidified atmosphere (37°C, 5% CO_2). To passage the cells, they were initially rinsed in α-MEM. Trypsin-ethylenediaminetetraacetic acid pH 7(EDTA) was used to detach the cells from the culture flask. Addition of osteoblast medium inactivated the trypsin, and cells were then pelleted by centrifugation at 1000g for 5mins. Supernatant was removed and cells resuspended in osteoblast medium. Cells were counted using a haemocytometer and plated in multi-well plates at a density of $1x10^4$cell/cm^2 (unless stated otherwise). Medium was changed every 2-3 days.

2.2.2 Freezing/thawing MC3T3 cells

To maintain the line cells were stored at -150°C. For freezing, cells were trypsinised and counted as described in section 2.2.1. They were then suspended in a 50/50 solution of freezing medium and osteoblast medium in cryovials (Corning, Surrey, UK) at a concentration of $3x10^6$cells/ml. These vials were stored upright in a polystyrene box filled with cotton wool for 3-5days at -80°C. Long term storage was at -150°C.

Cells were thawed in a 37°C water bath. Osteoblast medium (5mls) was then added in a drop wise manner. Centrifugation at 1000g for 5mins removed the dimethyl sulfoxide (DMSO) (component of the freezing medium) by pelleting the cells.

Supernatant was removed and cells resuspended in osteoblast medium. Cells were maintained as described in section 2.2.1.

2.2.3 Isolating primary osteoblasts

Under sterile conditions primary osteoblasts were isolated from calvaria dissected from 3-5 day old mice, sacrificed by decapitation, using a protocol adapted from (Zhu *et al.* 2011). All solutions used were sterilise filtered through a 0.20μm filter and heated to 37°C. In brief, dissected calvaria were digested in 1mg/ml collagenase type II (Worthington Biochemical Cooperation, UK) in Hank's balanced salt solution (HBSS) for 10mins with agitation. This removed fibroblasts and marrow cells. Subsequent digestions at 37°C in 1mg/ml collagenase in HBSS (45mins), 4mM EDTA in PBS (10mins) and 1mg/ml collagenase in HBSS (45mins) all with agitation, produced 3 fractions of cells. Each population was washed in phosphate buffered saline (PBS), HBSS, and PBS, respectively then centrifuged at 2000g for 5mins and supernatant removed. Osteoblasts from all three fractions were re-suspended in osteoblast medium and cultured in T75 flasks (Costar) (approximately 3 calvaria per flask in 12mls medium) in a humidified atmosphere (37°C, 5% CO_2).

2.2.4 Isolating murine metatarsals

Isolation of metatarsals was complete following an established method (Pass *et al.* 2012; MacRae *et al.* 2007; Mushtaq *et al.* 2004). Matings were set up and females checked daily for a vaginal plug. If a plug was observed females were singly housed to ensure an accurate date of conception. This was counted as day 0. Seventeen day old embryos or postnatal day 3 pups were sacrificed by decapitation and the middle three metatarsals isolated from each foot under a dissecting microscope under sterile conditions. All solutions were sterilise filtered through a 0.20μm filter and heated to 37°C. Metatarsals were kept moist during dissection in preparation medium.

Following extraction, metatarsals were immersed in 300µl of embryonic metatarsal medium or postnatal metatarsal medium (depending on age at extraction). Metatarsals were cultured 1 bone per well in 24-well plates (Costar). . Medium was changed every 2-3 days. Culture plates containing metatarsals were incubated in a humidified atmosphere (37°C, 5% CO_2) for up to 13 days. Metatarsal length was measured at the same time as medium change. Metatarsals were measured between the proximal to distal articulation surfaces through the middle of the bone using a Nikon eclipse TE300 microscope with digital camera attached, using Image Tool (Image Tool Version 3.00, University of Texas Health Life Science Centre, San Antonio, TX).

2.3 Transfecting MC3T3 cells

2.3.1 The SOCS2 overexpressing and control plasmids

The SOCS2 overexpression plasmid (pEF-FLAG-I/mSOCS2) and control plasmid (pEF-FLAG-I) were kingly obtained from Prof. D. Hilton (The Walter and Eliza Hall Institute for Medical Research, Parkville, Victoria, Australia). The plasmids had been previously used by Dr Chloe Pass (University of Glasgow) to assess the effects of SOCS2 overexpression in ATDC5 chondrocyte like cells (Pass *et al.* 2012). Since these two plasmids did not have resistance to any antibiotic that would be suitable for selection during transfection, they were co-transfected with pcDNA3.1$^{(+)}$ (Invitrogen; derived from pcDNA3) which contains the neomycin gene which confers resistance to geneticin.

2.3.2 Preparing glycerol stocks

Glycerol stocks of the three plasmids were kindly obtained from Dr Chloe Pass. DNA concentration and quality were assessed using a nanodrop spectrophotometer (Thermo Scientific, UK). Purity was assessed by the ratio of wavelengths 260nm/280nm, where 1.8-2.0 was considered optimal. Concentrations ranged from

911-2880ng/µl. New glycerol stocks were made from 50µl of original glycerol stock added to 200ml liquid lysogeny (LB)-broth containing 100µg/ml ampicillin. This was incubated overnight at 37°C with agitation. Ten microlitres of the resulting culture was added to 4mls of LB-broth and incubated for a further 7hrs at 37°C with agitation. Two millilitres of 50% glycerol in H_2O was then added and the resulting solution was aliquoted and stored at -80°C.

2.3.3 EndoFree maxipreparation of plasmid DNA

An EndoFree plasmid maxiprep kit (Qiagen) was used to purify the plasmid DNA and remove endotoxins found in E.coli. Manufacturer's instructions were followed. In brief, E.coli cells were pelleted from the glycerol stock by centrifugation at 6000g for 15mins at 4°C. Supernatant was removed and pellets resuspended in 10ml buffer P1 and 10mls lysis buffer P2. The solutions was mixed thoroughly and incubated for 5mins at room temperature. Precipitation of genomic DNA, proteins, cell debris and SDS was achieved by the addition of 10ml chilled neutralisation buffer P3. The lysate was added to a QIAfilter cartridge and incubated for 10mins at room temperature. The lysate passed into a sterile tube removing the precipitate. Endotoxins were removed by the addition of 2.5ml endotoxin removal buffer, inversion, and incubation for 30mins on ice. The lysate was then added to a QIAGEN-tip 500; equilibrated with QBT buffer; and allowed to enter the resin by gravity flow. Binding of the plasmid DNA to the resin, allowed contaminants to be removed through washes with 2x15mls QC buffer. DNA was eluted by the addition of 15mls buffer QN and 10.5mls isopropanol. DNA was pelleted by centrifugation at 15000g for 90mins at 4°C. Supernatant was removed and pellet washed with 70% ethanol for 10mins at 15000g. Pellet was air dried and resuspended in 50µl endotoxin-free TE buffer and stored at -80°C.

2.3.4 Restriction digest

To ensure the plasmids were complete and of correct size a restriction digest was completed with DNA from the maxiprep. The specific restriction enzymes used and band sizes expected are outlined in Appendix II. Reaction volumes for Nde I and Asc I restriction enzymes were 1µl DNA (1µg/µl), 0.05µl enzyme (20U), 5µl buffer, and 43.95µl H_2O. For EcoR1, Nhe I, and Pst I reaction volumes were 1µl DNA (1µg/µl), 0.25µl enzyme, 2.5µl buffer, and 21.25µl H_2O. All reactions were incubated for 1hr at 37°C followed by 25mins at 65°C. DNA fragments were run on a 1.8% agarose/1xTBE (Ambion, Cambridge, UK) gel containing 0.5ug/ml ethidium bromide. 5x blue loading buffer (5:1) (New England Biolabs, Herts, UK) was added to each sample to aid loading. Electrophoresis was carried out at 160V in a gel tank containing TBE buffer. Hyperladder 1 (Bioline) was used as a molecular weight marker. Gels were imaged using a Gel Logic 200 imaging system and software (Kodak, Hemel Hempstead, Herts, UK).

2.3.5 Transfection of MC3T3 cells

MC3T3 cells were transfected using FuGene 6 (Roche). FuGene 6 (6µl) was incubated with 92.5µl OptiMEM (used for lipid infections) for 5mins at room temperature. DNA containing the plasmids pEF-FLAG-I or pEF-FLAG-I/mSOCS2 were then added along with pcDNA3.1$^{(+)}$ (to give antibiotic resistance) at a ratio of 5:1 (1.25µl and 0.25µl, respectively). This ensured that there was optimal chance that if pcDNA3.1$^{(+)}$ was transfected then the other two plasmids would also be transfected. The resulting transfection reagent was incubated at room temperature for 15mins before being carefully added to MC3T3 cells (70% confluency) cultured in antibiotic free osteoblast medium. Cells were maintained in a humidified atmosphere (37°C, 5% CO_2) for 6hrs and then the medium was changed to normal osteoblast medium. Following 48hrs the medium was changed again to osteoblast medium containing geneticin. This was used to select transfected cells (500µg/ml; Gibco, Invitrogen). Further medium changes were every 2 days.

To ensure that colonies were grown form a single cell population, individual cell position was marked and proliferation tracked. Once a colony had reached a desirable size they were isolated by trypsinisation within a cloning ring (8mm x 8mm). This was completed for 5 individual colonies containing the pEF-FLAG-I/mSOCS2 plasmid and 3 colonies containing the control pEF-FLAG-I plasmid. The collected cells form different colonies were separately pelleted by centrifugation and resuspended in osteoblast medium in a 6 well plate (Costar). Geneticin (500μg/ml) was added 24hrs later to allow the cells time to attach. Osteoblast medium containing geneticin (500μg/ml) was changed every 2 days. Cells were propagated until there was sufficient to be frozen down as described in section 2.2.2.

2.4 *In vivo* studies

2.4.1 Animal welfare

Mice were maintained under conventional housing conditions with 12h light/dark cycle. All animal experiments were approved by The Roslin Institute's Animal Users Committee and the animals were maintained in accordance with Home Office guidelines for the care and use of laboratory animals

2.4.2 Generation of *Socs2*$^{-/-}$ mice

All mice used in this thesis were from an established colony. The *Socs2*$^{-/-}$ colony was generated as previously described (MacRae *et al.* 2009).

2.4.3 Genotyping

DNA was extracted from earclips taken from 3-4 week old mice using a DNeasy blood and tissue kit (Qiagen, Crawley, UK) following manufacturer's protocol. In brief, the kit contained an overnight proteinase K lysis stage with agitation (performed at 37°C) to digest the tissue. This was followed by use of a spin column which provided optimal DNA binding conditions on a silica-based membrane, and allowed for the removal of contaminants and enzyme inhibitors through two wash

steps. The DNA was finally eluted in a low-salt buffer and passes through the membrane. DNA concentration and quality were assessed using a nanodrop spectrophotometer (Thermo Scientific, UK). Purity was assessed by the ratio of wavelengths 260nm/280nm, where 1.8-2.0 was considered optimal.

Primers had been previously designed to identify both WT and *Socs2* knockout (KO; neo-cassette) bands (Pass *et al.* 2012). Therefore, each sample was run with both sets of primers separately. The WT PCR solution contained – 3µl DNA (10ng/µl); 2.5µl 10x NH_4 buffer (Bioline, London, UK); 1.125µl 50mM $MgCl_2$ (Bioline), 2.5µl 2mM dNTPs (Invitrogen); 0.5µl 20pmol/µl forward and reverse WT primers; 15.625µl nuclease free H_2O; 0.25µl 5U/µl BioTaq DNA polymerase (Bioline). The PCR was performed under the following conditions on a DNA Engine Dyad machine (Peltier Thermal Cycler, Bio-Rad Laboratories, Hertfordshire, UK) – 3mins at 94°C (denaturing), 35 thermocycles consisting of 20s at 94°C (denaturing), 20s at 50°C (annealing), and 45s at 72°C (extension); 10mins at 72°C. The KO PCR solution contained – 3µl DNA (10ng/µl); 2.5µl 10x NH_4 buffer; 0.75µl 50mM $MgCl_2$ (Bioline), 2.5µl 2mM dNTPs; 0.5µl 20pmol/µl forward and reverse WT primers; 16µl nuclease free H_2O; 0.25µl 5U/µl BioTaq DNA polymerase. The PCR was performed under the following conditions on a DNA Engine Dyad machine (Peltier Thermal Cycler, Bio-Rad Laboratories, Hertfordshire, UK) – 2mins at 92°C (denaturing) followed by 32 thermocycles consisting of 1mins at 92°C (denaturing), 1min at 58°C (annealing), and 1min at 72°C (extension). There was a final step of 10mins at 72°C.

PCR products were run on a 1.8% agarose/1xTBE (Ambion, Cambridge, UK) gel containing 0.5ug/ml ethidium bromide. 3µl of 5x blue loading buffer (New England Biolabs, Herts, UK) was added to PCR product and 13ul of samples was added to the gel. Electrophoresis was carried out at 160V in a gel tank containing TBE buffer. Hyperladders 1 and V (Bioline) were used as molecular weight markers for WT and KO PCR's, respectively. Gels were imaged using a Gel Logic 200 Imaging System and software (Kodak, Hemel Hempstead, Herts, UK).

2.4.4 Calcein labelling

Mice received a subcutaneous injection of 10mg/kg calcein diluted in sodium bicarbonate solution ($NaHCO_3$). In juvenile mice (6 weeks of age), injections were given 9 and 2 days prior to sacrifice. In adult mice (17 weeks of age), injections were given 16 and 2 days prior to sacrifice.

2.4.5 Long term *in vivo* GH treatment

From 14 days of age mice received subcutaneous injection of recombinant human GH (rhGH) (3mg/kg) (a generous gift from Professor Faisal Ahmed) twice daily for 14 days. Vehicle treated animals received an injection of sterile H_2O. Injection site was changed each time to minimise discomfort to the animal and local inflammation. GH administration was spaced the maximum time part within the working day (~7hrs). Mouse weight was measured daily before first injection to track weight gain. Three hours after the final injection on day 14 of treatment mice were sacrificed by asphyxiation.

Immediately following sacrifice, blood samples were extracted by cardiac puncture and collected in serum Z/1.3 tubes (Greiner Bio-One, Gloucestershire, UK), promoting clotting. Samples were left on ice for 30mins and then centrifuged at 1000g for 10mins. Supernatant was removed, aliquoted, and stored at -80°C. The left femurs were dissected and the epiphysis removed. Marrow was removed by centrifugation. Along with the dissected livers, samples were snap frozen in liquid nitrogen and stored at -80°C for RNA extraction. Right femurs were dissected and stored in H_2O at -20°C for micro-computed tomography (micro-CT) imaging.

2.4.6 Short term *in vivo* GH treatment

At 17 and 24 days of age mice were given a single intraperitoneal injection of rhGH (3mg/kg) (a generous gift from Professor Faisal Ahmed) or sterile H_2O for 15mins, before being sacrificed by cervical dislocation. Liver and tibiae were quickly dissected. The epiphysis of the tibiae were removed, and marrow extracted by

centrifugation. Livers and tibiae were then snap frozen and stored at -80°C for protein extraction.

2.4.7 Micro-computed tomography imaging

Micro-CT imaging was carried out with guidance from Professor Rob van'f Hof. This was used to assess trabecular architecture and cortical geometry of bone. Bones samples were stored in H_20 at -20°C and thawed prior to scanning. In chapters 4 and 6 (bones from DSS induced colitis study) tibiae were scanned using a micro-CT system (Skyscan 1172 X-ray microtomograph, Bruker Corporation, Kontich, Belgium). In chapter 5 and 6 (bones from $Il10^{-/-}$ study) femurs and tibiae were scanned using a micro-CT system (Skyscan 1272 X-ray microtomograph, Bruker Corporation, Kontich, Belgium). The methods outlined below focus of the use of the Skyscan 1172. Specific changes to analysis are outlined in the material and methods sections of each results chapter (sections 4.4.2, 5.4.2, and 6.4.1). For analysing trabecular bone parameters, high resolution scans with an isotropic voxel size of 5μm were acquired (60kV, 0.5mm aluminium filter, 0.6° rotation angle between images over 180°). The isotropic voxel size was changed to 10μm for cortical scanning. Two images were averaged at each rotation angle to reduce noise. Scans were reconstructed using NRecon software (Bruker).

A volume of interest was selected using Data Viewer (Bruker). A 1mm section of the metaphysis was used for analysis of trabecular bone, using the base of the growth plate as a standard reference point (Fig. 2.1A). A 500μm section of the mid-shaft was taken for analysis of cortical bone, using the articulation with the fibula as a standard reference point. CTAn software (Bruker) was used to analyse appropriate parameters. A region of interest was selected for trabecular analysis to ensure cortical bone was not included in trabecular analysis (Fig. 2.1B). This stage was not completed for cortical bone as no trabecular bone was present at the midshaft. CTAn software was used to reduce noise in the reconstructed images by applying a median filter with a radius of 1 pixel. To ensure only bone was analysed, and not

surrounding soft tissue, a threshold was set, remaining consistent in all samples. Calcium hydroxyapatite phantoms of a known density were scanned using the same settings as above for calibration, from which BMD values were calculating. Parameters analysed using CTAn software are outlined in Table 2.1.

2.4.8 Mechanical testing

A Lloyd LRX5 materials testing machine (Lloyd Instruments, West Sussex, UK) fitted with a 500N load cell was used to determine failure load, work to failure, load to maximum and maximum stiffness of tibiae. The span was fixed at 10mm and the cross-head lowered at 1mm/min. Data were recorded after every 0.2mm change in deflection. Each bone was tested to point of failure which was identified from the load-extension curve (Fig. 2.2) as the point of maximum load. The remaining parameters were calculated from a polynomial curve fitted to the rising region of the load-extension curve in Sigmaplot (Systat Softwatre Inc., San Jose, USA). The maximum stiffness was defined as the maximum gradient of the rising portion of the curve (Fig. 2.2). Load at maximum stiffness was calculated as the load at point of maximum stiffness (Fig. 2.2). Work to failure was calculated as the area under the load extension curve up to point of failure (Fig. 2.2).

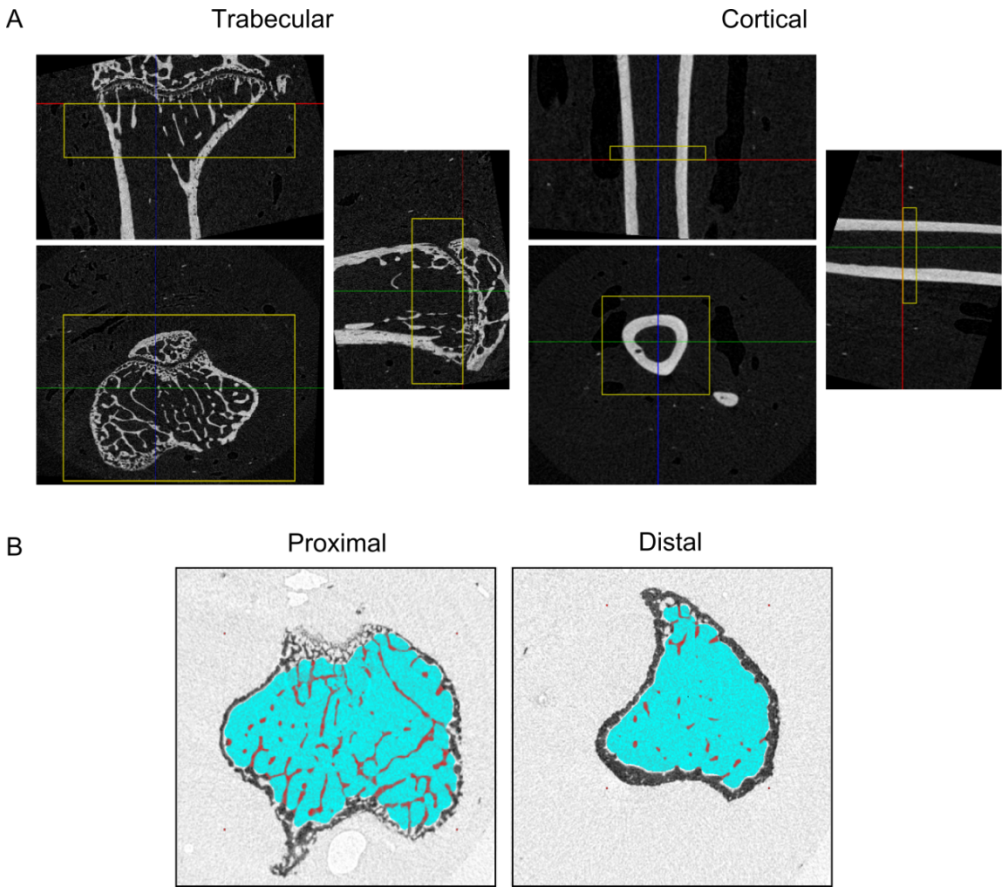

Figure 2.1 Selecting volume and region of interest for micro-CT analysis

A. Representative images in Data Viewer of proximal tibia and midshaft (both showing 3 planes of view), highlighting the selection of a volume of interest (yellow box). **B.** Representative transverse images in CTAn of a tibia showing the proximal and distal areas of the volume of interest. Blue area highlights the region of interest for trabecular analysis.

Table 2.1 Parameter analysed using micro-CT

Trabecular and cortical parameters measured by micro-CT, their abbreviations, and units measured in.

Parameter	Abbreviation	Units
Trabecular bone		
Percent bone volume	BV/TV	%
Trabecular number	Tb.N	1/mm
Trabecular Thickness	Tb.Th	mm
Trabecular Separation	Tb.Sp	mm
Structural model index	SMI	na
Bone mineral density	BMD	g/cm^3
Cortical Bone		
Tissue Area	Tt.Ar	mm^2
Cortical Area	Ct.Ar	mm^2
Marrow Area	Ma.Ar	mm^2
Cortical Thickness	Ct.Th	mm
Polar moment of inertia	J	mm^4
Bone mineral density	BMD	g/cm^3

na – non applicable as SMI is measured as relative prevalence of plates and rods

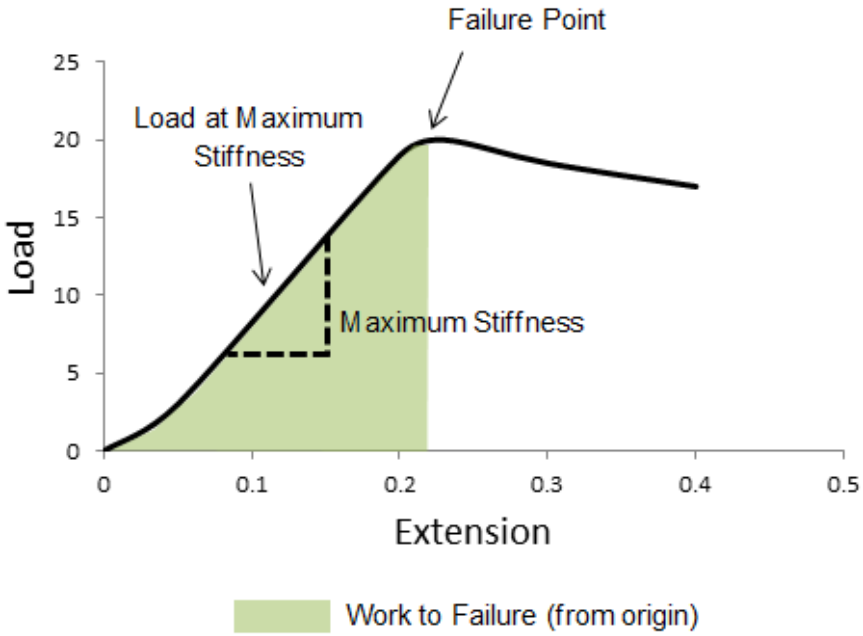

Figure 2.2 Three point bending load extension curve

Diagram of a typical load extension curve obtained with 3-point bending highlighting the measured parameters.

2.4.9 Methylmethacylate embedding

Tibiae were initially stripped of all soft tissue and fixed in 4% paraformaldehyde for 24hrs at 4°C and stored in 70% ethanol at 4°C for no longer than 1 month. Samples were dehydrated through increasing concentrations of ethanol - PBS for 45mins, 50% ethanol for 2hrs, 70% ethanol for 2hrs, 80% ethanol for 2hrs, 96% ethanol for 2hrs, 100% ethanol for 3hrs, 100% ethanol for 3hrs. Fat was then removed from the sample through 2 washes in xylene for 1hr and 12hrs. Samples were added to a filtration solution under vacuum (89% liquid Methylmethacylate (MMA), 10% dibutyl phthalate (increases plasticity), 1% perkadox) for 5mins. Samples were stored for 1 week at 4°C. Bones were embedded in MMA in an air tight holder to reduce oxygen levels (oxygen slows setting of MMA). Care was taken to keep the orientation of the tibia similar. Samples were left in a 30°C water bath for 48hrs then mounted on cassettes and 5µm sections cut using a Leica RM2265 microtome (Leica Biosystems, UK). Sections were kept moist in 96% ethanol and left in a 37°C incubator for 2-3 days.

2.4.10 Von Kossa and paragon staining

Staining recipes can be found in appendix I. Slides embedded in MMA (section 2.4.9) were stained with Von Kossa (stains calcium deposits black and cytoplasm light pink) and paragon (stains nucleic acids blue and polysaccharides purple). Before staining resin was removed by methoxyethyl acetate (MEA) and rehydrated through decreasing concentrations of ethanol –MEA for 20mins, MEA for 20mins, xylene for 10mins, xylene for 10mins, dipped in 100% ethanol twice, dipped in 96% ethanol, dipped in 80% ethanol, dipped in 70% ethanol, dipped in 50% ethanol and stored in H_2O. Sections were then immersed in silver nitrate solution in the dark for 5mins. Following 3 washes in H_2O samples were reduced in freshly prepared 0.5% hydroquinone until mineralised tissue turned black (~2mins). Sections were stained in paragon solution for 30s. Finally, sections were rinsed with dH_2O, air dried then dehydrated in xylene for 5mins before cover slips were mounted using DePeX mountant.

2.5 RNA methods

2.5.1 Isolation of RNA from cells, tissues and metatarsals

Primary osteoblasts were rinsed in ice cold PBS to remove excess medium. Cells were then scraped in 200µl PBS, pelleted and stored at -80°C. RNA was extracted using a Qiagen RNeasy kit, according to manufacturer's instructions. In brief, samples were initially homogenised in the presence of a denaturing buffer, inactivating RNases. Addition of ethanol provided optimal binding conditions to the silica-based membrane. This was then centrifuged in the presence of wash buffers to remove contaminants. The RNA was then eluted in RNase free H_2O and passed through the membrane. The RNA was stored at -80°C.

Liver and bone samples were extracted using an RNeasy Lipid Tissue Kit following manufacturer's protocol. The kit was similar to the RNeasy kit, but contained and additional phenol/guanidine-based sample lysis step which facilitates the breakdown of fatty tissues. RNA was then extracted through the addition of chloroform and run on spin columns. Liver was initially homogenised in QIAzol Lysis Reagent (RNeasy Lipid and Tissue kit) using a hand held homogeniser (Cole-Parmer Instruments Ltd, London UK). Bone samples were submerged in liquid nitrogen and homogenised using a mortar and pestle followed by a hand held homogeniser in QIAzol Lysis Reagent. RNA was stored at -80°C.

Metatarsals were grouped (3-4 bones) to make one sample. RNA was extracted using Trizol reagent following manufacturer's protocol. In brief, metatarsals are homogenised in 200µl of Trizol using the hand held homogeniser. 40µl of chloroform was added to the samples and shaken vigorously. Following 3mins incubation the samples were centrifuged at 12000g for 15mins at 4°C. RNA was extracted from the upper aqueous phase and added to 100µl of 100% isopropanol and incubated for 10mins. Samples were then centrifuged at 12000g for 10mins at 4°C. The supernatant was removed leaving only the RNA pellet. This was washed

in 200µl of 75% ethanol, vortexed briefly, and centrifuged at 7500g for 5mins at 4°C. Wash was discarded and pellet allowed to air dry (~5mins), before being resuspended in 50µl RNase-free H_2O.

RNA concentration and quality of all samples were assessed using a nanodrop spectrophotometer (Thermo Scientific, UK). Purity was assessed by the ratio of wavelengths 260nm/280nm, where ~2.0 was considered optimal. Samples from the same study were diluted in nuclease-free water (NFW) to the concentration of the lowest sample.

2.5.2 Reverse transcription

RNA was converted into complementary DNA (cDNA) using the DNA polymerase enzyme reverse transcriptase. RNA samples (10µl) were incubated with 2µl of random primers (1:60, (Invitrogen) from 10mins at 70°C (DNA Engine Dyad machine) and immediately cooled on ice. A master mix was used; composed of 4µl 5xFirst strand buffer, 2µl dithiothreitol (DTT) (0.1M) (Invitrogen), 1µl deoxyribonucleotide triphosphate (dNTP) (10mM), and 1µl Superscript II RNase H enzyme (200U/µl). 8µl of the master mix was added to each sample. The reverse transcription was performed under the following conditions on a DNA Engine Dyad machine – 10min at 25°C (annealing), 50mins at 42°C (elongation), 10min at 70°C (termination). The cDNA samples were stored at -20°C.

2.5.3 Quantitative polymerase chain reaction (qPCR)

All cDNA samples were diluted to 5ng/µl in NFW. Master mix containing 10µl 2x FastStart Universal SYBR Green Master Mix (Roche), 0.5µl forward primer and 0.5µl reverse primer (10pmol/µl; MWG Eurofins London, UK) or 1µl primer assay (0.5µM; Invitrogen) and 4µl NFW was added to 25ng cDNA (5µl). FastStart Universal SYBR Green Master Mix contains a fluorescent dye which binds to double stranded cDNA generating a quantifiable readout for amplified cDNA levels. The qPCR was performed under the following conditions on a Stratagene Mx3000P PCR cycler (Agilent Technologies, Santa Clara, USA) – 15mins at 95°C (denaturing), 40

thermocycles consisting of 15s at 94°C (denaturing), 30s at 55°C (annealing), and 30s at 72°C (elongation). Fluorescence levels were measured during each elongation step. A dissociation curve was generated after each run to assess primer specificity with a single peak indicating one amplified product. Reactions containing H_2O instead of cDNA sample were used as a negative control.

To initially test primer efficiency, cDNA samples known to express the gene of interest were serially diluted and run with the sample programme as described above producing a standard curve. Primers were considered acceptable if the standard curve had an R^2 value between 0.90 and 1.00, with an amplification efficiency between 90-110% (Fig 2.3A). To confirm specificity of new primers the product was run on a 1.8% agarose gel and visualised as outlined in section 2.4.3 (Fig. 2.3B). qPCR products from un tested primers were sent to Edinburgh Genomics (University of Edinburgh) for sequencing to confirm primer specificity. NCBI Blast was used to match product sequence with sequence of interest. Information on primers can be found in Appendix II.

Analysis of qPCR was carried using MxPro software (Cheshire, UK). Gene expression was initially normalised to a house keeping gene *Gapdh* (unless stated otherwise). *Gapdh* was selected using a gNorm kit (Primer Design, UK). This test was completed on RNA from bone samples and tested an array of common housekeeping genes to ensure that their expression was not altered by genotype. *Gapdh* was found to be stable between genotypes (WT and *Socs2*$^{-/-}$). Furthermore, *Gapdh* expression is not influenced by GH treatment (Mrak *et al*. 2007). Data were then presented as relative expression of the gene calculated using the $\Delta\Delta C_T$ method (Livak & Schmittgen 2001).

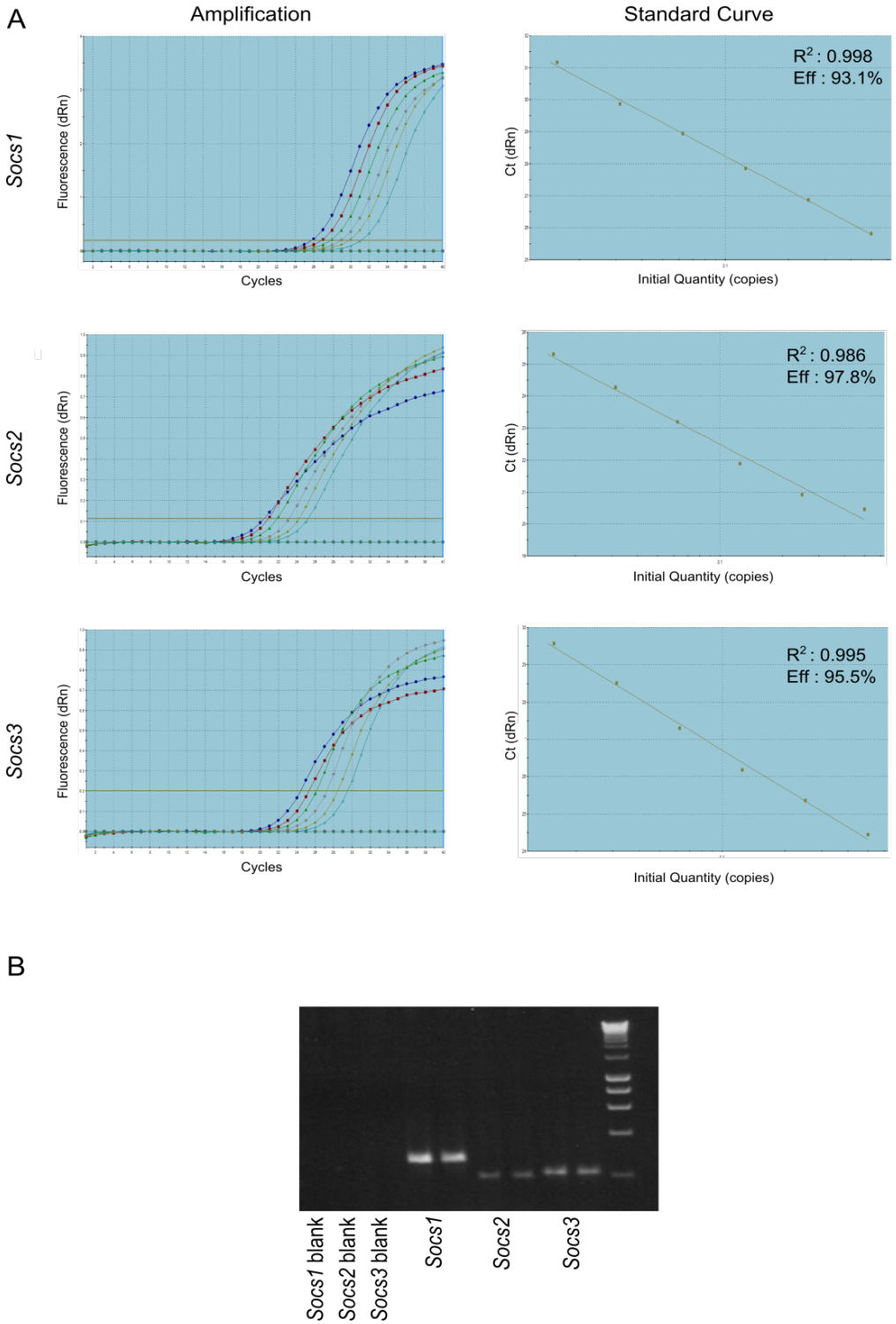

Figure 2.3 Primer optimisation

A. Amplification plots and standard curves (highlighting R^2 and efficiency) for *Socs1*, *Socs2*, and *Socs3*. **B.** qPCR product for *Socs1*, *Socs2* and *Socs3* run on a gel to confirm primer specificity (one band). Samples run in duplicate.

2.6 Protein methods

2.6.1 Protein extraction

Primary osteoblasts and MC3T3 cells were rinsed in ice cold PBS twice to remove excess medium. Generally, 2 wells were combined for 1 sample. Depending on protein of interest, cells were scraped in either Phosphosafe extraction reagent (Novagen, Merck Biosciences, Nottingham, UK) containing 0.15 x volume protease inhibitor cocktail (Roche, Burgess Hill, West Sussex, UK) or RIPA buffer containing 0.15 x volume protease inhibitor depending on protein of interest. Detection of phosphorylated (p-) proteins such as p-STATs, p-AKT, and p-ERK1/2 required scraping in Phosphosafe, whereas cells used for the detection of SOCS proteins were scraped in RIPA. Samples were vortexed to ensure cell disruption and protein release. Liver samples were homogenised in RIPA buffer containing 0.15 x volume protease inhibitors and 0.01 x volume phosphatase inhibitor cocktail using a hand held homogeniser (Cole-Parmer Instruments CO. Ltd, London, UK). Bone samples were submerged in liquid nitrogen and homogenised using a mortar and pestle. Once added to the RIPA solution (as for liver) bone samples were further homogenised using the hand held homogeniser. All samples were stored at -20°C.

2.6.2 Quantification of protein

Protein samples were thawed, vortexed, centrifuged at 2000g for 5mins, and pellet discarded. Protein content was determined using a DS protein assay (Bio-Rad Laboratories, Herts, UK). This assay is similar to the Lowry assay. Protein undergoes a reaction with an alkaline copper tartrate solution which reduces Folin reagent producing a blue colour. Standards were made using lyophilised bovine plasma gamma globulin protein, 2mg/ml (Bio-Rad) diluted in the same solution that protein was extracted in. Each reaction was carried out in a 96-well plate. All samples were carried out in duplicate. Initially, 25µl Reagent A' (containing 20µl Reagent S per 1ml Reagent A) was pipetted in each well, followed by 5µl of sample/standard. To this 200µl of Reagent B was added and the plate was incubated

for between 15-60mins. Protein levels were measured by absorbance at 690nm using a Synergy HT Multi-Mode Microplate Reader (BioTech Instruments, Bedfordshire, UK). The standard curve was used to determine the protein concentration of each sample.

2.6.3 Western blotting

Samples were prepared so that each sample contained the same quantity of protein. Quantities ranged from 5µg to 30µg. An appropriate volume of sample was added to a solution of LDS sample buffer (3:1) and sample reducing reagent (10:1, Invitrogen). Samples were denatured at 70°C for 10mins. The denatured proteins were chilled on ice for 1min before being loaded onto pre-cast 3-8% Tris –Acetate ((p-)STATs, (p-) Akt, and (p-) ERK1/2) or 10% Bis-Tris gels (SOCS) (both Invitrogen) (unless stated otherwise). Gels were run in a Novex Gel Tank (Invitrogen) containing 1x Tris Acetate or 1x MOPS running buffer, respectively. All blue protein standards were used as molecular weight markers (All Blue, Bio-Rad, Hemel Hempstead, UK). Anti-oxidant was added to the centre compartment of the tank to preserve reduced proteins (2.5µl/ml; Invitrogen). Proteins were separated by electrophoresis at 200V for 40mins.

Protein was transferred onto a Hybound-ECL nitrocellulose membrane (GE Healthcare, Amersham), sandwiched between transfer buffer (Appendix I) soaked filter paper and sponges. This created a wet transfer within a transfer module (Invitrogen). Transfer was run on ice at 30V for 90mins.

The nitrocellulose membrane was washed in TBS/T (Tris-buffered saline/Tween-20) and blocked at room temperature for 1hour in 5% BSA (Albumin, Bovine Serum, Fraction V) in TBS/T. Following this stage the nitrocellulose was incubated at 4°C overnight with the primary antibody diluted in TBS/T. The nitrocellulose was then washed again in TBS/T before being incubated at room temperature for 1.5hours with the secondary antibody diluted in 5% marvel. Bound antibody was detected

using chemiluminescence detection with Amersham ECL western blotting detection reagents A and B (GE Healthcare) which were pipetted onto the nitrocellulose at a ratio of 1:1 for 1min. Chemiluminescence was detected with Amersham ECL Hyperfilm (GE Healthcare), which was developed using a Medical Film Processor (SRX-101A; Konica Minolta, Banbury, UK).

2.6.4 Stripping nitrocellulose

Restore Plus Stripping buffer (Thermo Scientific) was used to strip nitrocellulose. Stripping buffer was incubated with nitrocellulose for up to 30mins at 37°C followed by up to 1hr at room temperature. Probing with the appropriate secondary antibody and detecting with chemiluminescence ensured the antibody had been effectively stripped.

2.6.5 Immunocytochemistry

Cells for immunocytochemistry were plated in collagen coated 6 well plates (Costar) containing a 22mmx22mm glass coverslip (Scientific Laboratory Supplies, Yorkshire, UK). At the end point of experiment medium was aspirated and cells fixed in 4% paraformaldehyde for 15mins. Cells were washed in PBS (3x5mins) before being permeabilised in ice cold 100% methanol for 5mins at -20°C. Following a 5mins wash in PBS cells were blocked in blocking buffer (1xPBS, 5% normal goat serum, 0.3% triton X-100) for 1hr. Blocking solution was aspirated and cells were incubated with primary antibody diluted in antibody dilution buffer (1xPBS, 1% BSA, 0.3% Triton X-100) overnight at 4°C. Primary antibody was removed and cells were washed in PBS (3x5mins). The fluorochrome-conjugated secondary antibody diluted in antibody dilution buffer was added to the cells for 90mins at room temperature in the dark. Cover slips were mounted to slides using ProLong Gold Antifade Mountant with DAPI (Invitrogen). Slides were analysed using a Nikon EC-1 confocal microscope.

2.7 Statistical Analysis

Statistical analysis was completed using SigmaPlot (v11.0) (Systat Software Inc., London, UK). For comparisons involving 2 independent variables data were analysed using a 2 way ANOVA for which suitable post-tests for multiple comparisons were conducted. Studies which involved repeated measures were analysed using a repeated measures 2 way ANOVA and suitable post-tests. Direct comparisons between groups were analysed using the Student's t-test or a suitable non-parametric test if the data were not normally distributed. Data were checked for normal distribution using a Shapiro-Wilk normality test. All data were expressed as the mean ± standard error of the mean (SEM). $p<0.05$ was considered to be significant.

Chapter 3

SOCS2 regulation of GH induced longitudinal bone growth

3.1 Introduction

The anabolic role of GH in long bones is well accepted, however its mode of action makes it difficult to delineate the relative contributions of GH's systemic and local effects on longitudinal growth (Le Roith *et al.* 2001). At a systemic level, GH acts indirectly through IGF-1, which is produced by the liver. At a local level (growth plate cartilage), GH activates the GHR and regulates chondrocyte function via IGF-1 dependent (indirect) or independent (direct) mechanisms (Gevers *et al.* 2002b). The phenotypic analysis of *Ghr*$^{-/-}$ and GHRH receptor knockout (*Ghrhr*$^{-/-}$) mice reveal reductions in body weight and growth retardation (Wajnrajch *et al.* 1996; Sims *et al.* 2000; Greenhalgh *et al.* 2005). A comparable phenotype is present in humans with severe primary IGF-1 deficiency, characterised by insensitivity to GH (Laron 2004). Similar growth deficiencies are reported in global *Igf1*$^{-/-}$ and *Igf1r*$^{-/-}$ mice (Liu *et al.* 1993; Lupu *et al.* 2001; Mohan *et al.* 2003). The relative contributions of GH's systemic and local effects, as well as GH's direct (IGF-1 independent) effects on longitudinal growth however remain unclear (Isaksson 1982; Lupu *et al.* 2001).

The importance of systemically derived IGF-1 on linear growth has been challenged by two independent studies, showing that LID mice had a 80% reduction of circulating IGF-1, but body weight and bone length were largely unaffected (Sjogren *et al.* 1999; Yakar *et al.* 1999). Further reductions in serum IGF-1 levels were achieved by the generation of triply deficient LID/ALSKO/BP3KO mice. By knocking out all components of the ternary complex to which IGF-1 binds in circulation, systemic IGF-1 levels were virtually undetectable (2.5% of WT IGF-1). Despite this, these mice only exhibited a 6% decrease in body length. This was comparable to that of the ALSKO mice alone, which had a 60% reduction in IGF-1 levels (Yakar *et al.* 2009). It has been proposed that a threshold concentration of systemic IGF-1 is required for normal growth, as ALSKO+LID mice (85-90% reduction in systemic IGF-1) have a significant reduction in linear growth (Yakar *et al.* 2002). In addition, when hepatic IGF-1 production was achieved in mice lacking *Igf1* gene expression in all other tissues, it was found that systemic IGF-1 contributed to 30% of the adult body size,

and sustained postnatal development (Stratikopoulos *et al.* 2008). Similarly, in *Igf1* null mice with hepatic overexpression of the rat *Igf1, s*erum IGF-1 production supported normal body growth during and after puberty (Wu *et al.* 2009; Elis *et al.* 2010). Although it is difficult to reconcile these results, it is likely that both systemic and local acting GH function in a highly coordinated manner to regulate the growth plate and subsequently linear bone growth.

Alternative strategies to distinguish between systemic and local IGF-1 effects on linear bone growth have involved the targeted deletion of *Igf1* in epiphyseal chondrocytes. These mice had a 40% reduction in cartilage *Igf1* expression and normal serum IGF-1 levels (Govoni *et al.* 2007a). Linear growth was reduced by 27% between 2 and 4 weeks of age, highlighting that local chondrocyte-produced IGF-1 is an important regulator of longitudinal growth. Whilst highly informative, these studies fail to address the possibility of GH actions on longitudinal growth that are independent of downstream IGF-1 effects. *Ghr*/*Igf1r*$^{-/-}$ mice have a more severe phenotype than *Ghr*$^{-/-}$ or *Igf1*$^{-/-}$ alone. This suggests that there are GH actions on linear bone growth that are independent of IGF-1 (Lupu *et al.* 2001).

A role for local GH in the regulation of bone growth is also suggested by data from *Socs2*$^{-/-}$ mice (Metcalf *et al.* 2000; MacRae *et al.* 2009). SOCS2 is expressed by epiphyseal chondrocytes, and is a recognised negative regulator of GH signalling via inhibition of the JAK/STAT pathway (Hilton 1999; Greenhalgh *et al.* 2002; Flores-Morales *et al.* 2006; Rico-Bautista *et al.* 2006; Pass *et al.* 2009). These mice are characterised by increased growth, including increased long bone length, without elevated systemic levels of IGF-1 or GH (Metcalf *et al.* 2000; Greenhalgh *et al.* 2005; MacRae *et al.* 2009). It can therefore be assumed that local direct and/or indirect (IGF-1 mediated) effects of GH are driving this increased linear bone growth.

The *ex vivo* metatarsal culture method has been exploited in many studies as a method of analysing endochondral bone growth. It provides a more physiological

environment than cultured chondrocytes (Mushtaq *et al.* 2004; MacRae *et al.* 2007; Chagin *et al.* 2010). In this organ culture model, chondrocyte interactions with each other and the ECM are maintained. Recently, it has been reported that GH is able to stimulate longitudinal growth of metatarsals only in the absence of SOCS2 (Pass *et al.* 2012). The *Socs2*$^{-/-}$ metatarsal culture is therefore a valuable model in investigating the mechanisms by which local GH enhances linear bone growth.

3.2 Hypothesis

WT metatarsals do not respond to GH due to an increase in *Socs2* expression. Increased growth of *Socs2*$^{-/-}$ metatarsals is mediated through the upregulation of IGF-1.

3.3 Aims

I. To quantify the expression of *Socs1*, *2*, and *3* in WT metatarsals following GH treatment.

II. To determine mRNA expression and protein levels of IGF-1 and IGFBP3 in WT and *Socs2*$^{-/-}$ metatarsals following GH treatment.

III. To determine the effects of GH treatment on *Socs2*$^{-/-}$ metatarsal growth in the presence of an IGF-1R inhibitor.

IV. To quantify the relative expression levels of *Igf1* in the growth plate of *Socs2*$^{-/-}$ mice.

3.4 Material and Methods

3.4.1 Murine metatarsals

Metatarsals were isolated from 17 day old embryos or postnatal day 3 pups as described in section 2.2.4. rhGH and rhIGF-1 (both Bachem, Merseyside, UK) and rmIGF-2 (R&D systems, Minneapolis, USA) were added at 100ng/ml. 1μM NVP-AEW541 (IGF-1R inhibitor) was added 16 hours prior to the addition of GH. As NVP-AEW541 was diluted DMSO, an equivalent concentration of DMSO was added to control groups. Culture plates containing metatarsals were incubated in a humidified atmosphere (37°C, 5% CO_2), for up to 13 days. Metatarsals were measured as described in section 2.2.4. Linear growth was assessed as percentage increase in growth from initial length. This method of analysis was chosen as high variation between initial metatarsals lengths would mask the effects of treatment if length of bones was compared directly.

3.4.2 Histological analysis of metatarsal zones

Embryonic day 17 metatarsals were stored in 80% ethanol following 12 days GH treatment. Metatarsal embedding, staining, and sectioning were completed by the Easter Bush Pathology Department, University of Edinburgh. In brief, metatarsals were demineralised in 10% EDTA for 2 days. Samples were embedded using the following protocol – 70% ethanol for 1hr, 95% ethanol for 1hr, 5 washes in absolute ethanol for 1hr each, and 2 washes in xylene for 1hr each. Finally, samples were embedded in paraffin wax for 4hrs, wax changed every 1hr. 5μm sections were cut and mounted on polysine slides (Thermo Scientific, UK). Sections were dewaxed and dehydrated through graded alcohol solutions, immersed in Harris haematoxylin, followed by 1% eosin, before being cleared and mounted in DePeX (VWR, Lutterworth, UK). A minimum of 4 metatarsals per group (control and GH treated) were measured at x10 magnification to calculate the widths of the proliferating and hypertrophic chondrocyte zones as a percentage of the total length of unmineralised tissue (Nikon eclipse TE300 microscope with digital camera

attached, using Image Tool (Image Tool version 3.00)). Proliferative and hypertrophic zones were defined from cell morphology. Multiple sections were measured, and an average percentage hypertrophic zone and proliferating zone calculated.

3.4.3 qPCR analysis

At defined time points following GH treatment RNA was extracted from metatarsals as described in section 2.5.1. cDNA was prepared as outlined in section 2.5.2, and qPCR analysis completed as detailed in section 2.5.3. Results were normalised to *Gapdh* housekeeping gene and the relative gene expression levels were calculated relative to untreated samples.

3.4.4 Conditioned medium ELISAs

Conditioned medium was collected from metatarsal cultures following 5, 7, and 12 days GH treatment and stored at -80°C. IGF-1 and IGFBP3 levels in were assessed by ELISA (Quantikine, R&D Systems, Minneapolis, MN, USA) according to manufacturer's instructions. IGF-2 levels in conditioned medium were assessed at day 7 and 12 (Ray Biotech, Inc) according to the manufacturer's instructions.

3.4.5 Dynamic and static histomorphometry

Six and 17 week old male WT and *Socs2*$^{-/-}$ mice received an injection of 10mg/kg calcein solution as described in section 2.4.4. Tibiae, fixed overnight in 4% paraformaldehyde (PFA) were embedded in methylmethacrylate, stained and sectioned as described in sections 2.4.9 & 2.4.10.

Calcein is taken up by newly mineralised bone and can therefore be used to determine longitudinal bone growth rate. This is calculated as the distance between the chondro-osseous junction and calcein labelling front using a Leica DMBR fluorescent microscope. Measurements are then divided by the number of days between injection and sacrifice (2 days) to give a bone formation rate per day. The

proximal growth rate of the tibia was measured in 4 WT and *Socs2*$^{-/-}$ tibia. Multiple sections were measured, and an average bone formation rate calculated. Bone formation rate was not calculated in 17 week old mice as the distance between chondro-osseous junction and calcein labelling was so small it was unmeasurable.

Using the Leica DMBR, growth plate width of the proximal tibia was measured in 5, 6 week old WT and *Socs2*$^{-/-}$ mice. At 17 weeks of age, 5 WT and 3 *Socs2*$^{-/-}$ growth plates were measured. Again, multiple sections were measured, and an average growth plate width calculated.

3.4.6 Micro-dissection and quantification of *Igf1* levels in the growth plate

Micro-dissection and quantification of *Igf1* levels in the growth plate was completed by Seema Jasim, an MSc student (University of Edinburgh) completing a project within the laboratory. Tibiae were dissected from 7 week old male WT (n=4) and *Socs2*$^{-/-}$ mice (n=3). Bones were briefly immersed in 4% aqueous (wt./vol.) polyvinylalcohol (PVA; Grade GO4/140, Wacker Chemicals, Walton-on-Thames, UK), chilled by precipitate immersion in n-hexane (BDH, Poole, UK; grade low in aromatic hydrocarbons) and stored at -80^{0}C. Using optimal cutting temperature (OCT) embedding medium (Brights, Huntingdon, UK), 30µm thick longitudinal sections of the proximal tibia were cut at -30^{o}C (Brights, OT model cryostat), mounted on Superfrost Plus slides (Fischer Scientific, Chicago, IL) before storage at -80°C. Slides were briefly thawed as described previously (Nilsson *et al.* 2007; Staines *et al.* 2012), and then dehydrated in graded solutions of ethanol (70%, 95% and 100%) with sections kept under a xylene droplet throughout the microdissection. The entire growth plate was dissected free from the perichondrium, the secondary ossification zone and the primary spongiosa. Growth plates from both tibae of each mouse were pooled in 2.88µl β-mercaptoethanol and 400µl Solution C (0.322g guanidine thiocyanate, 377µl nuclease free water, 23µl 0.75M sodium citrate). From each animal approximately 40-60µg of growth plate tissue was obtained and RNA isolation was performed using proteinase K digestion

followed by phenol:chloroform extraction as previously described (Heinrichs *et al.* 1994). Reverse transcription of RNA and quantification of *Igf1* levels was carried out as described in sections 2.5.2 & 2.5.3, respectively.

3.4.7 Statistical analysis

Statistical analysis was completed on software described in section 2.7. For metatarsal growth, experimental data were analysed using a repeated measures 2 way ANOVA for which suitable post-tests for multiple comparisons were conducted. All other results within the chapter were analysed using the Student's t-test or a suitable non-parametric test if the data were not normally distributed. Data were checked to be normally distributed using a Shapiro-Wilk normality test.

3.5 Results

3.5.1 SOCS2 regulation of GH induced growth in embryonic metatarsals

It has previously been shown that in the absence of SOCS2, embryonic metatarsals respond to GH with increased growth. This highlights an important role for SOCS2 in the regulation of GH action on endochondral bone growth (Pass *et al.* 2012). To confirm the importance of GH induced SOCS2 in the regulation of longitudinal growth, WT and *Socs2*$^{-/-}$ metatarsals were cultured in the presence of GH (Fig. 3.1). GH treatment failed to stimulate WT metatarsal growth (Fig. 3.1A). This was likely due to the regulatory effects of increased SOCS2 levels, as transcript analysis at day 7 revealed an increase in *Socs2*, but not *Socs1* and *3* expression in GH treated metatarsals (17–fold, $p<0.01$) (Fig. 3.1B). *Socs2*$^{-/-}$ metatarsals showed significantly increased growth in response to GH from day 7 ($p<0.05$), and had grown 23%, ($p<0.001$) and 25% ($p<0.001$) more than untreated bones by days 9 and 12 respectively (Fig. 3.1C). Untreated metatarsals from WT and *Socs2*$^{-/-}$ animals displayed similar growth rates (Fig. 3.1D). This indicates that GH stimulation is required to up regulate *Socs2* expression, which subsequently inhibits growth.

Treatment with IGF-1, stimulated growth of WT and *Socs2*$^{-/-}$ metatarsals (Fig. 3.1A&C). In accordance with previous studies, the level of stimulation in the presence of IGF-1 was comparable. This suggests that SOCS2 does not regulate IGF-1 induced growth in this model (Pass *et al.* 2012).

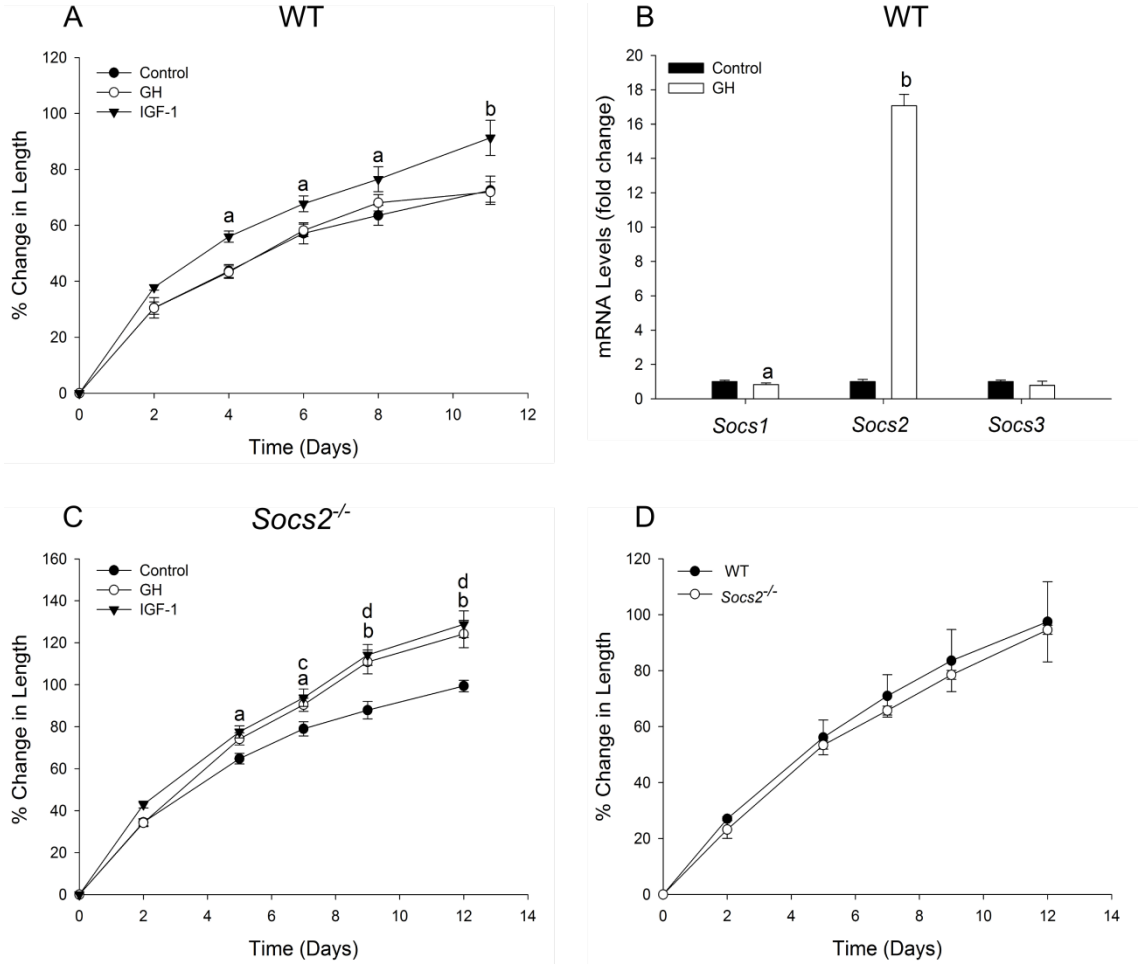

Figure 3.1 SOCS2 regulation of GH induced longitudinal growth of embryonic metatarsals

A. WT and **C.** *Socs2*$^{-/-}$ E17 metatarsal growth in response to GH or IGF-1 (both 100ng/ml) treatment for up to 12 days. Data are presented as mean ± SEM (n≥6). Significance from untreated (control) metatarsals denoted by IGF-1 from control ^{a} $p<0.05$, ^{b} $p<0.001$; GH from control ^{c} $p<0.05$, ^{d} $p<0.001$. **B**. *Socs1, 2,* and *3* mRNA expression levels in WT E17 metatarsals following 7 days GH (100ng/ml) treatment. Data presented as mean ± SEM (n=3 groups of 3-4 pooled bones) relative to untreated (control) samples. Significance from untreated (control) samples denoted by ^{a} $p<0.05$, ^{b} $p<0.01$. **D.** Growth of WT and *Socs2*$^{-/-}$ metatarsals over a 12 day period. Data are presented as mean ± SEM.

3.5.2 GH action on zones of the embryonic metatarsal growth plate

Embryonic metatarsals comprise of cells in the proliferative (PZ), hypertrophic (HZ) and mineralising stage of chondrocyte differentiation (Mushtaq *et al.* 2004). The HZ and PZ were measured in WT and *Socs2*$^{-/-}$ metatarsals cultured in the presence of GH, in order to determine the site of GH action. Following 12 days culture, the PZ of WT metatarsals constituted 63% of the total un-mineralised tissue. The HZ made up the remaining 37%. GH treatment did not significantly alter this ratio (Fig. 3.2). In *Socs2*$^{-/-}$ metatarsals, following 12 days GH treatment the PZ size decreased as a percentage of the total un-mineralised tissue (control – 74%, GH – 64%; $p<0.05$). There was an associated increase in HZ (control - 25%, GH – 36%; $p<0.05$) (Fig. 3.2). These data show that in the absence of a growth response to GH (as observed with WT metatarsals) the composition of the growth plate remains unchanged. When linear bone growth is stimulated in *Socs2*$^{-/-}$ metatarsals challenged with GH, the width of the HZ increased. This suggests that GH promotes linear growth by eliciting its effects on the hypertrophic chondrocytes.

3.5.3 Experimental setup for mRNA and conditioned medium analysis of embryonic metatarsals in response to GH

To determine whether GH action on *Socs2*$^{-/-}$ metatarsals was a result of increased IGF-1 levels, transcript and conditioned medium was analysed from WT and *Socs2*$^{-/-}$ bones following GH treatment. GH induced linear growth was initially observed in *Socs2*$^{-/-}$ metatarsals following 5 days GH treatment ($p<0.05$) and by day 7, GH stimulation had resulted in 15% increase in growth ($p<0.01$). A similar stimulation of linear growth was not observed in WT metatarsals (Fig. 3.3). Following 12 days GH treatment, *Socs2*$^{-/-}$ metatarsal growth had increased by 23% ($p<0.01$) while WT metatarsals continued to show no stimulation (Fig. 3.3).

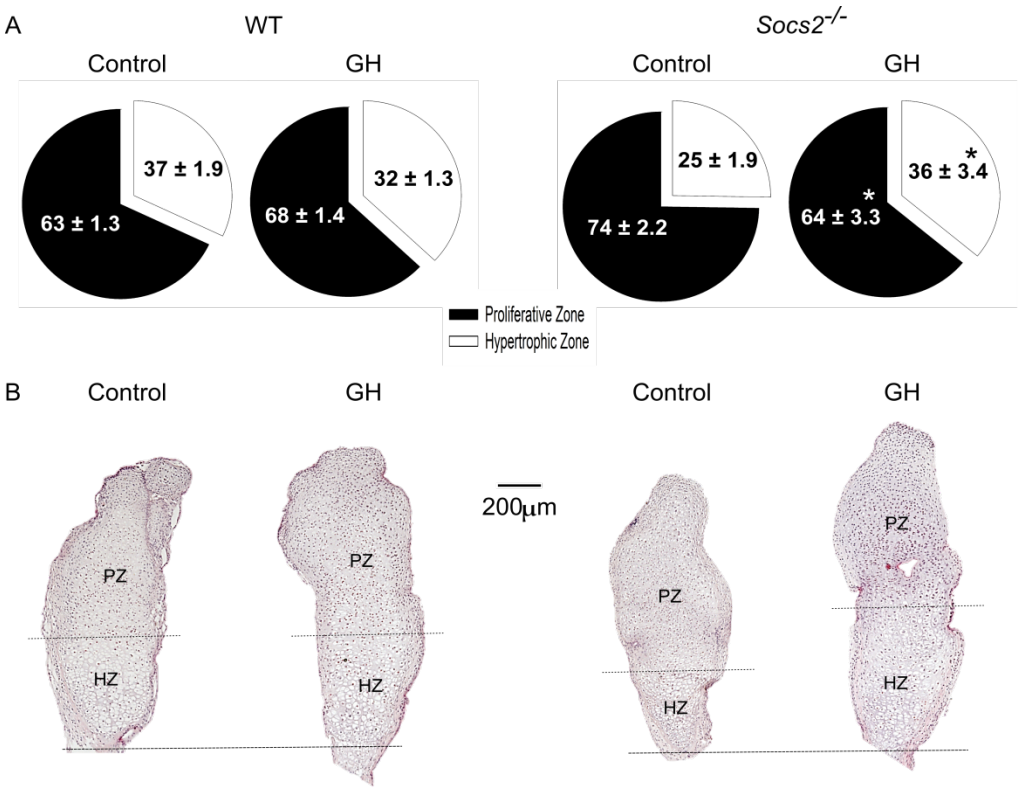

Figure 3.2 SOCS2 regulation of GH induced alternation in proliferative and hypertrophic zone proportions of embryonic metatarsals

A. The percentage of un-mineralised tissue containing cells in the proliferative zone or hypertrophic zone following 12 days GH (100ng/ml) treatment in WT and *Socs2*$^{-/-}$ E17 metatarsals. Data are presented as mean ± SEM (n≥5). Significance from untreated (control) metatarsals denoted by $^{*}p<0.05$. **B**. Representative H&E sections from WT and *Socs2*$^{-/-}$ E17 metatarsals treated with GH (100ng/ml) for 12 days. Intersecting dotted lines define proliferative and hypertrophic zones. Scale bar represents 200µm.

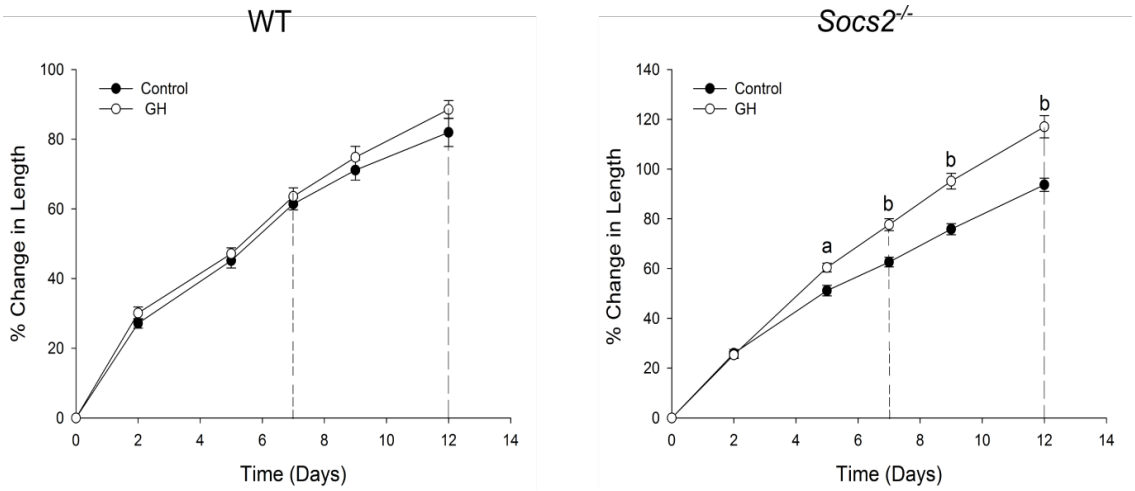

Figure 3.3 Experimental setup for mRNA analysis of embryonic metatarsals in response to GH

WT and *Socs2*$^{-/-}$ E17 metatarsal growth in response to GH (100ng/ml) over a 12 day period. Dotted lines represent points at which *Igf1* (section 3.5.4), *Igfbp3* (section 3.5.6) and *Igf2* (section 3.5.8) mRNA expression levels were measured. Data are presented as mean ± SEM (n≥6). Significance from untreated (control) metatarsals denoted by ^{a} $p<0.05$, ^{b} $p<0.01$.

3.5.4 The effects of GH treatment on IGF-1 production by embryonic metatarsals

Expression levels of *Igf1* did not increase in WT and *Socs2*$^{-/-}$ metatarsals following both 7 and 12 days GH treatment (Fig. 3.4).

Conditioned medium was collected from WT and *Socs2*$^{-/-}$ metatarsal cultures following 5, 7, and 12 days GH treatment. At all-time points protein analysis revealed no increase in IGF-1 levels in WT or *Socs2*$^{-/-}$ metatarsal medium following GH treatment (Table 3.1). These data reveal that the increased longitudinal growth in response to GH which is observed in the *Socs2*$^{-/-}$ metatarsal model is not mediated by increased IGF-1 levels.

3.5.5 *Igf1* mRNA levels in the *Socs2*$^{-/-}$ growth plate

Detailed analysis of 6 week old *Socs2*$^{-/-}$ mice revealed a trend towards increased tibia growth plate width, but this did not reach significance (Fig. 3.5A & Table 3.2). The linear growth rate at the chondro-osseous junction was increased in *Socs2*$^{-/-}$ mice at this age (21%; $p<0.05$) (Fig. 3.5B & Table 3.2). At 17 weeks of age, the growth plate width had significantly decreased in size in WT and *Socs2*$^{-/-}$ mice, with no significant differences being observed between genotypes (Fig. 3.5A & Table 3.2). At this age, the linear growth rate was negligible in WT and *Socs2*$^{-/-}$ mice, and was therefore not measured (Fig. 3.5B). Despite the increase in longitudinal growth rate reported at 6 weeks, *Socs2*$^{-/-}$ mice showed no elevation in *Igf1* transcript levels in the growth plate compared to WT mice at 7 weeks (Fig. 3.5C).

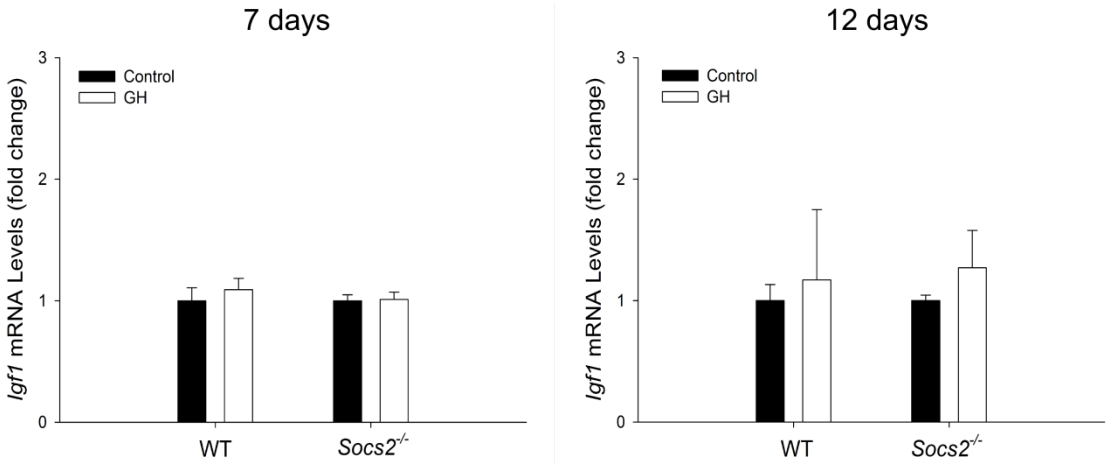

Figure 3.4 No alteration in *Igf1* mRNA expression levels in *Socs2*$^{-/-}$ embryonic metatarsals following GH treatment

Igf1 mRNA expression level in WT and *Socs2*$^{-/-}$ E17 metatarsals following 7 or 12 days GH (100ng/ml) treatment. Data are presented as mean ± SEM (n=3 groups of 3-4 pooled bones) relative to untreated (control) samples.

Table 3.1 No alteration in IGF-1 protein levels in embryonic metatarsal cultures following GH treatment

IGF-1 protein levels in conditioned medium from E17 WT and *Socs2*$^{-/-}$ metatarsals following 5, 7, or 12 days GH (100ng/ml) treatment.

Day	Treatment	WT (ng/ml)	*Socs2*$^{-/-}$(ng/ml)
5	Control	2.4 ± 0.48	2.7 ± 0.59
	GH	2.1 ± 0.23 (0.595)	2.6 ± 0.26(0.857)
7	Control	6.4 ± 0.86	3.3 ± 0.39
	GH	4.0 ± 0.70 (0.066)	2.8 ± 0.28 (0.292)
12	Control	11.6 ± 1.16	9.9 ± 0.90
	GH	9.5 ± 1.06 (0.205)	7.0 ± 0.39 (0.084

Data are presented as mean ± SEM (n≥5). Significance from untreated (control) samples denoted asP-values in brackets.

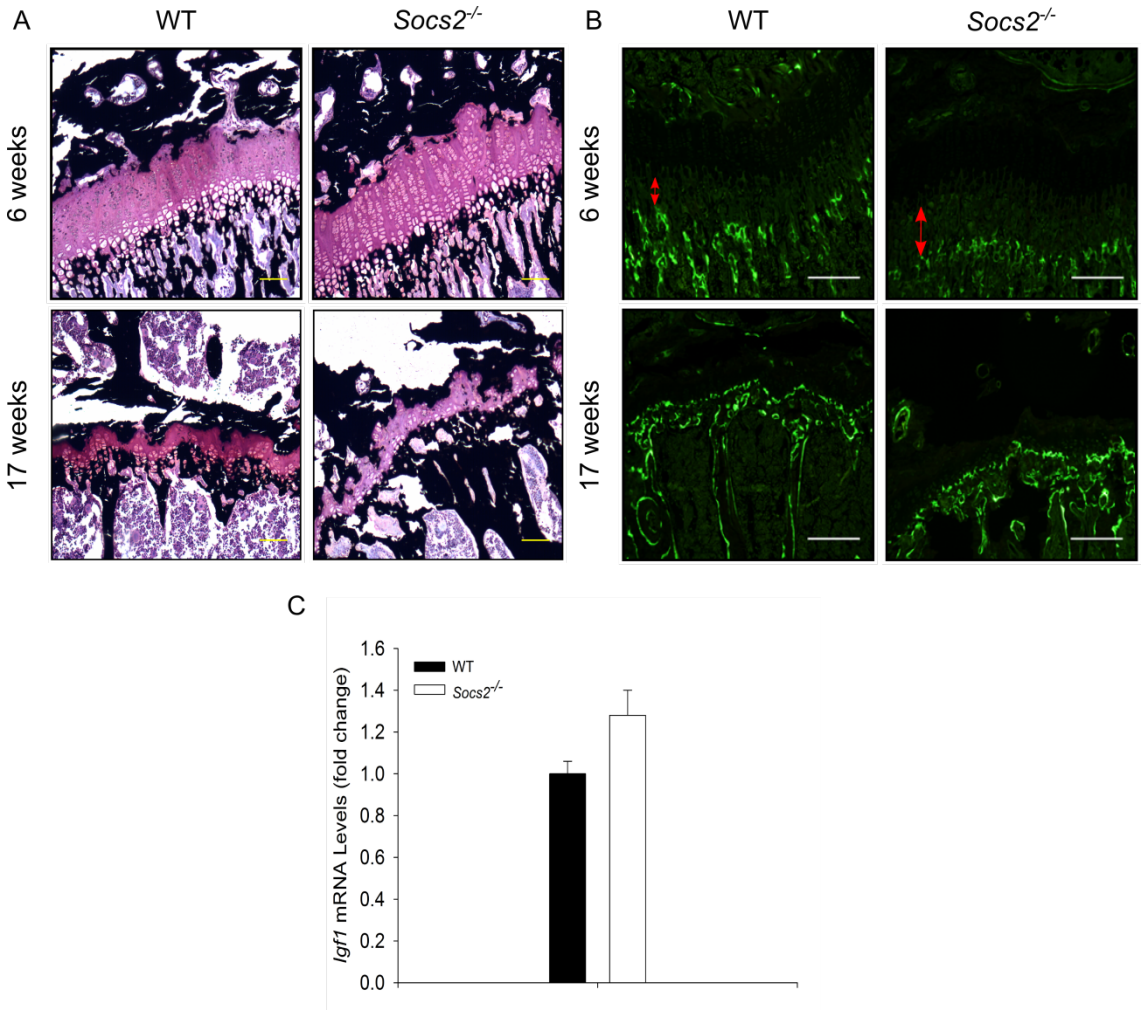

Figure 3.5 *Igf1* mRNA expression in growth plate from *Socs2*$^{-/-}$ mice is comparable to WT

A. Representative images of Von Kossa and paragon stained growth plate of proximal tibia of 6 and 17 week old male WT and *Socs2*$^{-/-}$ mice. Scale bar = 50 μm **B**. Calcein labelling highlighting linear bone growth rate of proximal tibia from 6 and 17 week old male WT and *Socs2*$^{-/-}$ mice. Linear growth rate measured from calcein label to chondro-osseous junction (red arrows). Scale bars = 100μm **C.** *Igf1* mRNA expression levels in growth plates micro-dissected from proximal tibia of 7 week old WT and *Socs2*$^{-/-}$ mice. Data are presented as mean ± SEM (n≥6) relative to WT growth plate samples.

Table 3.2 Increased linear bone growth rate in 6 week old male *Socs2*$^{-/-}$ mice

Quantification of static and dynamic histomorphometry of the proximal tibia growth plates of 6 and 17 week old male WT and *Socs2*$^{-/-}$ mice.

Age	Genotype	Growth Plate Width (μm)	Linear Bone Growth Rate (μm/day)
6 weeks	WT	183.4 ± 10.61	36.8 ± 1.57
	Socs2$^{-/-}$	203.2 ± 3.93	44.5 ± 1.80[a]
17 weeks	WT	57.4 ± 2.26	nd
	Socs2$^{-/-}$	61.3 ± 6.5	nd

Data are presented as mean ± SEM (n≥4). Significance from age matched WT growth plates denoted by [a] $p<0.05$. nd = no data.

3.5.6 The effects of GH treatment on IGFBP3 production by embryonic metatarsals

GH is also a major regulator of IGFBP3 levels (Clemmons 1998). Following 7 days GH treatment, expression levels of *Igfbp3* were unaltered in WT and *Socs2*$^{-/-}$ metatarsals (Fig. 3.6). At day 12, WT metatarsals continued to show no increase in *Igfbp3* expression in response to GH. Conversely, at this point *Igfbp3* expression increased 3.5 fold ($p<0.05$) in *Socs2*$^{-/-}$ samples (Fig. 3.6). Protein analysis of conditioned medium from WT metatarsals revealed no increase in IGFBP3 levels in response to GH at day 5 and 7 (Table 3.3). At day 12, IGFBP3 levels increased 59% ($p<0.05$) (Table 3.3). IGFBP3 levels in conditioned medium from *Socs2*$^{-/-}$ metatarsals were more responsive to GH. Increased IGFBP3 level were noted at day 5 (186%; $p<0.01$), 7 (334%; $p<0.01$), and 12 (123%; $p<0.001$) (Table 3.3). The transcript and protein analysis carried out here highlights an important role for SOCS2 in the regulation of GH induced IGFBP3 levels.

3.5.7 The effects of GH treatment on *Socs2*$^{-/-}$ embryonic metatarsals in the presence of an IGF-1R inhibitor

To further investigate the possibility of an IGF-1 independent effect of GH on longitudinal growth, *Socs2*$^{-/-}$ metatarsals were cultured in the presence of GH and an IGF-1R inhibitor. To ensure a functional inhibitor was used in this study, two well-known IGF-1R inhibitors were first tested on osteoblasts to ensure inhibition of IGF-1R signalling (Garcia-Echeverria *et al.* 2004; Girnita *et al.* 2004). At concentrations of 0.5 and 5 μM picropodophyllin (PPP), an insulin-like, cell-permeable cis-cyclolignan compound, failed to inhibit IGF-1 induced autophosphorylation of the IGF-1R and downstream AKT activation (Fig. 3.7A). NVP-AEW541 (NVP), a selective IGF-1R kinase, inhibited IGF-1 induced autophosphorylation of the IGF-1R, and subsequently blocked downstream AKT activation at concentrations of 0.5 and 5μM (Fig. 3.7A). NVP was therefore used in future experiments.

Preliminary studies were carried out on WT metatarsals to determine a concentration of NVP that would inhibit IGF-1 activity, without being toxic. Metatarsals were cultured in the presence of 1, 2, 3, or 4μM NVP for 5 days. All treatment groups showed significantly less growth than the non-treated group (Fig. 3.7B). It was observed that concentrations of 3 and 4μM NVP almost completely inhibited longitudinal growth, with a proportion of the metatarsals decreasing in length between day 2 and 5. In the presence of lower concentrations of NVP (1 and 2μM), metatarsals continued to display a modest increase in length over 5 days (Fig. 3.7B). On day 5, the inhibitor was removed and metatarsal growth was tracked for a further 4 days. Metatarsals treated with 3 and 4 μM NVP showed no signs of recovery following its removal, yet those treated with 2 μM NVP continued to grow at a similar pace to when inhibited. Metatarsals treated with 1μM NVP showed inhibited growth until day 7, and then showed enhanced growth (Fig. 3.7B). This indicated that at the higher concentrations NVP (3 and 4μM) were possibly toxic to the bones whereas at 1μM the growth inhibitory effects were reversible after the inhibitor was removed. Aside from highlighting an appropriate concentration of inhibitor to use for future studies, these data also showed the importance of IGF-1R signalling in the growth of metatarsals.

As observed in WT, *Socs2*$^{-/-}$ metatarsals treated with NVP (1μM) showed significantly decreased growth compared to untreated metatarsals (Fig. 3.7C). GH treatment stimulated growth of metatarsals from day 5 ($p<0.05$). In the presence of the IGF-1R inhibitor GH was unable to stimulate growth (Fig. 3.7C). This suggests that the effects of GH on longitudinal bone growth are mediated through the IGF-1R.

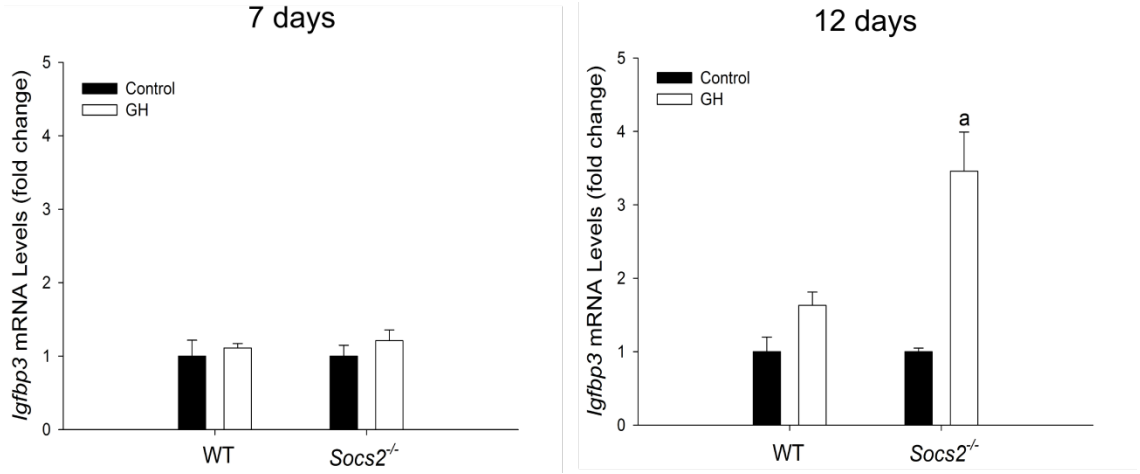

Figure 3.6 Increased *Igfbp3* mRNA expression levels in *Socs2*$^{-/-}$ embryonic metatarsals following GH treatment

Igfbp3 mRNA expression levels in WT and *Socs2*$^{-/-}$ E17 metatarsals following 7 or 12 days GH (100ng/ml) treatment. Data are presented as mean ± SEM (n=3 groups of 3-4 bones) relative to untreated (control) samples. Significance from untreated (control) samples denoted by [a] $p<0.05$.

Table 3.3 Enhanced IGFBP3 protein levels in *Socs2*$^{-/-}$ embryonic metatarsal cultures following GH treatment

IGFBP3 protein levels in conditioned medium from E17 WT and *Socs2*$^{-/-}$ metatarsals following 5, 7, or 12 days GH (100ng/ml) treatment.

Day	Treatment	WT (ng/ml)	*Socs2*$^{-/-}$ (ng/ml)
5	Control	9.0 ± 1.43	8.2 ± 1.35
	GH	9.7 ± 1.41 (0.727)	23.5 ± 5.76(0.002)
7	Control	12.2 ± 1.68	5.2 ± 0.94
	GH	19.7 ± 4.57 (0.155)	22.6 ± 3.34(0.004)
12	Control	25.0 ± 5.09	22.2 ± 3.51
	GH	39.8 ± 3.69(0.050)	49.6 ± 1.89(<0.001)

Data are presented as mean ± SEM (n≥5). Significance from untreated (control) samples denoted by p-values in brackets.

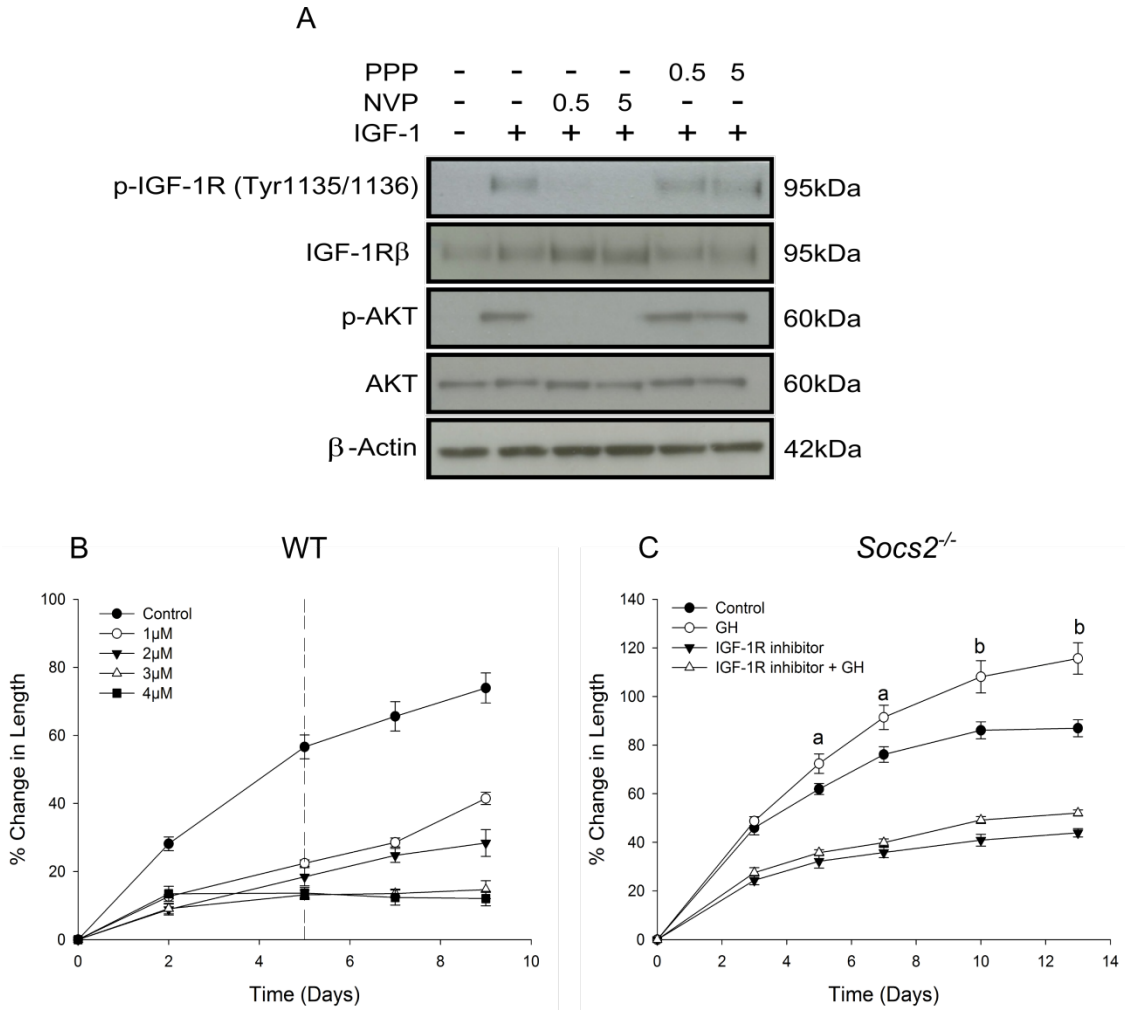

Figure 3.7 Failure of growth stimulation of *Socs2*$^{-/-}$ embryonic metatarsals by GH in the presence of an IGF-1R inhibitor

A. Western blotting of (p-) AKT and (p-) IGF-1R in osteoblasts following 24 hours pre-incubation with 0.5μM or 5 μM, PPP or NVP and 15mins IGF-1(50ng/ml) treatment. β-Actin serves as loading control. **B.** WT metatarsal growth in the presence of varying concentrations of NVP (1 μM - 4 μM) for 5 days (dotted line), followed by untreated medium for a further 4 days. Data are presented as mean ± SEM (n≥3). **C.** *Socs2*$^{-/-}$ metatarsal growth in response to GH (100ng/ml), NVP (1μM) or GH (100ng/ml) + NVP (1μM). Data are presented as mean ± SEM (n≥6). Significance from untreated (control) metatarsals denoted by ^{a} $p<0.05$, ^{b} $p<0.01$,

3.5.8 The effects of GH treatment on IGF-2 production by embryonic metatarsals

The cellular responses of IGF-1 and IGF-2 are mediated through the IGF-1R. As the stimulatory effects of GH are ablated in the presence of an IGF-1R inhibitor (Fig. 3.7), and IGF-1 levels are not increased in GH treated metatarsals (Fig. 3.4 & Table 3.1) IGF-2 was assessed for its responsiveness to GH. No elevation was observed in *Igf2* mRNA levels in WT and *Socs2*$^{-/-}$ metatarsals following 7 days GH treatment (Fig. 3.8A). At day 12, WT metatarsals showed large individual variation in *Igf2* mRNA levels. No increase in *Igf2* expression in response to GH was noted. In *Socs2*$^{-/-}$ metatarsals, *Igf2* expression increased 4.6 fold in response to GH ($p<0.05$) (Fig. 3.8A). Protein analysis of conditioned medium from WT metatarsals at day 12 revealed no increase in IGF2 in response to GH (Table 3.4). Conversely, conditioned medium from GH treated *Socs2*$^{-/-}$ metatarsals had increased IGF-2 levels (Control 1.7ng/ml ± 0.34, GH 17.1ng/ml ± 1.72; $p<0.001$) (Table 3.4).

As GH-induced linear growth in *Socs2*$^{-/-}$ metatarsals was associated with an increase in IGF-2 levels (Table 3.4), metatarsals were treated with exogenous IGF-2 to establish whether it could stimulate longitudinal growth. IGF-2 was added at an equimolar concentration to IGF-1 which has been shown to be a potent stimulator of longitudinal growth (Fig. 3.1). IGF-2 treatment significantly increased growth of *Socs2*$^{-/-}$ metatarsals from day 5 (8.3%; $p<0.05$) to 12 (11.1%; $p<0.01$) (Fig. 3.8B). The enhanced growth by IGF-2 was considerably less than that observed following IGF-1 treatment, which resulted in a 28.4% increase in growth by day 12. This indicates that whilst IGF-1 and IGF-2 can both stimulate linear growth, IGF-1 is the more potent of the two IGF ligands (Fig. 3.8B). Similar results were observed in WT metatarsals treated with IGF-2 for 7 days (Fig. 3.8B).

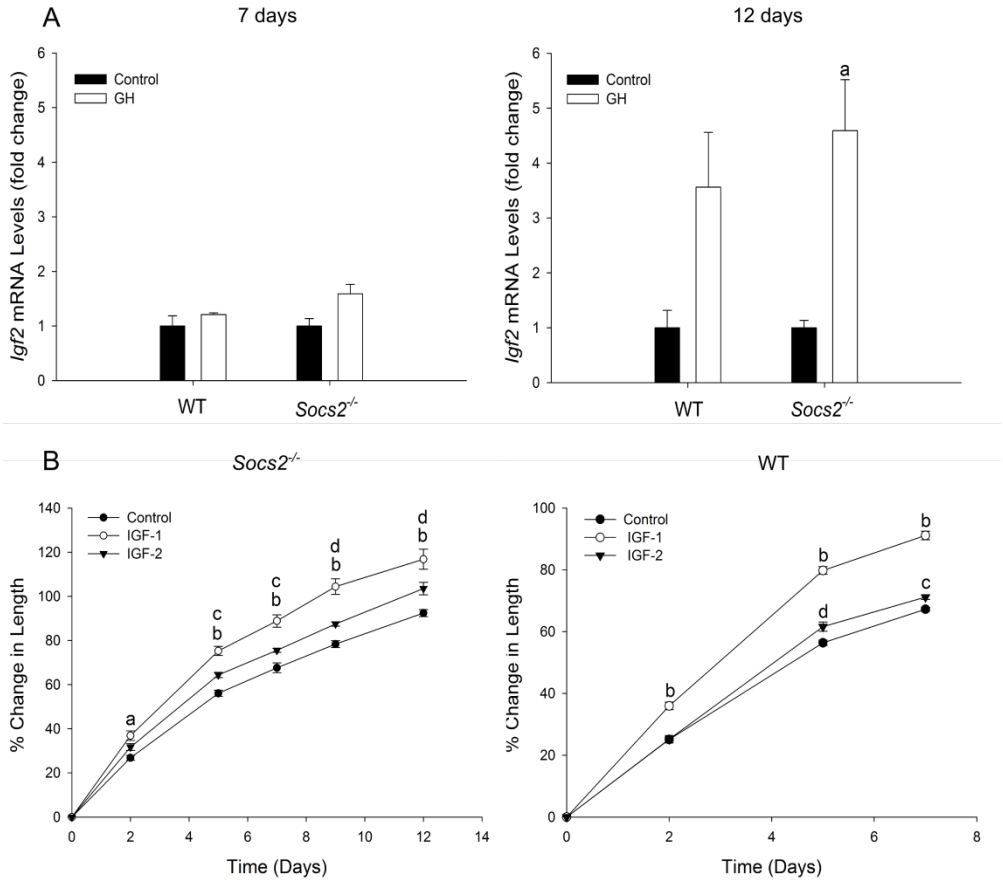

Figure 3.8 Increased *Igf2* mRNA expression levels in *Socs2*$^{-/-}$ embryonic metatarsals following GH treatment

A. *Igf2* mRNA expression levels in WT and *Socs2*$^{-/-}$ E17 metatarsals following 7 or 12 days GH (100ng/ml) treatment. Data are presented as mean ± SEM (n=3 groups of 3-4 pooled bones) relative to untreated (control) samples. Significance from untreated (control) samples denoted by ^{a} $p<0.05$. **B.** *Socs2*$^{-/-}$ and WT metatarsal growth following 12 or 7 days IGF-1 or IGF-2 (both 100ng/ml) treatment. Data are presented as mean ± SEM (n≥6). Significance from untreated (control) metatarsals denoted by IGF-1 from control ^{a} $p<0.01$, ^{b} $p<0.001$; IGF-2 from control ^{c} $p<0.05$, ^{d} $p<0.01$.

Table 3.4 Enhanced IGF-2 protein levels in *Socs2*$^{-/-}$ embryonic metatarsal cultures following GH treatment

IGF-2 protein levels in conditioned medium from E17 WT and *Socs2*$^{-/-}$ metatarsals following 12 days GH (100ng/ml) treatment.

Day	Treatment	WT (ng/ml)	*Socs2*$^{-/-}$ (ng/ml)
12	Control	7.0 ± 1.39	1.7 ± 0.34
	GH	8.4 ± 0.97 (0.426)	17.1 ± 1.72(<0.001)

Data are presented as mean ± SEM (n≥5). Significance from untreated (control) samples denoted by p-value in brackets. .

3.5.9 Growth of postnatal metatarsals

Up to this point, the metatarsal model has used bones extracted from E17 pups. To determine if there were prenatal and postnatal differences of GH action on metatarsals, a postnatal metatarsal model was established. Initially, metatarsals were extracted from WT and *Socs2*$^{-/-}$ animals at 3 and 4 days postnatal (PN3 and PN4), and growth assessed over a 12 day period. Independent of genotype, a correlation between age of animal at extraction and linear growth was observed (Fig. 3.9). By day 12, WT PN3 and PN4 metatarsals had grown 60% and 52%, respectively, which was significantly less than the 126% growth observed in E17 metatarsals. A similar trend was observed in the *Socs2*$^{-/-}$ metatarsals (E17- 97%, PN3-67%, PN4-20%) (Fig. 3.9). The growth of PN4 *Socs2*$^{-/-}$ metatarsals was highly varied, and it was noted that in some cases individual PN4 metatarsals had ceased growing. Future experiments would consequently focus on PN3 metatarsals as a level of continuous growth was observed over the 12 day culture period.

3.5.10 SOCS2 regulation of GH induced growth in postnatal metatarsals

The response of PN3 metatarsals to GH was similar to that observed in embryonic metatarsals (section 3.5.1 & Fig. 3.10). GH treatment failed to stimulate WT metatarsal growth over the 12 day culture period (Fig. 3.10A). Similar to E17 WT metatarsals, the failure of GH to stimulate growth was likely the result of increased SOCS2 levels. Transcript analysis of metatarsals at day 12 revealed a 4.2 fold increase in *Socs2* expression in GH treated metatarsals ($p<0.05$). *Socs1* and *3* expression were unaffected by GH treatment (Fig. 3.10B). *Socs2*$^{-/-}$ metatarsals showed significantly increased growth in response to GH from day 7 ($p<0.01$), and had grown 12%, more than untreated bones by days 9 and 12 ($p<0.001$) (Fig. 3.10C). These results, coupled with results from section 3.5.1 suggest that SOCS2 has a regulatory function on both pre and postnatal endochondral growth.

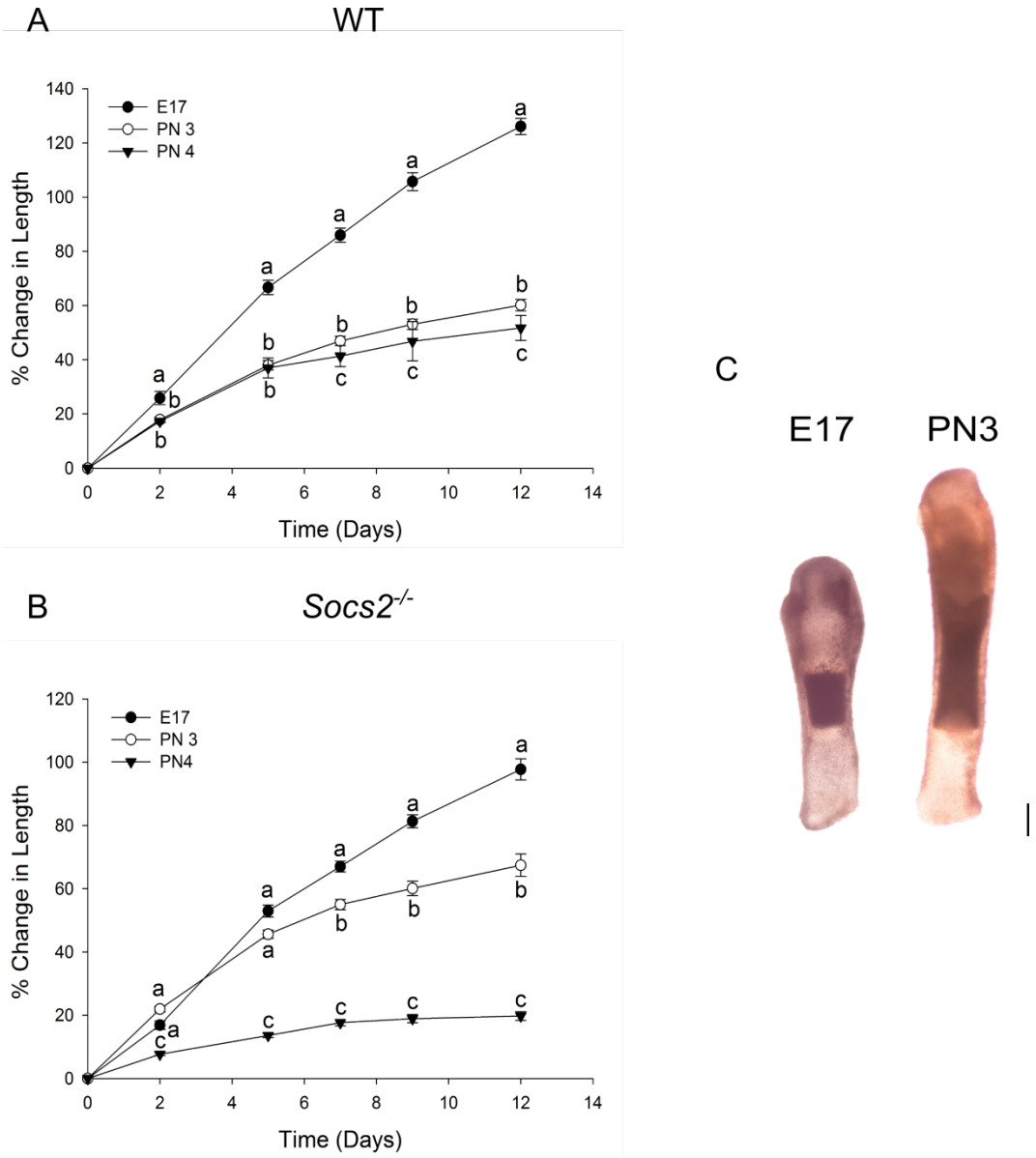

Figure 3.9 Decreased growth rate of postnatal metatarsals

A. WT and **B.** *Socs2*$^{-/-}$ metatarsal (extracted from E17, postnatal day 3 (PN3) or PN4 mice) growth over a 12 day period. Data are presented as mean ± SEM (n=12). Different letters at each timepoint indicate significance ($p<0.05$) from metatarsals extracted at different ages. **C.** Representative images of E17 and PN3 metatarsals day after extraction. Scale bar = 200μm.

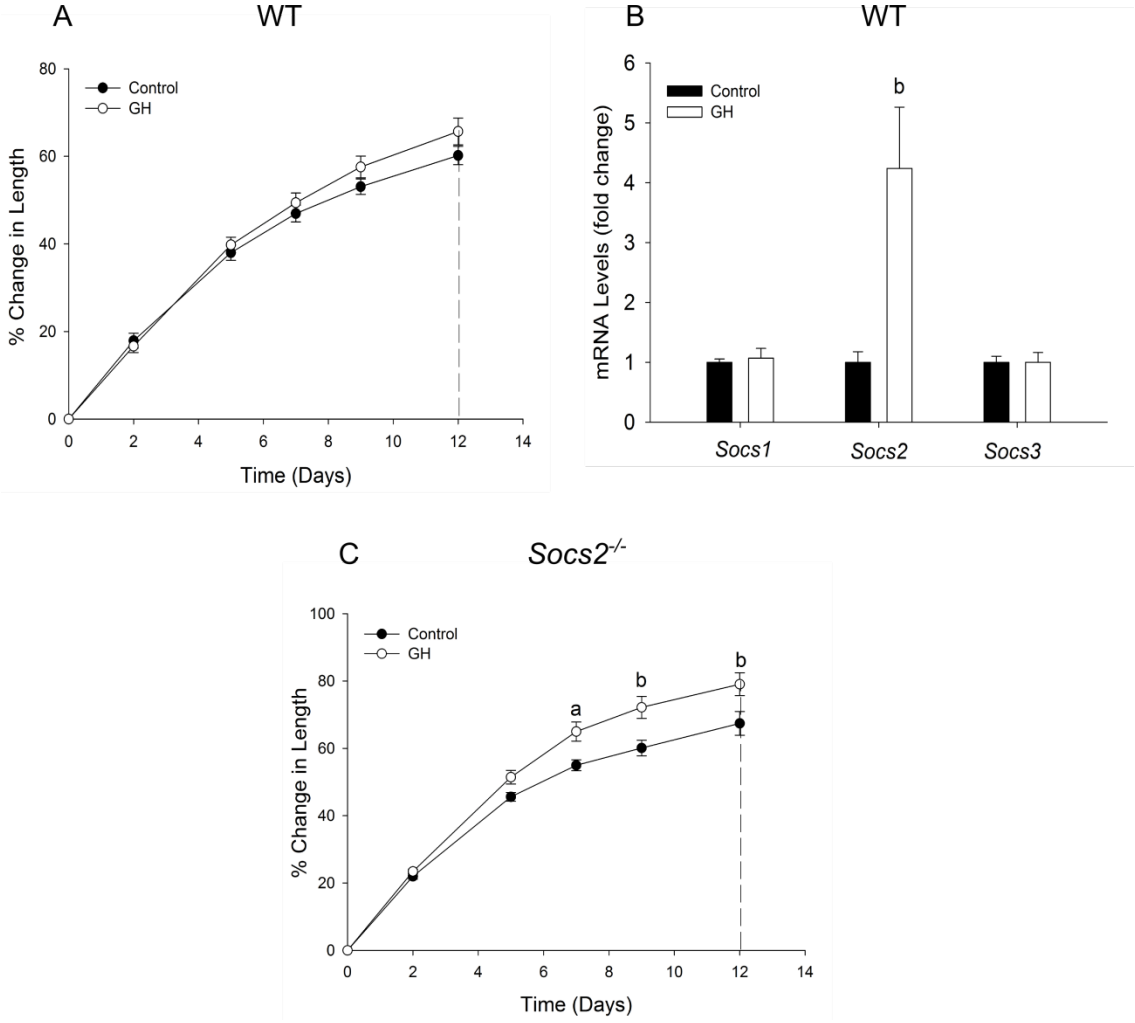

Figure 3.10 SOCS2 regulation of GH induced longitudinal growth of postnatal metatarsals

A. WT and **C.** *Socs2*$^{-/-}$ PN3 metatarsal growth in response to GH (100ng/ml) treatment for 12 days. Data are presented as mean ± SEM (n=12). Significance from untreated (control) metatarsals denoted by ^{a} $p<0.01$, ^{b} $p<0.001$. Dotted lines indicate point at which *Igf1, Igfbp3*, and *Igf2* mRNA expression levels were measured section 3.5.11. **B.** *Socs1, 2,* and *3* mRNA expression levels in WT metatarsals following 12 days GH (100ng/ml) treatment. Data are presented as mean ± SEM (n=3 groups of 3-4 pooled bones) relative to untreated (control) samples. Significance from untreated (control) samples denoted by ^{b} $p<0.01$.

3.5.11 Altered IGF-1, IGF-2 and IGFBP3 production by postnatal metatarsals in response to GH

The effect of GH treatment on *Igf1*, *Igfbp3* and *Igf2* expression in postnatal metatarsals was largely similar to that observed in prenatal metatarsals (sections 3.5.4, 3.5.6 & 3.5.8). Twelve days GH treatment did not stimulate *Igf1* expression in WT or *Socs2*$^{-/-}$ metatarsals (Fig. 3.11A). In WT metatarsals, GH did not stimulate *Igfbp3* or *Igf2* expression. Conversely, in *Socs2*$^{-/-}$ metatarsals, 12 days GH treatment resulted in a 3.4 fold increase in *Igfbp3* mRNA levels ($p<0.05$) and a 4.7 fold increase in *Igf2* mRNA levels ($p<0.01$) (Fig. 3.11B&C).

Conditioned medium collected at day 7 and 12 was used to assess protein levels. At this age there was high individual sample variation. Increased growth of postnatal *Socs2*$^{-/-}$ metatarsals was not associated with an increase in IGF-1 levels (Table 3.5). At day 12, GH treatment enhanced IGF-1 levels (49%) in WT metatarsals, despite no increase in growth (Fig. 3.10 & Table 3.5). No significant increase was observed in GH treated *Socs2*$^{-/-}$ samples (Table 3.5).

IGFBP3 levels were elevated in conditioned medium from GH treated WT metatarsals at both 7 and 12 days (Table 3.5). GH treated *Socs2*$^{-/-}$ metatarsals did not have increased IGFBP3 levels at 7 days, however the increase in protein levels was highly exaggerated at 12 days (WT 172% ($p<0.001$); *Socs2*$^{-/-}$ 262% ($p<0.01$)) (Table 3.5).

At day 7, IGF-2 levels were significantly increased to a similar level in GH treated WT ($p<0.05$) and *Socs2*$^{-/-}$ ($p<0.01$) samples (Table 3.5). At day 12, IGF-2 levels were still elevated in GH treated WT and *Socs2*$^{-/-}$, samples ($p<0.05$) (Table 3.5). The level of increase at day 12 was not majorly different in WT (96%) and *Socs2*$^{-/-}$ (84%) samples.

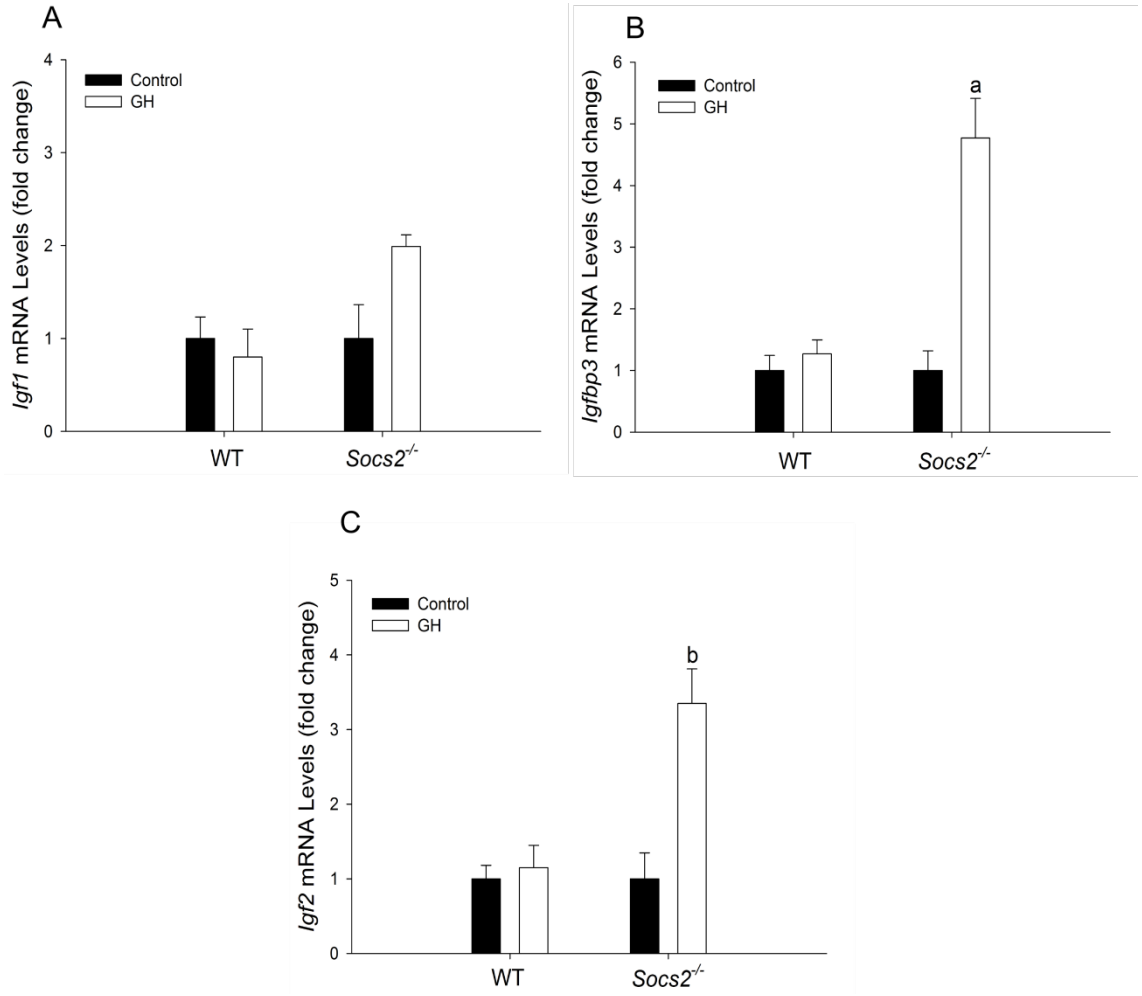

Figure 3.11 Increased *Igfbp3* and *Igf2* mRNA expression levels in *Socs2*$^{-/-}$ postnatal metatarsals in response GH treatment

A. *Igf1* **B.** *Igfbp3* **C.** *Igf2* mRNA expression levels in WT and *Socs2*$^{-/-}$ PN3 metatarsals following 12 days GH (100ng/ml) treatment. Data presented as mean ± SEM (n=3 groups of 3-4 pooled bones) relative to untreated (control) samples. Significance from untreated (control) samples denoted by [a] $p<0.05$, [b] $p<0.01$.

Table 3.5 Altered protein levels in WT and *Socs2*$^{-/-}$ postnatal metatarsal cultures following GH treatment

IGF1, IGFBP3, and IGF2 protein levels in conditioned medium from PN3 WT and *Socs2*$^{-/-}$ metatarsals following 7 and 12 days GH (100ng/ml) treatment.

		WT	*Socs2*$^{-/-}$
Day	**Treatment**	**IGF-1 (ng/ml)**	
7	Control	3.4 ± 0.24	4.6 ± 0.54
	GH	3.5 ± 0.71 (0.937)	4.4 ± 0.67 (0.845)
12	Control	7.3 ± 0.91	10.5 ± 2.08
	GH	10.9 ± 1.20 (0.036)	13.6 ± 1.7 (0.272)
		IGFBP3 (ng/ml)	
7	Control	5.4 ± 2.16	21.1 ± 7.2
	GH	16.5 ± 4.68 (0.047)	40.0 ± 10 (0.173)
12	Control	14.5 ± 4.86	35.9 ± 18.4
	GH	39.4 ± 5.00(0.007)	130.0 ± 28.2(0.019)
		IGF-2 (ng/ml)	
7	Control	3 ± 0.37	3.1 ± 0.87
	GH	10.9 ± 3.17(0.004)	10.7 ± 1.49(0.001)
12	Control	5.6 ± 0.8	7.0 ± 1.66
	GH	11 ± 1.61(0.014)	12.9 ± 1.93(0.047)

Data are presented as mean ± SEM (n≥5). Significance from untreated (control) samples denoted by p-value in brackets.

3.6 Discussion

As hypothesised, in this chapter SOCS2 was identified as a key regulator of GH induced longitudinal bone growth. Only in the absence of SOCS2 was GH able to stimulate longitudinal growth of metatarsals. *Ex vivo* and *in vivo* results presented here are in conflict with the understanding that GHs effects on the growth plate are mediated through the upregulation of IGF-1. The increase in IGF-2 and IGFBP3 gene and protein levels in response to GH offer a possible alternative to the current dogma.

The *ex vivo* metatarsal culture method offers a valid model to investigate endochondral bone growth (Mushtaq *et al.* 2004; MacRae *et al.* 2007; Chagin *et al.* 2010). The ability to grow metatarsals in long term cultures without foetal bovine serum allows for the manipulation of medium conditions and investigation of the effects of various treatments. The present study has focussed on the effects of GH in promoting longitudinal growth of metatarsals. Recently, it has been reported that GH is able to stimulate longitudinal metatarsal growth in the absence of SOCS2 (Pass *et al.* 2012). The effects of GH on *Socs2*$^{-/-}$ metatarsals was therefore investigated to better understand the mechanisms of GH induced longitudinal bone growth.

GH induces expression of several SOCS family members (CIS, SOCS1-3) which regulate GH signalling (Adams *et al.* 1998; Tollet-Egnell *et al.* 1999; Pass *et al.* 2012). In this study GH induced *Socs2* expression (Fig. 3.1B), and it is therefore likely that the lack of growth in response to GH in WT metatarsals was the result of increased SOCS2 levels. Similar results have been observed in primary chondrocyte culture, where GH was shown to stimulate SOCS2 levels (Pass *et al.* 2012). The importance of SOCS2 in regulating GH action has previously been reported. In the absence of endogenous GH, *Socs2*$^{-/-}$ longitudinal bone growth is increased to a greater magnitude than WT, following GH treatment (Greenhalgh *et al.* 2005).

A number of studies have utilised the metatarsal model to investigate the anabolic effects of IGF-1 on linear bone growth. IGF-1 treatment increases metatarsal proliferation, hypertrophic cell size and subsequently growth (Mushtaq *et al.* 2004; MacRae *et al.* 2006a; MacRae *et al.* 2007; Chagin *et al.* 2010). SOCS2 may also have an important role in regulating IGF-1 signalling. GH and IGF-1 stimulation of collagen in intestinal mesenchymal cells is regulated by SOCS2 (Fruchtman *et al.* 2005). Furthermore, SOCS2 is able to bind to the IGF-1R and potentially regulate downstream STAT3 signalling (Dey *et al.* 1998; Zong *et al.* 2000). However, the current observation that WT and *Socs2*$^{-/-}$ metatarsals respond similarly to IGF-1 confirms previous studies, and indicates that SOCS2 does not regulate IGF-1 actions on endochondral bone growth (Fig. 3.1 A&C) (Pass *et al.* 2012). In addition to this, endogenous IGF-1 was detected in the conditioned medium of untreated WT and *Socs2*$^{-/-}$ metatarsals at numerous stages of growth (Table 3.1). As IGF-1 has been demonstrated to enhance linear growth in a number of studies, endogenous levels are presumed to play an important role in growth (Mushtaq *et al.* 2004; MacRae *et al.* 2007; Pass *et al.* 2012). If SOCS2 did regulate IGF-1 signalling, an increase in *Socs2*$^{-/-}$ compared to WT metatarsal growth would be expected due to the lack of IGF-1 suppression. This was however not observed in this study (Fig 3.1D).

The broad distribution of GHR and IGF-1R within the growth plate suggests local GH/IGF-1 may play a role in chondrocyte proliferation, differentiation, and hypertrophy (Lupu *et al.* 2001; Gevers *et al.* 2002a; Parker *et al.* 2007). The germinal zone of the growth plates are significantly enlarged in *Igf1*$^{-/-}$ mice, supporting the idea that GH stimulates longitudinal bone growth directly (by stimulating the differentiation of growth plate precursor cells), and indirectly (by inducing *Igf1* expression in differentiating chondrocytes which then in-turn stimulate clonal expansion) (Isaksson *et al.* 1987; Wang *et al.* 1999a; Wang *et al.* 2004). Current data highlights that GH is able to stimulate linear growth by increasing the size of the HZ (Fig. 3.2). Care must be taken in the interpretation of these results. It appears that the *Socs2*$^{-/-}$ metatarsals have reduced lengthening which is restored to control

(WT) levels by the addition of GH. This however may not be the case, as slightly variations in the time of metatarsal extraction may have large effects on initial metatarsal size. As females are only plug checked once daily it is possible that the starting point of the experiment can vary up to a much as half a day. To fully assess the difference between non-treated WT and *Socs2*$^{-/-}$ metatarsals numerous litters would have to be examined. It must also be noted that fixation solutions such as PFA have been shown to cause shrinkage artefacts due to the high osmolarity of these solutions (Loqman *et al.* 2010). It is generally understood that IGF-1 acts mainly on the HZ, although it is expressed throughout the growth plate (Wang *et al.* 1999a). While the actions of IGF-1 on the HZ are established, there is some dispute over its action on the PZ as proliferation rate and zone size are reported to be normal or decreased in *Igf1*$^{-/-}$ mice (Wang *et al.* 1999a; Lupu *et al.* 2001).

The intimate relationship between GH and IGF-1 makes it difficult to distinguish between direct GH actions, or those resulting indirectly through IGF-1. Tibial growth is reduced in both *Ghr* and *Igf1* null mice. This becomes more severe in the double *Ghr*/*Igf1* mutants, inferring that GH and IGF-1 have independent functions (Lupu *et al.* 2001). In agreement with this, *Ghr*$^{-/-}$ mice show a much greater reduction in longitudinal bone growth compared to *Igf1*$^{-/-}$ (Wang *et al.* 2004). IGF-1 levels however increase in response to GH within the PZ, suggesting a regulatory role for GH on IGF-1 (Nilsson *et al.* 1986). The present study demonstrates that despite normal IGF-1 gene and protein expression levels in *Socs2*$^{-/-}$ E17 metatarsals, GH enhances bone growth (Fig. 3.3, 3.4 & Table 3.1) . This indicates that not only is GH unable to regulate IGF-1 levels, but also that the growth promoting effects of GH are independent of IGF-1. This was supported by the observation of normal *Igf1* expression levels in the growth plates of *Socs2*$^{-/-}$ tibia, which are characterised by wider growth plates and longer bones (MacRae *et al.* 2009; Pass *et al.* 2012); and as demonstrated in this study by increased linear bone growth.

IGF-1 and IGF-2 bind to the IGF-1R, and the cellular responses of both ligands are mediated through this receptor. In this study, inhibition of the IGF-1R abrogated the growth promoting effects of GH (Fig. 3.7). It therefore stands to reason that IGF's are responsible for mediating the increase in linear growth. As there is no increase in the IGF-1 levels in response to GH, it is possible that IGF-2 is responsible for the growth of the *Socs2*$^{-/-}$ metatarsals.

Although care was taken to establish an appropriate dose of IGF-1R inhibitor to use for metatarsals, this experiment would have benefited from more work being carried out on determining the toxicity of the drug. Although metatarsals showed increased growth on the removal of 1μM NVP, this may have been due to catch up growth. It must be noted that without the completion of a viability assay it is not possible to full understand the effect of NVP on growth plate chondrocyte viability.

IGF-1 and IGF-2 are both regulators of skeletal growth. While IGF-1 is important in foetal and postnatal growth, IGF-2 is thought to function only in the former. IGF-2 is expressed highly in a variety of tissues in the embryo and neonatal, but is subsequently down-regulated (Parker *et al.* 2007; Lui *et al.* 2008). Disruption of the *Igf2* gene has negative effects on longitudinal growth (Mohan *et al.* 2003). It is widely accepted that IGF-2 actions are independent of GH regulation. GH has however been shown to regulate *IGF2* transcription in the human liver (von Horn *et al.* 2002). Furthermore, increased growth plate *Igf2* levels in *Igf1*$^{-/-}$ mice are concomitant with increased GH levels. Conversely, decreased growth plate *Igf2* levels are observed in the *Ghr* null mouse. Taken together, this infers that IGF-2 could mediate GH effects on the growth plate (Wang *et al.* 2004).

In the present study, IGF-2 levels increased in response to GH (Fig. 3.8A & Table 3.4). It is possible that the increase in linear growth observed in *Socs2*$^{-/-}$ metatarsals is a result of elevated IGF-2 levels. IGF-2 has previously been shown to stimulate growth of rat metatarsals, and can promote the expansion of foetal hypertrophic

chondrocytes in cultured limb explants, possibly through activation of the PI3K and TGF-ß pathways, and downstream elevation of transcription factors (Hamamura *et al.* 2008; Chen *et al.* 2010). In agreement with this, the present results show that IGF-2 was able to stimulate longitudinal bone growth in metatarsals from WT and *Socs2*$^{-/-}$ mice (Fig. 3.8B. Due to the time constraints of this thesis it was not possible to carry out a comprehensive study assessing the effects of IGF-2 on metatarsal growth, however further work on this would be highly informative.

A significant increase in IGFBP3 levels in response to GH was more apparent in *Socs2*$^{-/-}$ metatarsals, where there was increased growth (Fig 3.6 & Table 3.3) . IGFBP3 is produced in a number of tissues and is regulated mainly by GH, but also to some degree by IGF-1 (Kiepe *et al.* 2005). It is the principal carrier of IGF's in serum, where it functions to control tissue IGF concentrations, and reduces bioavailability (Clemmons 1998). Depending on incubation time and dose, it can inhibit or potentiate the actions of IGF's (Demellow & Baxter 1988; Stewart *et al.* 1993; Bagi *et al.* 1994). IGFBP3 has also been shown to have pro-apoptotic functions on chondrocytes (independent of IGFs), which are likely mediated through their own cell surface bound receptors (Oh *et al.* 1993; Spagnoli *et al.* 2002). The complex relationship between IGF's and IGFBP3 make it difficult to deduce what its role may be in this system. As there appears to be a correlation between increased IGFBP3 and increased growth in response to GH, it is unlikely that the effects of IGFBP3 are inhibitory.

The foetal metatarsal culture method is used as a highly physiological model to study longitudinal growth. This is because the growth rate of embryonic bones in culture is similar to that found *in vivo* (Scheven & Hamilton 1991; Coxam *et al.* 1996; Mushtaq *et al.* 2004; Pass *et al.* 2012). The term highly physiological must however be used with some caution. The metatarsal organ culture method does not take into account the possibility of mechanical stress on these bones which may have an effect on growth. To be defined as a truly physiological model all factors that affect metatarsal growth *in vivo* would have to be determined and addressed.

Given that there are clear differences between prenatal and postnatal regulation of growth, studies were carried out on E17 and PN3 metatarsals. Current results are similar to those previously published, clearly showing that the growth of postnatal metatarsals is less than prenatal metatarsals (Fig. 3.9) (MacRae *et al.* 2006b; Chagin *et al.* 2010). This may be due to a number of factors such as the less differentiated nature of the cells and hence a greater proliferative capacity within the prenatal metatarsals. More differentiated cells are also more likely to require a more sophisticated growth factor cocktail than that which can be supplied by serum free conditions. Also, the greater size of the cultured postnatal bone may limit their growth due to the poor diffusion of nutrients into the cells of the bones. Despite this decrease in growth rate, postnatal bones responded to GH in a similar manner to prenatal bones (Fig. 3.10). This suggests that independent of age, GH induced growth of *Socs2*$^{-/-}$ metatarsals is independent of IGF-1.

In conclusion, using the murine metatarsal model this study underscores the critical role of SOCS2 in controlling the GH anabolic effects on linear bone growth. It also provides compelling evidence to support the notion that GH can regulate linear growth via local mechanisms that are independent of IGF-1 production, while highlighting a potential role for IGF-2 in mediating GH.

Chapter 4

The *Socs2*$^{-/-}$ bone phenotype: actions of local GH signalling

4.1 Introduction

The regulatory role of SOCS2 in linear bone growth is well defined. A number of studies have reported increased long bone length in *Socs2*$^{-/-}$ mice as a result of increased growth plate width (Metcalf *et al.* 2000; MacRae *et al.* 2009; Pass *et al.* 2012). Confirmatory results were presented in chapter 3 of this thesis, where *Socs2*$^{-/-}$ mice showed an increased longitudinal bone formation rate compared to WT mice. This is likely to be a major contributor to the overgrowth phenotype of the *Socs2*$^{-/-}$ mouse. Aside from increased longitudinal growth, *Socs2*$^{-/-}$ mice also have an altered trabecular and cortical bone phenotype. The effects of SOCS2 ablation on bone architecture are however far less conclusive. Two independent studies have assessed the *Socs2*$^{-/-}$ bone phenotype, and have produced largely conflicting results (Lorentzon *et al.* 2005; MacRae *et al.* 2009). MacRae and colleagues reported an anabolic bone phenotype with no changes in BMD, while Lorentzon and colleagues highlight a largely catabolic bone phenotype (Lorentzon *et al.* 2005; MacRae *et al.* 2009). The difference in sex and age of mice analysed may account for the difference in results. There is therefore the need for a comprehensive study to assess the bone phenotype of *Socs2*$^{-/-}$ mice which encompasses different ages and sexes. Furthermore, there is no evidence as to the effects of altered bone architecture on bone strength in this model.

As discussed in chapter 3, the *Socs2*$^{-/-}$ mouse offers a novel model to investigate the local effects of GH on target tissues. The anabolic actions of GH on bone accrual are well established (Andreassen *et al.* 1995; Ohlsson *et al.* 1998). GHR deficiency leads to decreased bone remodelling, bone mass, bone mineral content (BMC), and BMD (Sjogren *et al.* 2000; Sims *et al.* 2000). The delineation of the relative contribution of local versus systemic GH however poses similar problems to that observed with regards to longitudinal bone growth (Le Roith *et al.* 2001). Global deficiency in GH signalling results in a decrease in systemic IGF-1 levels (Zhou *et al.* 1997). An altered bone phenotype in *Igf1*$^{+/-}$ and *Igf1*$^{-/-}$ mice indicates an important function of IGF-1 in regulating bone mass (Bikle *et al.* 2001; Mohan & Baylink 2005; He *et al.* 2006).

The current dogma states that systemic IGF-1 is critical for the maintenance of cortical bone, whereas locally (osteoblast) derived IGF-1 regulates trabecular bone formation. Alteration of systemic IGF-1 levels predominantly alters cortical geometry, with minimal changes to trabecular bone (Sjogren *et al.* 2002; Yakar *et al.* 2002b; Yakar *et al.* 2010; Elis *et al.* 2010). Interestingly, hepatic overexpression of *Igf1* in global *Igf1*$^{-/-}$ mice compensates for the lack of skeletally derived IGF-1 after puberty (Elis *et al.* 2010). Interpretation of some of these observations is complicated by the 4.5 fold increase in systemic GH levels in LID mice (Yakar *et al.* 2002). This increase in GH level may contribute to the bone phenotype of the LID mouse, and mask the effects of low circulating IGF-1 levels in this, and other mouse models (Yakar *et al.* 2002). Studies with the GHR antagonist, pegvisomant, highlight that in states of hepatic IGF-1 insufficiency, GH protects the skeleton against severe inhibition of bone remodelling during growth (Courtland *et al.* 2011).

Local osteoblast disruption of the GH/IGF-1 axis has focused predominantly on the mouse knockout of *Igf1*, or its receptor (Zhang *et al.* 2002; Wang *et al.* 2007; Govoni *et al.* 2007b). These mice present with a catabolic bone phenotype with no reports of decreased circulating IGF-1 levels. Targeted overexpression of *Igf1* to osteoblasts (OC-IGF-1) has anabolic effects on trabecular architecture, but does not alter cortical width (Zhao *et al.* 2000). These studies, although highly informative, fail to advance the understanding of a possible local GH action, independent of IGF-1. It has been shown that GH treatment stimulates periosteal bone formation in *Igf1*$^{-/-}$ mice, suggesting that IGF-1 is not solely essential for mediating GH action on bone (Bikle *et al.* 2001).

Socs2$^{-/-}$ mice have elevated serum markers for bone turnover (Lorentzon *et al.* 2005; MacRae *et al.* 2009). Bone mass and turnover is maintained by the balance between osteoblast bone formation and osteoclast bone resorption. GH stimulates both osteoblasts and osteoclasts. Evidence to date suggests that GH stimulates bone resorption through both direct actions (on osteoclast differentiation) and indirect

action (through activation of mature osteoclasts) via stromal osteoblasts (Mochizuki *et al.* 1992; Nishiyama *et al.* 1996; Guicheux *et al.* 1998). However, given the known anabolic action of GH, and phenotype of the *Socs2*$^{-/-}$ mouse, it is likely that increased GH signalling in osteoblasts is mediating the bone phenotype (Metcalf *et al.* 2000). Previous results have clearly shown that osteoblasts express both the GHR and SOCS2 (Ohlsson *et al.* 1998; MacRae *et al.* 2009). This suggests a potential regulatory role of SOCS2 in GH signalling. The mechanisms however remain undefined.

4.2 Hypothesis

Socs2$^{-/-}$ mice have an anabolic bone phenotype, which results in stronger bones. The bone phenotype is the result of enhanced JAK/STAT signalling in osteoblasts resulting in increased proliferation.

4.3 Aims

I. Complete an in depth analysis of the skeletal phenotype of juvenile and adult, male and female *Socs2*$^{-/-}$ mice.

II. Identify the SOCS proteins involved in regulating GH signalling in osteoblasts.

III. Compare the temporal activation levels of key GH induced signalling proteins in primary osteoblasts from WT and *Socs2*$^{-/-}$ mice.

IV. Confirm the importance of SOCS2 in mediating GH signalling through the generation of a SOCS2 over expressing osteoblast-like cell line.

V. Quantify the relative expression levels of *Igf1* in WT and *Socs2*$^{-/-}$ osteoblasts following GH treatment.

VI. Assess the levels of proliferation in WT and *Socs2*$^{-/-}$ osteoblasts in response to GH.

4.4 Material and Methods

4.4.1 Dynamic histomorphometry

Calcein injections were given as outlined in section 2.4.4. Weight gain was measured as the weight gained per day between calcein injections. Tibiae, fixed overnight in 4% paraformaldehyde (PFA) were embedded in methylmethacrylate as described in section 2.4.9. Sections stained with aniline blue solution (Appendix I) for 20mins, washed in tap water and then cover slips mounted. As calcein binds to newly mineralised tissue it can be used as a marker of bone formation. Endosteal and periosteal MAR were measured as the distance between the two calcein labels using a Leica DMBR fluorescent microscope. Measurements were divided by the number of day between to give a rate per day. MAR was measured in right tibiae from 6 WT and 5 *Socs2*$^{-/-}$ 6 weeks old mice. Multiple sections were measured, and an average MAR calculated. MAR could not be quantified in 17 week old mice due to insufficient double labelling.

4.4.2 Micro-CT analysis and mechanical testing

Micro-CT analysis and 3 point bending was carried out on the tibia 6 and 17 week old male and female WT and *Socs2*$^{-/-}$ mice as described in sections 2.4.7, & 2.4.8, respectively. Prior to scanning tibiae were stored in dH_20 at -20°C. Six tibiae were analysed in each group. Three point bending was carried out on previously scanned tibiae.

4.4.3 Cell culture

Primary osteoblasts were isolated from calvaria extracted from 3-5day old WT and *Socs2*$^{-/-}$ mice as described in section 2.2.3. SOCS2 overexpressing and control MC3T3 cells were generated as described in section 2.2.1. Cells were cultured in 6 well plates in osteoblast medium until 80-90% confluent. Prior to stimulation all cells were serum starved in 0.1% BSA for 24hrs. Cells were treated with GH or IGF-1 (500ng/ml and 50ng/ml, respectively, unless stated otherwise; Bachem, UK) for up to 48hrs. Specific incubation times are outlined in figures, and figure legends.

4.4.4 Western blotting

At defined time points following GH treatment, protein was extracted from primary osteoblasts and MC3T3 cells and western blot analysis carried out on as previously described in sections 2.6. Primary and secondary antibodies are detailed in Appendix II.

4.4.5 Immunocytochemistry

WT and *Socs2*$^{-/-}$ primary osteoblasts, and SOCS2 overexpressing and control MC3T3 cells were plated for immunocytochemistry (sections 2.2.1 & 2.2.3). Following standard culture protocol (above) cells were stimulated with GH for 20mins. Immunocytochemistry analysis was then carried out as described in section 2.6.5.

4.4.6 qPCR analysis

Six week old mice sacrificed for micro-CT analysis also had their liver and right femur removed. Both were snap frozen in liquid nitrogen and stored at -80°C. Before being snap frozen femurs had the epiphyses removed and marrow spun out by centrifugation. RNA was extracted as described in section 2.5.1. At defined time points following GH treatment RNA was also extracted from primary osteoblasts as described in section 2.5.1. cDNA was prepared from all RNA as outlined in section 2.5.2, and qPCR analysis completed as detailed in section 2.5.3. Results were normalised to *Gapdh* housekeeping gene (unless stated otherwise) and the relative gene expression levels were calculate relative to untreated samples.

4.4.7 Conditioned medium ELISAs

Conditioned medium was collected from primary WT and *Socs2*$^{-/-}$ osteoblasts following 48hrs GH treatment and stored at -80°C. IGF-1 and IGFBP3 levels in conditioned medium were analysed by ELISA (Quantikine, R&D Systems, Minneapolis, MN, USA) according to manufacturer's instructions.

4.4.8 Gene expression profiling

A gene expression profiling for JAK/STAT target genes (84 target genes) was performed on WT and *Socs2*$^{-/-}$ osteoblasts using RT^2 profiler PCR arrays (Qiagen, Manchester, UK). In accordance with previous studies, osteoblasts were challenged with GH for 4hrs to detect genes directly stimulated by STAT translocation to the nucleus, and not those downstream of secondary messengers (Greenhalgh *et al.* 2005; Govoni *et al.* 2006). Following manufacturer's protocol, RNA was extracted, and 1 μg RNA was reverse transcribed with the RT^2 profiler PCR array first strand synthesis assay, followed by real-time PCR with RT^2 real-time PCR master mix SYBR green. Each group (WT or *Socs2*$^{-/-}$ osteoblasts ± GH) was assessed in triplicate.

4.4.9 [^{3}H] Thymidine proliferation assay

Cell proliferation was measured in MC3T3 cells, and WT and *Socs2*$^{-/-}$ osteoblasts, following GH or IGF-1 treatment. Cells were incubated with 0.2μCi/ml [^{3}H]-thymidine (Amersham, Buckinghamshire, UK) for the final 12hrs of incubation. Cells were washed in αMEM and fixed in ice-cold 5% trichloroacetic acid for 15mins. Following 2 PBS washes (2x5mins) cells were lysed in 0.1M NaOH for 15mins. Lysed cells were transferred to a scintillation vial and mixed with 3ml scintillation fluid (optiPhase HiSafe 2, Fisons Chemicals, Loughborough, UK). The DNA incorporating [^{3}H]-thymidine was determined using a scintillation counter (Wallac 1410, Pharmacia, Biotech, Uppsala, Sweden).

4.4.10 Statistical analysis

Statistical analysis was completed on software described in section 2.7. For weight, micro-CT, and 3 point bending, experimental data were analysed using a repeated measures 2 way ANOVA for which suitable post-tests for multiple comparisons were conducted. All other results within the chapter were analysed using the Student's t-test or a suitable non-parametric test if the data were not normally distributed. Data were checked to be normally distributed using a Shapiro-Wilk normality test.

4.5 Results

4.5.1 Weight and growth of *Socs2*$^{-/-}$ mice

Before conducting a detailed analysis of the bone phenotype of *Socs2*$^{-/-}$ mice, it was important to confirm the overgrowth phenotype in the SOCS2 colony. Female *Socs2*$^{-/-}$ mice were 18% ($p<0.01$) and 20% ($p<0.01$) heavier than WT mice at 6 and 17 weeks of age, respectively (Fig. 4.1). Despite this increase in body weight, no difference in daily weight gain was observed at either age (6 weeks of age WT: 0.14g/day, *Socs2*$^{-/-}$: 0.21g/day; 17 weeks of age WT: 0.06g/day, *Socs2*$^{-/-}$: 0.02g/day) (Fig. 4.1).

Male *Socs2*$^{-/-}$ mice were significantly heavier than age matched WT mice at 6 (23%; $p<0.001$) and 17 weeks of age (26%; $p<0.001$) (Fig. 4.1). The increased weight of 6 week old *Socs2*$^{-/-}$ mice was associated with an increase in weight gain (Fig. 4.1). Male *Socs2*$^{-/-}$ mice gained 0.6g of weight per day compared to 0.3g per day observed in WT ($p<0.001$) (Fig. 4.1). At 17 weeks of age no difference in weight gain was observed between male *Socs2*$^{-/-}$ and WT mice (WT: 0.02g/day, *Socs2*$^{-/-}$: 0.02g/day) (Fig. 4.1).

4.5.2 Cortical bone growth of male *Socs2*$^{-/-}$ mice

The increase in body weight observed in *Socs2*$^{-/-}$ mice is likely a consequence of enlarged organs including cartilage and bone of the skeleton. To investigate the latter, appositional growth was assessed in male *Socs2*$^{-/-}$ mice at 6 and 17 weeks of age (Fig. 4.2). At 6 weeks, periosteal MAR of the tibia was increased by 42% in *Socs2*$^{-/-}$ mice ($p<0.01$) (Fig. 4.2). Endosteal MAR remained comparable to WT mice (Fig. 4.2). At 17 weeks, double calcein labelling was rarely observed in WT and *Socs2*$^{-/-}$ tibia. It was therefore not possible to quantify periosteal or endosteal MAR at this age.

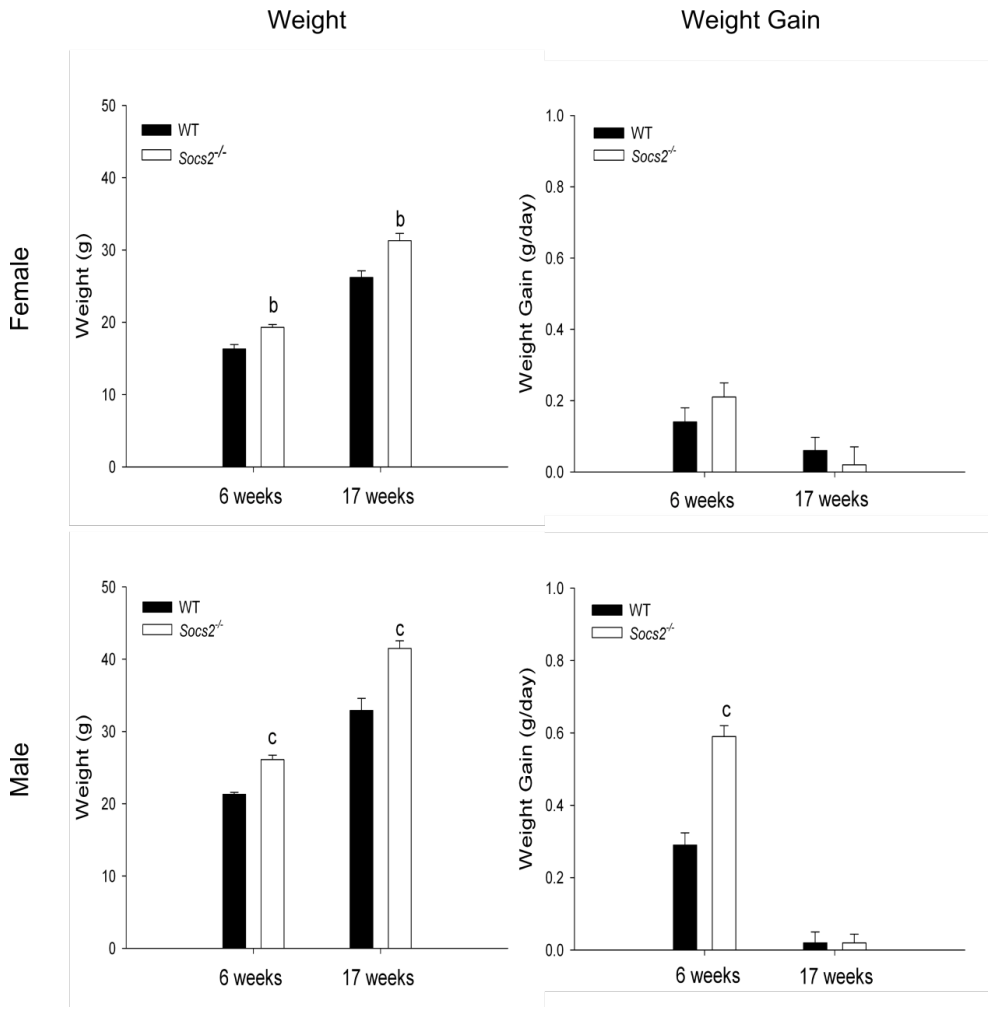

Figure 4.1 Increased weight of *Socs2*$^{-/-}$ mice

Weight and weight gain of male and female, WT and *Socs2*$^{-/-}$ mice at 6 and 17 weeks of age. Data are presented a mean ± SEM (n=6). Significance from age and sex matched WT mice denoted by ^{b} $p<0.01$, ^{c} $p<0.001$.

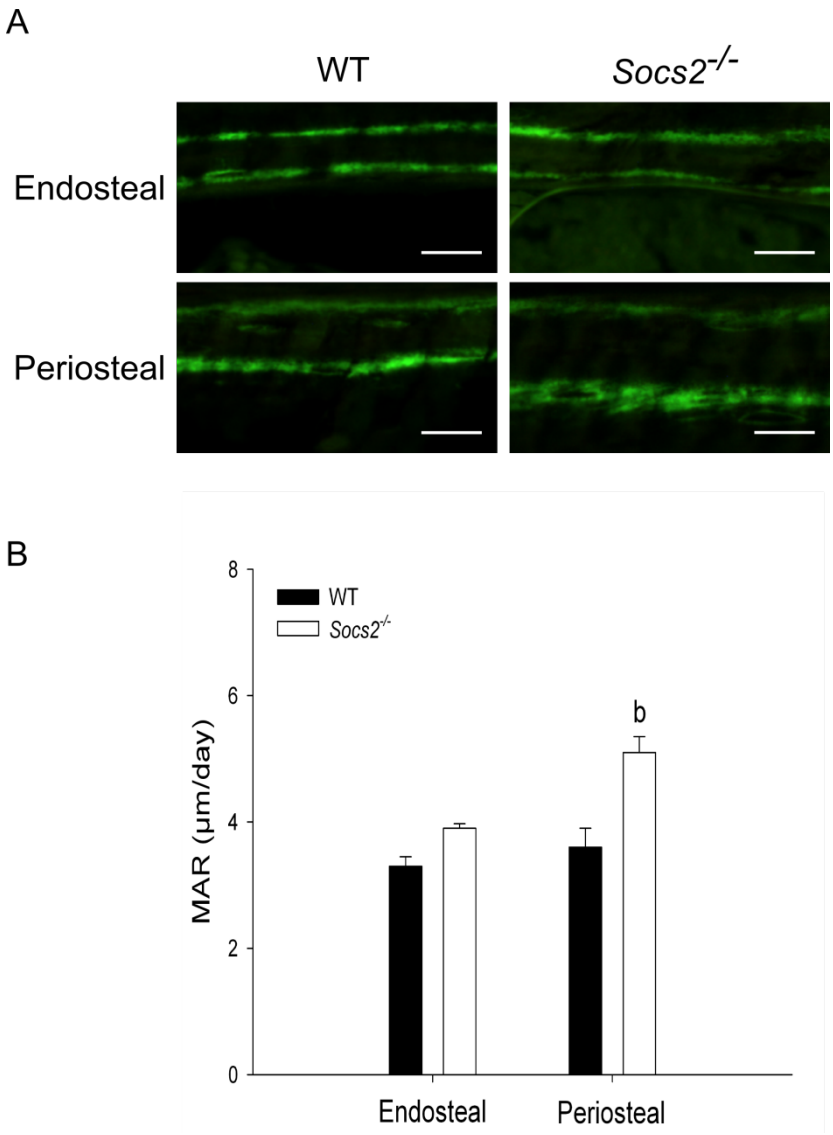

Figure 4.2 Increased periosteal MAR in *Socs2*$^{-/-}$ tibia

A. Representative images of endosteal and periosteal MAR of tibia from 6 week old male WT and *Socs2*$^{-/-}$ mice. Scale bars = 25µm. **B.** MAR of tibia from 6 week old male WT and *Socs2*$^{-/-}$ mice. Data presented as mean ± SEM (n≥5). Significance from WT samples denoted by ^{b} $p<0.01$.

4.5.3 Micro-CT analysis of *Socs2*$^{-/-}$ tibia

High resolution micro-CT analysis of the tibia of male and female, juvenile and adult mice disclosed the full effects of SOCS2 deficiency on trabecular architecture and cortical geometry (Tables 5.1 & 5.2). The trabecular BV/TV of the proximal tibia was increased in all *Socs2*$^{-/-}$ mice (6 weeks: male 34% ($p<0.01$), female 31% ($p<0.01$); 17 weeks: male 32% ($p<0.05$) female 24% ($p<0.05$)). The increased BV/TV was likely due to increased trabecular thickness (Tb.Th); noted in the *Socs2*$^{-/-}$ tibia at 6 weeks (female 15% ($p<0.01$), male 14% ($p<0.01$)) and 17 weeks (female 39% ($p<0.001$), male 12% ($p<0.01$)). Female 6 week old *Socs2*$^{-/-}$ mice also had increased trabecular number (Tb. N) (13%; $p<0.05$). Only female 17 week old *Socs2*$^{-/-}$ mice had increased trabecular separation (Tb.Sp) ($p<0.05$). The structural model index (SMI) and trabecular BMD remained unchanged in the *Socs2*$^{-/-}$ tibia (Tables 5.1 & 5.2).

Analysis of cortical bone revealed a significant increase in total tissue area (Tt.Ar) of male and female, 6 and 17 week old *Socs2*$^{-/-}$ tibia ($p<0.05$) (Tables 5.1 & 5.2). Cortical bone area (Ct.Ar) was also increased by 27% ($p<0.001$) and 28% ($p<0.001$) in tibia from 6 and 17 week old male *Socs2*$^{-/-}$ mice, respectively. These changes were not noted in the equivalent *Socs2*$^{-/-}$ female mice (Tables 5.1 & 5.2). Increases in marrow space were far less marked, with only 6 week old female ($p<0.001$) and 17 week old male ($p<0.001$) *Socs2*$^{-/-}$ tibia showing increased medullary area (Ma.Ar). Analysis of male *Socs2*$^{-/-}$ tibia compared to WT, revealed a significant increase in cortical thickness (Ct.Th) ($p<0.01$). Age defined analysis revealed this increase was limited to 6 week old *Socs2*$^{-/-}$ tibia ($p<0.01$). Cortical thickness was unchanged in female *Socs2*$^{-/-}$ tibia (Tables 5.1 & 5.2). Polar moment of inertia (J) is a measure of the cortex's ability to resist torsion. This was increased in the *Socs2*$^{-/-}$ compared to WT tibia, at 6 weeks (female 37% ($p<0.05$), male 51% ($p<0.05$)), and 17 weeks (female 24% ($p<0.05$), male 82% ($p<0.001$)) (Tables 5.1 & 5.2). At 6 weeks, there was no significant difference in cortical BMD between *Socs2*$^{-/-}$ and WT mice. At 17 weeks however both male ($p<0.05$) and female *Socs2*$^{-/-}$ ($p<0.01$) tibia had a significantly decreased BMD (Tables 5.1 & 5.2).

Table 4.1 Altered bone phenotype of female *Socs2*$^{-/-}$ mice

Micro- CT analysis of 6 and 17 week old female WT and *Socs2*$^{-/-}$ mice tibia.

	6 weeks				17 weeks			
	WT		*Socs2*$^{-/-}$		WT		*Socs2*$^{-/-}$	
Trabecular								
BV/TV (%)	9.7 ± 0.25		12.7 ± 0.88[b]		8.0 ± 0.38		9.9 ± 0.52[a]	
Tb.N (1/mm)	2.4 ± 0.09		2.7 ± 0.13[a]		1.6 ± 0.10		1.4 ± 0.09	
Tb. Th (mm)	0.04 ± 0.001		0.05 ± 0.002[b]		0.05 ± 0.002		0.07 ± 0.001[c]	
Tb.Sp (mm)	0.22 ± 0.01		0.23 ± 0.01		0.28 ± 0.01		0.33 ± 0.03[a]	
SMI	2.0 ± 0.04		2.0 ± 0.05		2.4 ± 0.28		2.3 ± 0.10	
BMD (g/cm^3)	1.48 ± 0.006		1.47 ± 0.01		1.56 ± 0.01		1.57 ± 0.01	
Cortical								
Tt.Ar (mm^2)	0.6 ± 0.02		0.7 ± 0.01[b]		0.7 ± 0.02		0.8 ± 0.04[a]	
Ct.Ar (mm^2)	0.4 ± 0.01		0.5 ± 0.01		0.6 ± 0.004		0.6 ± 0.02	
Ma.Ar (mm^2)	0.19 ± 0.008		0.26 ± 0.008[c]		0.16 ± 0.008		0.12 ± 0.039	
Ct.Th (mm)	0.21 ± 0.005		0.20 ± 0.002		0.26 ± 0.009		0.27 ± 0.007	
J (mm^4)	0.05 ± 0.003		0.07 ± 0.003[a]		0.08 ± 0.007		0.09 ± 0.007[a]	
BMD (g/cm^3)	1.34 ± 0.007		1.32 ± 0.006		1.44 ± 0.005		1.41 ± 0.006[b]	

Data are presented as mean ± SEM (n=6). Trabecular data - BV/TV = bone volume/tissue volume, Tb.N = trabecular number, Tb.Th = trabecular thickness, Tb.Sp = trabecular separation, SMI = structural model index. BMD = bone mineral density. Cortical data - Tt.Ar = total tissue area, Ct.Ar = cortical bone area, Ma.Ar = medullary area, Ct.Th = cortical thickness, J = polar moment of inertia. BMD = bone mineral density. Significance from age matched WT mice is denoted by [a] $p<0.05$, [b] $p<0.01$, [c] $p<0.001$.

Table 4.2 Altered bone phenotype of male *Socs2*$^{-/-}$ mice

Micro- CT analysis of 6 and 17 week old male WT and *Socs2*$^{-/-}$ mice tibia.

	6 weeks				17 weeks			
	WT		*Socs2*$^{-/-}$		WT		*Socs2*$^{-/-}$	
Trabecular								
BV/TV (%)	15.4 ± 0.69		20.6 ± 1.72[b]		14.9 ± 1.9		19.6 ± 1.07[a]	
Tb.N (1/mm)	3.4 ± 0.01		4.0 ± 0.25		3.0 ± 0.41		3.5 ± 0.19	
Tb. Th (mm)	0.04 ± 0.001		0.05 ± 0.002[b]		0.05 ± 0.002		0.06 ± 0.001[b]	
Tb.Sp (mm)	0.17 ± 0.01		0.16 ± 0.01		0.2 ± 0.01		0.18 ± 0.01	
SMI	1.9 ± 0.05		1.7 ± 0.08		1.7 ± 0.18		1.5 ± 0.05	
BMD (g/cm^3)	1.44 ± 0.01		1.46 ± 0.03		1.55 ± 0.006		1.45 ± 0.06	
Cortical								
Tt.Ar (mm^2)	0.8 ± 0.03		1.0 ± 0.03[b]		0.9 ± 0.06		1.3 ± 0.04[c]	
Ct.Ar (mm^2)	0.6 ± 0.01		0.7 ± 0.03[c]		0.7 ± 0.03		0.9 ± 0.02[c]	
Ma.Ar (mm^2)	0.23 ± 0.016		0.25 ± 0.015		0.25 ± 0.029		0.41 ± 0.018[c]	
Ct.Th (mm)	0.25 ± 0.008		0.28 ± 0.011[b]		0.27 ± 0.003		0.28 ± 0.003	
J (mm^4)	0.10 ± 0.003		0.15 ± 0.012[a]		0.13 ± 0.016		0.24 ± 0.014[c]	
BMD (g/cm^3)	1.31 ± 0.016		1.29 ± 0.04		1.42 ± 0.002		1.35 ± 0.008[a]	

Data are presented as mean ± SEM (n=6). Trabecular data - BV/TV = bone volume/tissue volume, Tb.N = trabecular number, Tb.Th = trabecular thickness, Tb.Sp = trabecular separation, SMI = structural model index. BMD = bone mineral density. Cortical data - Tt.Ar = total tissue area, Ct.Ar = cortical bone area, Ma.Ar = medullary area, Ct.Th = cortical thickness, J = polar moment of inertia. BMD = bone mineral density. Significance from age matched WT mice is denoted by [a] $p<0.05$, [b] $p<0.01$, [c] $p<0.001$.

4.5.4 Biomechanical properties of *Socs2*$^{-/-}$ tibia

The alterations in bone phenotype observed in *Socs2*$^{-/-}$ mice are likely to have a biomechanical impact. To assess this, 3- point bending was carried out on the contralateral tibia from mice used for micro-CT. Failure load, work to failure, load to maximum stiffness, and maximum stiffness were unaltered in tibia from female *Socs2*$^{-/-}$ mice at 6 and 17 weeks of age (Fig. 4.3 & Table 4.3).

Tibia from 6 week old male *Socs2*$^{-/-}$ mice showed a 41% increase in work to failure ($p<0.05$), indicating that more energy was required to reach failure point (Fig. 4.3 & Table 4.3). At 17 weeks of age, work to failure (90%, $p<0.05$) was still increased in male *Socs2*$^{-/-}$ mice. In addition, there was also an increase in failure load (32%, $p<0.05$) (Fig. 4.3 & Table 4.3). This highlights that not only increased energy, but also a greater force was necessary to cause the *Socs2*$^{-/-}$ tibia to fail. Load to maximum stiffness and maximum stiffness of tibia from male *Socs2*$^{-/-}$ mice were not altered at either age (Fig. 4.3 & Table 4.3).

4.5.5 Liver *Igf1* expression in *Socs2*$^{-/-}$ mice

The increased body weight (section 4.5.1), tibial MAR (section 4.4.2), and altered bone phenotype (section 4.4.3) observed in 6 week old *Socs2*$^{-/-}$ mice was not associated with an increase in *Igf1* expression in livers from both male and female mice (Fig. 5.4). An increase in *Igfbp3* levels was observed in male *Socs2*$^{-/-}$ compared to sex matched WT livers (Fig. 5.4). A similar increase in *Igfbp3* levels was not observed in female livers (Fig. 5.4). These results indicate that the altered bone phenotype observed in sections 2 & 3 are not via an increase in hepatic IGF-1 levels.

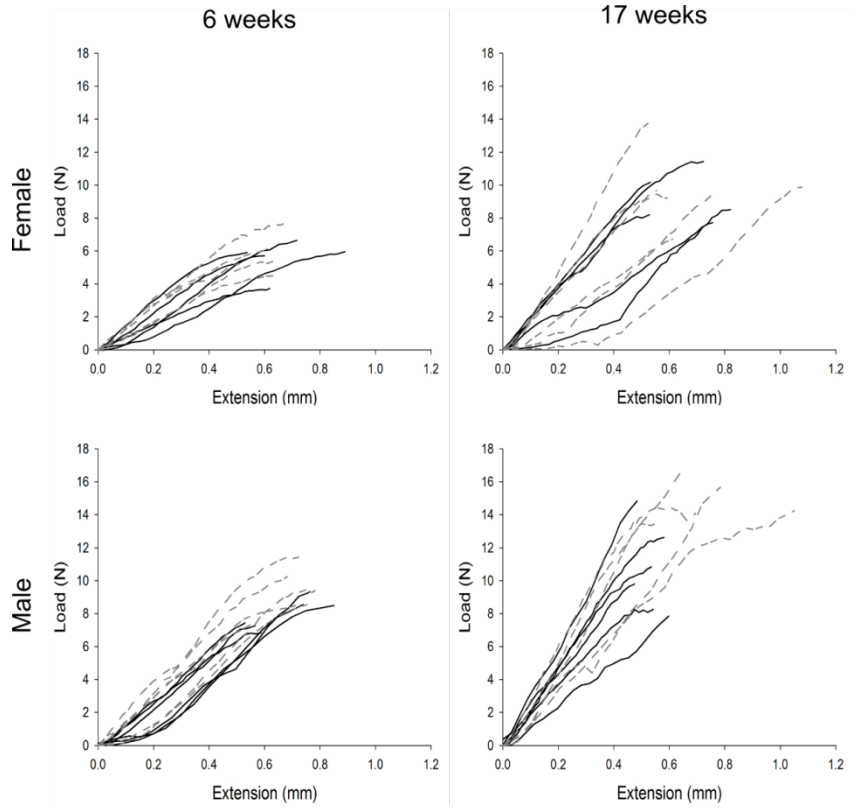

Figure 4.3 Load vs extension curve from 3 point bending of *Socs2*$^{-/-}$ tibia

Load vs. extension curves to point of failure of tibia from 6 week old and 17 week old, male and female WT (black) and *Socs2*$^{-/-}$ (grey broken) mice.

Table 4.3 Increased breaking strength of male *Socs2*$^{-/-}$ tibia

Three point bending analysis of 6 and 17 week old, female and male WT and *Socs2*$^{-/-}$ mice tibia.

	6 weeks				17 weeks			
	WT		*Socs2*$^{-/-}$		WT		*Socs2*$^{-/-}$	
Female								
Failure Load (N)	5.6	± 0.51	5.7	± 0.45	9.3	± 0.54	10.0	± 0.90
Work to Failure (mJ)	2.4	± 0.31	2.0	± 0.22	3.0	± 0.27	3.0	± 0.26
Load to Maximum (N)	2.7	± 0.35	2.1	± 0.27	5.5	± 0.8	5.7	± 0.50
Maximum Stiffness (N/mm)	11.1	± 1.32	12.5	± 0.95	18.2	± 1.47	22.7	± 3.42
Male								
Failure Load (N)	8.0	± 0.39	9.4	± 0.57	11.1	± 2.46	14.6	± 1.59[a]
Work to Failure (mJ)	2.6	± 0.23	3.6	± 0.34[a]	3.3	± 0.71	6.2	± 2.35[a]
Load to Maximum Stiffness (N)	4.4	± 0.33	4.7	± 0.41	6.2	± 1.62	6.8	± 1.21
Maximum Stiffness (N/mm)	18.6	± 1.52	19.6	± 3.18	28.4	± 8.57	30.3	± 10.57

Data are presented as mean ± SEM (n=6). Significance from age matched WT mice is denoted by [a] $p<0.05$.

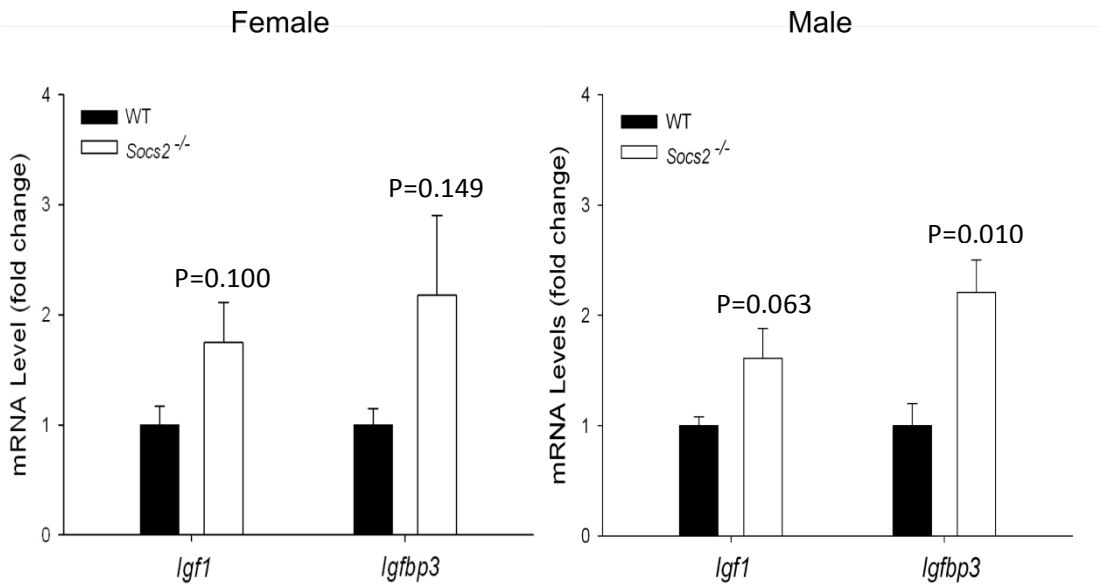

Figure 4.4 No alteration in *Igf1* mRNA expression levels in liver from 6 week old, male and female *Socs2*$^{-/-}$ mice

Analysis of *Igf1* and *Igfbp3* mRNA expression levels in livers extracted from 6 week old female and male WT and *Socs2*$^{-/-}$ mice. Data are presented as mean ± SEM (n≥5) relative to age and sex matched WT liver samples. Significance form age and sex matched WT liver sample denoted byp-values.

4.5.6 SOCS expression in osteoblasts

To address the importance of local GH action in driving the *Socs2*$^{-/-}$ bone phenotype, it first had to be established that the negative feedback loop of SOCS2 regulation existed in osteoblasts. SOCS1, 2, and 3 transcript and protein levels were assessed in WT primary osteoblasts following GH treatment. GH increased *Socs2*, but not *Socs1* and *Socs3* mRNA expression after 24 hours treatment ($p<0.001$) (Fig. 4.5A). This was confirmed and extended by western blot analysis following 24 and 48 hour GH challenge. GH treatment increased SOCS2 levels at both time points studied. SOCS1 and 3 protein levels were not raised at any time point studied (Fig. 4.5B).

Due to the intimate relationship between GH and IGF-1, SOCS levels were also measured following IGF-1 treatment. As expected, IGF-1 had no effect on SOCS1, 2 and 3 transcript or protein levels in WT osteoblasts (Fig. 4.5).

4.5.7 Regulation of GH induced STAT signalling in osteoblasts by SOCS2

Having identified SOCS2 as the predominant GH-regulated SOCS protein in osteoblasts, it was next determined if the absence of SOCS2 increased the phosphorylation status of STAT1, 3, and 5 (p-STAT) in response to GH. In WT osteoblasts, STAT3 was not activated in response to GH, whereas increased p-STAT1 was observed following 15mins of GH exposure, but not at later time points. In contrast, p-STAT5 was increased by GH at all time points studied. It was also noted that phosphorylation of STAT5 decreased with prolonged GH stimulation (Fig. 4.6). When compared to WT osteoblasts, *Socs2*$^{-/-}$ osteoblasts showed increased and prolonged phosphorylation status of STAT1, 3 in response to GH (Fig. 4.6). Activation of STAT1 was extended in *Socs2*$^{-/-}$ osteoblasts, and was observed after 15 and 30mins GH exposure. A similar response was observed with STAT3 activation. The difference in activation patterns was most evident with STAT5. Greatly increased p-STAT5 was observed in response to GH stimulation at all time points studied (Fig. 4.6). This was further confirmed by immunofluorescence of cultured osteoblasts. The stimulation of pSTAT5 by GH (in both the cytoplasm and nucleus)

was much higher in *Socs2*$^{-/-}$ osteoblasts (Fig. 4.7). These data strongly suggest an increase in STAT dependent gene transcription in *Socs2*$^{-/-}$ osteoblasts, and confirms the negative role of SOCS2 on GH-induced STAT signalling.

4.5.8 Regulation of IGF-1 induced STAT signalling in osteoblasts by SOCS2

Previous studies have reported that IGF-1 was able to signal via the STAT3 pathway (Zong *et al.* 2000). Activation of STAT3 by IGF-1 was not observed in WT primary osteoblasts (Fig. 4.8). IGF-1 treatment also failed to activate STAT 5; a potent mediator of GH signalling (section 4.5.7). The failure of IGF-1 to stimulate STAT3 and 5 was also observed in *Socs2*$^{-/-}$ primary osteoblasts (Fig. 4.8).

4.5.9 Regulation of GH or IGF-1 induced AKT and ERK1/2 signalling in osteoblasts by SOCS2

The ERK1/2 and AKT pathways are also responsible for mediating GH and IGF-1 action. In WT osteoblasts, GH stimulated ERK1/2 (p-ERK1/2), but not AKT activation (p-AKT) after 15mins GH exposure. A similar activation pattern was observed in *Socs2*$^{-/-}$ osteoblasts (Fig. 4.9).

IGF-1 treatment stimulated both AKT (p-AKT) and ERK1/2 (p-ERK1/2) activation following 15mins exposure. By 30mins, p-ERK1/2 had returned to basal level, whereas p-AKT levels remained elevated. Again, the activation patterns were similar in *Socs2*$^{-/-}$ osteoblasts (Fig. 4.9). Taken together, these results indicate that SOCS2 does not regulate AKT or ERK1/2 signalling in osteoblasts, in response to GH or IGF-1.

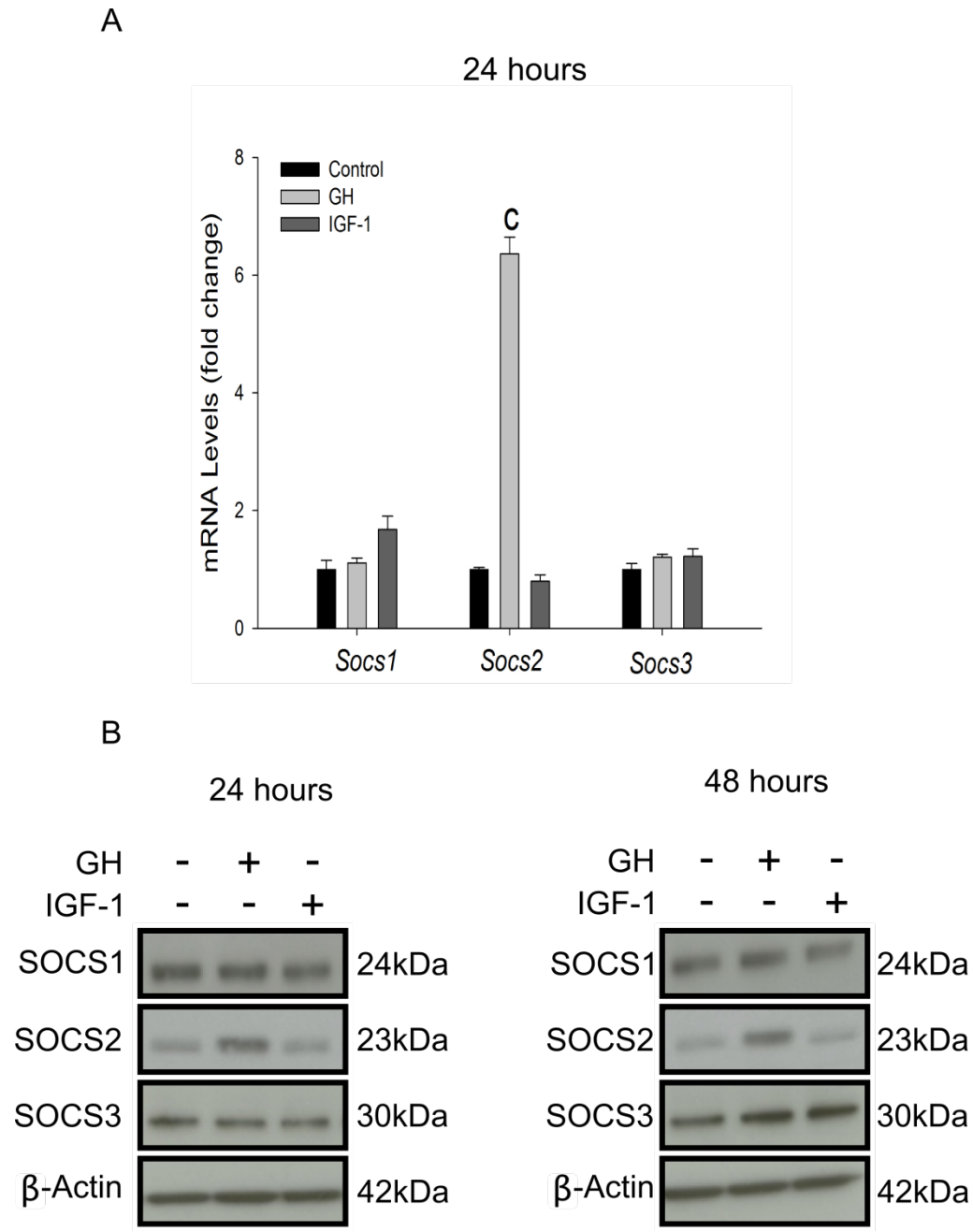

Figure 4.5 Increased SOCS2 levels in WT osteoblasts in response to GH

A. *Socs1, 2,* and *3* mRNA expression levels in WT osteoblasts following 24hours GH (500ng/ml) or IGF-1 (50ng/ml) exposure. Samples were initially normalised to housekeeping gene *atp5b*. Data are presented as mean ± SEM (n=3) relative to untreated samples. Significance from untreated samples denoted by ^{c} $p<0.001$. **B.** Western blotting of SOCS1, 2, and 3 in WT osteoblasts following 24 and 48hours GH (500ng/ml) or IGF-1 (50ng/ml) exposure. β-actin protein shown as loading control.

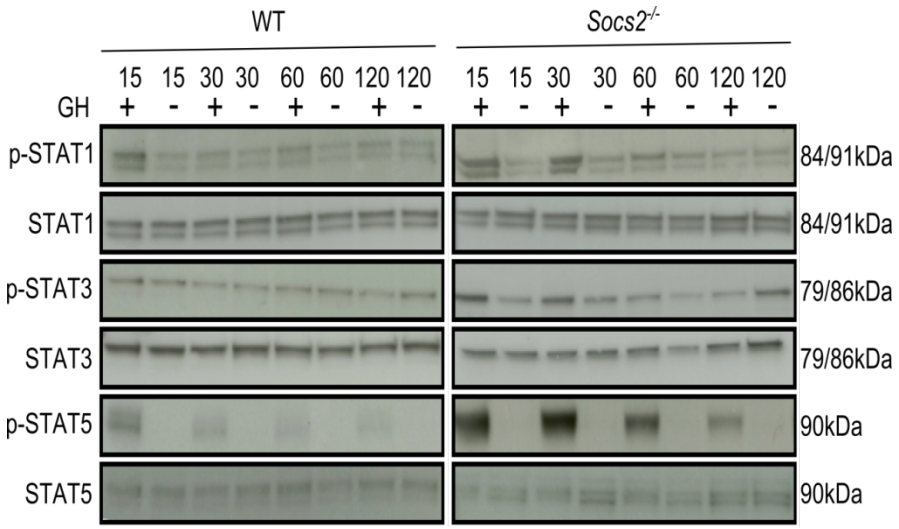

Figure 4.6 SOCS2 regulation of GH induced STAT signalling in osteoblasts

Western blotting of phosphorylated (P-) STAT1, 3, and 5 in WT and *Socs2*$^{-/-}$ osteoblasts following up to 120mins GH (500ng/ml) exposure. Total STAT proteins shown as loading control.

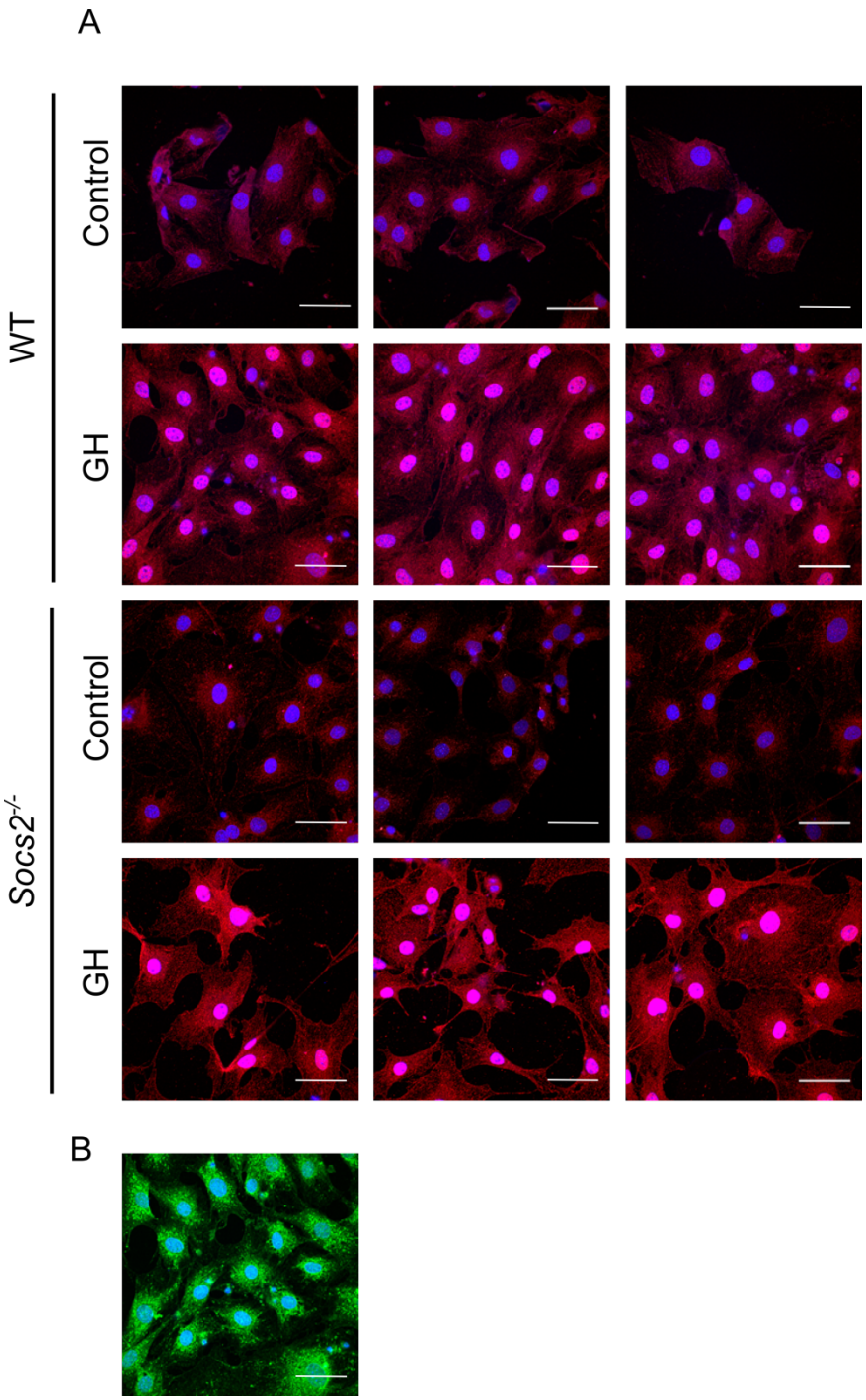

Figure 4.7 SOCS2 regulation of GH induced STAT5 activation and translocation into the nucleus in osteoblasts

A. Representative immunofluorescence detection of p-STAT5 in WT and *Socs2*$^{-/-}$ osteoblasts following 20mins GH (500ng/ml) exposure. Scale bars = 50µm. Nucleus –Blue; pSTAT5 – pink. **B.** Immunofluorescence detection of acetyl tubulin defining cell cytoplasm. Images taken from 3 experimental replicates.

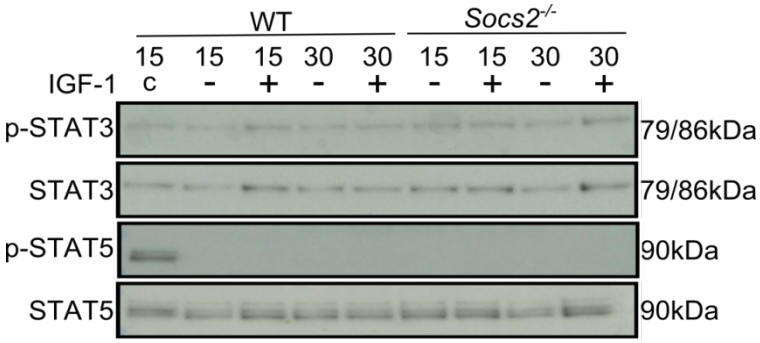

Figure 4.8 SOCS2 does not regulate IGF-1 induced STAT signalling in osteoblasts

Western blotting of phosphorylated (P-) STAT3 and 5 in WT and *Socs2*$^{-/-}$ osteoblasts following up to 30mins IGF-1 (50ng/ml) exposure. Total STAT proteins shown as loading control. C = GH treated WT osteoblasts serve as loading control.

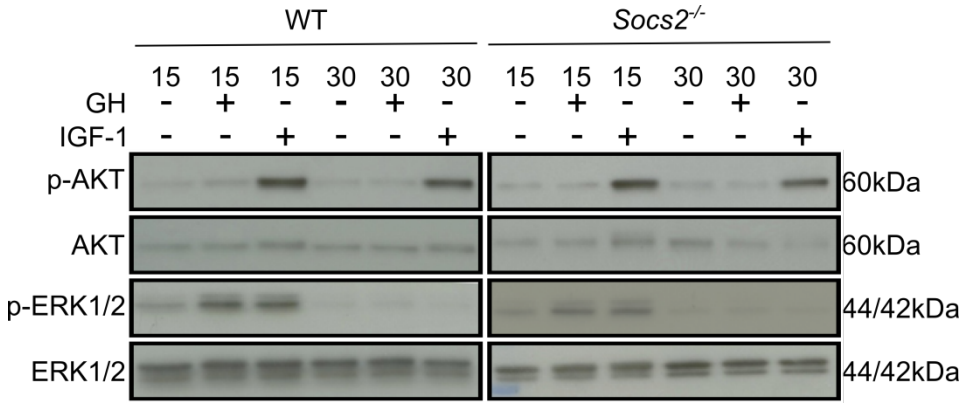

Figure 4.9 SOCS2 does not regulate GH or IGF-1 induced AKT or ERK1/2 signalling in osteoblasts

Western blotting of phosphorylated (P-) AKT and (P-) ERK1/2 in WT and *Socs2*$^{-/-}$ osteoblasts following up to 30mins GH (500ng/ml) or IGF-1 (100ng/ml) exposure. Total AKT and ERK1/2 serve as loading control.

4.5.10 The effects of SOCS2 overexpression in osteoblast like cells on GH induced STAT signalling

To fully appreciate the role of SOCS2 in GH signalling in osteoblasts, MC3T3 osteoblast like cells overexpressing SOCS2 were produced. To confirm SOCS2 overexpression in cells containing the SOCS2 plasmid, 5 overexpressing colonies were selected, and *Socs2* expression levels measured. *Socs2* mRNA varied from a 10 fold increase (SOCS2+ colony 3), to a 103 fold increase (SOCS2 + colony 5) in the overexpressing colonies (Fig. 4.10A). The presence of the overexpressed SOCS2 attached to the FLAG epitope was confirmed in colony 5 by western blot. The overexpression of SOCS2 was not observed in colony 3 at the protein level (Fig. 4.10B).

Cells expressing the control plasmid showed STAT5 activation at all time points studied (15-120mins), although phosphorylation decreased with prolonged GH stimulation. This activation profile was greatly decreased in SOCS2 overexpressing cells with only negligible levels of p-STAT5 observed at 60 and 120mins (Fig. 4.10C). The decreased p-STAT5 in GH treated SOCS2 overexpressing cells was further confirmed by immunofluorescence (Fig. 4.11). The stimulation of p-STAT5 in both the cytoplasm and nucleus by GH was much lower in SOCS2 overexpressing cells.

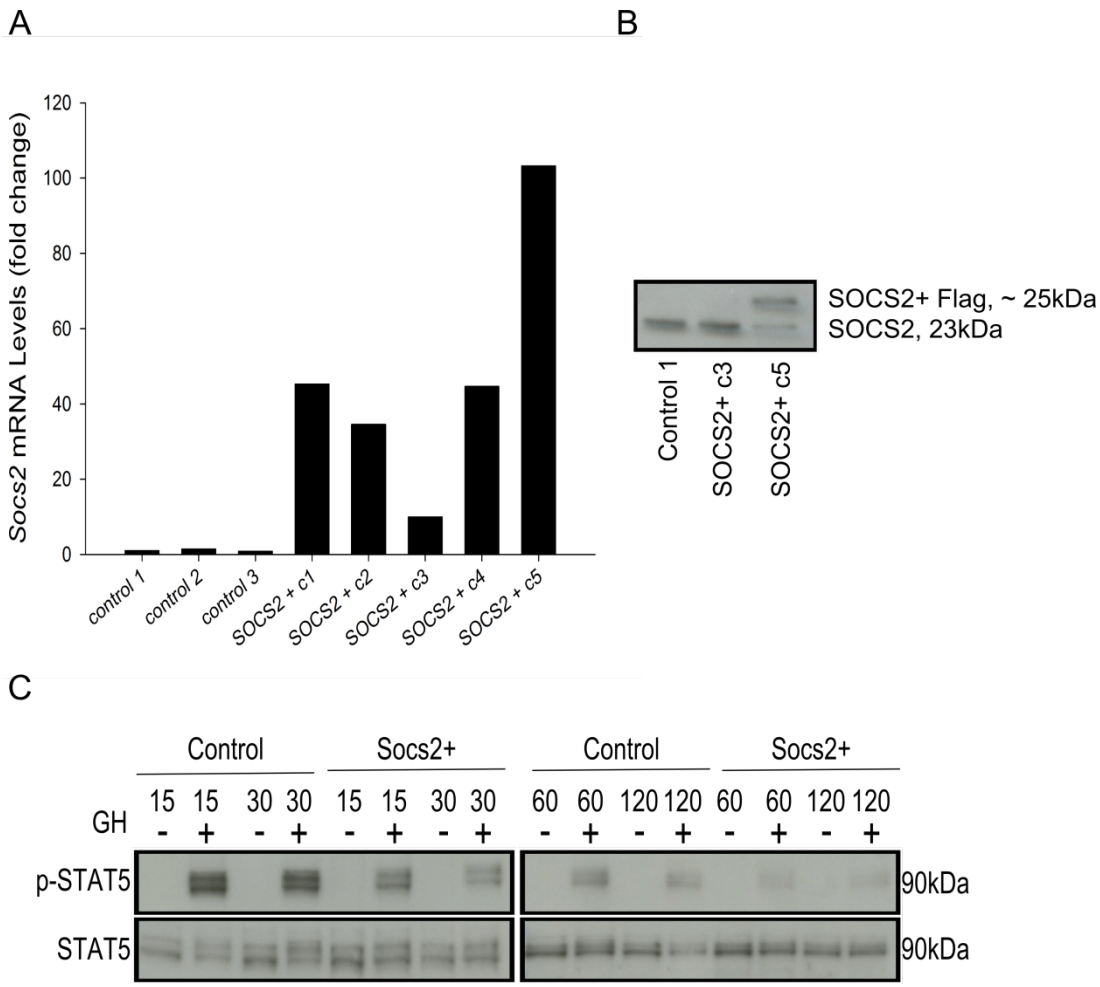

Figure 4.10 Inhibited STAT5 activation in SOCS2 overexpressing osteoblast like cells

A. Analysis of *Socs2* mRNA expression levels in 5 colonies of MC3T3 cells containing SOCS2 overexpression plasmid (SOCS2+) compared to cells containing the control plasmid. **B.** Confirmation of SOCS2 overexpression in colonies 3 and 5 by western blotting. The extra SOCS2 produced in over expressing cells was a higher weight than physiological SOCS2 due to attachment to the FLAG epitope. **C**. Western blotting of phosphorylated (P-) STAT5 in SOCS2 overexpressing osteoblast like cells following up to 120mins GH (500ng/ml) exposure. Total STAT5 protein shown as loading control.

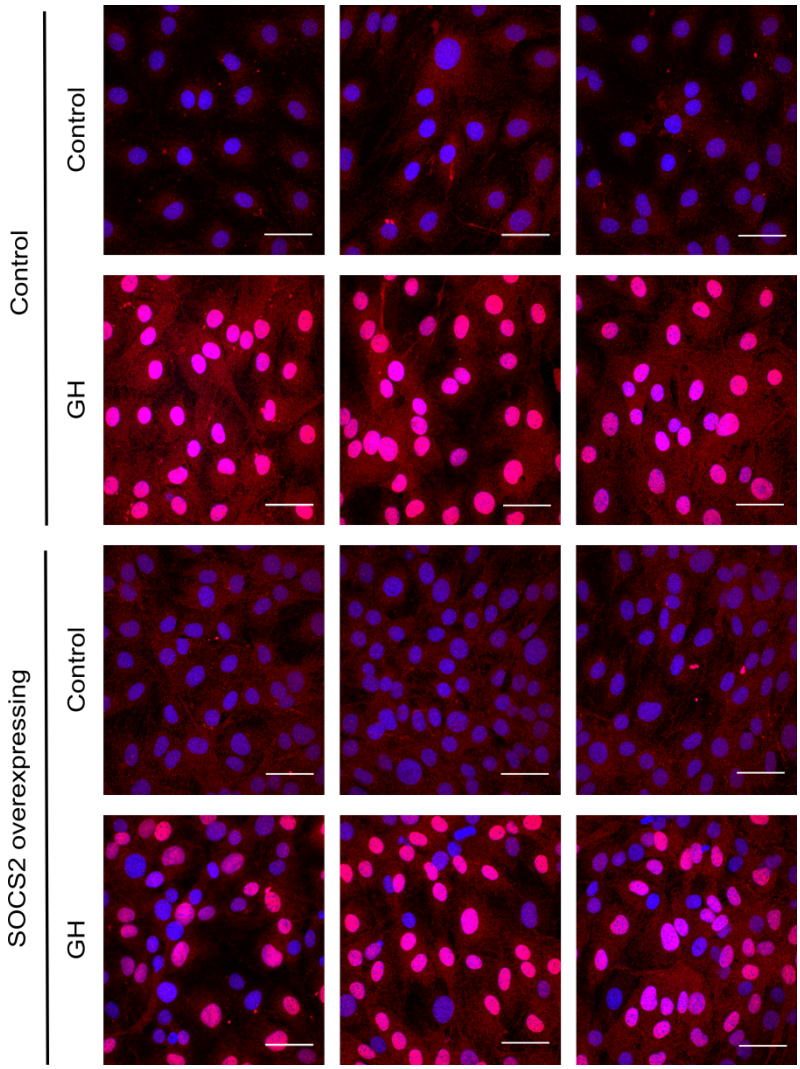

Figure 4.11 SOCS2 regulation of GH induced STAT5 activation and translocation into the nucleus in SOCS2 overexpressing osteoblast like cells

A. Representative immunofluorescence detection of pSTAT5 in SOCS2 overexpressing or control MC3T3s following 20mins GH (500ng/ml) exposure. Scale bars = 50μm. Nucleus – Blue; pSTAT5 – pink. Images are taken from 3 experimental replicates.

4.5.11 Regulation of GH induced gene expression in osteoblasts by SOCS2

Socs2 expression was greatly enhanced in WT osteoblasts following GH treatment ($p<0.001$). Aside from highlighting that GH treatment up regulates gene expression in WT osteoblasts, these results also strengthen previous protein data (section 4.5.6). In WT osteoblasts, GH caused a small but significant increase in *Igf1* (1.32 fold, $p<0.01$) and *Igfbp3* (1.53 fold, $p<0.001$) expression (Fig. 4.12A). In *Socs2*$^{-/-}$ osteoblasts, the increase in both *Igf1* (2.39 fold, $p<0.001$) and *Igf1bp3* (2.83 fold, $p<0.001$) expression was of a slightly greater magnitude (Fig. 4.12A). Protein analysis of IGF-1 and IGFBP3 in the conditioned medium was used to confirm transcript data. In *Socs2*$^{-/-}$ osteoblasts, GH treatment increased IGF-1 and IGFBP3 levels by 1.14 fold ($p<0.001$) and 1.20 fold ($p<0.001$), respectively (Fig. 4.12B). No significant changes were noted in WT osteoblasts.

Analysis of markers of differentiation osteopontin (*Spp1*) and alkaline phosphatase (*Akp2*) revealed no alteration in expression in response to GH, in WT or *Socs2*$^{-/-}$ osteoblasts (Fig. 4.12C). These markers were also assessed in a population of more mature osteoblasts (cultured for 5 days post confluency before GH challenge). GH stimulated an increase in *Socs2* expression in WT osteoblasts (6.7 fold; $p<0.001$), similar to that observed in previous experiments with less mature osteoblasts (Fig. 4.13A). Enhanced *Igf1* expression in response to GH in *Socs2*$^{-/-}$ osteoblasts was also confirmed in the more mature cells. GH treatment did not alter the expression of *Spp1* or *Akp2* in mature WT osteoblasts. Similar results were obtained with regards to *Spp1* in *Socs2*$^{-/-}$ mature osteoblasts, however *Akp2* expression significantly decreased after GH challenge in these cells (-2.9 fold, $p<0.001$) (Fig. 4.13B).

4.5.12 Identification of osteoblast genes associated with the JAK/STAT pathway stimulated by GH

In order to gain a full appreciation for the regulatory role of SOCS2 on GH induced osteoblast gene expression, a RT^2 profiler assay was used to analyse 84 genes associated with the JAK/STAT pathway. *Socs2* expression was used as a positive

control in WT osteoblasts, to ensure that the GH was potent. In this study *Socs2* expression increased 5 fold in response to 4hrs GH treatment ($p<0.01$). In WT osteoblasts, the RT^2 profiler assay revealed a significant increase in 7 genes following 4hrs GH treatment (*Sh2b2*, *Bcl2l1*, *Gata3*, *Fr2*, *Fcgr1*, *Gbp1* and *Socs2*). Only 2 genes showed a greater than 2 fold increase (*Fcgr1*, 4.46 fold, $p<0.05$; *Socs2*, 4.55 fold, $p<0.01$) (Fig 4.14 & Table 4.4). In *Socs2*$^{-/-}$ osteoblasts, 1 gene (*Cdkn1a*) showed a significant increase, and 2 genes (*Sla2* and Stat4) significantly decreased following GH treatment. Only *Stat4* showed a greater than 2 fold change (-6.1 fold, $p<0.01$). GH treatment did increase *Fcgr1* expression (3.7 fold), but this did not reach significance ($p<0.076$) (Fig. 4.14 & Table 4.4).

4.5.13 Bone *Igf1* Expression in *Socs2*$^{-/-}$ mice

To directly address the higher bone mass noted in the *Socs2*$^{-/-}$ mice, *Igf1* and *Igfbp3* mRNA expression was quantified in femurs from mice previously analysed for μCT (section 4.5.3). The transcript levels of *Igf1* and *Igfbp3* in *Socs2*$^{-/-}$ and WT bones, extracted from 6 week old male and female mice remained similar (Fig. 4.15). These data highlight that in the *in vivo* situation of enhanced bone growth observed in *Socs2*$^{-/-}$ mice, *Igf1* and *Igfbp3* levels are not increased.

4.5.14 Osteoblast proliferation in response to GH and IGF-1

To assess the effects of enhanced GH signalling (section 4.5.7) on proliferation, WT and *Socs2*$^{-/-}$ osteoblasts were administered GH or IGF-1, and thymidine uptake measured. A preliminary study was first completed on MC3T3 cells to determine an optimum plating density and IGF-1 concentration to use for future experiments. In previous signalling experiments (sections 4.5.8 & 4.5.9) cells were treated with IGF-1 (50ng/ml). A number of reports investigating the effects of IGF-1 on osteoblast/osteoblast like cell proliferation used a concentration of 100ng/ml (Kim *et al.* 2005; DiGirolamo *et al.* 2007). When plated at a density of $5x10^3$cell/cm^2, GH and IGF-1 (50ng/ml and 100ng/ml) failed to stimulate MC3T3 cell proliferation. Cells plated at a density of $1x10^4$cell/cm^2 showed increased proliferation in response to

24hrs exposure to GH (105%; $p<0.05$), IGF-1(50ng/ml) (103%; $p<0.05$) and IGF-1 (100ng/ml) (247%; $p<0.05$) (Fig. 4.16A). Due to the enhanced level of proliferation observed with IGF-1 (100ng/ml) treatment, this concentration was used in future experiments on primary osteoblasts.

IGF-1 (100ng/ml) treatment enhanced proliferation of WT (79%; $p<0.05$) and *Socs2*$^{-/-}$ (72%; $p<0.05$) primary osteoblasts following 24 hours exposure. No significant difference in proliferation was observed between genotypes. Following 24 hours GH exposure, proliferation was not altered in WT or *Socs2*$^{-/-}$ osteoblasts (Fig. 4.16B). To ensure that this lack of response was not dependent on duration of GH exposure, a further experiment was set up where proliferation was measured following 24 and 48hrs. GH challenge did not alter proliferation at any time point studied (Fig. 4.16C).

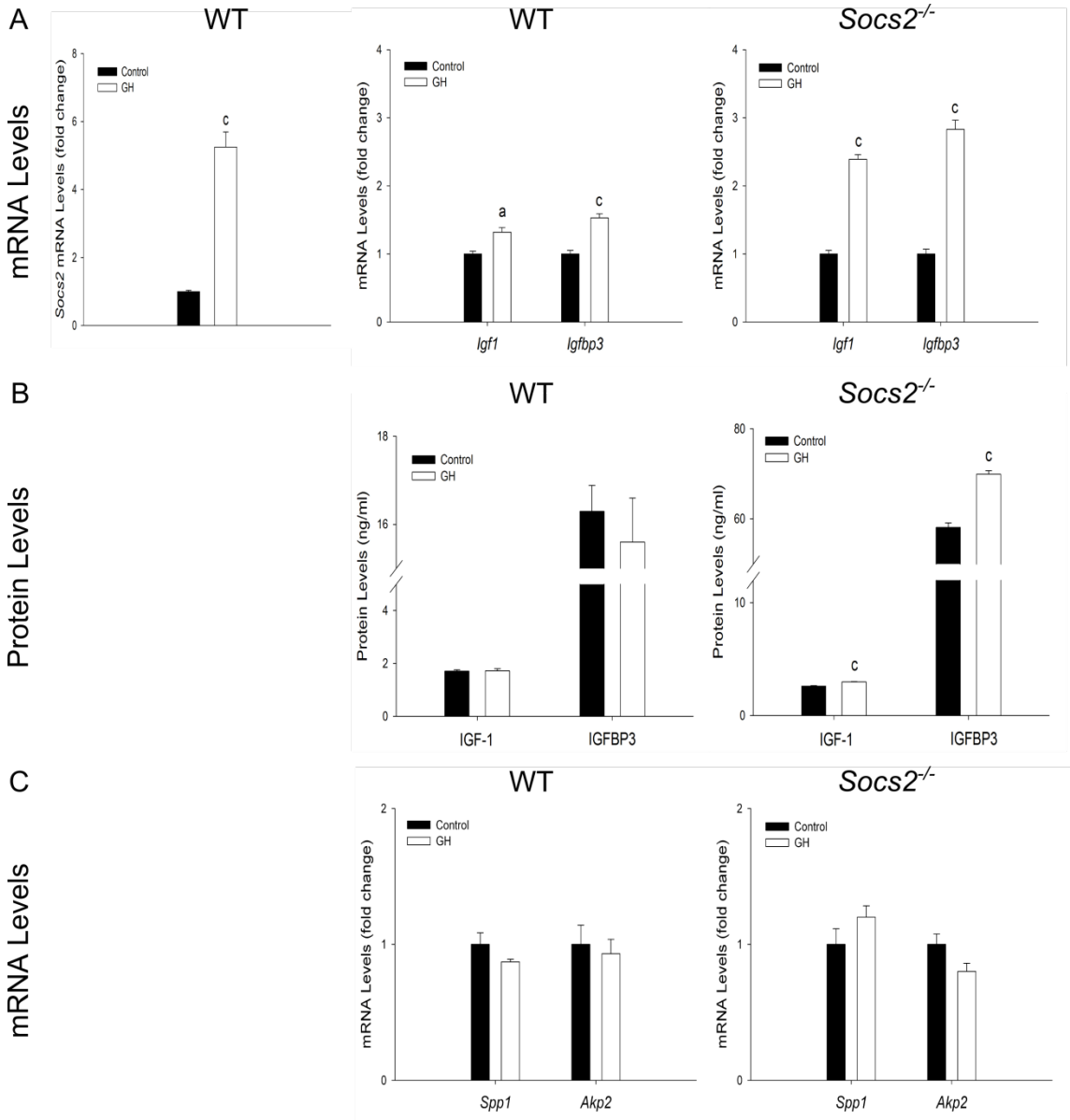

Figure 4.12 Enhanced IGF-1 and IGFBP3 levels in GH treated *Socs2*$^{-/-}$ osteoblasts

A. Analysis of *Socs2* mRNA expression levels in WT, and *Igf1* and *Igfbp3* mRNA expression levels in WT and *Socs2*$^{-/-}$ osteoblasts following 48hrs GH (500ng/ml) treatment. Data are presented as mean ± SEM (n=5) relative to control samples. Significance from control samples denoted by ^{a} $p<0.05$, ^{c} $p<0.001$. **B.** Protein analysis of IGF-1 and IGFBP3 from conditioned medium from WT and *Socs2*$^{-/-}$ osteoblasts following 48hrs GH (500ng/ml) treatment. Data are presented as mean± SEM (n=5). Significance from untreated samples denoted by ^{c} $p<0.001$. **C.** *Spp1* and *Akp2* mRNA expression levels in WT and *Socs2*$^{-/-}$ osteoblasts following 48hrs GH (500ng/ml) treatment. Data are presented as mean ± SEM (n=3) relative to untreated samples.

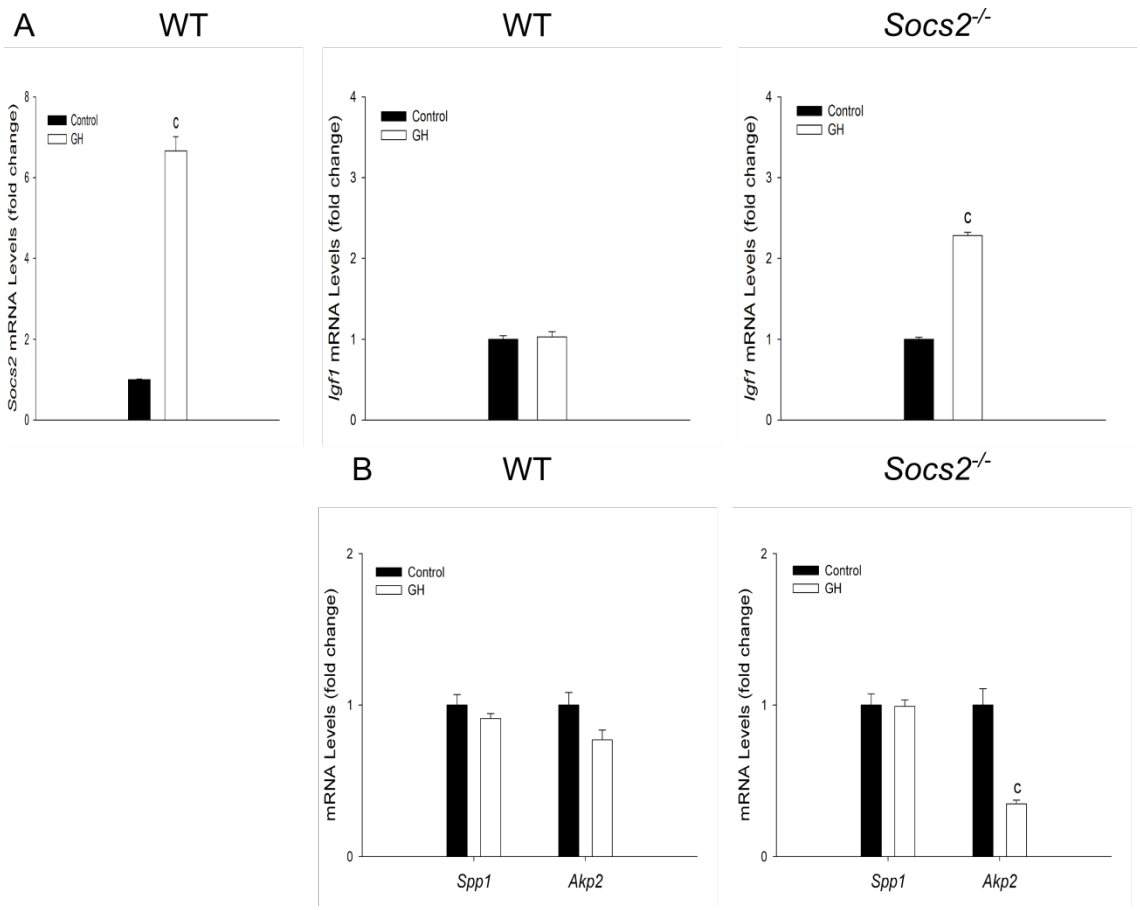

Figure 4.13 Decreased *Akp2* mRNA expression levels in mature *Socs2*$^{-/-}$ osteoblasts

A. Analysis of *Socs2* mRNA expression levels in WT, and *Igf1* and *Igfbp3* in WT and *Socs2*$^{-/-}$ osteoblasts following 48hrs GH (500ng/ml) treatment .Data are presented as mean ± SEM relative to untreated samples (n=5). Significance from untreated samples denoted by ^{a} $p<0.05$, ^{c} $p<0.001$. **B.** Analysis of *Spp1* and *Akp2* mRNA expression levels in WT and *Socs2*$^{-/-}$ osteoblasts following 48hrs GH (500ng/ml) treatment. Data are presented as mean ± SEM (n=5) relative to untreated samples. Significance from untreated samples denoted by $p<0.001$.

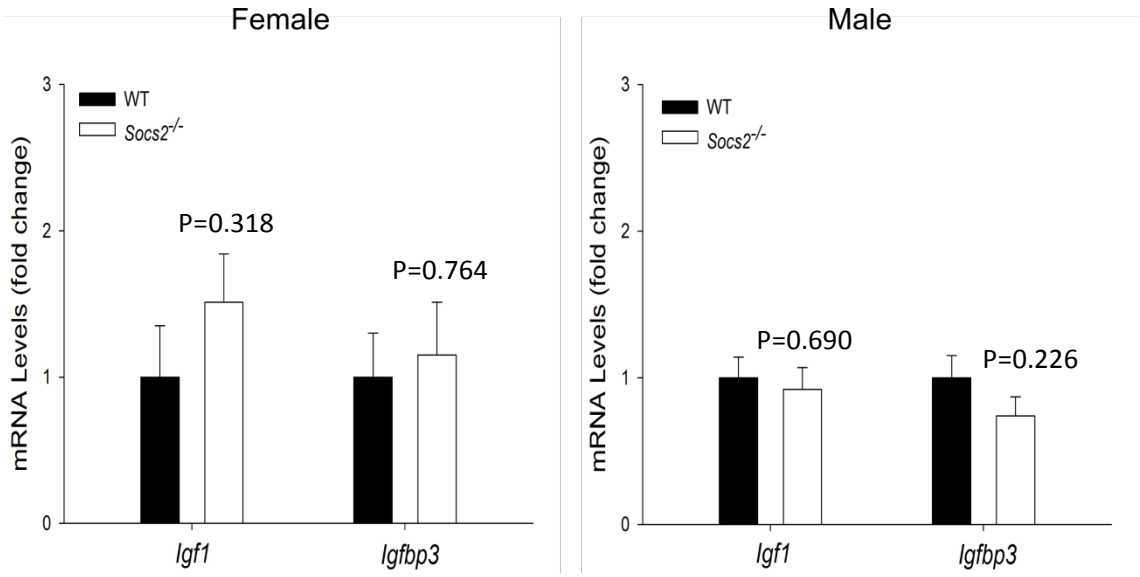

Figure 4.14 No alteration in *Igf1* mRNA expression levels in bone from 6 week old, male and female *Socs2*$^{-/-}$ mice

Analysis of *Igf1* and *Igfbp3* mRNA expression levels in femur extracted from 6 week old female and male WT and *Socs2*$^{-/-}$ mice. Data are presented as mean ± SEM (n≥5) relative to age and sex matched WT femur samples. Significance form age and sex matched WT femur samples denoted by p-values.

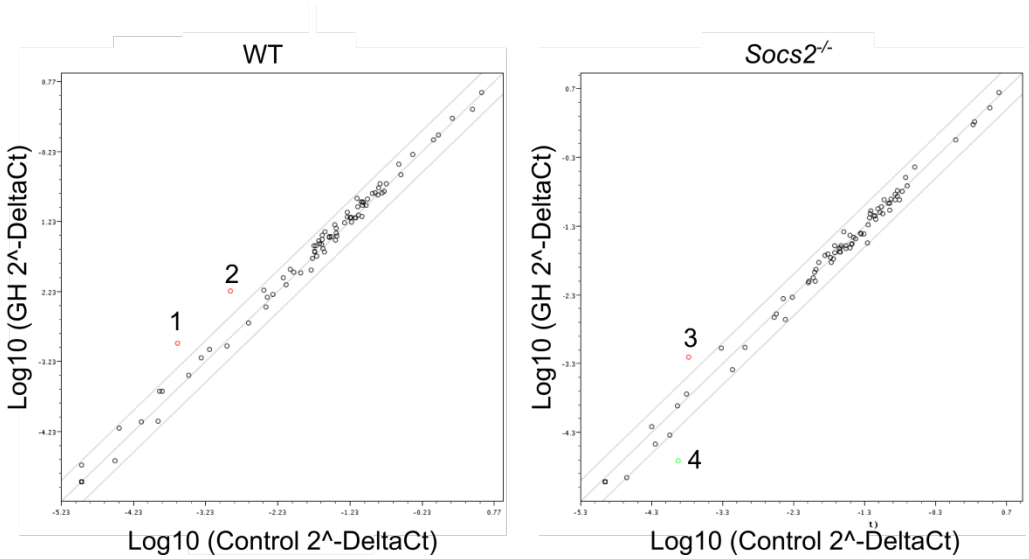

Figure 4.15 SOCS2 regulation of genes associated with the JAK/STAT pathway

Comparison of normalised expression of genes related to the JAK/STAT pathway in WT and *Socs2*$^{-/-}$ osteoblasts following 4hrs GH treatment. Graphs represent the means of 3 experimental replicates. Genes are plotted against one another to visualise gene expression changes. Boundaries indicate a fold change of 2. Numbered dots refer to genes listed in Table 4.

Table 4.4 Genes regulated by GH downstream of JAK/STAT in WT and *Socs2*$^{-/-}$ osteoblasts

List of genes altered by 4hrs GH (500ng/ml) treatment in WT and *Socs2*$^{-/-}$ osteoblasts

WT					*Socs2*$^{-/-}$				
Gene	No.	Ref. Seq.	Fold Change	p value	Gene	No.	Ref. Seq.	Fold Change	p value
Sh2b2		NM_018825	1.33	0.025	*Cdkn1a*		NM_007669	1.42	0.033
Bcl2l1		NM_009743	1.45	0.010	*Fcgr1*	3	NM_010186	3.71	0.076
Fr2		NM_010169	1.35	0.023	*Sla2*		NM_029983	-1.66	0.034
Gata3		NM_008091	1.45	0.020	*Stat4*	4	NM_011487	-6.08	0.023
Gbp1		NM_010259	1.72	0.003					
Socs2	1	NM_007706	4.55	0.020					
Fcgr1	2	NM_010186	4.46	0.034					

No. refers to numbered dots on Fig. 4.15

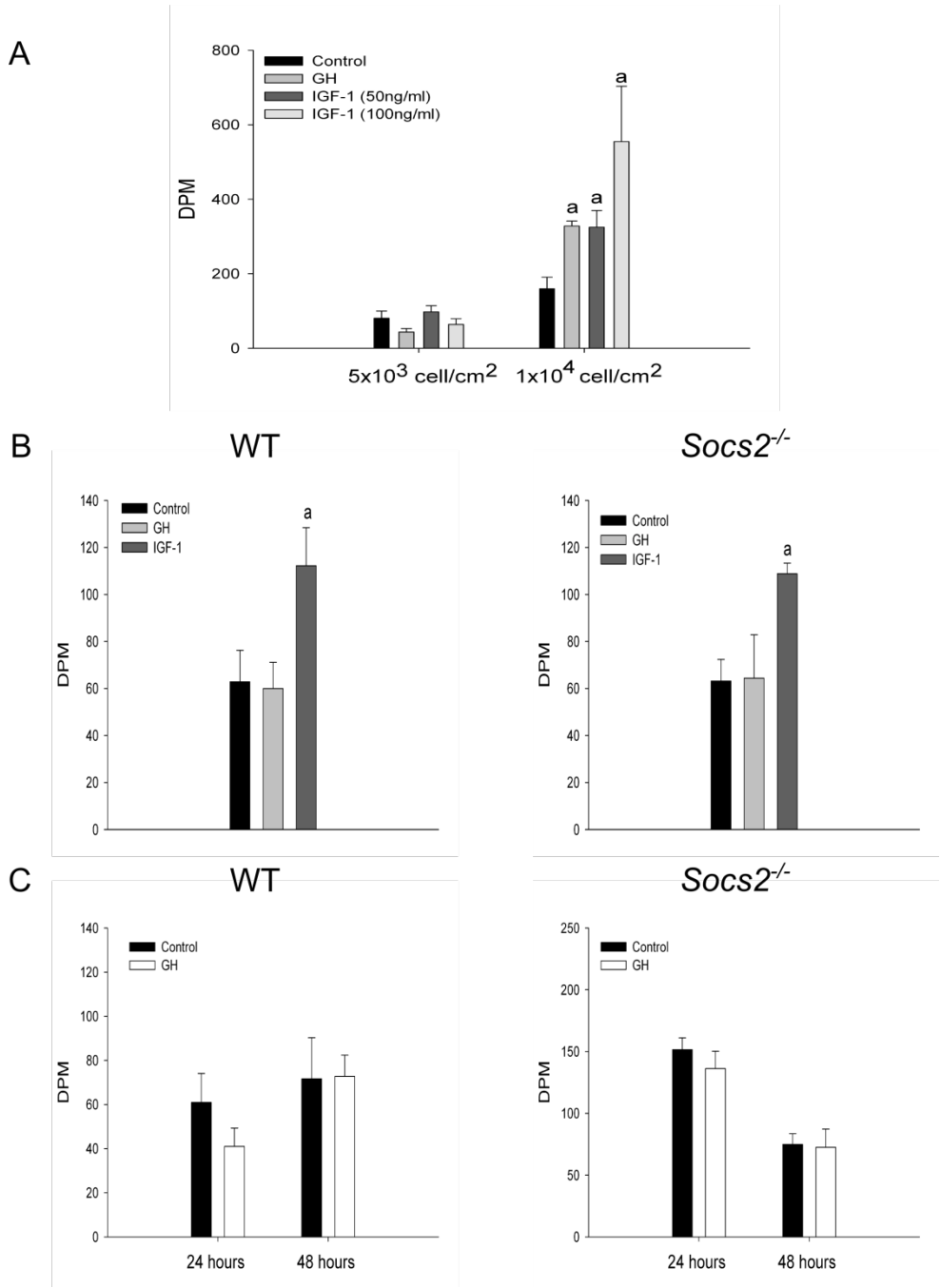

Figure 4.16 WT and *Socs2*$^{-/-}$ osteoblasts do not respond to GH with increased proliferation

A. Proliferation (as measured by thymidine uptake) of MC3T3 osteoblast like cells plated at 5x10^3 cell/cm^2 or 1x10^4 cell/cm^2 and treated with GH (500ng/ml), IGF-1 (50ng/ml) or IGF-1 (100ng/ml) for 24hrs. Data presented as mean ± SEM (n≥6). Significance denote by ^{a} $p<0.05$. **B.** Proliferation of WT and *Socs2*$^{-/-}$ osteoblasts following 24hrs GH (500ng/ml) or IGF-1 (100ng/ml) treatment. Data presented as mean ± SEM (n≥6). Significance relative to untreated samples denote by ^{a} $p<0.05$. **C**. Proliferation of WT and *Socs2*$^{-/-}$ osteoblasts following 24 and 24hrs GH (500ng/ml) treatment. Data presented as mean ± SEM (n≥6).

4.6 Discussion

Results presented in this chapter confirm the anabolic bone phenotype of *Socs2*$^{-/-}$ mice and give insight into the alteration in mechanical properties of these bones. The comprehensive study conducted on both male and female mice of two ages also highlights sex specific difference in the bone phenotype. *In vitro* primary osteoblast cell cultures were exploited to unravel the mechanisms driving the bone phenotype. In osteoblasts, SOCS2 was identified as being an important regulator of GH induced STAT signalling while having no effects on IGF-1 signalling. The importance of IGF-1 in mediating this signal was investigated however difference between *in vitro* and *in vivo* data made it difficult to draw conclusions.

SOCS2 is a key regulator of GH action. The overgrowth phenotype observed in the *Socs2*$^{-/-}$ mouse exhibits several features of deregulated GH signalling, including collagen accumulation in the dermis, and the production of major urinary proteins (Metcalf *et al.* 2000; Greenhalgh *et al.* 2005). Analysis of the *Socs2*$^{-/-}$ phenotype has focused primarily on its regulation of longitudinal bone growth (Metcalf *et al.* 2000; Greenhalgh *et al.* 2002a; Pass *et al.* 2012). The bone phenotype of *Socs2*$^{-/-}$ mice remains a matter of debate (Lorentzon *et al.* 2005; MacRae *et al.* 2009). Therefore, in this chapter, an in depth analysis of the bone phenotype of *Socs2*$^{-/-}$ mice was performed. To gain a full appreciation of this phenotype, male and female, juvenile and adult mice were analysed. Furthermore, primary osteoblast and SOCS2 overexpressing osteoblast like cell cultures were used to delineate the local actions of GH.

Socs2$^{-/-}$ mice are indistinguishable from WT littermates until 4-6 weeks of age, at which point the overgrowth phenotype becomes apparent. By 12 weeks, male *Socs2*$^{-/-}$ mice are reported to be 40% heavier than male WT mice. The overgrowth phenotype of female *Socs2*$^{-/-}$ mice is less evident. At 12 weeks, female *Socs2*$^{-/-}$ mice are only 28% heavier (Metcalf *et al.* 2000). In this study, *Socs2*$^{-/-}$ male and female mice were significantly heavier than WT mice at both ages (Fig. 4.1). Increased in weight was coupled with an increase in weight gain, observed in 6 week old male *Socs2*$^{-/-}$

mice (Fig. 4.1). The increase in body weight of *Socs2*$^{-/-}$ mice is the result of an increase in size of a number of organs including bone (Metcalf *et al.* 2000). Six week old male *Socs2*$^{-/-}$ mice had increased cortical periosteal MAR, with no alteration to endosteal MAR (Fig. 4.2). Increased periosteal MAR, at this age, is likely due to increased GH signalling during a period of GH dependent appositional growth (Callewaert *et al.* 2010). The level of bone turnover decreases with increased age. Consistent with this, analysis of MAR in tibia from 17 week old mice, revealed a lack of double calcein labelling. Studies using similarly aged mice have also reported severely reduced MAR in older animals (Sheng *et al.* 1999; Baldock *et al.* 2006).

The GH/IGF-1 pathway is a critical regulator of osteoblast function, bone homeostasis, and ultimately bone mass (Giustina *et al.* 2008). Global GH overexpression results in increased midshaft cross sectional area, an observation that is more evident in males (Eckstein *et al.* 2004). Conversely, GH deficiency leads to decreased cortical periosteal circumference, cross sectional area, and thickness. Trabecular bone volume, number, and thickness however remain unchanged (Sims *et al.* 2000; Sjogren *et al.* 2000). Alterations in systemic IGF-1 levels in these models make it difficult to delineate the relative contributions of GH and IGF-1. Overexpression of GH in osteoblasts results in increased cortical area and strength, despite no increase in systemic IGF-1 levels (Baker *et al.* 1992; Tseng *et al.* 1996). Conversely, IGF-1 overexpression in osteoblasts reveals an important role for local IGF-1 in regulating trabecular architecture. There were minimal effects on cortical geometry, suggesting that GH effects are not all mediated through IGF-1 (Zhao *et al.* 2000). Furthermore, GH stimulates periosteal bone formation rate in global *Igf1*$^{-/-}$ mice (Bikle *et al.* 2001).

Micro-CT analysis revealed a bone phenotype which had similarities to both previous studies analysing the *Socs2*$^{-/-}$ mouse skeletal phenotype (Lorentzon *et al.* 2005; MacRae *et al.* 2009). The architecture of *Socs2*$^{-/-}$ mice tibiae was consistent with the known anabolic effects of GH on bone (Tseng *et al.* 1996; Eckstein *et al.* 2004).

Socs2$^{-/-}$ tibiae had increased trabecular BV/TV and Tt.Ar, resembling previous analysis on 7 week old female mice (Tables 4.1 & 4.2 (MacRae *et al.* 2009). Similar to the GH excess models, male *Socs2*$^{-/-}$ mice displayed a more pronounced anabolic cortical bone phenotype (Table 4.1 & 4.2) (Eckstein *et al.* 2004). The increased Ct.Th and Ct.Ar observed in male *Socs2*$^{-/-}$ mice provided greater support to the cortex, thus increasing bone strength (Fig. 4.3 & Table 4.3) (Davison *et al.* 2006). The gender specific differences observed may be a consequence of the reported regulatory role of oestrogen on SOCS2 expression. This relationship merits further investigation (Leung *et al.* 2003; Bolamperti *et al.* 2013). The cortical bone phenotype has also been studied in 4 and 15 week old male mice. In 4 week old mice the ablation of *Socs2* was shown to decrease Ct.Ar and Ct.Th. This is however before the initiation of the overgrowth phenotype. Therefore, the effects of enhanced GH are unlikely to be seen in bone (Lorentzon *et al.* 2005). By 15 weeks of age there was no alteration in the cortical bone phenotype observed in *Socs2*$^{-/-}$ mice (Lorentzon *et al.* 2005). Differences observed between these studies may be a result of the scanning equipment used. Lorentzon and colleagues used a pQCT scanner, operating at a resolution of 70μm (Lorentzon *et al.* 2005). The present study and that of MacRae and colleagues used a micro-CT scanner which allowed scanning at a much higher resolution of 5-10μm (MacRae *et al.* 2009). Current data does show an age dependent decrease in cortical BMD in *Socs2*$^{-/-}$ tibiae (Tables 4.1 & 4.2). Adult mice had a decreased cortical BMD, similar to that observed in the global GH excess model and reported by Lorentzon and colleagues (Eckstein *et al.* 2004; Lorentzon *et al.* 2005). Osteoblast specific GH is anabolic to bone. It has been proposed that this is at the expense of bone tissue integrity such as increased cortical porosity. This has previously been used as a predictor of BMD (Tseng *et al.* 1996; Wachter *et al.* 2002).

Tibiae are significantly longer in *Socs2*$^{-/-}$ mice compared to WT (MacRae *et al.* 2009; Pass *et al.* 2012). It is therefore possible that the method used in this thesis to determine the region on interest for micro-CT analysis has led to slightly different areas of bone being compared. It is unclear if a similar analysis strategy was used in

other micro-CT procedures (Yakar *et al.* 2002b; Elis *et al.* 2010; Courtland *et al,* 2011). Future studies should aim to better define micro-CT methods in order to allow for correct interpretation.

Several studies have reported no increase in basal systemic IGF-1 levels in *Socs2*$^{-/-}$ mice. This suggests that the *Socs2*$^{-/-}$ overgrowth phenotype is a result of increased endogenous GH signalling at a local level (Metcalf *et al.* 2000; Lorentzon *et al.* 2005; MacRae *et al.* 2009). In agreement with this, the present study confirms that the increased growth observed in juvenile, male and female *Socs2*$^{-/-}$ mice was not associated with increased hepatic *Igf1* expression which is recognised as the main source of systemic IGF-1 (Fig. 4.4) (Yakar *et al.* 1999; Sjogren *et al.* 1999). Other GH regulated genes, such as *Igfbp3,* are preferentially expressed in the *Socs2*$^{-/-}$ liver (Rico-Bautista *et al.* 2005). This was confirmed in male, but not female mice of the present study (Fig. 4.4). The gender specific effects of GH on *Igfbp3* expression have been noted previously (Bielohuby *et al.* 2011). These observations underline the importance of local GH signalling, and confirm the value of the *Socs2*$^{-/-}$ mouse model in investigating the direct (IGF-1 dependent or independent) effects of GH.

The activation of STAT1, 3 and 5 has been implicated in the regulation of gene transcription, downstream of the GHR in various cell types. In osteoblasts however, the activation patterns remain unclear (Smit *et al.* 1996). In the present study, STAT1 and 5 are activated in response to GH in WT osteoblasts (Fig. 4.6). In the absence of SOCS2, the GH-induced phosphorylation of osteoblast STAT1, 3 and 5, and the translocation of p-STAT5 into the osteoblast nucleus are increased compared to WT cells (Figs. 4.6 &4.7). The reliance of p-STAT5 for SOCS2 regulation of GH signalling has been clearly demonstrated in the *Socs2*$^{-/-}$; *Stat5b*$^{-/-}$ double knockout mouse whose overgrowth phenotype is minimised (Greenhalgh *et al.* 2002). These data suggest that like growth plate chondrocytes and linear bone growth STAT5 mediates GHs anabolic actions on bone (Teglund *et al.* 1998; Pass *et al.* 2012). Nevertheless, the bone phenotype of *Ghr*$^{-/-}$ mice is more severe than that of *Stat5ab*$^{-/-}$ mice, suggesting

that there are additional GH actions on osteoblasts that are STAT5 independent (Sims *et al.* 2000). GH treatment also induced ERK1/2 activation. Previous studies have shown ERK1/2 signalling to mediate important actions in osteoblasts (Lai *et al.* 2001; Xiao *et al.* 2002). There was however no evidence for a SOCS2 regulatory role in this pathway (Fig. 4.9). It is therefore proposed that the high bone mass of the *Socs2*$^{-/-}$ mouse was not due to increased GH signalling through the ERK1/2 pathway.

Although the precise mechanism(s) by which SOCS2 negatively regulates GH signalling is unclear, the increased GH-induced phosphorylation of STATs 1, 3 and 5 reported in osteoblasts, implies that the inhibitory actions of SOCS2 are not STAT5 specific (Pass *et al.* 2009; Ahmed & Farquharson 2010). The observation that ablation of SOCS2 does not modify GH-induced activation of the ERK1/2 and AKT pathways advocates that SOCS2 regulates STAT activation only in osteoblasts (Fig. 4.9). The specificity of SOCS2 in the regulation of STAT signalling suggests that, at least in osteoblasts, SOCS2 does not regulate signalling via targeting the GHR for proteasomal degradation (Vesterlund *et al.* 2011). Proteasomal degradation would result in enhanced signalling of all pathways downstream of the GHR in *Socs2*$^{-/-}$ osteoblasts. A role for SOCS1 and 3 in negatively regulating the osteoblast STAT response to GH was not supported by these data, and confirms previous observations in growth plate chondrocytes (Fig. 4.5) (Pass *et al.* 2012). SOCS2 was shown to have no regulatory role in IGF-1 induced AKT and ERK1/2 signalling. A previous study has indicated that IGF-1 may stimulate STAT3 signalling, and therefore be a possible target for SOCS2 regulation (Zong *et al.* 2000). IGF-1 did not however stimulate STAT3 or STAT5 (a recognised mediator of GH signalling targeted by SOCS2) phosphorylation (Fig. 4.8). This is not surprising, as the IGF-1R does not contain specific tyrosine motifs thought to be recognised by STAT proteins (Stahl *et al.* 1995; Decker & Kovarik 2000).

The JAK/STAT pathway is required for GH-induced IGF-1 production. Specifically, STAT5 has been identified as a key mediator of GH induced up regulation of IGF-1

in liver and skeletal muscle (Udy *et al.* 1997; Klover & Hennighausen 2007). Its role in bone however remains undefined. The increased STAT5 activation and translocation into the nucleus following GH treatment observed was associated with a modest increase in *Igf1* and *Igfbp3* expression. Previous studies on cultured osteoblasts have reported that GH has either no effect on *Igf1* expression in rat osteoblasts, or causes a slight increase in expression in mouse calvarial osteoblasts and in MC3T3 osteoblast like cells (Morel *et al.* 1993; Schmid *et al.* 1994; DiGirolamo *et al.* 2007). The difference in results may be due to the difference in GH incubation time, as longer GH treatment was associated with increased *Igf1* expression. GH also stimulates *Igfbp3* expression in mouse calvarial osteoblasts (DiGirolamo *et al.* 2007). It was proposed that the increased STAT5 phosphorylation and translocation into the nucleus would likely result in higher *Igf1* expression, and thereby offer an explanation for the increased bone mass of *Socs2*$^{-/-}$ mice. Enhanced *Igf1* and *Igfbp3* expression were noted in *Socs2*$^{-/-}$ osteoblasts in response to GH implying that SOCS2 can limit GHs ability to stimulate osteoblast *Igf1* and *Igfbp3* expression (Fig. 4.12). It was noted, however, that the level of increase in *Socs2*$^{-/-}$ osteoblasts compared to WT was minimal. Furthermore, the *in vitro* data were not confirmed in the *in vivo* model. *Socs2*$^{-/-}$ mice, with an overgrowth phenotype, increased bone mass, and strength, had unchanged levels of bone *Igf1* and *Igfbp3*. This is consistent with previous quantification of *Igf1* expression in bone form *Socs2*$^{-/-}$ mice (Metcalf *et al.* 2000). It must however be recognised that this analysis was done on whole bone samples, still containing bone marrow and epiphyseal cartilage. Differences between the bone phenotype (cortical BMD) of the *Socs2*$^{-/-}$ and osteoblast specific *Igf1* overexpressing mouse cast further doubt on the essential role of local *Igf1* in mediating the effects of GH in *Socs2*$^{-/-}$ mice (Zhao *et al.* 2000). If the *Socs2*$^{-/-}$ phenotype was solely mediated through local IGF-1 then similarities would be expected between these models.

To assess the full impact of enhanced GH induced STAT signalling in *Socs2*$^{-/-}$ osteoblasts, a JAK/STAT signalling pathway PCR array was completed (Fig 4.15 & Table 4.4). This array measured the expression of 84 genes related to JAK/STAT

signalling, including all JAK and STAT family members, the receptors that activate them, nuclear co-factors, co-activators associated with STAT proteins, STAT-inducible genes, and negative regulators of the pathway. Attempts to identify alternative changes in gene expression associated with enhanced STAT signalling, that are both stimulated by GH and negatively controlled by SOCS2 were however unrewarding. Further studies are required to identify the specific gene activation downstream of enhanced GH-STAT signalling in *Socs2*$^{-/-}$ osteoblasts.

The effects of IGF-1 on osteoblasts are well established. IGF-1 stimulates osteoblast proliferation and collagen synthesis, while inhibiting collagen degradation (Canalis 1980; Canalis *et al.* 1995; DiGirolamo *et al.* 2007; Zhang *et al.* 2012). The effects of GH on osteoblasts are less understood. Osteoblasts extracted from human trabecular explants plated at a subconfluent density show increased proliferation (160%) in response to 24 hours of GH treatment. Conversely, confluent osteoblasts do not respond to GH (Kassem *et al.* 1993). The proliferation of mouse calvarial osteoblasts is only minimally increased in response to GH (1% increase in BrdU incorporation) (DiGirolamo *et al.* 2007). In the present study, IGF-1 stimulated the proliferation of osteoblasts from WT and *Socs2*$^{-/-}$ animals to a similar level (Fig. 4.16). This was to be expected, as no alteration in IGF-1 signalling was observed in the absence of SOCS2. It was hypothesised that the noted increase GH signalling in *Socs2*$^{-/-}$ osteoblasts would lead to increased proliferation in response to GH. GH did not however stimulate osteoblast proliferation in WT or *Socs2*$^{-/-}$ osteoblasts at any time point studied (Fig. 4.16). Increased proliferation in response to GH may require longer incubation times in excess of 24 hours (DiGirolamo *et al.* 2007). The present study however reported no increase in proliferation up to 48 hours. Factors thought to influence osteoblasts response include species of origin, site of origin, and age of donor (Czekanska *et al.* 2012). The paucity of previous studies reporting the effects of GH on osteoblast proliferation make it difficult to deduce the reason behind the lack of response observed. Although beyond the scope of this thesis, it is recognised that an alternative organ culture method exists to assess osteoblast function. The *ex*

vivo calvarial culture method allows the long term assessment of osteoblasts in a serum free environment, while remaining in a more physiologically accurate state (Mohammad *et al.* 2008).

In conclusion, this study underscores the critical role for SOCS2 in controlling GH's effects on bone. It also provides compelling evidence to support the notion that SOCS2 is pivotal is regulating GH induced STAT signalling in osteoblasts.

Chapter 5

Mechanisms of GH control of body growth and bone structure

5.1 Introduction

GH predominantly exerts its actions through the secondary messenger IGF-1. A number of tissues including liver, growth plate, and muscle all respond to GH with increased IGF-1 production (Isgaard *et al.* 1988a; Isgaard *et al.* 1988b; Le Roith *et al.* 2001). The importance of IGF-1 in mediating GH induced growth is clear, as *Igf1*$^{-/-}$ mice do not respond to GH (Liu & LeRoith 1999). There is however little evidence to suggest that GH stimulates IGF-1 production in bone. An IGF-1 independent action of GH on bone formation is shown by the responsiveness of global *Igf1*$^{-/-}$ mice to GH treatment (Bikle *et al.* 2001).

The *Socs2*$^{-/-}$ mouse has been identified as a potential model to study the local effects of GH on bone, independent of systemic or local (bone) IGF-1 production. The *Socs2*$^{-/-}$ skeletal phenotype is evident despite normal systemic IGF-1 levels and *Igf1* expression in bone (Metcalf *et al.* 2000; Lorentzon *et al.* 2005; MacRae *et al.* 2009). Results presented in chapter 4 confirm that the anabolic bone phenotype of the *Socs2*$^{-/-}$ mouse is not associated with an increase in liver or bone *Igf1* expression. Conversely, primary osteoblast cultures revealed a larger increase of *Igf1* expression in GH treated *Socs2*$^{-/-}$ osteoblasts. Under basal conditions, SOCS levels remain low. Following GH stimulation, SOCS levels increase rapidly (SOCS1 & 3 and CIS) or gradually (SOCS2), forming a negative feedback loop (Adams *et al.* 1998; Tollet-Egnell *et al.* 1999). Therefore, GH stimulation is required for the upregulation of SOCS2, subsequently inhibiting GH signalling and downstream IGF-1 production. Previous *in vivo* measurements of downstream *Igf1* expression (including results in chapter 4) are potentially hindered by the uncertainty of GH secretion at the point of sacrifice (Metcalf *et al.* 2000). To fully appreciate the potential importance of IGF-1 in mediating the bone phenotype in GH challenged *Socs2*$^{-/-}$ mice, *Igf1* expression levels should be assessed directly following GH administration.

The JAK/STAT pathway is of primary importance in mediating GHs' actions. Similar to *Ghr*$^{-/-}$ mice, *Stat5b*$^{-/-}$ mice are indistinguishable from WT mice until 2-3 weeks of age (Udy *et al.* 1997; Lupu *et al.* 2001). This is similar to *Socs2*$^{-/-}$ mice which have comparable growth rates to WT mice during early postnatal development. This is before the onset of the overgrowth phenotype (Metcalf *et al.* 2000). The importance of STAT5 in mediating the *Socs2*$^{-/-}$ phenotype is clear from *Stat5b*$^{-/-}$; *Socs2*$^{-/-}$ double knockout mice which do not have the gigantism phenotype (Greenhalgh *et al.* 2002). STAT5b also has a key role in sexually dimorphic growth, taking place at around 3 weeks of age. Ablation of *Stat5b* causes a lack of enhanced growth in male mice at this age, while female growth remains largely unaffected (Udy *et al.* 1997). STAT5b is essential in mediating GH action in liver, and *Stat5b*$^{-/-}$ mice have low circulating IGF-1 levels despite elevated GH levels (Udy *et al.* 1997). *Stat5a*$^{-/-}$ mice show no reduction in growth with IGF-1 levels comparable to WT (Teglund *et al.* 1998). *Stat5a/b*$^{-/-}$ double knockout mice are however growth retarded, and have reduced serum IGF-1 levels. These mice share many similarities to *Ghr*$^{-/-}$ and GH-deficient (*lit/lit*) mice (Donahue & Beamer 1993; Zhou *et al.* 1997; Teglund *et al.* 1998). In these mouse models, the decrease in growth is attributed to the reduction of systemic IGF-1 levels. The role of STAT5 in mediating GH action in bone is less understood. GH induces STAT5 activation in osteoblasts (DiGirolamo *et al.* 2007). In addition, results presented in chapter 4 highlight enhanced GH-STAT5 signalling in *Socs2*$^{-/-}$ osteoblasts *in vitro;* a likely mediator of the skeletal overgrowth phenotype. Research would however benefit from an *in vivo* study assessing STAT5 signalling and its relation to GH induced bone formation. As GH action in both liver and bone has been identified as being involved in bone growth it is important that signalling cascades are assessed in both tissues. Furthermore, the gender differences outlined in chapter 4 highlight an importance for the assessment of both male and female mice.

5.2 Hypothesis

Increased bone formation in GH treated *Socs2*$^{-/-}$ mice is associated with increased local STAT5 activation, but not changes in local *Igf1* expression.

5.3 Aims

I. Compare the effects of GH treatment on body and bone growth in male WT and *Socs2*$^{-/-}$ mice.

II. Assess downstream GH signalling in liver and bone from male WT and *Socs2*$^{-/-}$ mice.

III. Identify *Igf1* expression levels in liver and bone following GH treatment.

IV. Complete similar experiments assessing body and bone growth, signalling and *Igf1* expression in response to GH treatment in female WT and *Socs2*$^{-/-}$ mice.

5.4 Material and Methods

All rhGH used in this chapter was a kind gift from Prof. Faisal Ahmed (University of Glasgow).

5.4.1 Long term *in vivo* GH treatment

GH injections and tissue collection were carried out as outlined in section 2.4.5.

5.4.2 Micro-CT analysis

Micro-CT analysis was carried out on femurs from mice treated as outlined in section 2.4.5 using a Skyscan 1272 scanner (Bruker). This scanner is different to the Skyscan 1172 used in chapters 4 and 6 and therefore scanning parameters were adjusted such that for cortical bone analysis, the rotation angle was set to 0.4°. All other scanning parameters remained the same. Analysis was completed as outlined in section 2.4.7 with one modification. Due to the lack of fibula articulation to the tibia as a reference point a volume of interest was selected 2000μm proximal of the distal growth plate (Fig. 5.1).

5.4.3 Short term *in vivo* GH treatment

GH injections and tissue collection for signalling analysis were carried out as outlined in section 2.4.6.

5.4.4 Western blotting

Protein was extracted from bone and liver samples, and western blot analysis carried out on as previously described in section 2.6. Primary and secondary antibodies are detailed in Appendix II. Densitometry of western blotting was measured on a minimum of three independent samples using Image J. Data is presented as phosphorylated protein levels normalised to total protein levels.

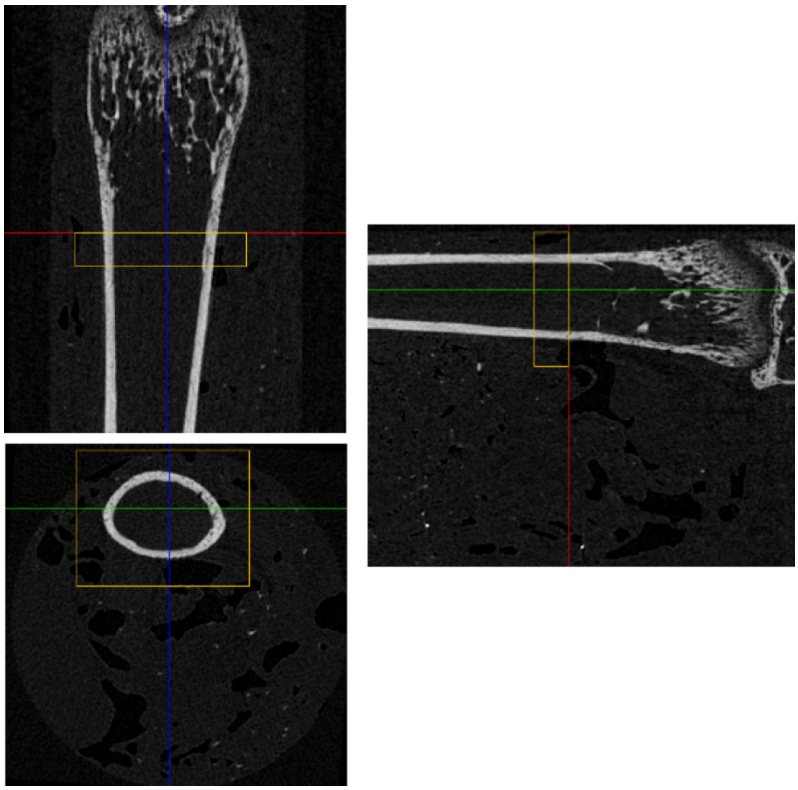

Figure 5.1 Selecting volume of interest for cortical analysis of femur

Representative images in Data Viewer of distal femur (3 planes of view), highlighting the selection of a volume of interest (yellow box).

5.4.5 qPCR analysis

Left femur and liver were dissected from male and female WT and *Socs2*$^{-/-}$ mice following 14 days GH treatment. Both were snap frozen in liquid nitrogen and stored at -80°C. Before being snap frozen femurs had the epiphyses removed and marrow spun out by centrifugation. RNA was extracted as described in section 2.5.1. cDNA was prepared from all RNA as outlined in section 2.5.2, and qPCR analysis completed as detailed in section 2.5.3. Results were normalised to *Gapdh* housekeeping gene and the gene expression levels were calculate relative to vehicle treated samples.

5.4.6 Serum IGF-1 ELISA

After 14 days GH treatment, immediately following sacrifice blood was collected from male and female WT and *Socs2*$^{-/-}$ mice by cardiac puncture. Blood was stored in serum tubes (Greiner Bio-One, Gloucestershire, UK) on ice for over 30mins to allow for clotting. Following 10mins centrifugation at 1000g supernatant was removed, aliquoted, and stored at -80°C. IGF-1 levels in was assessed by ELISA (Quantikine, R&D Systems, Minneapolis, MN, USA) according to manufacturer's instructions.

5.4.7 Statistical analysis

Statistical analysis was completed on software described in section 2.7. For growth studies, experimental data were analysed using a repeated measures 2-way ANOVA for which suitable post-tests for multiple comparisons were conducted. Final measurements, micro-CT, IGF-1 ELISAs, and signalling data were analysed using a 2 way ANOVA for which suitable post-tests for multiple comparisons were conducted. All other results within the chapter were analysed using the Student's t-test or a suitable non-parametric test if the data were not normally distributed. Data were checked to be normally distributed using a Shapiro-Wilk normality test.

5.5 Results

5.5.1 Growth of male WT and *Socs2*$^{-/-}$ mice treated with GH

Growth of male WT and *Socs2*$^{-/-}$ mice was similar from 14 - 27 days of age (Fig. 5.2A). GH treatment (starting at 14 days of age) did not alter growth of WT mice at any time point studied (Fig. 5.2B). Growth of *Socs2*$^{-/-}$ mice was not altered significantly in response to GH until 8 days of treatment (22 days of age). Between days 8-13 (22-27 days of age), GH treatment significantly enhanced growth of *Socs2*$^{-/-}$ mice (Fig. 5.2C).

5.5.2 Final measurements from male mice treated with GH

Following 14 days GH treatment, WT mice did not show any signs of enhanced growth (Fig. 5.3 & Table 5.1). Final measurements (weight, nose to rump length, tail length, femur length and tibia length) were unaltered in WT mice treated with GH compared to vehicle treated mice (Table 5.1). GH treated *Socs2*$^{-/-}$ mice were visibly larger than vehicle treated mice (Fig. 5.3). GH treatment resulted in a significant increase in weight of *Socs2*$^{-/-}$ mice (17%; $p<0.01$) (Table 5.1). All other parameters remained unchanged (Table 5.1).

5.5.3 Micro-CT analysis of femur from male mice treated with GH

Analysis of cortical geometry revealed anabolic changes to the femur of GH treated *Socs2*$^{-/-}$ mice. These mice had increased Ct.Ar (20%; $p<0.01$) and polar moment of inertia (J) (43%; $p<0.05$) (Table 5.2). No changes in cortical geometry were observed in GH treated WT mice (Table 5.2). Consistent with the lack of an overgrowth phenotype, (section 5.5.1) there were no changes in cortical geometry between vehicle treated WT and *Socs2*$^{-/-}$ mice (Table 5.2).

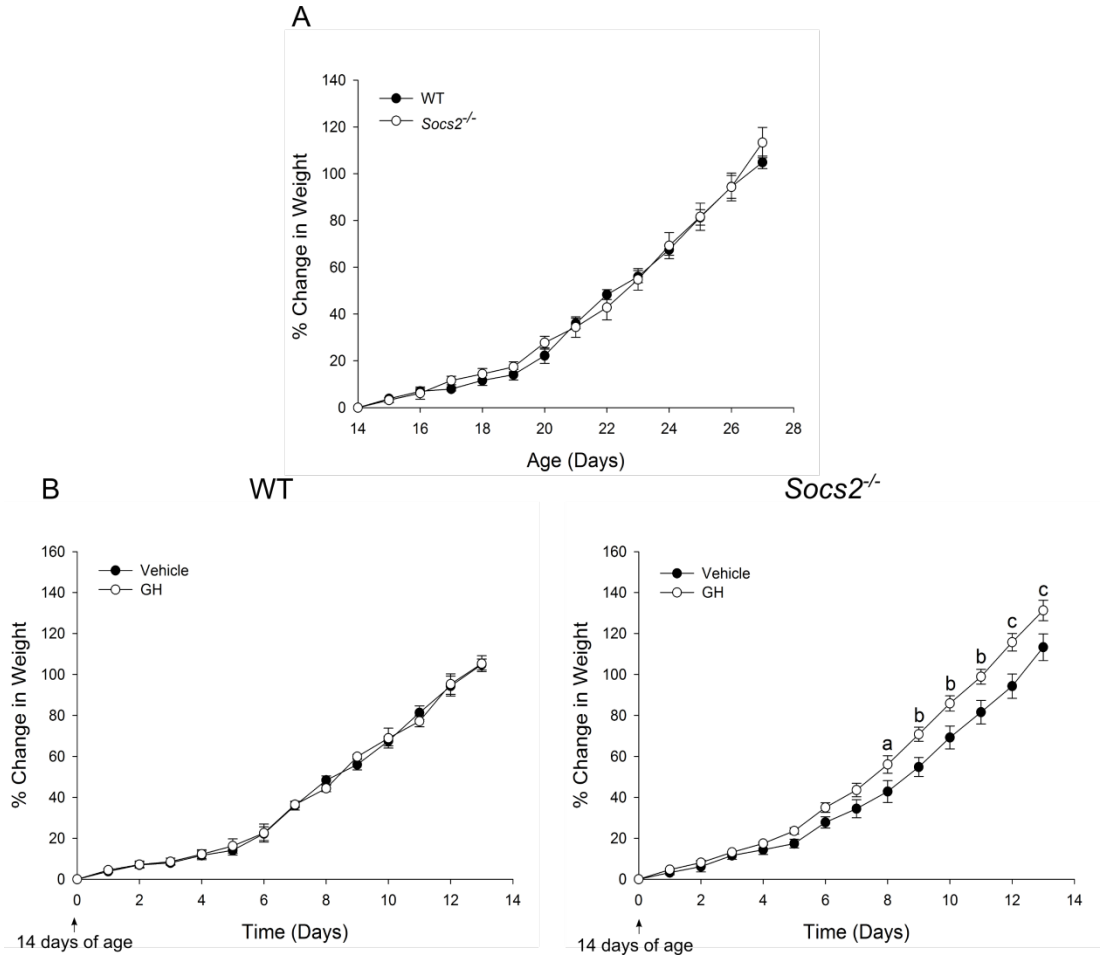

Figure 5.2 GH stimulates growth of male *Socs2*$^{-/-}$ mice

A. Weight gain of WT and *Socs2*$^{-/-}$ mice from 14-27 days of age. **B.** Growth (% change in weight) of WT and *Socs2*$^{-/-}$ mice in response to GH (3mg/kg) treatment from 14-27 days of age. Data are presented as mean ± SEM (n≥5). Significance from vehicle treated mice is denoted by ^{a} $p<0.05$, ^{b} $p<0.01$, ^{c} $p<0.001$.

Table 5.1 Increased weight of GH treated male *Socs2*$^{-/-}$ mice

Final measurement from 27 day old WT and *Socs2*$^{-/-}$ male mice treated with GH (3mg/kg) for 14 days.

Genotype	Treatment	Weight (g)	Nose to Rump Length (mm)	Tail Length (mm)	Femur Length (mm)	Tibia Length (mm)
WT	Vehicle	14.0 ± 0.69	75.2 ± 0.62	54.2 ± 1.58	11.1 ± 0.21	14.7 ± 0.26
	GH	14.4 ± 0.61	75.1 ± 1.81	54.7 ± 0.98	11.4 ± 0.20	14.5 ± 0.15
Socs2$^{-/-}$	Vehicle	15.0 ± 0.71	75.1 ± 1.46	54.2 ± 1.96	11.2 ± 0.18	14.6 ± 0.21
	GH	17.6 ± 0.55[b]	79.9 ± 0.98	56.8 ± 1.81	11.7 ± 0.20	15.0 ± 0.16

Data are presented as mean ± SEM (n≥5). Significance from genotype matched vehicle treated mice is denoted by [b] $p<0.01$.

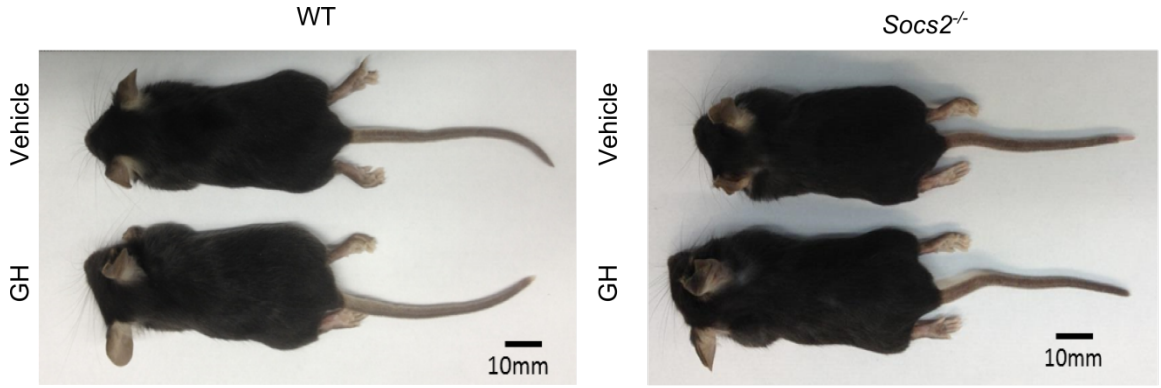

Figure 5.3 Enhanced growth of GH treated male *Socs2*$^{-/-}$ mice

Representative images of 27 day old male WT and *Socs2*$^{-/-}$ following 14 days GH (3mg/kg) treatment. Scale bar = 10mm

Table 5.2 Altered cortical geometry of GH treated male *Socs2*$^{-/-}$ mice

Micro-CT analysis of tibia from 27 day old WT and *Socs2*$^{-/-}$ male mice treated with GH (3mg/kg) for 14 days.

	WT				***Socs2*$^{-/-}$**			
	Vehicle		GH		Vehicle		GH	
Tt.Ar (mm²)	1.33 ± 0.051		1.30 ± 0.070		1.27 ± 0.050		1.45 ± 0.070	
Ct.Ar (mm²)	0.45 ± 0.023		0.43 ± 0.023		0.41 ± 0.009		0.49 ± 0.017[b]	
Ma.Ar (mm²)	0.88 ± 0.032		0.87 ± 0.048		0.86 ± 0.050		0.96 ± 0.061	
Ct.Th (mm)	0.12 ± 0.003		0.12 ± 0.003		0.12 ± 0.004		0.13 ± 0.004	
J (mm⁴)	0.17 ± 0.018		0.15 ± 0.017		0.14 ± 0.007		0.20 ± 0.015[a]	

Data are presented as mean ± SEM (n≥5). Tt.Ar = total area, Ct.Ar = cortical area, Ma.Ar = marrow area, Ct. Th = cortical thickness, and J = polar moment of inertia. Significance from genotype matched vehicle treated mice is denoted by [a] $p<0.05$, [b] $p<0.01$.

5.5.4 Regulation of GH induced signalling in male liver and bone by SOCS2

To identify the downstream signalling pathways involved in mediating GHs' actions on body (section 5.5.1) and bone growth (section 5.5.3) in *Socs2*$^{-/-}$ mice, activation of signalling proteins were measured in liver and bone samples.

At 24 days of age (*Socs2*$^{-/-}$ mouse growth rate increases in response to GH, WT mouse growth rate unaltered in response to GH), liver p-STAT5 levels increased significantly in WT ($p<0.05$) and *Socs2*$^{-/-}$ ($p<0.001$) mice. This increase was greatly exaggerated in liver samples from *Socs2*$^{-/-}$ mice (Fig. 5.4). Minimally increased p-AKT levels were present in liver samples from GH treated WT mice ($p<0.05$). This was not observed in *Socs2*$^{-/-}$ mice (Fig. 5.4). P-ERK1/2 levels were not altered in response to GH treatment in WT and *Socs2*$^{-/-}$ liver samples (Fig. 5.4).

Bone samples dissected from GH treated *Socs2*$^{-/-}$ mice revealed a significant increase in p-STAT5 levels ($p<0.01$) (Fig. 5.4). A significant p-STAT5 level response was not observed in bone from WT mice, but this was likely due to 1 of the 3 mice not responding to GH administration (Fig. 5.4). Even taking this into account, it was clear that STAT5 activation was greatly exaggerated in bone from GH *Socs2*$^{-/-}$ mice compared to WT (Fig. 5.4). No alteration in p-AKT and p-EKR1/2 levels were noted in bone from GH treated WT and *Socs2*$^{-/-}$ mice (Fig. 5.4).

5.5.5 Regulation of GH induced signalling in male liver and bone by SOCS2 during a period of no growth response

The results in section 5.5.1 (Fig. 5.2B) identified a period of growth in WT and *Socs2*$^{-/-}$ mice that was not stimulated by GH (14-~20 days of age). Therefore downstream signalling levels were measured in 17 day old mice. It was expected that the results obtained would give an indication to the importance of specific signalling pathways in mediating the *Socs2*$^{-/-}$ overgrowth phenotype.

At 17 days of age (WT and *Socs2*$^{-/-}$ mouse growth rates are unaltered in response to GH treatment), liver p-STAT5 levels significantly increase in response to GH in WT mice ($p<0.05$). A similar response was observed in *Socs2*$^{-/-}$ liver, but did not reach significance and again this was likely due to individual mice variation of basal p-STAT5 levels (Fig. 5.5). P-AKT levels in the liver were not detected at this age, and p-ERK1/2 levels were not altered in response to GH (Fig. 5.5).

Bone samples dissected from WT mice revealed a modest increase in p-STAT5 levels in response to GH ($p<0.001$). A similar trend was observed in bone from *Socs2*$^{-/-}$ mice, however this did not reach significance ($p<0.053$) (Fig. 5.5). P-AKT levels in the bone were not detected at this age and p-ERK1/2 levels were not elevated in response to GH (Fig. 5.5).

These data confirm an age dependent regulatory role of SOCS2 on GH-induced STAT5 signalling in bone and liver, and suggest a possible mechanism for the increased growth observed in GH treated *Socs2*$^{-/-}$ mice.

5.5.6 Regulation of GH induced mRNA expression levels in liver and bone by SOCS2 in male mice

GH treatment increased *Socs2* levels in liver (2.73fold; $p<0.05$), but not bone from WT mice (Fig. 5.6A). *Igf1* and *Igfbp3* levels were unaltered in response to GH in WT and *Socs2*$^{-/-}$ liver or bone (Fig. 5.6B&C). The lack of increase in hepatic *Igf1* expression was confirmed using an IGF-1 serum ELISA (Table 5.4). IGF-1 levels remained unaltered in serum from WT and *Socs2*$^{-/-}$ mice treated with GH.

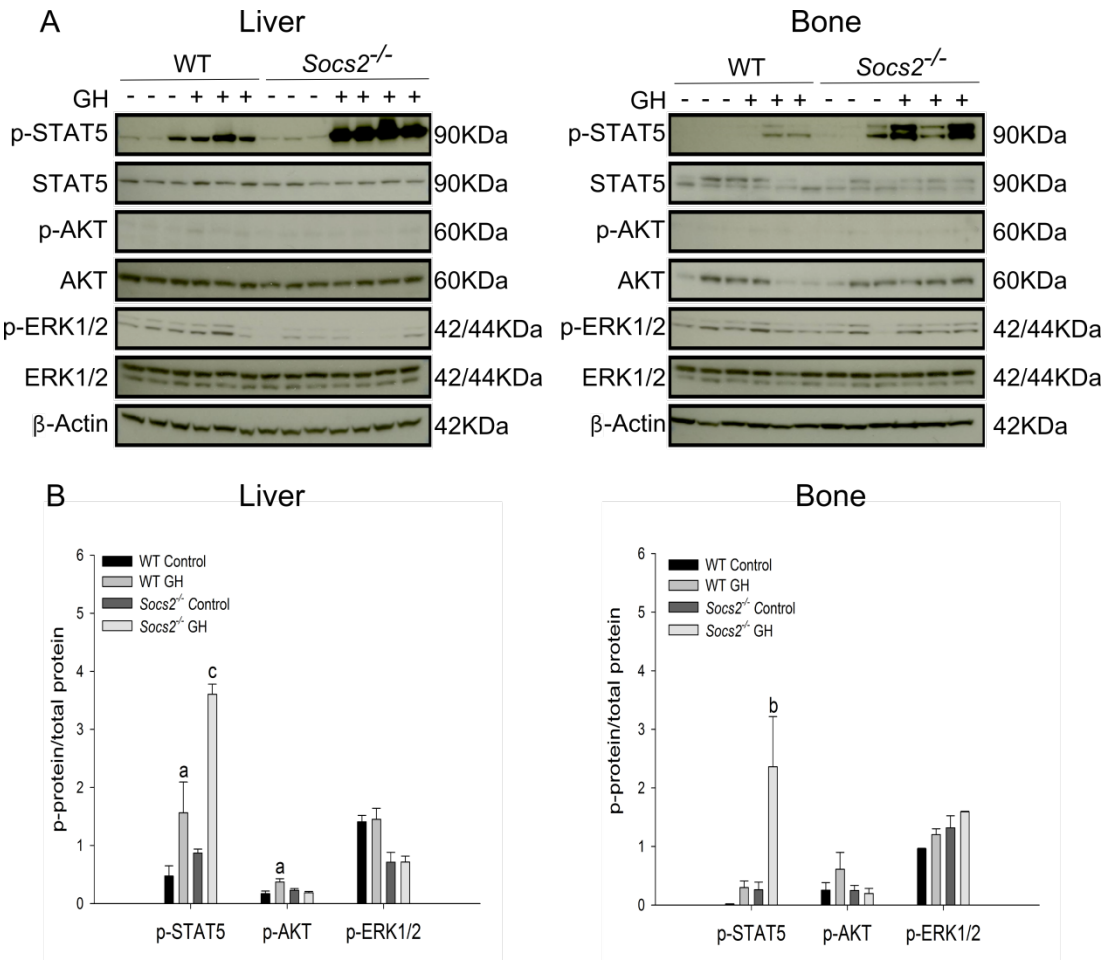

Figure 5.4 Exaggerated STAT5 activation in liver and bone from 24 day old *Socs2*$^{-/-}$ male mice following GH treatment

A. Western blotting of phosphorylated (P-) STAT5, AKT and ERK1/2 in liver or tibia extracted from 24 day old WT and *Socs2*$^{-/-}$ mice following 15mins GH (3mg/kg) treatment. β-actin proteins shown as loading controls. **B.** Quantification of densitometry analysis of western blotting. Data presented as p-protein normalised to total protein. All data presented as mean ± SEM (n≥3). Significance from genotype matched vehicle treated samples (control) is denoted by ^{a} $p<0.05$, ^{b} $p<0.01$, ^{c} $p<0.001$.

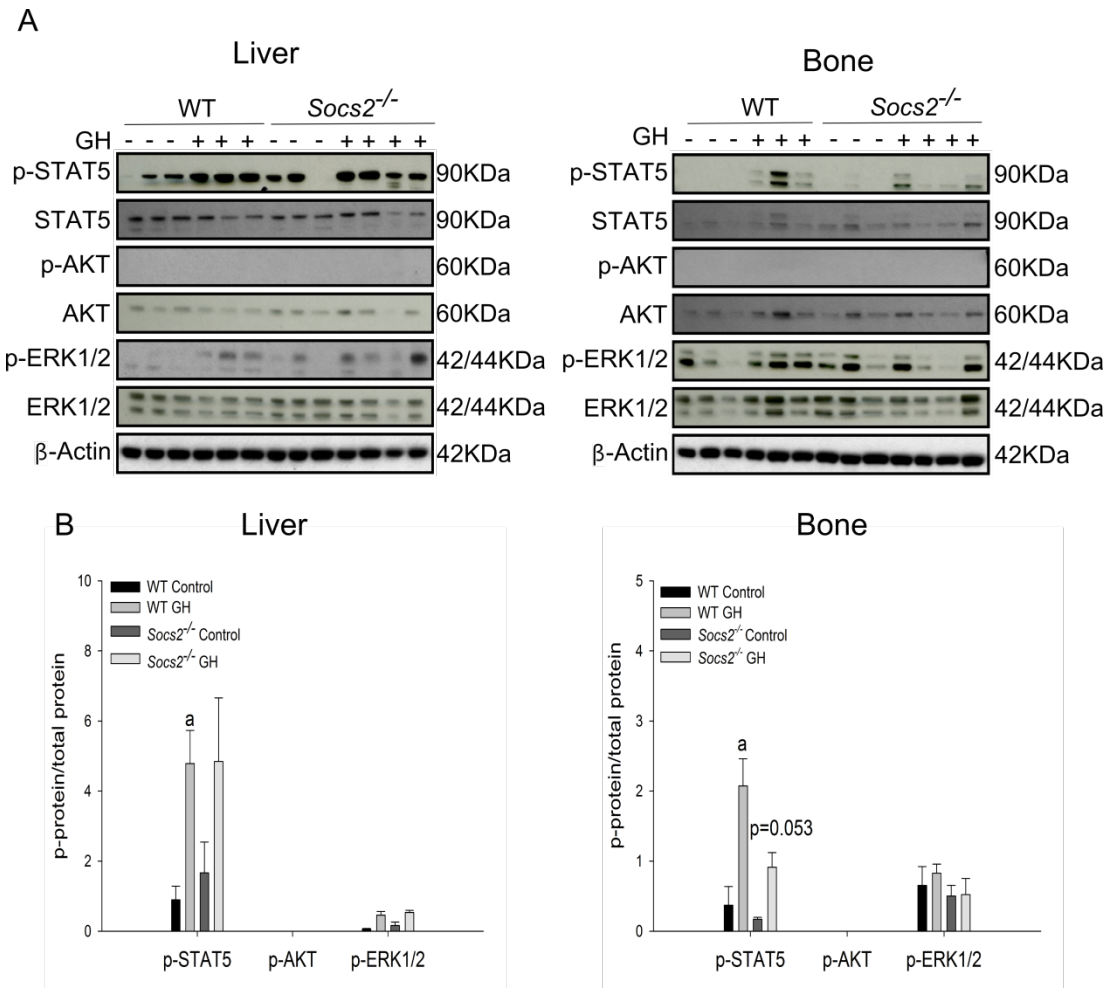

Figure 5.5 No exaggerated GH induced signalling in liver and bone from male 17 day old *Socs2*$^{-/-}$ mice

A. Western blotting of phosphorylated (P-) STAT5, AKT and ERK1/2 in liver or tibia extracted from 17 day old WT and *Socs2*$^{-/-}$ mice following 15mins GH (3mg/kg) treatment. β-actin proteins shown as loading controls. **B.** Quantification of densitometry analysis of western blotting. Data presented as p-protein normalised to total protein. All data presented as mean ± SEM (n≥3). Significance from genotype matched vehicle treated samples (control) is denoted by [a] $p<0.05$.

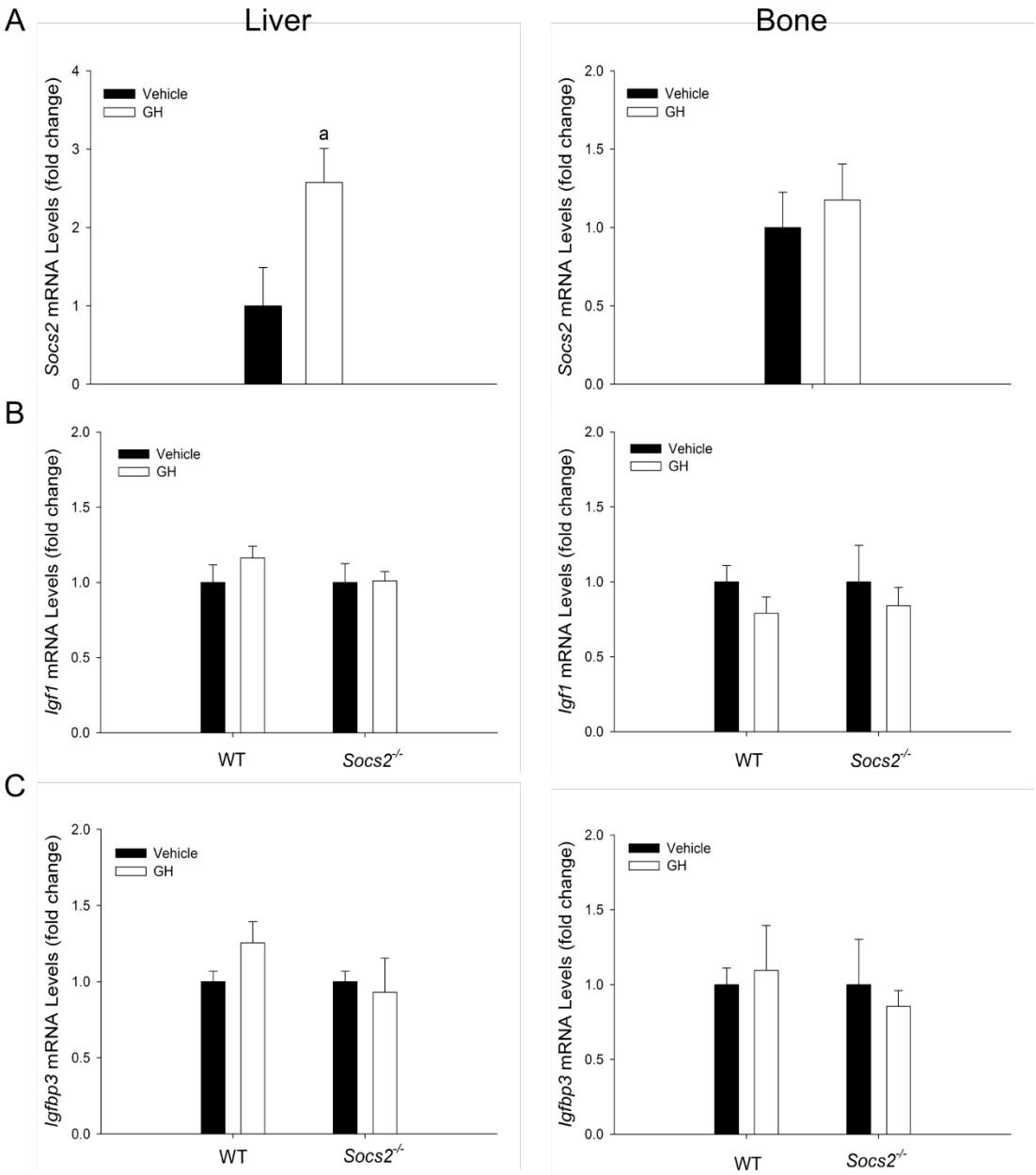

Figure 5.6 No alteration in *Igf1* and *Igfbp3* mRNA expression levels in liver and bone from male *Socs2*$^{-/-}$ mice following GH treatment

A. *Socs2* mRNA expression levels in liver and bone from male WT mice at 27 days of age following 14 days GH (3mg/kg) treatment. **B.** *Igf1* and **C.** *Igfbp3* mRNA expression levels in liver and bone from male WT and *Socs2*$^{-/-}$ mice at 27 days of age following 14 days GH (3mg/kg) treatment. Data are presented as mean ± SEM (n=5, except *Socs2*$^{-/-}$ *Igfbp3* + GH n=3) relative to untreated samples. Significance from genotype matched vehicle treated samples is denoted by ^{a} $p<0.05$.

Table 5.3 No alteration in male serum IGF-1 levels following GH treatment

Serum IGF-1 levels in 27 day old male WT and *Socs2*$^{-/-}$ mice following 14 days GH (3mg/kg) treatment.

Treatment	WT			*Socs2*$^{-/-}$		
Vehicle	389.6	±	9.90	351.0	±	20.43
GH	367.8	±	27.16	409.3	±	21.87

Data are presented as mean ± SEM (n≥5).

5.5.7 Growth of female WT and Socs2$^{-/-}$ mice treated with GH

The *Socs2*$^{-/-}$ overgrowth phenotype is more pronounced in male mice compared to females (Metcalf *et al.* 2000). Furthermore, results presented in chapter 4 of this thesis highlight sex specific differences in bone architecture in male and female *Socs2*$^{-/-}$ mice. To investigate this further, the effects of GH on growth and intracellular signalling was also explored in female *Socs2*$^{-/-}$ mice.

Growth of female WT and *Socs2*$^{-/-}$ mice was comparable from 14 - 22 days of age. At 23 days of age, the growth of *Socs2*$^{-/-}$ mice was significantly greater than WT ($p<0.05$). This was observed until the end point of the experiment (27 days of age). At this age, *Socs2*$^{-/-}$ mice had grown 46% more than WT mice ($p<0.001$) (Fig. 5.7A). This is in contrast to male mice where no divergence in growth was observed between *Socs2*$^{-/-}$ and WT (Fig. 5.2A).

GH treatment of female WT mice (starting 14 days of age) did not alter growth until day 9 of treatment (23 days of age). At this point, growth of GH treated mice was significantly greater than vehicle treated ($p<0.05$). By day 13 (27 days of age), GH treated WT mice had grown 30% more than vehicle treated ($p<0.001$) (Fig. 5.7B). This is in contrast to male WT mice that showed no alteration in growth in response to GH (Fig. 5.2B). GH treated *Socs2*$^{-/-}$ mice showed increased growth from 6 days of treatment (20 days of age) ($p<0.05$). By 13 days of GH treatment (27 days of age), *Socs2*$^{-/-}$ mice had grown 44% more than vehicle treated mice ($p<0.001$) (Fig. 5.7B). *Socs2*$^{-/-}$ mice tended to show a greater increase in growth in response to GH compared to WT, however this was not significant.

5.5.8 Final measurements from female mice treated with GH

Increased growth in response to GH in female mice was at the end of the study (day 27) associated with increased weight (WT 20%, $p<0.01$; *Socs2*$^{-/-}$ 27%, $p<0.01$) and nose to rump length (WT 5%; $p<0.01$; *Socs2*$^{-/-}$ 6%, $p<0.05$ (Table 5.4). No alterations were observed in tail, tibia, or femur length in GH treated WT or *Socs2*$^{-/-}$ mice. No

significant differences were observed between vehicle treated WT and *Socs2*$^{-/-}$ mice (Table 5.4). This indicates that at this age (27 days), despite the increase in growth rate observed in *Socs2*$^{-/-}$ mice (section 5.5.7), the overgrowth phenotype is not yet apparent.

5.5.9 Regulation of GH induced signalling in female liver and bone by SOCS2

At 24 days of age (WT and *Socs2*$^{-/-}$ mouse growth rate increase in response to GH), liver p-STAT5 was not significantly increased in WT or *Socs2*$^{-/-}$ mice after GH challenge (Fig. 5.8). There was a trend towards increased phosphorylation in both genotypes by GH, however high levels of variability meant that this did not reach statistical significance (Fig. 5.8). Contrasting to male results (section 5.5.4, Fig. 5.4), there was no apparent exaggeration of STAT5 activation in the liver of *Socs2*$^{-/-}$ female mice. GH treatment did not result in activation of the AKT or ERK1/2 pathways in liver from WT or *Socs2*$^{-/-}$ mice (Fig. 5.8).

High variability between bone samples meant that no significant differences in signalling were observed between WT and *Socs2*$^{-/-}$ mice in response to GH. Exaggerated STAT5 activation was noted in two of the three bone samples from *Socs2*$^{-/-}$ mice challenged by GH. However the third sample showed no p-STAT5 (Fig. 5.8). GH treatment did not result in activation of AKT or ERK1/2 pathways in bone from WT or *Socs2*$^{-/-}$ mice (Fig. 5.8).

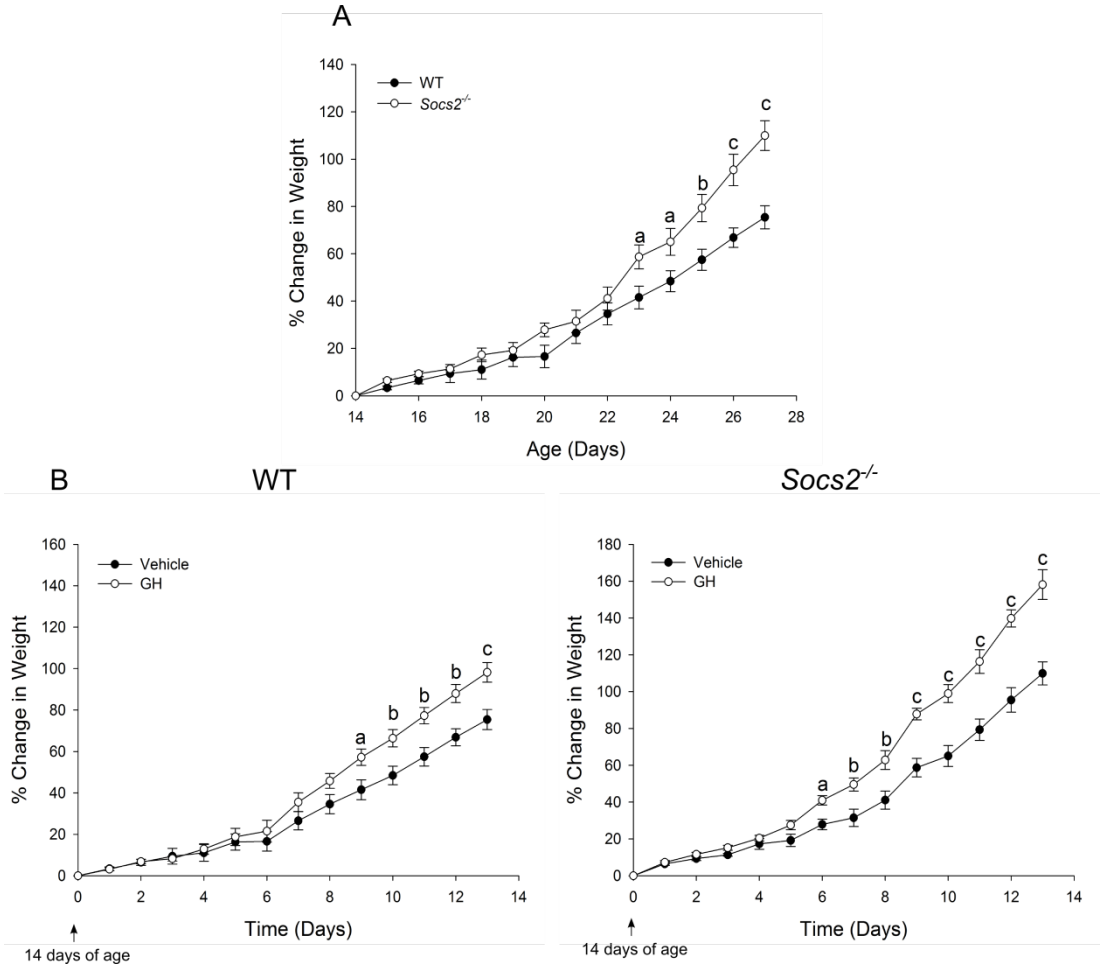

Figure 5.7 GH stimulates growth of female WT and *Socs2*$^{-/-}$ mice

A. Weight gain of WT and *Socs2*$^{-/-}$ mice from 14-27 days of age. **B.** Growth of WT and *Socs2*$^{-/-}$ mice in response to GH (3mg/kg) from 14-27 days of age. Data are presented as mean ± SEM (n≥5). Significance from vehicle treated mice is denoted by ^{a} $p<0.05$, ^{b} $p<0.01$, ^{c} $p<0.001$.

Table 5.4 Increased weight and length in WT and *Socs2*$^{-/-}$ female mice following GH treatment

Final measurement from 27 day old female WT and *Socs2*$^{-/-}$ mice treated with GH (3mg/kg) for 14 days.

Genotype	Treatment	Weight (g)	Nose to Rump Length (mm)	Tail Length (mm)	Femur Length (mm)	Tibia Length (mm)
WT	Vehicle	12.7 ± 0.59	75.6 ± 0.95	51.4 ± 2.57	11.0 ± 0.19	14.3 ± 0.20
	GH	15.2 ± 0.50[b]	79.5 ± 0.76[b]	55.0 ± 0.93	11.3 ± 0.21	14.9 ± 0.20
Socs2$^{-/-}$	Vehicle	12.2 ± 0.75	72.9 ± 1.58	53.1 ± 2.95	10.7 ± 0.28	13.9 ± 0.29
	GH	15.5 ± 0.88[b]	77.0 ± 0.51[a]	55.5 ± 2.87	11.0 ± 0.14	14.6 ± 0.30

Data are presented as mean ± SEM (n≥5). Significance from genotype matched vehicle treated mice is denoted by [a] $p<0.05$ [b] $p<0.01$.

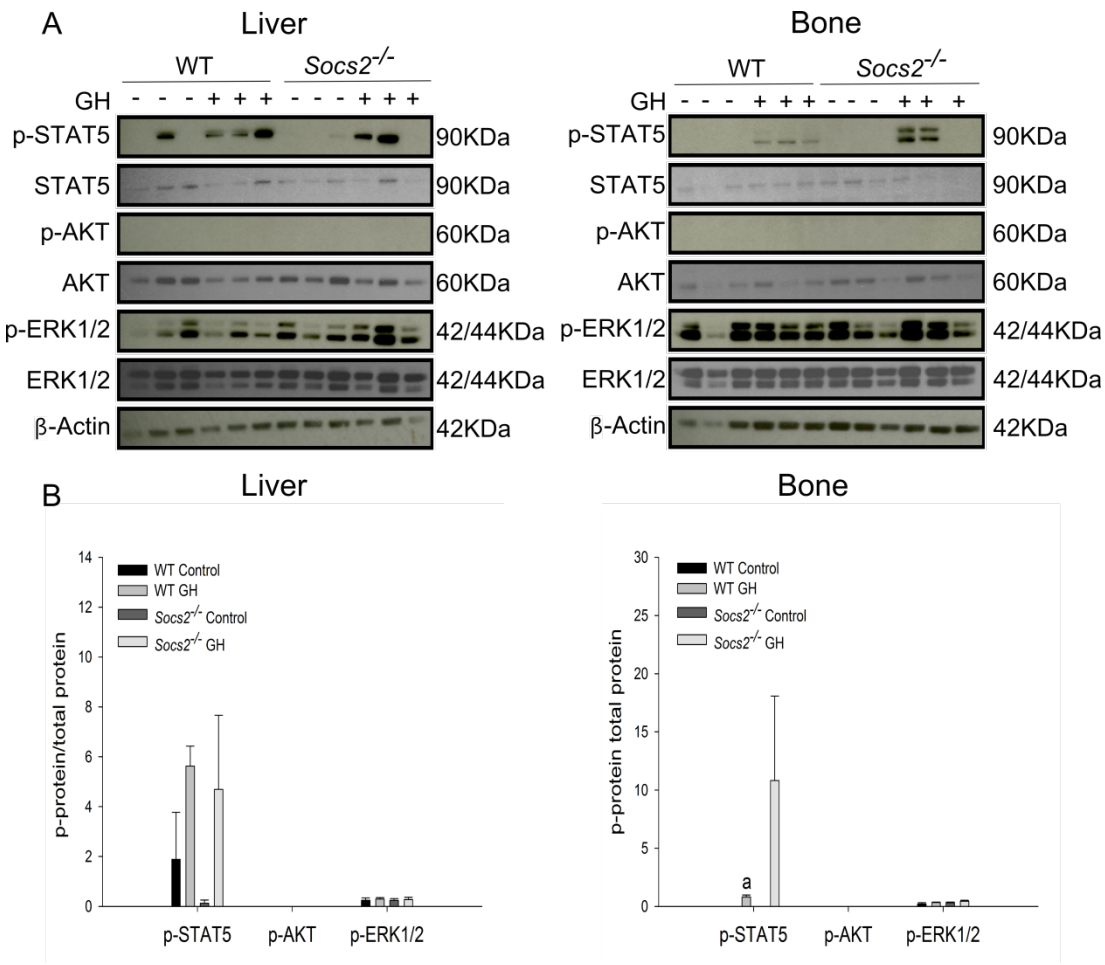

Figure 5.8 No obviously enhanced signalling in liver and bone from 24 day old female *Socs2*$^{-/-}$ mice following GH treatment

A. Western blotting of phosphorylated (P-) STAT5, AKT and ERK1/2 in liver or tibia extracted from 24 day old WT and *Socs2*$^{-/-}$ mice following 15mins GH (3mg/kg) treatment. β-actin proteins shown as loading controls. **B.** Quantification of densitometry analysis of western blotting. Data presented as p-protein normalised to total protein. All data presented as mean ± SEM (n=3). Significance from genotype matched vehicle treated samples (control) is denoted by ^{a} $p<0.05$.

5.5.10 Regulation of GH induced mRNA expression levels in liver and bone by SOCS2 in female mice

GH treatment increased *Socs2* levels in the liver (4.04 fold; $p<0.001$) and bone (1.91 fold; $p<0.05$) of female WT mice (Fig. 5.9A). *Igf1* levels were also increased in liver in response to GH in WT (2.44 fold; $p<0.01$) and *Socs2*$^{-/-}$ (2.08 fold; $p<0.05$) mice. There was however no significant difference between the levels of increase observed in each genotype. A similar increase was not observed in bone (Fig. 5.9B). This increase in liver *Igf1* levels did not translate to an increase in systemic IGF-1 levels, as measured by serum IGF-1 ELISA (Table 5.5). *Igfbp3* levels were not altered by GH treatment in liver or bone from WT or *Socs2*$^{-/-}$ mice (Fig 5.9C).

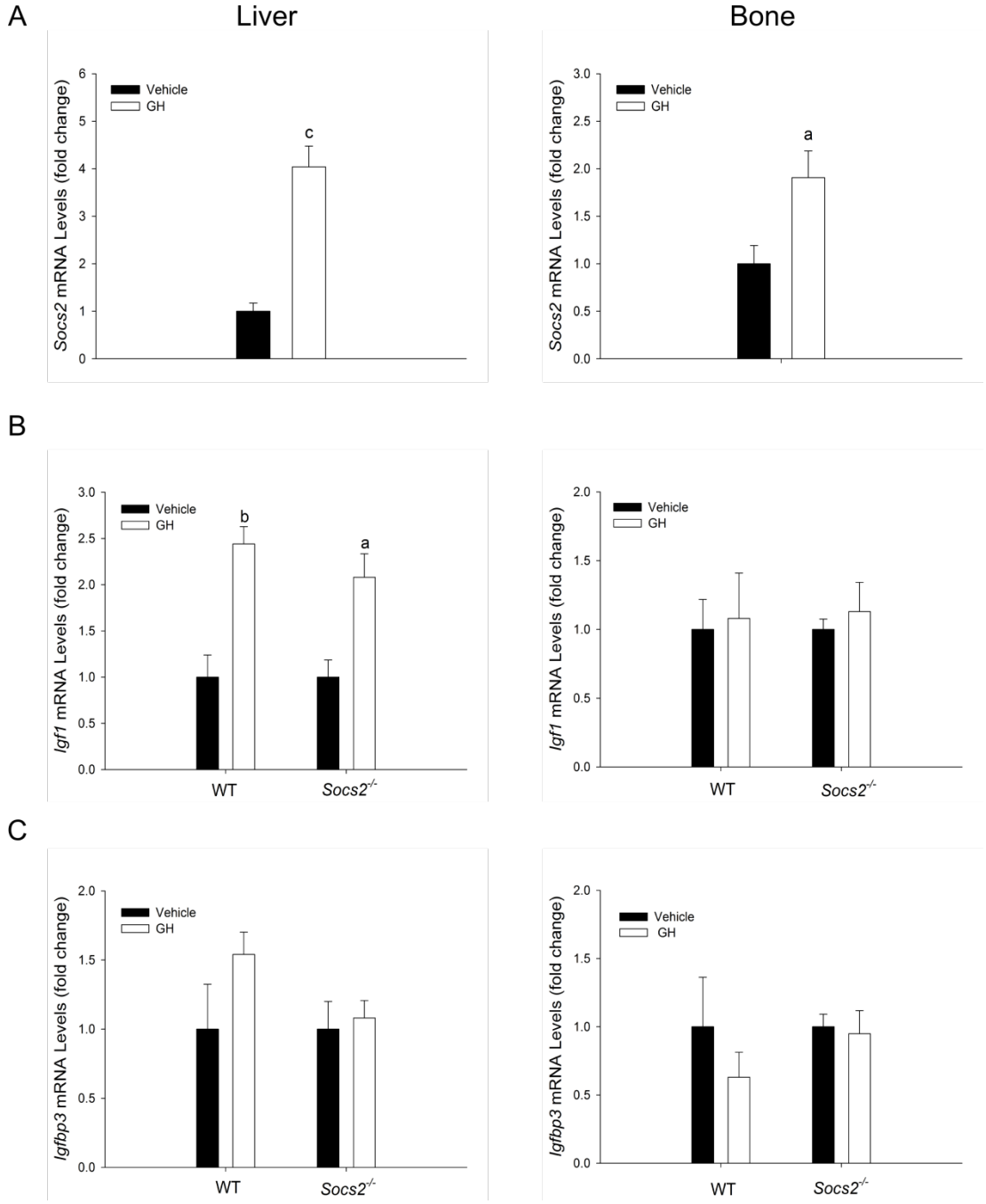

Figure 5.9 No alteration in *Igf1* and *Igfbp3* mRNA expression levels in liver and bone from female *Socs2*$^{-/-}$ mice following GH (3mg/kg) treatment

A. *Socs2* mRNA expression levels in liver and bone from female WT mice at 27 days of age following 14 days GH (3mg/kg) treatment. **B.** *Igf1* and **C.** *Igfbp3* mRNA expression levels in liver and bone from female WT and *Socs2*$^{-/-}$ mice at 27 days of age following 14 days GH (3mg/kg) treatment. Data are presented as mean ± SEM (n≥4) relative to untreated samples. Significance from genotype matched vehicle treated samples is denoted by [a] $p<0.05$, [b] $p<0.01$, [c] $p<0.001$.

Table 5.5 No alteration in female serum IGF-1 levels following GH treatment

Serum IGF-1 levels in 27 day old female WT and *Socs2*$^{-/-}$ mice following 14 days GH (3mg/kg) treatment.

Treatment	WT			*Socs2*$^{-/-}$		
Vehicle	338.1	±	33.96	297.1	±	26.82
GH	331.8	±	16.23	336.4	±	34.73

Data are presented as mean ± SEM (n≥5).

5.5.11 Growth of female and male WT mice treated with GH

The increased growth of WT female, but not male mice in response to GH was an unexpected finding. To help understand the extent of the sex specific differences in GH responsiveness, and to help identify potential mechanisms behind this, further analysis was completed by directly comparing male and female WT mice.

Comparison between vehicle treated male and female mice revealed a divergence of growth rate at 22 days of age (Fig. 5.10). Between 22-27 days of age, males showed a significant increase in weight gain compared to females ($p<0.001$). This period of sexually dimorphic growth coincided with the age (23-27 days of age) at which female mice showed increased growth in response to GH (Fig. 5.10). There was no significant difference in weight gain between vehicle treated male mice, GH treated male mice, and GH treated female mice (Fig. 5.10).

5.5.12 Micro-CT analysis of femur from WT female mice treated with GH

Analysis of cortical geometry revealed anabolic changes to the femur of GH treated female WT mice at 27 days of age. These mice had increased Tt.Ar (18%; $p<0.01$), Ct.Ar (28%; $p<0.01$), Ma.Ar (14%; $p<0.05$), and polar moment of inertia (J) (145%; $p<0.001$) (Table 5.6). No changes in cortical thickness were observed (Table 5.6). The increase in bone parameters noted here in GH treated female mice was not observed in GH treated male WT mice (Section 5.5.3 & Table 5.2). These data are shown in Table 5.6 to make gender specific comparisons easier. Despite the divergence in growth rates from 22-27 days of age (section 5.5.11), there were no changes in cortical geometry between vehicle treated female and male mice (Table 5.6).

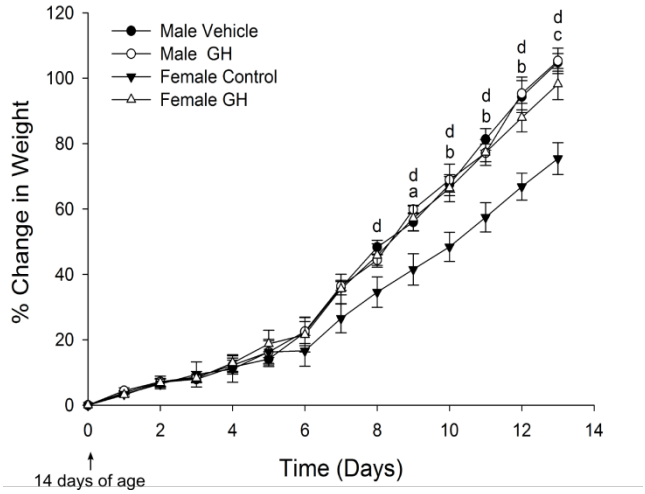

Figure 5.10 Sexually dimorphic response to GH coincides with growth divergence

Weight gain of female and male WT mice in response to GH (3mg/kg) treatment from 14-27 days of age. Data are presented as mean ± SEM. (n≥6). Significance denoted by; female GH treated from female vehicle treated [a] $p<0.05$, [b] $p<0.01$, [c] $p<0.001$; male vehicle treated and GH treated from female vehicle treated [d] $p<0.001$.

Table 5.6 Gender specific differences on the effects of GH on cortical geometry

Micro-CT analysis of tibia from 27 day old female and male WT mice treated with GH (3mg/kg) for 14days.

	Female		Male	
	Vehicle	GH	Vehicle	GH
Tt.Ar (mm^2)	1.43 ± 0.031	1.69 ± 0.070[b]	1.33 ± 0.051	1.30 ± 0.070
Ct.Ar (mm^2)	0.43 ± 0.025	0.55 ± 0.036[b]	0.45 ± 0.023	0.43 ± 0.023
Ma.Ar (mm^2)	1.00 ± 0.024	1.14 ± 0.079[a]	0.88 ± 0.032	0.87 ± 0.048
Ct.Th (mm)	0.11 ± 0.006	0.13 ± 0.007	0.12 ± 0.003	0.12 ± 0.003
J (mm^4)	0.17 ± 0.011	0.27 ± 0.020[c]	0.17 ± 0.018	0.15 ± 0.017

Data are presented as mean ± SEM (n≥5). Tt.Ar = total area, Ct.Ar = cortical area, Ma.Ar = marrow area, Ct. Th = cortical thickness, and J = polar moment of inertia. Significance from sex matched vehicle treated mice is denoted by [a] $p<0.05$, [b] $p<0.01$.

5.5.13 Gender specific differences in GH signalling in liver and bone

The importance of STAT5 signalling in mediating GHs gender specific control of growth was investigated. In light of the data presented in sections 5.5.4, 5.5.5, and 5.5.9, AKT and ERK1/2 phosphorylation were not measured.

At 24 days of age, GH treatment significantly increased p-STAT5 levels in liver from female mice ($p<0.05$; Fig. 5.11). An increase was not observed in liver from male mice. A significant increase in total STAT5 levels in female compared to male liver samples meant that for quantification p-STAT5 levels were normalised to β-actin, and not STAT5 as before (Fig. 5.11C). GH treatment greatly stimulated p-STAT5 levels in bone dissected from female ($p<0.001$), but not male mice (Fig. 5.11).

At 17 days of age, GH treatment significantly increased p-STAT5 levels in liver from female mice ($p<0.05$). Although an increase was observed in male mice, this did not reach significance (Fig. 5.12). GH treatment of female and male mice did not significantly increase p-STAT5 levels in bone (Fig. 5.12).

Taken together, these data indicate that female mice appear to be more sensitive to GH as measured by activation of p-STAT5 signalling in liver and bone. This enhanced sensitivity may explain the increased growth and bone formation of female mice when challenged by GH (Fig. 5.10 & Table 5.6).

5.5.14 Alterations in gene expression in liver and bone from female and male mice

Data presented in sections 5.5.6 & 5.5.10 emphasised the different effects of GH on gene expression in mouse liver and bone. However, it was also of interest to assess the differences in basal gene expression to assess if key genes may play a role in the sexually divergent growth.

Socs2 expression levels were significantly elevated in bone samples from male mice (2.34 fold; $p<0.05$), but not in the liver (Fig. 5.13A). *Igf1* and *Igfbp3* expression levels

were similar in bone from female and male mice, but were significantly elevated in male liver compared to female (*Igf1* 2.45 fold; $p<0.01$, *Igfbp3* 1.81 fold; $p<0.05$) (Figs. 5.13B&C). This increase in hepatic *Igf1* in male mice did not however translate to an increase in systemic IGF-1 levels (Tables 5.3 & 5.5).

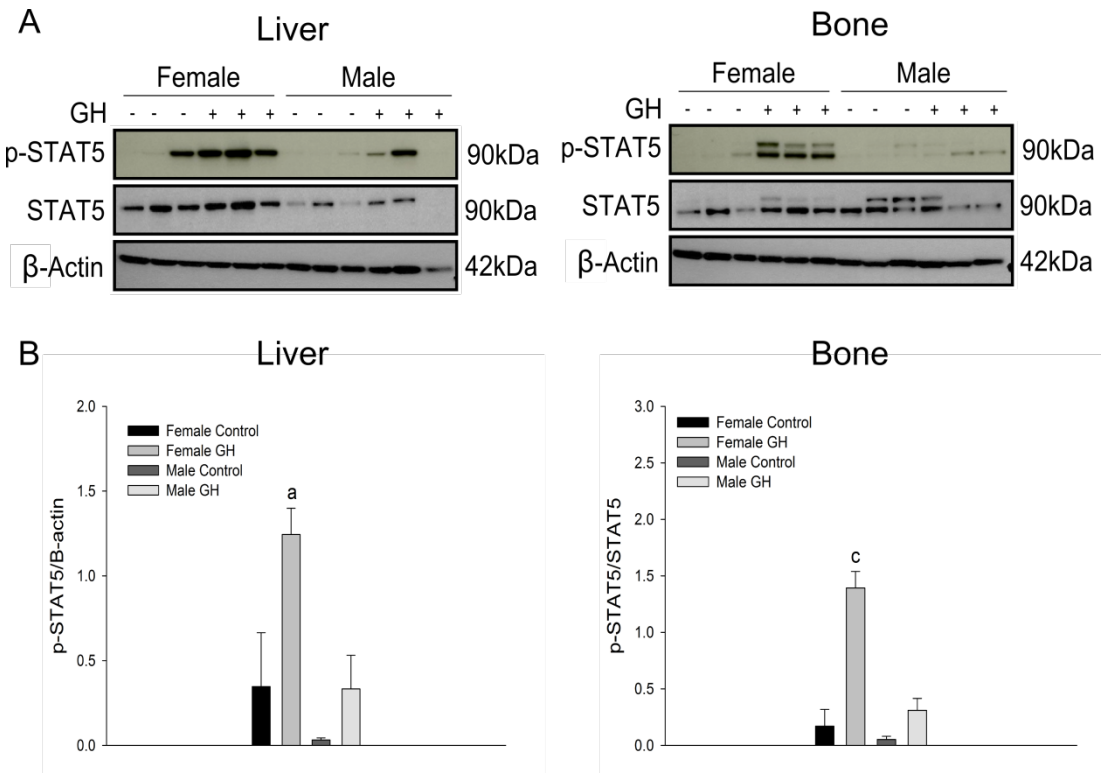

Figure 5.11 Exaggerated STAT5 activation in liver and bone from 24 day old female mice following GH treatment

A. Western blotting of phosphorylated (P-) STAT5 in liver or tibia extracted from 24 day old female and male mice following 15mins GH (3mg/kg) treatment. β-actin proteins shown as loading controls. **B.** Quantification of densitometry analysis of western blotting measuring total STAT5 levels relative to β-actin in liver from 24 day old female and male mice. Data presented as mean ± SEM (n=6). Significance denoted by ^{b} $p<0.01$. **C.** Quantification of densitometry analysis of western blotting. Liver data presented as p-STAT5 relative to β-actin. Bone data presented as p-STAT5 normalised to total STAT5. All data presented as mean ± SEM (n=3). Significance from sex matched vehicle treated samples (control) is denoted by ^{a} $p<0.05$, ^{c} $p<0.001$.

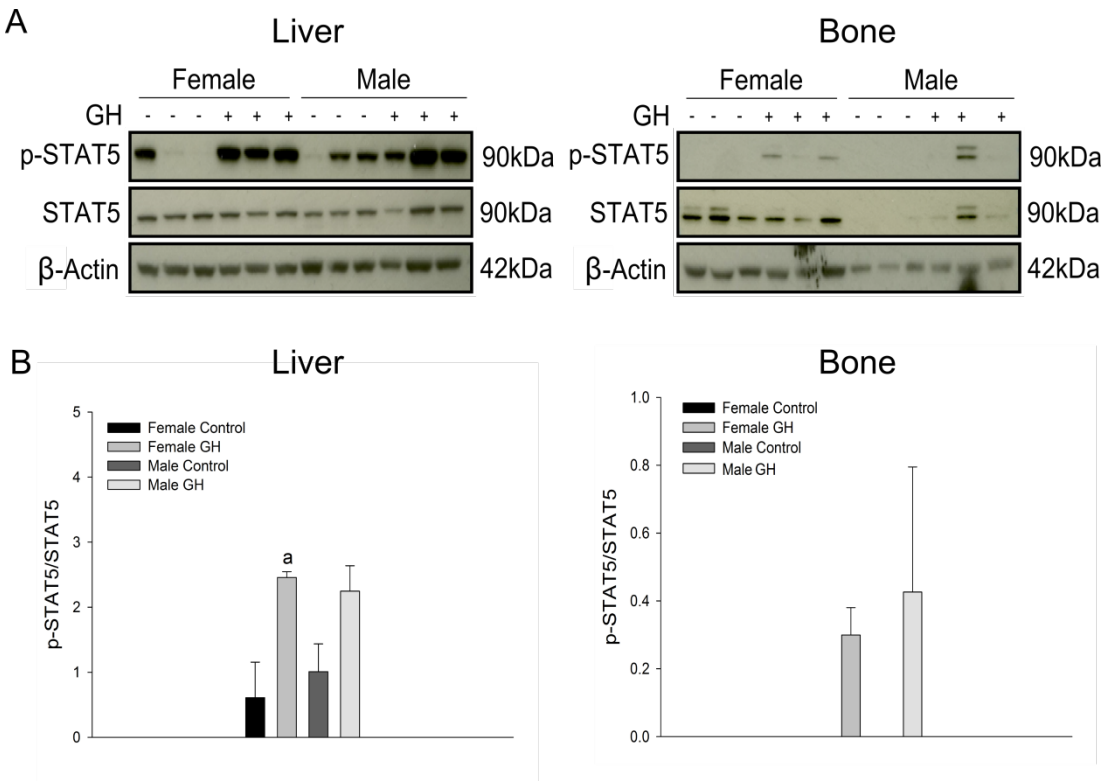

Figure 5.12 No exaggerated STAT5 activation in liver and bone from 17 day old female mice following GH treatment

A. Western blotting of phosphorylated (P-) STAT5 in liver or tibia extracted from 24 day old female and male mice following 15mins GH (3mg/kg) treatment. β-actin proteins shown as loading controls. **C.** Quantification of densitometry analysis of western blotting. Data presented as p-STAT5 normalised to total STAT5 (n=3). All data presented as mean ± SEM Significance from sex matched vehicle treated samples (control) is denoted by [a] $p<0.05$.

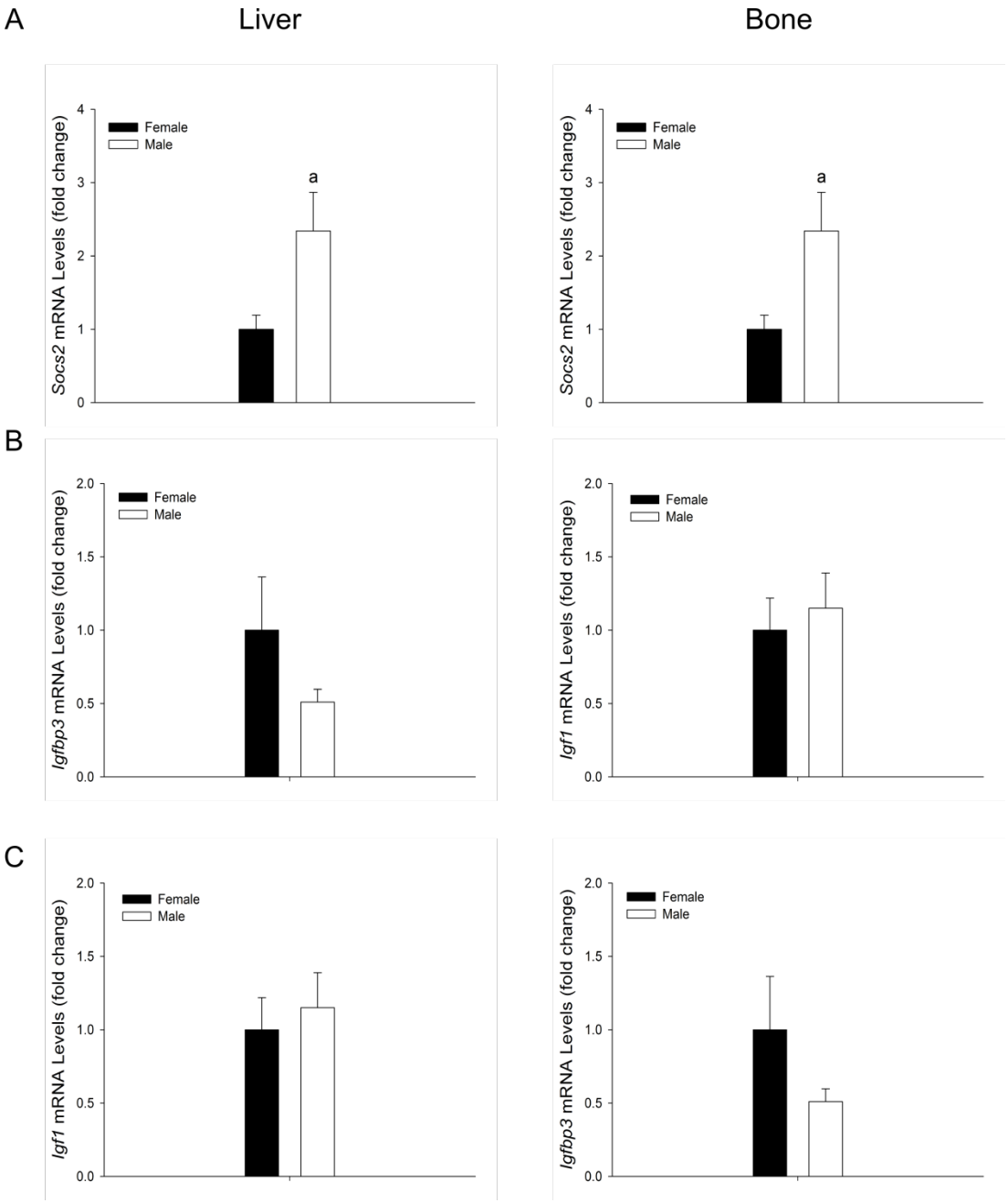

Figure 5.13 Altered gene expression in liver and bone in 27 day old female mice compared to male mice

Socs2 **(A)**, *Igf1* **(B)**, or *Igfbp3* **(C)** mRNA expression levels in liver and bone from 27 day old female and male mice. Data presented as mean ± SEM (n=5) relative to female samples Significance from female samples is denoted by [a] $p<0.05$, [b] $p<0.01$.

5.6 Discussion

Following analysis of the results presented in chapter 5 the main hypothesis was accepted. Increased bone formation in GH treated Socs2$^{-/-}$ mice is associated with increased local STAT5 activation, but not changes in local *Igf1* expression. The key findings of this chapter are summarised in Fig. 5.14.

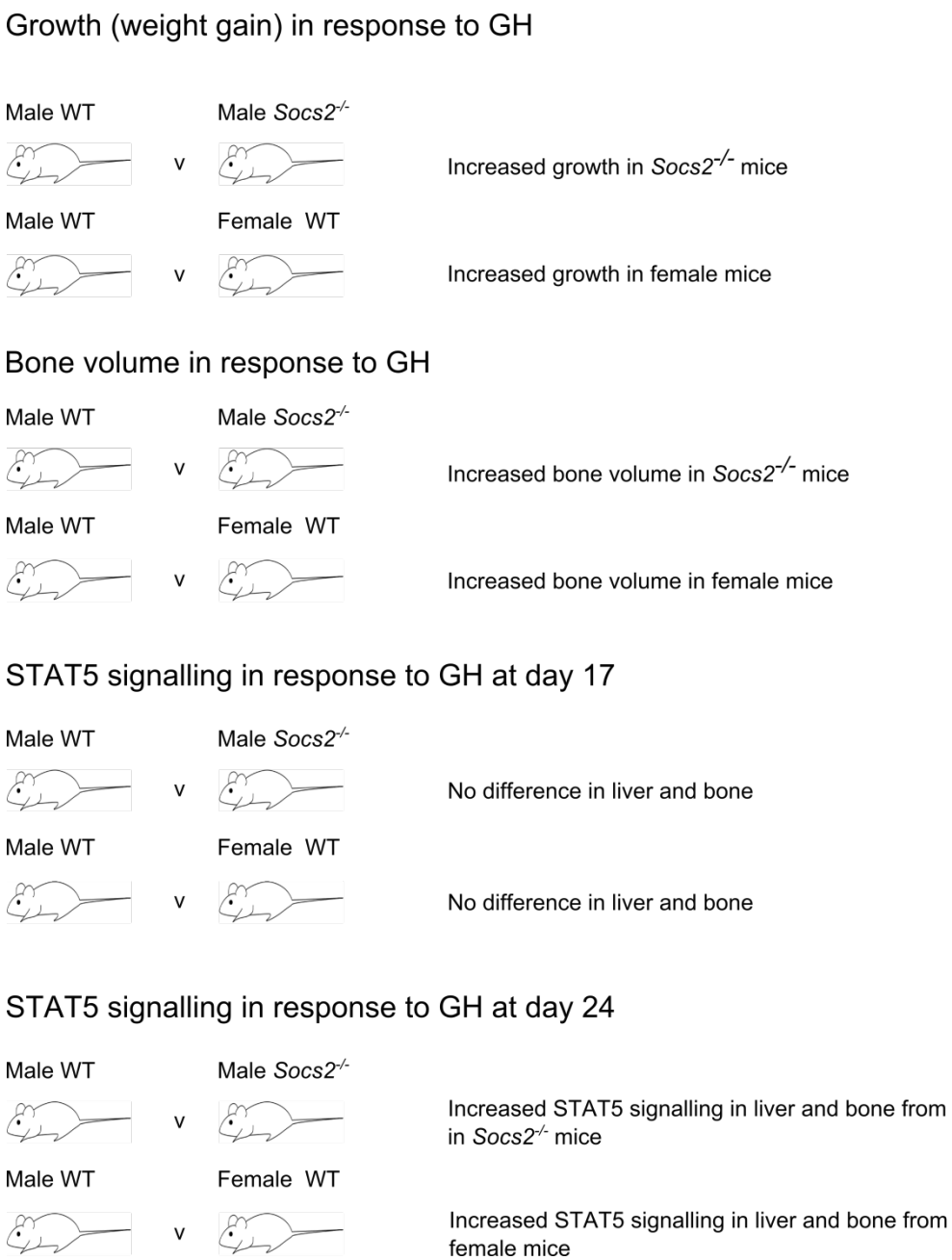

Figure 5.14 Summary of the key findings in chapter 5.

As reported in chapter 4 of this thesis, *Socs2*$^{-/-}$ mice are characterised by their overgrowth skeletal phenotype despite no elevation in systemic GH or IGF-1 levels (Metcalf *et al.* 2000; Greenhalgh *et al.* 2002a; MacRae *et al.* 2009). In accordance with this, the present study found that the anabolic bone phenotype observed in GH treated male *Socs2*$^{-/-}$ mice was not associated with an increase in hepatic *Igf1* expression or systemic IGF-1 levels (Fig. 5.6 & Tables 5.2, 5.3. These observations underline the importance of local GH signalling in mediating growth, and confirm the value of the *Socs2*$^{-/-}$ mouse model in investigating GH's direct (IGF-1 dependent or independent) effects. The importance of systemic IGF-1 in mediating GH action on bone development is further questioned by the observation that GH treatment promotes bone accrual in young female mice, despite no elevation in systemic IGF-1 levels. Similar results have been reported in relation to longitudinal bone growth in rats (Rol De Lama *et al.* 2000).

Hepatic STAT5 (but not ERK1/2 and AKT) activation was enhanced in male *Socs2*$^{-/-}$ mice treated with GH compared to WT (Fig 5.4). This is likely due to the lack of a negative SOCS2 regulatory effect on GH action. GH treatment of WT mice results in the up regulation of *Socs2* expression in the liver (Greenhalgh *et al.* 2002). A comparable increase in *Socs2* expression was noted in this study (Fig. 5.6). Functioning STAT5b signalling is essential for the *Socs2*$^{-/-}$ overgrowth phenotype, and elevated hepatic STAT5 activation has been previously reported in liver from *Socs2*$^{-/-}$ mice (Greenhalgh *et al.* 2002). Given that STAT5b is important for upregulating *Igf1* expression and numerous STAT5 binding sites have been identified on the *Igf1* gene it is surprising that enhanced GH induced hepatic STAT5 activation in male *Socs2*$^{-/-}$ mice did not result in raised hepatic IGF-1 transcript and systemic levels (Fig. 5.6) (Davey *et al.* 1999a; Davey *et al.* 2001; Eleswarapu *et al.* 2008). It has been suggested that STAT5 proteins are weak activators of transcription, and require co-activators to achieve this (Kornfeld *et al.* 2008). Hepatocyte nuclear factor 1α (HNF1α) (a transcription factor) upregulates the co-activator glucocorticoid receptor, which interacts with GH induced STAT5 to promote growth (Tronche *et al.* 2004). Furthermore, optimal GH dependent

activation of a salmon *Igf1* promoter construct requires the expression of both STAT5 and HNF1α (Meton *et al.* 1999). It is therefore possible that enhanced IGF-1 production in response to GH requires a number of cofactors that are not all elevated in *Socs2*$^{-/-}$ mice. Interestingly, liver *Igf1* expression levels were elevated to a similar level in female WT and *Socs2*$^{-/-}$ mice (Fig. 5.9). This did not however result in an increase in systemic IGF-1 levels, suggesting that, at least in the case of females, increased hepatic *Igf1* levels are insufficient to increase systemic IGF-1 levels. Further studies are required to investigate the relationship between enhanced hepatic STAT5 signalling and systemic IGF-1 levels.

It is widely understood that GH is anabolic to the skeleton. *Ghr*$^{-/-}$ mice have a catabolic bone phenotype, whereas GH overexpression increases bone size (Sims *et al.* 2000; Sjogren *et al.* 2000; Eckstein *et al.* 2004). GH treatment promotes periosteal bone formation in aged rats (Andreassen *et al.* 1995). This effect is also observed in zero gravity conditions, highlighting that it is not a secondary effect of increased weight (Ohlsson *et al.* 1998). There is little evidence for the effects of GH treatment in mice with normal GH secretion. The present study demonstrates that exogenous GH is unable to alter bone growth in young male WT mice (Table 5.2). GH treatment did however stimulate body and bone growth of male *Socs2*$^{-/-}$ mice indicating a key role for SOCS2 in GH regulation at this age (Fig. 5.2 & Table 5.2). The increase in bone volume in GH treated male *Socs2*$^{-/-}$ mice was associated with an exaggerated p-STAT5 signalling response in bone, but this was not coupled with an increase in *Igf1* expression (Figs. 5.4 & 5.6). This infers that IGF-1 may not be central in mediating local GH action. An IGF-1 independent action of GH on bone formation is suggested by the responsiveness of global *Igf1*$^{-/-}$ mice to GH treatment (Bikle *et al.* 2001).

Previous studies focusing on the effects of GH on early postnatal development have either failed to consider the sex of animals studied or focused primarily on a single gender. GH has been shown to have a peak activity between 20-40 days of age, as is

apparent by the reduced linear growth rate of *Ghr*$^{-/-}$ mice. The sex of the *Ghr*$^{-/-}$ animals used in this study are however unknown (Wang *et al.* 2004). This is also apparent in a study that identifies a period of early postnatal growth that cannot be stimulated by GH treatment (Liu & LeRoith 1999). Analysis of *Ghr*$^{-/-}$ mice revealed a tendency for females to be heavier than males. This did not reach significance, and the authors therefore combined sexes for future analysis (Lupu *et al.* 2001). The present study has shown a sex specific response to GH that manifests at approximately 3 weeks of age (Fig 5.10). Young (17 day old) male and female mice display similar GH induced signalling and no alteration in growth. A time point selected after 3 weeks of age (24 days) highlights that female mice are more responsive to GH treatment. These mice have elevated p-STAT5 levels in liver and bone (Fig 5.11). This increased STAT5 activation is likely responsible for mediating the increased growth and anabolic bone phenotype that is not observed in male mice. Interestingly, the switch from GH unresponsive to GH responsive growth in females coincides with the point at which male and female growth diverges (Goedbloed 1980; Lupu *et al.* 2001). The sexual dimorphic growth pattern is generally considered to arise due to differences in GH secretion patterns (Jansson *et al.* 1985; Chowen *et al.* 2004). In male mice, this consists of pulses of GH secretion with minimal interpulse GH levels. In females, there are also pulses of GH, but these occur more frequently than in males (Macleod *et al.* 1991). The extended interpulse interval in males results in sexually dimorphic liver gene expression and growth patterns that emerge at puberty (Davey *et al.* 1999b). It is therefore possible that the twice daily injections of female mice more closely resembles the male secretion pattern, and therefore stimulates female growth to a male level. Further studies assessing the differences in continuous and intermittent GH to young female mice are needed to investigate this. A sex specific response to GH has also been demonstrated in peripubertal rats. Female rats show increased body and tibial growth, whereas male rats do not (Rol De Lama *et al.* 2000). It is proposed that this is due to the inability of GH to further stimulate maximal growth in peripubertal male rats. GH stimulation of older rats promotes growth (Rol De Lama *et al.* 2000).

Ghr$^{-/-}$ mice show limited radial bone expansion during puberty, and no sexual dimorphism. This indicates that GH is key in determining pubertal bone growth (Callewaert *et al.* 2010). The sex specific effects of GH treatment on young mice have not previously been demonstrated. The anabolic bone phenotype of GH overexpressing mice is more evident in males. These mice have increased cortical cross-sectional area (apparent from 6 weeks of age). There are no changes in transgenic females (Eckstein *et al.* 2004). Similarly, *Socs2*$^{-/-}$ mice (characterised by the overgrowth phenotype due to enhanced GH signalling) show sex specific alterations in the skeletal phenotype (chapter 4). The data presented here shows that female mice are responsive to GH with increased growth and an anabolic cortical bone phenotype (Fig. 5.10 & Table 5.6). This sex specific difference may be an age dependent effect. Although analysis of bone was not completed in the study, an increase in weight is observed in 3 week old GH overexpressing female, but not male mice. Analysis of older mice reveals a bone overgrowth phenotype in males (Eckstein *et al.* 2004).

Lower *Socs2* transcript levels in bone from female mice indicate that sex specific differences in the expression of *Socs2* may be responsible for the difference in responsiveness to GH treatment (Fig 5.13). *Socs2* levels have previously been shown to be equally expressed in male and female rat liver, muscle, and fat (Tollet-Egnell *et al.* 1999). A similar result was obtained with regards to liver in the current study. Oestrogen has been implicated in the upregulation of GH signalling in human osteoblasts through the down regulation of SOCS2 expression (Bolamperti *et al.* 2013). It is therefore possible that an increase in oestrogen in female mice at this age may act to lower SOCS2 and therefore increase responsiveness to GH.

During the period of GH stimulated growth of females, increased STAT 5 activation was observed in liver and bone (Fig. 5.11). It must be noted that at this age liver p-STAT5 levels were measured relative to β-actin. This was required as total STAT5 levels were higher in livers from female mice at this age. A study looking at p-

STAT5 levels in liver found no differences between genders. This was completed in 2.5 week old mice (Martinez *et al.* 2013). The lack of a sex specific difference in STAT5 activation is similar to the results obtained in 17 day old mice in the present study (Fig. 5.12). This suggests that these effects are age dependent, manifesting after 3 weeks. It was hypothesised that these differences may be due to the role of sex steroids in regulating GH action. The role of oestrogen is still a matter of debate. Oestrogen has previously been shown to limit appendicular bone growth in rats, through inhibition of GH-dependent mechanisms (Zhang *et al.* 1999). Studies on mice however reveal that oestrogens inhibit cortical bone growth despite no alteration in systemic IGF-1 levels. The authors concluded that oestrogen's effects are therefore independent of the GH-IGF-1 axis (Callewaert *et al.* 2010). This conclusion fails to address the possibility of oestrogen regulating GH at the local level (bone). Ovariectomy of GH-transgenic mice impairs development of bone mass, thus suggesting that sex hormones are required for GH to exert its anabolic actions (Sandstedt *et al.* 1996). In males, oestrogens are thought to promote radial bone expansion through stimulation of the GH-IGF-1 axis (Venken *et al.* 2006; Callewaert *et al.* 2010). It is widely accepted that androgens stimulate bone growth independent of the GH-IGF-1 axis (Venken *et al.* 2006; Callewaert *et al.* 2009; Callewaert *et al.* 2010).

The mechanisms behind the GH unresponsive phase (embryonic and early postnatal) in mice are poorly understood. STAT5 activation is present in liver of 1 week old mice following GH treatment. The levels of phosphorylation however are less compared to older mice. This may be due to the lower levels of GHR, or increased levels of CIS and PTP1B (negative regulators) (Martinez *et al.* 2013). The current study found STAT5 phosphorylation in liver and bone from 17 day old animals following GH treatment. It therefore appears that young mice are responsive to GH treatment. This however is not sufficient to promote growth. Previous studies in rats have also observed STAT5 activation in foetal liver. This is a

point at which growth is widely considered to be GH independent (Phornphutkul *et al*. 2000).

In conclusion, the present study highlights the importance of SOCS2 in regulating GH induced bone growth. Identification of two models (*Socs2*$^{-/-}$ model and young female WT model) allows assessment of the importance of IGF-1 in mediating GH action. The increased growth and anabolic bone phenotype observed in male *Socs2*$^{-/-}$ and female WT and *Socs2*$^{-/-}$ mice, despite no elevation in systemic IGF-1 levels or bone *Igf1* transcript levels, suggests an important role for local GH action independent of IGF-1 in regulating bone mass. The activation of the STAT5 pathway is identified as being closely linked to the increase in growth, and is likely a key pathway in mediating the growth promoting effects of GH.

Chapter 6

Inflammatory induced bone loss in experimental colitis: role of SOCS2

6.1 Introduction

IBD is the term used to describe inflammatory conditions of the gastrointestinal tract; ulcerative colitis (UC), and Crohn's disease (CD). UC is limited to the colon, and characterised by lamina propria inflammation, and bowel epithelium destruction. CD can affect the entire digestive system, and is characterised by transmural inflammation and fibrosis (Sartor 1997). The aetiology of IBD remains poorly understood, however a number of genetic and environmental factors have been implicated in the pathogenesis (Papadakis & Targan 2000). IBD is common in the Western world, and within the USA it is ranked amongst the 5 most prevalent gastrointestinal diseases with 1.4 million sufferers, and an annual health care costs exceeding $1.7billion (Sandler *et al.* 2002; Lakatos 2006), Similar prevalence rates are noted elsewhere. In Europe 2.2 million people are affected (Alexeeva *et al.* 1994). In addition to the well-recognised gut inflammation, there are a number of extra-intestinal manifestations associated with IBD. Adults with IBD are at increased risk of developing osteoporosis with a relative risk of fracture that is 40% higher than normal (Compston *et al.* 1987). Children with IBD may also have a higher risk of fractures, especially in the vertebrae (Laakso *et al.* 2012; Wong *et al.* 2014). Recent studies in children have shown that trabecular bone density, reduced at diagnosis, showed inadequate improvement despite control of the underlying inflammation (Dubner *et al.* 2009). In addition, these patients have thinner and smaller bones (Dubner *et al.* 2009; Tsampalieros *et al.* 2013). Peak bone mass is compromised in childhood onset IBD despite adequate control of disease and progression through puberty (Laakso *et al.* 2014).

In order to increase the understanding of IBD, a number of mouse models have been generated. These include several gene-knockout strains which develop colitis (*Il2*$^{-/-}$ and *Il10*$^{-/-}$ (Sadlack *et al.* 1993; Kuhn *et al.* 1993)), and models where inflammation is chemically induced (dextran sodium sulphate (DSS) model and trinitrobenzene sulfonic acid (TNBS) model (Morris *et al.* 1989; Okayasu *et al.* 1990)). Colitis develops spontaneously in *Il10*$^{-/-}$ mice; a T helper cell regulatory cytokine (Kuhn *et al.* 1993;

Berg *et al.* 1996). IL-10 deficiency alone leads to a disruption of the intestinal immune response due to a failure in regulating the actions of $CD4^+$ T cells and the production of proinflammatory cytokines (Cohen *et al.* 2004). The onset and severity of colitis varies depending on mouse strain. Mice on a 129/SvEv and Balb/C background, develop severe colitis more rapidly than mice on a C57BL/6 background (Berg *et al.* 1996). Chronic inflammation can also be induced in *Il10*$^{-/-}$ mice challenged with non-steroidal anti-inflammatory drugs such as sulindac sulfone and piroxicam. Piroxicam treatment is thought to enhance apoptosis of the intestinal epithelium and facilitate adhesion and invasion of intestinal bacteria into the mucosal tissue (Hale *et al.* 2005). These drugs have little effect on WT gut inflammation when used alone (Berg *et al.* 2002; Hale *et al.* 2005). Inflammation in the *Il10*$^{-/-}$ mice closely resembles CD (MacDonald 1994; Rennick *et al.* 1997).

Chemically induced models are the most widely studied due to the simplicity of induction, and the relatively low cost involved. These models differ in their inflammation characterisation. DSS mice display a UC like colitis, whereas TNBS mice have a more CD like colitis. Nevertheless, both models share many similarities with the human conditions (Boismenu & Chen 2000). DSS induced inflammation is the result of deterioration of the epithelial barrier through an increase in epithelial cell apoptosis and a decrease in proliferation (Araki *et al.* 2010). The barrier exists as a physiological and immunological barrier between the mucosa and lumen. This deterioration of the epithelial barrier allows for the influx of antigens and micro-organisms, prompting an inflammatory response (Tlaskalova-Hogenova *et al.* 2005). Depending on treatment duration, DSS can be used to induce chronic or acute inflammation. Chronic inflammation is observed a number of weeks after initial DSS treatment, or can be stimulated through cyclical administration of DSS. Acute inflammation is observed soon after DSS treatment (Cooper *et al.* 1993; Dieleman *et al.* 1998; Melgar *et al.* 2005; Yan *et al.* 2009). Similar to human IBD, DSS induced colitis results in the increased production of numerous proinflammatory cytokines which are released into the blood stream (Alex *et al.* 2009; Harris *et al.* 2009).

Osteoporotic bone loss observed in people with IBD is also present in the DSS model of colitis. Both juvenile and adult treated mice present with altered trabecular architecture associated with decreased bone formation (Hamdani *et al.* 2008; Harris *et al.* 2009). The bone phenotype of *Il10*$^{-/-}$ mice is more poorly characterised, but it is known *Il10*$^{-/-}$ mice, independent of piroxicam, have a lower BMD compared to WT mice (Cohen *et al.* 2004). Both the *Il10*$^{-/-}$, and DSS induced colitic mouse model have increased proinflammatory cytokine levels (Perse & Cerar 2012; Holgersen *et al.* 2014). Proinflammatory cytokines, including IL-1β, IL-6 and TNFα have been shown to stimulate SOCS2 expression in a number of tissues (Greenhalgh & Hilton 2001; Rico-Bautista *et al.* 2006; MacRae *et al.* 2009). Given that SOCS2 has been identified as critical regulator of GH induced bone accrual (chapters 4 & 5), it is possible that SOCS2 may act as a central mediator through which pro-inflammatory cytokines inhibit the local anabolic effects of GH on bone leading to low bone mass and osteoporosis in IBD.

6.2 Hypothesis

The osteoporotic phenotype in experimental mouse models of colitis mice is associated with an increase in *Socs2* expression in bone. In the absence of SOCS2, mice with colitis will be partly protected from the bone loss phenotype.

6.3 Aims

I. Identify the bone phenotype of *Il10*$^{-/-}$ mice to assess the suitability as a model for IBD associated bone loss.

II. Establish the DSS model of experimental colitis.

III. Quantify relative levels of *Socs2* expression in bone from DSS induced colitic mice.

IV. Determine the effects of SOCS2 ablation on the gut pathology of DSS induced colitic mice.

V. Determine the effects of SOCS2 ablation on the bone phenotype of DSS induced colitic mice.

6.4 Material and Methods

6.4.1 Micro-CT analysis

Micro-CT analysis of trabecular and cortical bone of tibia from *Il10*$^{-/-}$ mice was carried out on a Skyscan 1272 scanner (Bruker) (same scanner used in chapter 5) and therefore there were appropriate modifications to the protocol outlined in section 2.4.7. The rotation step for trabecular scans was changed to 0.3° and for cortical scans to 0.4°. Two images were not averaged at each rotation angle. The remainder of the analysis was as outlined in section 2.4.7. Micro-CT analysis of DSS treated mice was completed as outlined in section 2.4.7.

6.4.2 Histology

The colon was dissected from WT and *Socs2*$^{-/-}$ mice ± DSS treatment (6 per group) and fixed and stored in 10% neutral buffer formalin. Each colon was divided into 5 transverse segments including proximal to distal portions. Embedding, staining, and sectioning of tissue was completed by the Easter Bush Pathology Department. In brief, samples were embedded using the following protocol – 70% ethanol for 1hr, 95% ethanol for 1hr, 5 washes in absolute ethanol for 1hr each, 3 washes in xylene for 1hr each. Finally, embedded in paraffin wax for 4hrs, wax changed every 1hr 20mins. 5μm sections were cut and mounted on Superfrost slides (Thermo Scientific, UK). Sections were dewaxed and dehydrated through graded alcohol solutions, immersed in Harris haematoxylin, followed by 1% eosin before being cleared and mounted in DePeX (VWR). Gut pathology was assessed on sections from all 5 gut segments with the help of Professor Elspeth Milne (Pathology Department, University of Edinburgh). Each colon was graded blind using an established histological grading scheme (Dieleman *et al.* 1998). The scoring scheme is outlined in table 6.1. Segments of colon were assessed separately for inflammation (0-3), extent (0-3), regeneration (0-4), and crypt damage (0-4). Each grade was then multiplied by the grade for percentage involved of that feature (1-4). Scores

therefore ranged from 0-12 for inflammation and extent, and 0-16 for regeneration and crypt damage. Scores from all five segments were averaged for each sample.

6.4.3 Serum IGF-1 ELISA

Immediately following sacrifice blood was collected from WT and *Socs2*$^{-/-}$ mice ± DSS treatment by cardiac puncture. Blood was stored in serum tubes (Greiner Bio-One) on ice for over 30mins to allow for clotting. Following 10mins centrifugation at 1000g supernatant was removed, aliquoted, and stored at -80°C. IGF-1 levels were assessed by ELISA (Quantikine, R&D Systems, Minneapolis, MN, USA) according to manufacturer's instructions.

6.4.4 qPCR analysis

Left femur and gastrocnemius muscle were dissected from WT and *Socs2*$^{-/-}$ mice ± DSS treatment. Both were snap frozen in liquid nitrogen and stored at -80°C. Before being snap frozen femurs had the epiphyses removed and marrow spun out by centrifugation. RNA was extracted as described in section 2.5.1. cDNA was prepared from all RNA as outlined in section 2.5.2, and qPCR analysis completed as detailed in section 2.5.3. Results were normalised to *Gapdh* housekeeping gene and the relative gene expression levels were calculate relative to non-treated samples.

6.4.5 Statistical analysis

Statistical analysis was completed on software described in section 2.7. For growth studies, experimental data were analysed using a repeated measures 2-way ANOVA for which suitable post-tests for multiple comparisons were conducted. Final measurements, micro-CT, IGF-1 ELISAs, and histology scoring data were analysed using a 2-way ANOVA for which suitable post-tests for multiple comparisons were conducted. All other results within the chapter were analysed using the Student's t-test or a suitable non-parametric test if the data were not normally distributed. Data were checked to be normally distributed using a Shapiro-Wilk normality test.

Table 6.1 Histology grading scheme for colitis

Feature Graded	Grade	Description
Inflammation	0	None
	1	Slight
	2	Moderate
	3	Severe
Extent	0	None
	1	Mucosa
	2	Mucosa and submucosa
	3	Transmural
Regeneration	4	No tissue Repair
	3	Surface epithelium not intact
	2	Regeneration with crypt depletion
	1	Almost complete regeneration
	0	Complete regeneration or normal tissue
Crypt damage	0	None
	1	Basal 1/3 damage
	2	Basal 2/3 Damaged
	3	Only surface epithelium intact
	4	Entire crypt and epithelium lost
Percent involvement	1	1-25%
	2	26-50%
	3	51-75%
	4	76-100%

6.5 Results

6.5.1 Bone phenotype of *Il10*$^{-/-}$ mouse

To assess the bone phenotype of *Il10*$^{-/-}$ mice (C57Bl6) treated with piroxicam, tibiae were kindly obtained from Dr Thomas Lindebo Holm (Novo Nordisk, Denmark). Gut inflammation had been previously confirmed in these mice by the Novo Nordisk scientists as part of a separate study. Micro-CT analysis revealed limited changes in bone architecture in *Il10*$^{-/-}$ mice treated with piroxicam, but there was a 6% decrease ($p<0.01$) in trabecular thickness in untreated *Il10*$^{-/-}$ tibiae compared to WT. This decrease was exacerbated with piroxicam treatment, where trabecular thickness had decreased by a further 7% ($p<0.05$). Piroxicam treatment of WT mice did not alter trabecular thickness, highlighting that the bone phenotype was *Il10*$^{-/-}$ specific (Table 6.2). BV/TV, trabecular separation, number, and pattern factor, and structural model index remained comparable between all groups (Table 6.2).

Markers for cortical geometry such as total area, bone area, marrow area, polar moment of inertia, and cortical thickness were similar between all groups (Table 6.3). As a result of the minimal changes to bone architecture, the *Il10*$^{-/-}$ mouse treated with piroxicam was deemed an inadequate model to assess the role of SOCS2 in inflammatory driven bone loss.

Table 6.2 Altered trabecular architecture of the *Il10*$^{-/-}$ mouse model

Micro-CT analysis of trabecular architecture of tibia from 12 week old WT, WT + piroxicam, *Il10*$^{-/-}$, and *Il10*$^{-/-}$ + piroxicam mice.

	WT				***Il10*$^{-/-}$**			
	Control		Peroxicam		Control		Peroxicam	
BV/TV	11.72 ± 0.670		12.58 ± 0.504		11.75 ± 0.368		11.69 ± 0.446	
Tb.Th (mm)	0.047 ± 0.001		0.048 ± 0.0005		0.044 ± 0.001[a]		0.041 ± 0.001[ab]	
Tb.Sp (mm)	0.22 ± 0.005		0.22 ± 0.006		0.22 ± 0.004		0.22 ± 0.008	
Tb.N (1/mm)	2.49 ± 0.133		2.62 ± 0.099		2.65 ± 0.063		2.82 ± 0.098	
Tb.Pf (1/mm)	27.68 ± 1.225		25.94 ± 0.845		26.17 ± 1.265		25.23 ± 0.538	
SMI	2.29 ± 0.070		2.23 ± 0.047		2.09 ± 0.072[a]		1.97 ± 0.034[a]	

Data are presented as mean ± SEM (n≥7). BV/TV = bone volume/tissue volume, Tb.Th = trabecular thickness, Tb.Sp = trabecular separation, Tb.N = trabecular number, Tb.Pf = trabecular pattern factor, SMI = structural model index. Significance from WT (control) mice is denoted by [a] $p<0.05$, from *Il10*$^{-/-}$ untreated (control) mice is denoted by [b] $p<0.05$

Table 6.3 No alteration in cortical geometry of the *Il10*$^{-/-}$ mouse model

Micro-CT analysis of cortical geometry of tibia from 12 week old WT, WT + piroxicam, *Il10*$^{-/-}$, and *Il10*$^{-/-}$ + piroxicam mice.

	WT		***Il10*$^{-/-}$**	
	Control	Peroxicam	Control	Peroxicam
T.Ar (mm²)	0.90 ± 0.012	0.90 ± 0.009	0.90 ± 0.021	0.87 ± 0.021
Ct.Ar (mm²)	0.58 ± 0.011	0.57 ± 0.003	0.58 ± 0.013	0.55 ± 0.017
Ma.Ar (mm²)	0.31 ± 0.008	0.33 ± 0.010	0.32 ± 0.020	0.32 ± 0.011
MMI (mm⁴)	0.12 ± 0.003	0.12 ± 0.002	0.11 ± 0.005	0.11 ± 0.006
Ct. Th (mm)	0.23 ± 0.006	0.23 ± 0.006	0.22 ± 0.005	0.22 ± 0.003

Data are presented as mean ± SEM (n≥7). Tt.Ar = total tissue area, Ct.Ar = cortical bone area, Ma.Ar = medullary area, Ct.Th = cortical thickness, J = polar moment of inertia.

6.5.2 Establishing a SOCS2 colony on a pure C57BL/6 background

Effective establishment of a DSS model for colitis required a pure SOCS2 colony as it is recognised that different genetic strains respond differently to DSS (Melgar *et al.* 2005; Perse & Cerar 2012). Previous background strain characterisation using a Mouse 384 SNP panel (Charles Rivers Laboratories) of four mice from the original SOCS2 colony (G0) showed them to be 76% C57BL/6 (Table 6.4). To increase line purity, a breeding programme was set up that involved 5 generations of backcrossing to pure C57BL/6 mice (Fig. 6.1). To ensure the Y chromosome was derived from the C57BL/6 line, 1 mating consisting of a male C57BL/6 crossed with a female *Socs2*$^{-/-}$ were included. Only male offspring were used for future mating (G2). Following 4 generations of backcrossing (G4), 5 mice were further background strain characterised as described above. Two mice were selected with high C57BL/6 strain percentage (98.6% and 98.7%), and were crossed with a C57BL/6 mice (G5); further purifying the strain (Table 6.4 & Fig. 6.1). The offspring from these matings were used to establish a new SOCS2 colony for the DSS studies.

To confirm the overgrowth phenotype in the new SOCS2 colony, male and female, WT and *Socs2*$^{-/-}$ mice were weighed at 4, 5, and 6 weeks of age. It has previously been reported that the *Socs2*$^{-/-}$ overgrowth phenotype becomes apparent between 4-6 weeks of age (Metcalf *et al.* 2000; MacRae *et al.* 2009). In accordance with this, both male and female *Socs2*$^{-/-}$ mice were significantly heavier than age and sex matched WT mice at 4 weeks ($p<0.001$; Fig. 6.2). This increase in body weight was still evident at 6 weeks, where *Socs2*$^{-/-}$ male mice were 44% heavier than male WT mice ($p<0.001$). Female *Socs2*$^{-/-}$ mice were a similar weight to WT males and were significantly heavier than WT females (22%; $p<0.001$; Fig. 6.2).

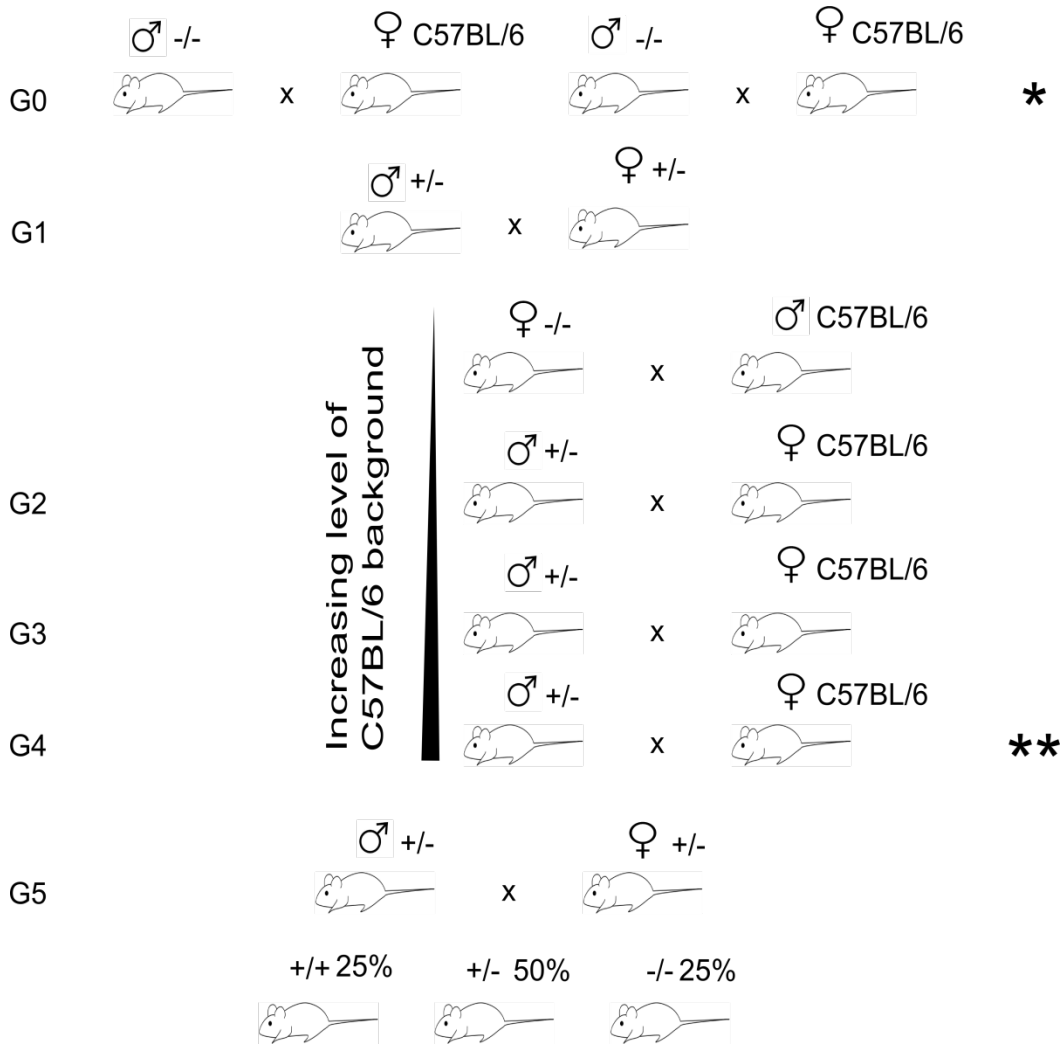

Figure 6.1 Breeding regime for SOCS2 colony

Breeding regime set up to purify the C57BL/6 background of the SOCS2 colony. Asterix indicate point at which strain characterisation was performed (see Table 6.4). G = backcross generation.

Table 6.4 Strain characterisation of SOCS2 colony

Strain characterisation of original SOCS2 colony, and colony following 4 generations of backcrossing to a pure C57BL/6 strain.

Mouse	G0 (%)	G4 (%)
1	73.9	96.3
2	74.6	98.7*
3	78.2	98.6*
4	77.5	97.3
5		96.6
Average	76.0	96.7

Data are presented as percentage C57BL/6 background. Asterix indicates mice used for future matings.

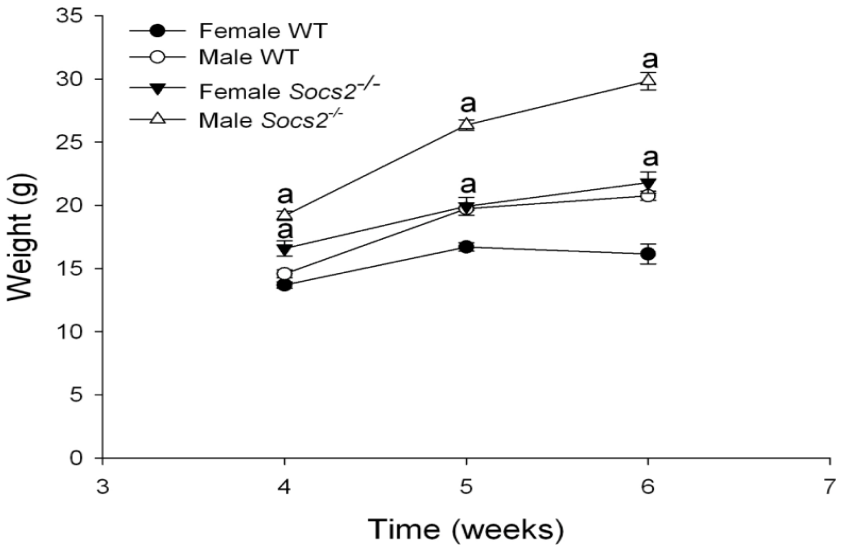

Figure 6.2 Increased weight of male and female *Socs2*$^{-/-}$ mice

Weight of male and female, WT and *Socs2*$^{-/-}$ mice at 4, 5, and 6 weeks of age. Data presented as mean ± SEM (n≥3) Significance from age and sex matched WT mice is denoted by ^{a} $p<0.001$.

6.5.3 DSS induced colitis concentration curve

The severity of colitis induced by DSS is dependent on a number of factors, including DSS concentration and duration, as well as the genetic influences discussed above (Melgar *et al.* 2005; Perse & Cerar 2012). It was therefore necessary to conduct a pilot study to investigate which concentration and duration of DSS treatment was appropriate for the newly established SOCS2 colony. WT mice were given 2.5%, 3%, 3.5%, or 4% DSS for 5 days, or 3% DSS for 4 days, followed by a 13 or 14 day recovery period, respectively. Any mice that lost more than 25% body weight were culled, in accordance with the Home Office animal licence regulations. Development of colitis by DSS is generally characterised by weight loss, beginning 5 days after the start of DSS treatment. This continues for a further 5-6 days, followed by a period of weight gain (Williams *et al.* 2001; Melgar *et al.* 2005). Mice given 2.5% DSS showed very little illness and minimal weight loss. Conversely, mice given 3%, 3.5%, and 4% DSS for 5 days started to lose weight at around day 5. Between days 8-9 a proportion of the mice had lost close to, or over 25% body weight and therefore the experiment was stopped and the mice humanely culled (Fig. 6.3). In some cases' this severe decrease in weight was coupled with loose stool consistency, bloody stool, and a hunched posture. Mice given 3% DSS for 4 days began to lose weight around day 5. Weight loss continued until approximately day 8. At this point, the weight of DSS mice was approximately 87% of starting weight. This was followed by a recovery phase, with weight increasing from day 9 onwards (Fig. 6.3). These results indicate that that for the mice to be used in the colitis studies the optimum concentration and duration of DSS to allow for induction of colitis and recovery was 3% DSS for 4 days.

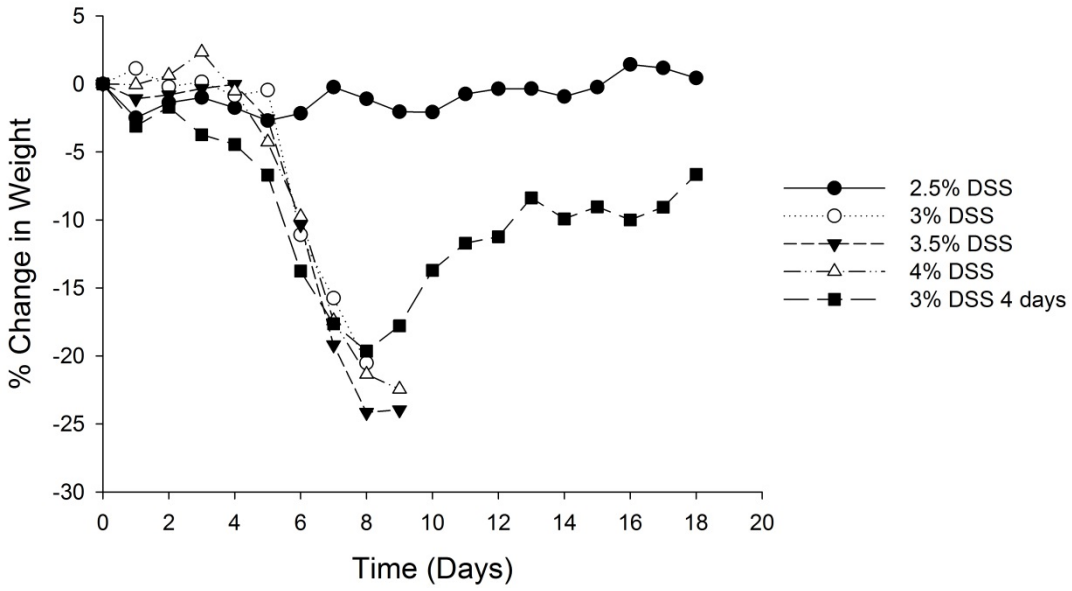

Figure 6.3 DSS concentration curve

Percentage change in weight of 8-9 week old male WT mice treated with 2.5%, 3%, 3.5%, or 4% DSS for 5 days, or 3% DSS for 4 days. Data presented as mean (n=3).

6.5.4 DSS study design

Following the protocol established in section 2, a study was designed to investigate the effects of IBD on bone development in *Socs2*$^{-/-}$ mice (Fig. 6.4). In addition to mouse weight being measured throughout the experiment, food levels were also measured at three points. Previous studies have shown that weight loss observed in DSS treated mice may be attributed to a reduction in food intake (Harris *et al.* 2009). Based on data collected in section 6.5.3, the experiment was divided into three stages - DSS intake (1), weight loss (2), and recovery (3) (Fig. 6.4). To ensure differentiation between a reduced food intake and an inflammation induced phenotype, non DSS WT and *Socs2*$^{-/-}$ mice were pair fed with DSS mice using a strategy adapted from Ballinger and colleagues (Ballinger *et al.* 2000). DSS treated water would also be measured in WT and *Socs2*$^{-/-}$ mice to give an indication of the level of DSS intake by each mouse (Fig. 6.4).

6.5.5 DSS study

To investigate the effects of DSS induced colitis on bone development and the possible role of SOCS2 in mediating bone loss, 8-9 week old male WT and *Socs2*$^{-/-}$ mice were treated with DSS as outlined in section 6.5.4. During DSS treatment, (0-4 days) no significant weight loss was observed in WT or *Socs2*$^{-/-}$ mice (Fig. 6.5A). All mice exhibited significant weight loss from day 6-8 (WT) or day 6-7 (Socs2$^{-/-}$) (Fig. 6.5). Maximum body weight loss was similar between WT (15%) and *Socs2*$^{-/-}$ (13%) DSS treated mice (Fig. 6.5A). Following the period of weight loss, DSS treated mice gained body weight until the end of the experiment (Fig. 6.5A). Pair fed control mice did not show any significant alterations in body weight (Fig. 6.5A). WT mice showed high variation in susceptibility to DSS, as measured by weight loss (Fig. 6.5B). Maximum body weight loss ranged between -6% and -21% in DSS treated WT mice before recovery, and 2 out of the 8 experimental animals fell below -25%, and therefore had to be culled (Fig. 6.5B). Body weight loss observed in *Socs2*$^{-/-}$ mice treated with DSS, was more uniform. It ranged between -11% and -15% before recovery (Fig. 6.5B).

6.5.6 Food and water intake of DSS treated mice

During the period of DSS treatment, water intake per gram of body weight was similar in WT and *Socs2*$^{-/-}$ mice (Fig. 6.6A). Food levels measured during the experiment revealed no difference in food intake during DSS intake, weight loss, and recovery (section 6.5.5) (Fig. 6.6B). Food intake between WT and *Socs2*$^{-/-}$ was also not significantly different.

6.6.7 End point measurement of DSS treated mice

At the end point of the experiment, the weight of WT and *Socs2*$^{-/-}$ mice treated with DSS was comparable to genotype matched non-treated mice (Table 6.5). No changes were observed in nose to rump length, tibia length, or femur length between DSS treated and non-treated mice. At this point, the overgrowth phenotype was apparent in *Socs2*$^{-/-}$ mice. Untreated mice were 39% ($p<0.001$) heavier than untreated WT mice. Increased length of nose to rump (13%; $p<0.001$), tibia (6%; $p<0.001$), and femur (8% $p<0.001$) were also noted in untreated *Socs2*$^{-/-}$ mice (Table 6.5).

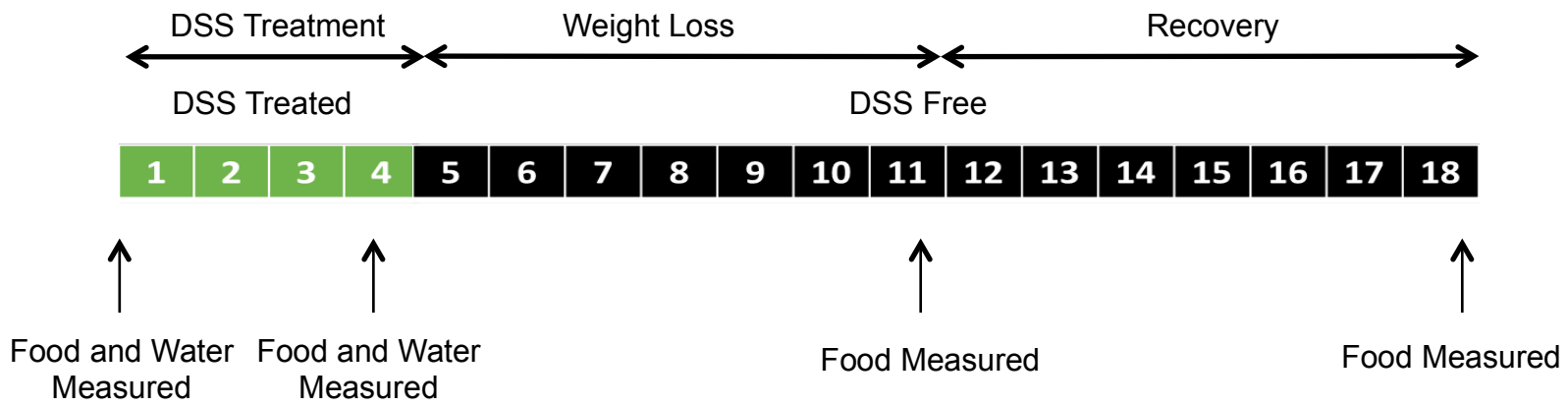

Figure 6.4 DSS Study Protocol

DSS study design outlining DSS treatment regime including day's food and water were measured.

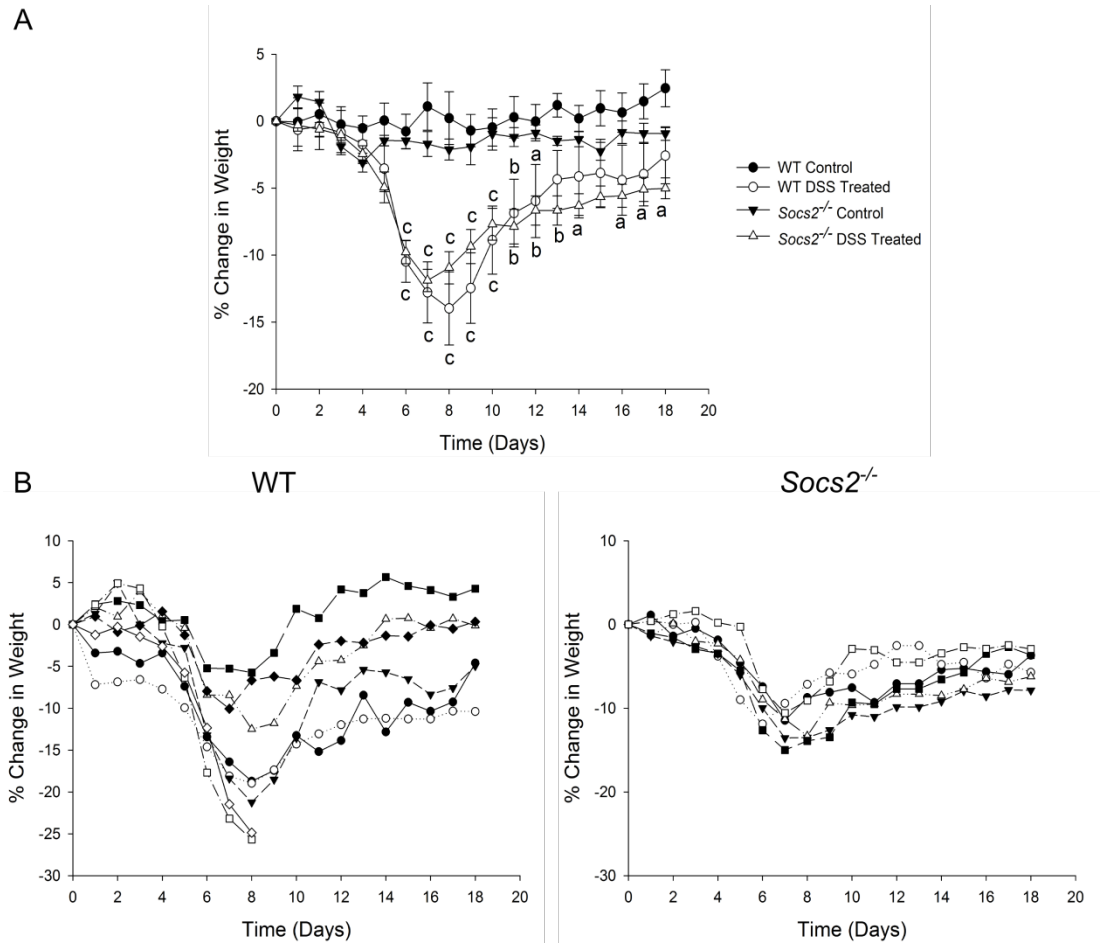

Figure 6.5 Mouse weights during DSS study

A. Percentage change in weight of 8-9 week old male WT and *Socs2*$^{-/-}$ mice treated with 3% DSS for 4 days. Data are presented as mean ± SEM (n=6). Significance from genotype matched untreated (control) mice denoted by ^{a} $p<0.05$, ^{b} $p<0.01$, ^{c} $p<0.001$ in comparison to genotype matched control mice. **B.** Individual percentage change in weight of WT and *Socs2*$^{-/-}$ mice treated with 3% DSS for 4 days. Each line represents an individual mouse % change in weight over the whole experiment.

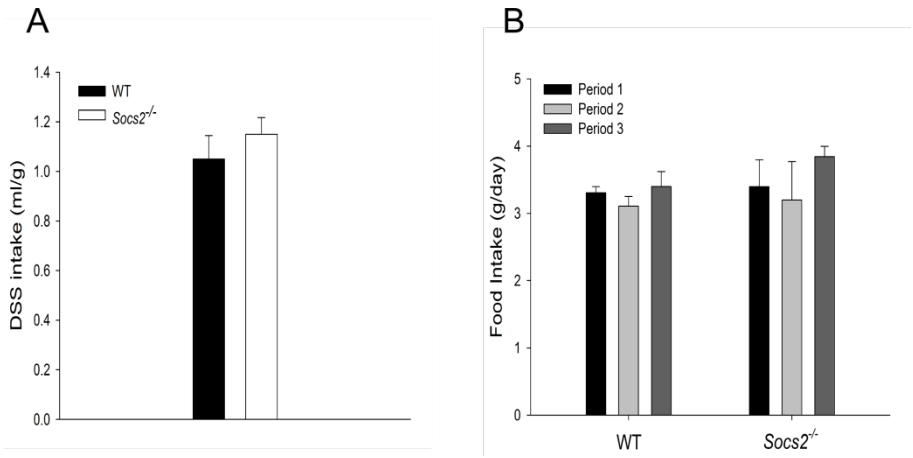

Figure 6.6 DSS and food intake during DSS study

A. Water consumption by DSS treated WT and *Socs2*$^{-/-}$ mice during DSS treatment. Water consumption normalised to body weight. Data presented as mean ± SEM (n≥5). **B.** Food consumption by WT and *Socs2*$^{-/-}$ mice during DSS treatment, weight loss, and recovery (Section 4). Data presented as mean ± SEM (n≥3).

Table 6.5 No changes in mouse weight and length at end point of DSS study

Weight and length measurements of WT and *Socs2*$^{-/-}$ mice at end point of DSS study.

	WT				***Socs2*$^{-/-}$**	
	Control	DSS Treated	Control	DSS Treated		
Weight (g)	23.5 ± 0.34	22.6 ± 0.38	32.6 ± 0.38[a]	31.5 ± 0.46		
N to R Length (mm)	88.7 ± 1.11	87.9 ± 1.40	100.5 ± 1.15[a]	103.2 ± 1.35		
Tail Length (mm)	72.5 ± 1.09	72.0 ± 0.82	76.0 ± 1.56	77.6 ± 1.24		
Left Tibia (mm)	17.7 ± 0.14	17.6 ± 0.16	18.7 ± 0.18[a]	18.9 ± 0.10		
Left Femur (mm)	14.4 ± 0.21	14.4 ± 0.10	15.6 ± 0.08[a]	15.2 ± 0.20		

Data presented as mean ± SEM (n=6). Significance denoted by [a] $p<0.001$ in comparison to WT control mice. N to R Length = nose to rump length.

6.5.8 Gut pathology of DSS treated mice

To assess the effects of DSS on mucosal integrity, detailed analysis of histology was performed on WT and *Socs2*$^{-/-}$ colon. As expected, histology scores were minimal in pair fed mice, with total inflammation scores of 3 and 3.2 respectively. There were also no notable morphological differences between the two non DSS control groups suggesting the lack of SOCS2 had no obvious effects on gut morphology (Fig. 6.7 & Fig. 6.8B).

Histological analysis of the colon from WT and *Socs2*$^{-/-}$ DSS treated mice, revealed extensive levels of inflammation. DSS treated mice were characterised as having signs of both acute and chronic inflammation throughout the colon (Fig. 6.8A). Signs of acute inflammation included infiltration of neutrophils and macrophages into the lamina propria and submucosa, and epithelial degeneration (Fig. 6.8A). In a number of sections there were also signs of crypt loss. These signs of acute inflammation were often concomitant with signs of chronic inflammation. Aside from acute phase cells such as neutrophils in the lamina propria, there were also high levels of mononuclear leucocytes which are associated with chronic inflammation (Fig. 6.8A). Atypical crypt regeneration (Fig. 6.8A) and transmural inflammation were also noted in colons from DSS treated mice, indicating chronic inflammation.

Scores for inflammation severity and extent of inflammation were significantly increased in DSS treated mice (Fig. 6.8B). The histological scores for inflammation severity (WT: 6.8, *Socs2*$^{-/-}$: 5.2) and extent of inflammation (WT: 7.3, *Socs2*$^{-/-}$: 5.9) following DSS treatment were not significantly different between genotypes (Fig. 6.8B). DSS treatment of WT mice slightly increased crypt damage/regeneration score ($p<0.01$). A significant difference was not observed in DSS treated *Socs2*$^{-/-}$ mice (Fig. 6.8B). Analysis of the crypt damage/regeneration revealed a significant interaction between treatment and genotype ($p<0.05$). This indicates that the effect of treatment on crypt damage/regeneration score was dependent on genotype (Fig. 6.8B). The minimal change in crypt damage/regeneration however was not sufficient to alter

total pathology scores (Fig. 6.8B). Taken together, these results indicate that the absence of SOCS2 had little effect in protecting against DSS-induced gut inflammation.

6.5.9 Systemic IGF-1 levels in DSS treated mice

GH resistance associated with IBD is characterised by a decrease in systemic IGF-1 levels (Ballinger *et al.* 2000; Katsanos *et al.* 2001). Analysis of serum from DSS treated animals revealed that despite obvious gut pathology (section 6.5.8), there was no alteration in IGF-1 levels in WT (control 263.8 ± 6.3, DSS treated 243.6 ± 10.8) or *Socs2*$^{-/-}$ (control 264.8 ± 9.8, DSS treated 276.9 ± 17.6) mice (Table 5).

6.5.10 Muscle and bone gene expression in DSS treated mice

Gene expression of *Socs1, 2, 3*, and *Igf1* were measured in muscle and bone samples from WT mice ± DSS. Previous studies have reported an increase in *Socs2* expression in muscle in response to inflammation (Mak & Cheung 2007; Cheung *et al.* 2008). In muscle, *Socs2* mRNA levels were increased 4.3 fold ($p<0.01$) in DSS treated mice. No significant differences were observed in *Socs1* and *3* mRNA levels (Figure 9A). Analysis of bone sample revealed increased *Socs2* (2.7 fold; $p<0.05$) and *Socs3* (4.1 fold; $p<0.05$) levels in DSS treated mice. No difference was observed in *Socs1* levels (Fig. 6.9A). Bone samples showed no alteration in *Igf1* expression levels in DSS treated mice (Fig. 6.9B).

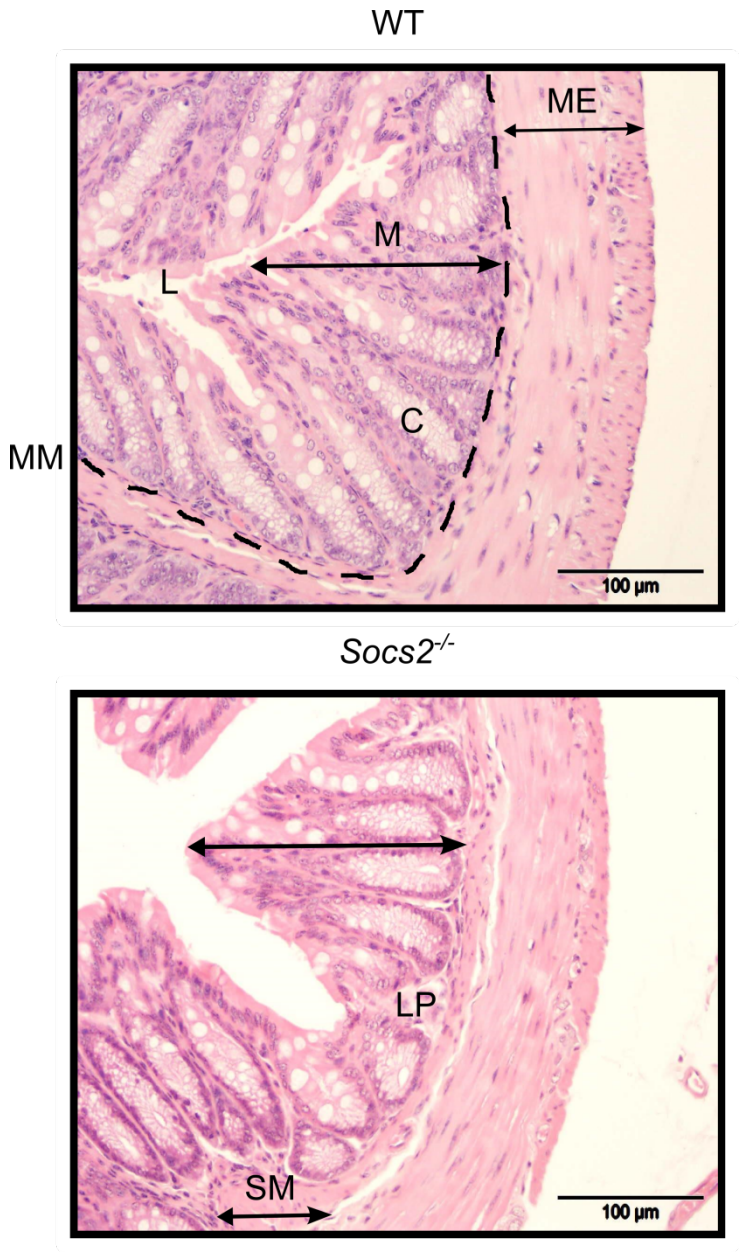

Figure 6.7 WT and *Socs2*$^{-/-}$ colon histology

Representative H&E stained sections of colon from control WT and *Socs2*$^{-/-}$ mice marking major anatomical features. L = lumen, M = mucosa, C = crypt, MM (dotted line) = muscularis mucosa, ME = muscularis externa, LP = lamina propria, and SM= submucosa. Scale bar = 100µm.

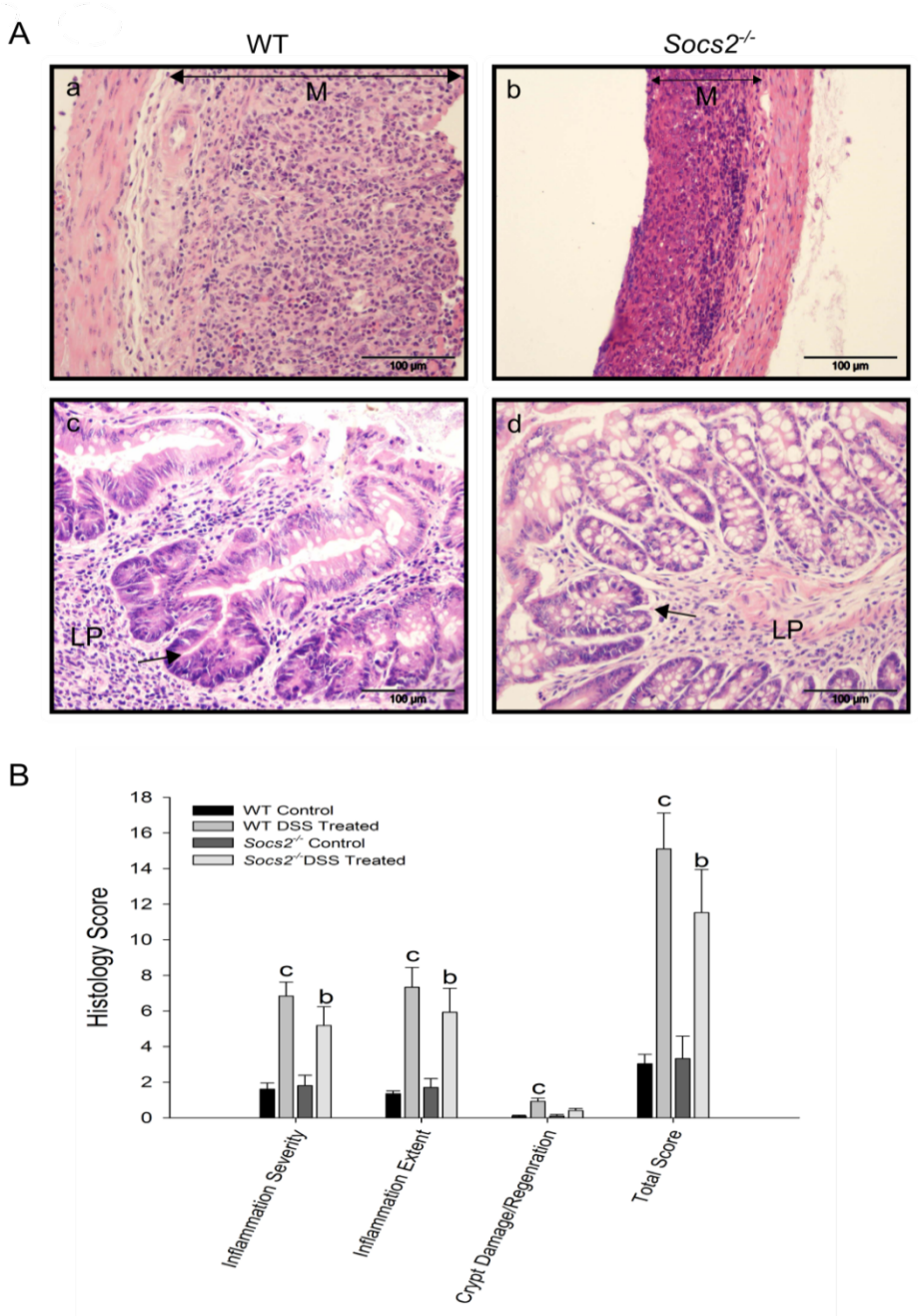

Figure 6.8 Minimal differences in gut pathology in DSS Treated WT and *Socs2*$^{-/-}$ mice

A. Representative H&E stained sections of colon from DSS treated WT and *Socs2*$^{-/-}$. M = mucosa, LP = lamina propria. Arrows indicate points of atypical crypt regeneration. Scale bar =100µm. **B**. Histological scoring of DSS treated, and control WT and *Socs2*$^{-/-}$ colons. Data represented as mean ± SEM. (n=6) Significance from genotype matched untreated (control) samples is denoted by ^{b} $p<0.01$, ^{c} $p<0.001$

Table 6.6 No alteration in systemic IGF-1 levels in DSS treated mice

IGF-1 levels in serum from WT and *Socs2*$^{-/-}$ mice at endpoint of DSS study.

	IGF-1 (ng/ml)	
	Control	DSS Treated
WT	263.8 ± 6.2	243.6 ± 10.8
***Socs2*$^{-/-}$**	264.8 ± 9.8	276.9 ± 17.6

Data presented as mean ± SEM (n=6).

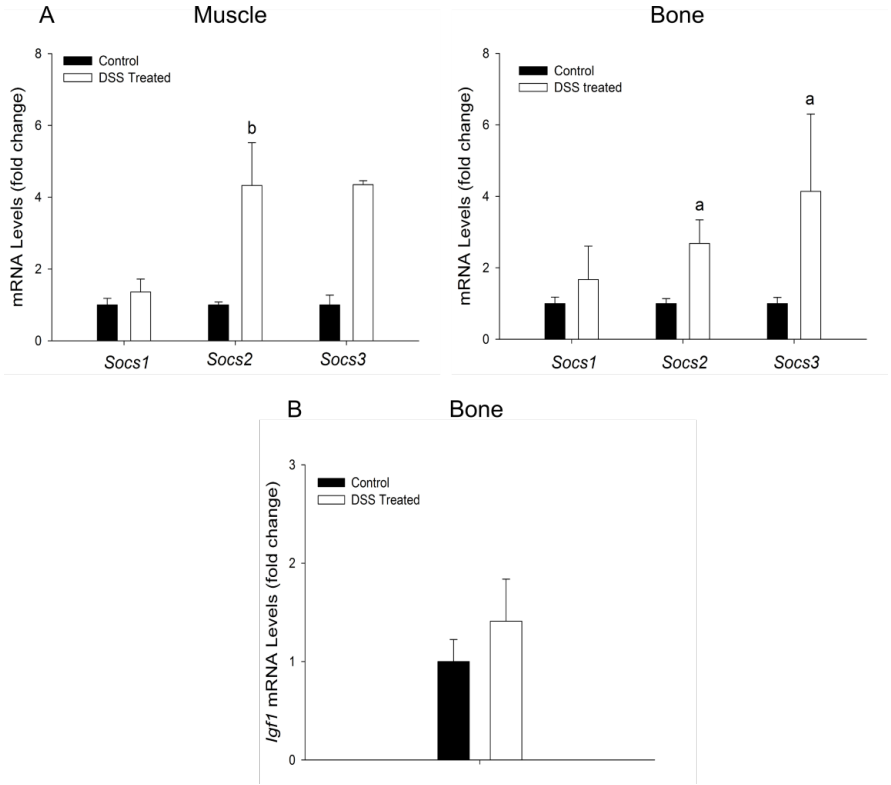

Figure 6.9 Elevated *Socs2* mRNA expression levels in bone and muscle from DSS treated WT mice

A. Analysis of *Socs1*, *2*, and *3* mRNA expression levels in muscle and bone from DSS treated WT mice at endpoint of DSS study. **B.** Analysis of *Igf1* mRNA expression levels in bone from WT mice at endpoint of DSS study. All data are presented as mean ± SEM relative to untreated (control) samples (n≥4) Significance from untreated (control) samples is denoted by [a] $p<0.05$, [b] $p<0.01$.

6.5.11 Bone phenotype of DSS treated mice

DSS induced colitis has previously been shown to have detrimental effects on bone quality, in both juvenile (4 week old) and young adult (10 week old) mice (Hamdani *et al.* 2008; Harris *et al.* 2009). In this study, DSS treated WT mice showed declined trabecular architecture compared to control mice (Fig. 6.10A). DSS treated WT mice had significantly decreased BV/TV (41%; $p<0.001$), trabecular thickness (16%; $p<0.01$), trabecular number (30%; $p<0.001$), and resulting increased trabecular separation (19%; $p<0.01$) (Fig. 6.10B). Increased trabecular pattern factor (40%; $p<0.001$) and structural model index ($p<0.001$) indicated a more disconnected 'rod-like' trabecular structure. This is associated with a reduction in quality of trabecular micro-architecture (Fig. 6.10B).

DSS induced *Socs2*$^{-/-}$ mice also showed altered trabecular architecture compared to control mice. The level of trabecular deterioration was however far less than that observed in WT mice (Fig. 6.10). DSS treated *Socs2*$^{-/-}$ mice had significantly decreased BV/TV (21%; $p<0.01$), trabecular number (14%; $p<0.05$), and increased trabecular pattern factor (20%; $p<0.05$). Trabecular thickness, trabecular separation, and structural model index were not significantly different from control mice (Fig. 6.10B). Analysis of BV/TV revealed a significant interaction between treatment and genotype ($p<0.05$). This indicates that the effect of treatment was dependent on genotype. Taken together, these results highlight that the absence of SOCS2 is protective against the trabecular bone loss phenotype observed in the DSS-colitis mouse model.

Similar to results obtained in *Il10*$^{-/-}$ mice treated with piroxicam, analysis of cortical bone revealed no change in any parameters following DSS treatment (Table 6.7). At this point, the anabolic bone phenotype (characterised by increased cortical tissue area ($p<0.001$), bone area ($p<0.001$), marrow area ($p<0.001$), and cortical thickness ($p<0.05$)) was apparent in untreated *Socs2*$^{-/-}$ mice (Table 6.7).

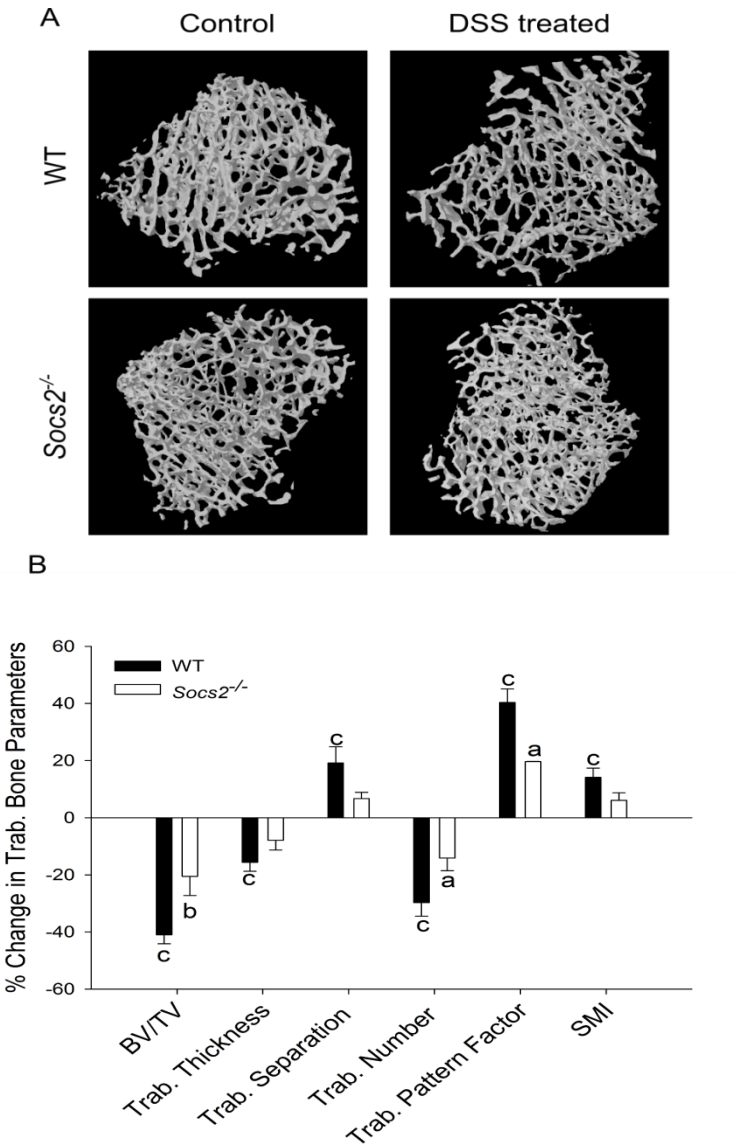

Figure 6.10 Protected trabecular architecture in DSS treated *Socs2*$^{-/-}$ mice

A. Representative 3D micro-CT reconstructions of tibial trabecular bone from control and DSS treated, WT and *Socs2*$^{-/-}$ mice. **B.** Percentage change of trabecular parameters in DSS treated mice relative to genotype matched controls. Data are presented as mean ± SEM (n≥4). Significance from genotype matched untreated (control) samples is denoted by ^{a} $p<0.05$, ^{b} $p<0.01$, ^{c} $p<0.001$.

Table 6.7 No alteration in cortical geometry of tibia from DSS treated mice

Micro-CT analysis of cortical geometry of tibia from WT and *Socs2*$^{-/-}$ mice at endpoint of DSS study.

	WT		***Socs2*$^{-/-}$**	
	Control	DSS Treated	Control	DSS Treated
Tt.Ar (mm²)	0.84 ± 0.001	0.82 ± 0.002	1.03 ± 0.003[b]	1.01 ± 0.003
Ct.Ar (mm2)	0.54 ± 0.014	0.54 ± 0.012	0.67 ± 0.028[b]	0.65 ± 0.022
Ma.Ar (mm²)	0.30 ± 0.005	0.28 ± 0.005	0.37 ± 0.009[b]	0.36 ± 0.001
Ct.Th (mm)	0.23 ± 0.003	0.23 ± 0.004	0.25 ± 0.008[a]	0.25 ± 0.006

Data are presented as mean ± SEM (n≥3). Tt.Ar = total tissue area, Ct.Ar = cortical bone area, Ma.Ar = medullary area, Ct.Th = cortical thickness.

6.6 Discussion

In chapter 6 the DSS model was successfully established as an appropriate model to study the bone loss phenotype associated with IBD. Furthermore, work carried out utilising this model on *Socs2*$^{-/-}$ mice highlighted a key role for SOCS2 in regulating this process. Despite no apparent differences in gut inflammation *Socs2*$^{-/-}$ mice were partially protected from bone deterioration following DSS induced colitis. IBD is often associated with secondary osteoporosis and increased risk of fracture (Bjarnason *et al.* 1997; Dinca *et al.* 1999; Ali *et al.* 2009). Poor bone health cannot be solely attributed to steroid medication, and poor nutrient intake and absorption. Inflammatory activity itself also has a role to play (Tilg *et al.* 2008; Ali *et al.* 2009). It is well established that IBD is associated with GH resistance, likely to contribute to the bone loss observed (Tenore *et al.* 1977; Wong *et al.* 2010). A number of proinflammatory cytokines have been shown to upregulate *Socs2* gene expression (Starr *et al.* 1997; Krebs & Hilton 2001). To investigate this, inflammatory models displaying bone loss are required. The current study therefore established the DSS model for colitis in order to assess the importance of SOCS2 in mediating the bone loss phenotype observed in IBD.

Micro-CT analysis of piroxicam treated *Il10*$^{-/-}$ mice revealed minimal bone loss (Tables 6.2 & 6.3). *Il10*$^{-/-}$ mice have previously been shown to have decreased BMD and BMC. However, this was only found to be significant when genders were combined (Cohen *et al.* 2004). The negative effects of piroxicam treatment on mucosal integrity and inflammation are widely understood (Berg *et al.* 2002; Hale *et al.* 2005). In keeping with other models of gut inflammation, it was expected that the increase in proinflammatory cytokines in *Il10*$^{-/-}$ mice treated with piroxicam would result in a greatly altered bone phenotype (Lin *et al.* 1996; Hamdani *et al.* 2008; Holgersen *et al.* 2014). In the present study, piroxicam was administered for 12 days. Future experiments assessing the bone phenotype in *Il10*$^{-/-}$ mice treated with

piroxicam may benefit from extending this period, to allow time for the potential negative effects of inflammation on bone turnover to be elucidated.

To assess the potential role for SOCS2 in mediating the bone loss phenotype observed in IBD, it was necessary to establish the DSS induced model for colitis. There are a number of factors that contribute to the susceptibility of a mouse to DSS, and each needs to be carefully addressed in order to establish a working and reproducible model (Perse & Cerar 2012). The responsiveness to DSS-induced colitis is different among inbred mouse strains (Mahler *et al.* 1998; Melgar *et al.* 2005). C57BL/6 mice are more susceptible to DSS than other mouse strains including BALB/c (Melgar *et al.* 2005). As previous characterisation of the SOCS2 colony revealed a mixed background (consisting of approximately 75% C57BL/6) it was important to increase the purity of the strain. This was done successfully to allow the DSS studies to be completed (Fig. 6.1, 6.2 & Table 6.4.

The molecular weight of the DSS used to induce colitis is important. A study by Kitajima and colleagues revealed that varying molecular weights of DSS (5kD, 40kD and 500kD) contributed to varying levels of inflammation, localised to different areas of the colon (Kitajima *et al.* 2000). A molecular weight of 500kD was unable to penetrate the mucosal membrane, whereas 5kD treatment resulted in mild inflammation in the caecum and upper colon. A molecular weight of 40kD resulted in severe inflammation in the lower colon, and has been used to induce colitis in a number of studies (Kitajima *et al.* 2000; Williams *et al.* 2001; Melgar *et al.* 2005; Harris *et al.* 2009). This molecular weight of DSS was also used in the present study.

A DSS concentration curve was undertaken to establish the optimal concentration to use to induce colitis in the SOCS2 colony. Previous reports on C57BL/6 mice have used concentrations of 3%-5% for 5 days, resulting in severe weight loss associated with inflammation followed by a period of weight gain (Melgar *et al.* 2005; Harris *et al.* 2009). Previous unpublished work (prior to the commencement of the current

studies) within the laboratory suggested that a concentration of 4% for 5 days was optimal, with higher concentrations resulting in high mortality, and lower concentration having little effect on health. It must however be noted that these early studies were done on a mixed strain of mice and it was unclear if a similar result would be seen in a genetic strain (~98% C57Bl/6) that was recognised to be more susceptible to DSS. The mice used in the present study were highly susceptible to DSS treatment, as concentrations of 3%, 3.5%, and 4% for 5 days all resulted in a high mortality rate. Lowering the number of days to 4 had a large effect on disease severity (Fig. 6.3). Mice on this treatment regime still lost weight following DSS treatment, however 5 days after treatment stopped the mice started to regain weight and show signs of recovery. Although it is likely that the altered level of susceptibility to DSS observed in this study is a result of increased purity of mouse strain, there are a number of variables that contribute to alter DSS susceptibility. Increased stress levels have been implicated in relapsing chronic inflammation (Melgar *et al.* 2008). No studies have been carried out on stress in relation to the initiation of DSS induced inflammation, however it may be possible that the increased stress of being moved to a new environment (shared cage to singly housed) may also have contributed to increased susceptibility.

Histologic scoring in the present study was carried out using a validated scoring scheme, allowing an in depth assessment of the mucosal integrity (Table 6.1) (Dieleman *et al.* 1998; Williams *et al.* 2001). Acute and chronic colitis are characterised by distinct pathological changes to the colon. Acute inflammation is associated with an influx of neutrophils into the lamina propria, and in some cases epithelial degeneration. Chronic inflammation on the other hand is associated with mononuclear leukocyte infiltration, crypt architectural disarray, and crypt regeneration (Melgar *et al.* 2005; Perse & Cerar 2012). In this study, histological analysis revealed signs of both acute and chronic inflammation, suggesting that the current experimental design was sufficient to induce chronic inflammation (Fig. 6.8). Previous reports have shown that acute inflammation can progress to chronic in

C57BL/6 mice following a single treatment of DSS (Melgar *et al.* 2005). Little difference was observed between the severity of inflammation in the WT and *Socs2*$^{-/-}$ mice (Fig. 6.8). This indicates that the absence of SOCS2 does not protect against the deterioration of mucosal integrity. There have been reports that increased GH activity promotes mucosal repair during inflammation. A small clinical trial of patients with active CD reported that GH therapy improved the CD activity index, and decreased the need for other medication (Slonim *et al.* 2000). Furthermore, GH transgenic mice display a similar extent of colon pathology during the onset of inflammation compared to WT mice, but show improved mucosal repair over an extended time period (Williams *et al.* 2001). Increased mucosal repair in the GH transgenic mice may have been a result of increased systemic IGF-1(Mathews *et al.* 1988; Howarth *et al.* 1998; Metcalf *et al.* 2000; MacRae *et al.* 2009). *Socs2*$^{-/-}$ mice however show no alteration in systemic IGF-1.

GH resistance during inflammation is associated with decreased systemic IGF-1 levels (Katsanos *et al.* 2001). In states of systemic inflammation, pro-inflammatory cytokines upregulate SOCS expression (Colson *et al.* 2000). IL-6 inhibits hepatic GH signalling through the upregulation of CIS and SOCS3 (Denson *et al.* 2003). TNF-α also down regulates hepatic GHR (Denson *et al.* 2001). In the present study, IGF-1 levels were not altered in DSS treated WT and *Socs2*$^{-/-}$ mice (Table 6.6). This suggests inflammation does not result in hepatic GH resistance. It must however be noted that systemic IGF-1 levels were measured at the end of the experiment. At this point, the DSS treated animals presented with severe inflammation of the colon, but had shown recovery of weight loss. Previous studies have shown decreased systemic IGF-1 levels immediately following DSS treatment, increasing over period of weeks (Harris *et al.* 2009). To therefore fully assess the importance of systemic IGF-1 levels during inflammation, IGF-1 levels would have to be measured at numerous points during the initiation and progression of colitis. In keeping with previous research, systemic IGF-1 levels in WT and *Socs2*$^{-/-}$ control animals were

comparable, further confirming the importance of the direct anabolic effects of GH (Metcalf *et al.* 2000; Lorentzon *et al.* 2005; MacRae *et al.* 2009).

The importance of SOCS proteins in regulating local GH signalling during inflammation has been investigated in muscle during uraemia. In this model, there were increased *Socs2* mRNA levels (Guarnieri *et al.* 2004; Cheung *et al.* 2008). Given the known regulatory role of SOCS2 on GH signalling, it is conceivable that the inhibited GH action may be responsible for the associated muscle wasting (Cheung *et al.* 2008). GH induced STAT5 activation in muscle is attenuated in states of uraemia (Sun *et al.* 2004). In the DSS model, there was increased *Socs2* expression in muscle and bone from WT mice (Fig. 6.9). This infers that SOCS2 may be a critical mediator through which pro-inflammatory cytokines inhibit GH/IGF-1 signalling in extra intestinal tissues. The role of SOCS2 in regulating the anabolic effects of GH on bone is evident from the anabolic bone phenotype discussed in chapter 4 and 5. *Socs3* mRNA levels were also increased in bone from WT mice treated with DSS. Due to the embryonic lethality of the *Socs3*$^{-/-}$ mouse, it is difficult to determine the potential role of SOCS3 in bone turnover, but it may have a contributory role (Roberts *et al.* 2001). SOCS3 has been identified as a potent regulator of osteoclast function It's precise role however remains unclear. SOCS3 has been shown to have both inhibitory and stimulatory roles in osteoclastogenesis (Fox *et al.* 2003; Wong *et al.* 2006). Also, the increased *Socs3* may act together with higher *Socs2* levels to inhibit GH action in DSS colitis and inhibit bone formation. No alteration in *Igf1* expression was observed in bone samples from DSS treated mice. This indicates that the increase in *Socs2* does not result in deregulated *Igf1* expression. These results are not surprising, as previous data discussed in chapter 4 & 5 show that SOCS2 is a critical regulator of GH action on bone, independent of local IGF-1.

The lack of evidence for a protective role of SOCS2 in mucosal integrity, coupled with the increase in *Socs2* levels in bone indicates that the differences in bone phenotype between DSS treated WT and *Socs2*$^{-/-}$ mice are likely due to the inhibitory

effects of SOCS2 on GH promotion of bone formation (chapter 4). DSS induced colitis results in bone loss in juvenile (4 weeks old) and adult (9 weeks old) mice (Hamdani *et al.* 2008; Harris *et al.* 2009). In juvenile mice, the adverse trabecular and cortical bone phenotype was associated with decreased serum osteocalcin and IGF-1, and increased TNFα. Trabecular deterioration is also apparent in older animals treated with DSS, however cortical bone remains unchanged (Hamdani *et al.* 2008; Harris *et al.* 2009). Taken together, these studies suggest that there is an age specific effect of inflammation on bone loss. During early puberty (3 to 5 weeks) there is extensive radial bone expansion, up to a point where adult bone size is reached (Callewaert *et al.* 2010). Decreased bone formation during this critical period may well be the cause behind the bone loss observed in juvenile mice (Harris *et al.* 2009). The present study found a severe trabecular bone loss phenotype in WT mice treated with DSS, consistent with previous reports in adult mice (Fig. 6.10) (Hamdani *et al.* 2008). This was associated with a loss of trabecular architecture, including alterations to trabecular pattern factor and structural model index (discussed in chapter 4). Trabecular pattern factor is an index of connectivity of trabecular bone. A higher trabecular pattern factor; as observed in DSS treated WT mice, signifies a more disconnected trabecular structure (Hahn *et al.* 1992). Bone loss observed in *Socs2*$^{-/-}$ mice treated with DSS was far less than that observed in WT mice, with a number of parameters comparable to non-treated bone (Fig. 6.10). This highlights that the absence of SOCS2 is partly protective against the bone loss phenotype associated with DSS induced inflammation. Complete protection of the skeleton was not observed however, and this is likely due to many other cellular mechanism including increased osteoclastic resorption and diminished GH signalling through the elevated *Socs3* levels. The effects of knocking out both *Socs2* and *Socs3* in the DSS model would be of great interest as it may offer greater protection to the skeleton.

In conclusion, these studies have identified, and established a working model for IBD, allowing the assessment of associated bone loss. Furthermore, the results

highlight that despite a similar level of gut inflammation, *Socs2*$^{-/-}$ mice are partly protected against the deteriorated bone loss associated with IBD. This work identifies SOCS2 as a critical regulator through which pro-inflammatory cytokines inhibit GH/IGF-1 signalling and decrease bone health.

Chapter 7

General discussion and future work

7.1 General Discussion

Recombinant human GH (rhGH) is approved for the treatment of a number of disorders which result in short stature. These include growth hormone deficiency (GHD), Turner syndrome (TS), Prader-Willi syndrome, short stature homeobox-containing gene deficiency (SHOX-D), and chronic renal insufficiency (Bang *et al.* 2012). GH therapy is also used to treat adult onset GHD that is associated with low bone turnover osteoporosis and increased fracture risk (Ohlsson *et al.* 1998). Whilst GH treatment is considered to be generally effective, there are a number of reports of an unsatisfactory growth promoting response (Allen 2011; Bang *et al.* 2012). In cases of GHD in children, one study has indicated that approximately 28% of participants do not respond to GH therapy (Bang *et al.* 2011). There is therefore a need to better understand the mechanisms of GH actions to aid the development of new strategies in the effective treatment of growth disorders. Furthermore, an in depth understanding of the GH signalling pathway and its regulation has the potential to uncover new therapeutic targets.

GH therapy, especially at high doses, has been shown to increase insulin levels in patients with idiopathic short stature (ISS); a disorder characterised by poor growth velocity despite little alteration in GH and IGF-1 levels. Although insulin levels appear to return to normal after treatment, these have to be monitored during long term treatment (Allen 2011). Reports of increased insulin levels and decreased insulin sensitivity have also been observed in a follow up study of young women with Turner syndrome treated with GH (Bannink *et al.* 2009). Surprisingly, adults with GHD have impaired insulin sensitivity, and in these cases, low doses of GH may act to improve the condition (Yuen *et al.* 2005). The full effects of GH therapy on insulin sensitivity are however still being elucidated. GH transgenic mice are insulin resistant, similar to individuals with acromegaly (Hansen *et al.* 1986; Kopchick *et al.* 1999). Although the anabolic structural bone changes in *Socs2*$^{-/-}$ mice are comparable to that observed in GH transgenic mice, *Socs2*$^{-/-}$ mice do not suffer

from insulin resistance. *Socs2*$^{-/-}$ mice could therefore represent an important model to study the pathways that promote bone accretion without leading to insulin resistance (Rico-Bautista *et al.* 2005; Zadjali *et al.* 2012). Caution must however be exercised as diet induced obesity causes increased insulin resistance in *Socs2*$^{-/-}$ mice compared to WT (Zadjali *et al.* 2012).

In order for future translational advances to benefit clinical applications of GH therapy there is a need for an improved basic understanding of the mechanisms of GH action. The emerging concept that GH functions not only at a systemic level, but also locally, has led to the generation of a number of transgenic mouse models (Le Roith *et al.* 2001; Kaplan & Cohen 2007). Previous models focussing on the importance of systemic IGF-1 through the generation of liver specific *Igf1*$^{-/-}$ mice have been called into question. This is due to the deletion of liver *Igf1* that is achieved with the cre-lox method of gene deletion using an albumin promoter. This results in progressive gene deletion long after the post weaning growth spurt (Yakar *et al.* 1999; Tang *et al.* 2005; Stratikopoulos *et al.* 2008). Furthermore, increased GH levels in these mice (as a consequence of low serum IGF-1 levels) may mask the potential effects of decreased systemic IGF-1 (Yakar *et al.* 2009). Investigation of the local effects of GH on longitudinal and radial bone growth have focused predominantly on the alteration of local *Igf1* and *Igf1r* levels. There are few studies that have directly addressed the possibility of a local GH action that is independent of IGF-1 (Zhang *et al.* 2002; Govoni *et al.* 2007a; Govoni *et al.* 2007b; Wang *et al.* 2011). The *Socs2*$^{-/-}$ mouse is therefore a valuable model to study the effects of local GH action on longitudinal bone growth and accrual, as systemic GH and IGF-1 levels remain at a physiological levels (Metcalf *et al.* 2000; Greenhalgh *et al.* 2002a; MacRae *et al.* 2009).

Results presented in the current thesis help settle the contested bone phenotype of *Socs2*$^{-/-}$ mice (Lorentzon *et al.* 2005; MacRae *et al.* 2009). The current studies have shown that alteration in *Socs2*$^{-/-}$ bone architecture has a beneficial knock-on effect on

the biomechanical properties of bone. The increased bone volume observed is consistent with the known effects of GH on bone (Ohlsson *et al.* 1998). GH treatment has been shown to increase BMD and BMC in patients with idiopathic osteoporosis and this is associated with a significant increase in systemic IGF-1 levels (Gillberg *et al.* 2002). GH treatment has also been reported to increase BMD and BMC in post-menopausal women and this has also been associated with increased systemic IGF-1 (Landin-Wilhelmsen *et al.* 2003). In contrast, the present studies show that increased GH action in the absence of SOCS2 results in an altered bone phenotype, despite no changes in trabecular BMD in young or older mice. Cortical BMD remains unchanged in young, but is decreased in older animals. This suggests that mechanisms that are not altered in the absence of SOCS2 are responsible for maintaining BMD. IGF-1 has been identified as being key in coupling matrix biosynthesis to mineralisation (Zhang *et al.* 2002). The evidence in this thesis points towards a GH action independent of IGF-1. This may potentially account for the diminished BMD in these older mice.

Both the architectural and biomechanical data also highlights a sex specific difference in the bone phenotype of the *Socs2*$^{-/-}$ mice. This is not surprising as the overgrowth phenotype of *Socs2*$^{-/-}$ male mice is much greater than female mice (Metcalf *et al.* 2000). In the clinical setting, in cases of GH deficiency, males are generally considered to be more responsive to GH than females (Burman *et al.* 1997; Span *et al.* 2000). The results presented here highlight that this is also the case in *Socs2*$^{-/-}$ mice when GH action is enhanced above normal levels. It is therefore important to analyse both sexes to gain a full appreciation of the role of SOCS2 in GH regulation. There may however be other factors involved in the sex specific regulation of GH signalling.

The use of both *ex vivo* culture and *in vivo* techniques have shown GH to have growth promoting effects on bone, independent of an increase in IGF-1. This is an exciting prospect as there is concern that raised systemic GH or IGF-1 levels may

promote tumourgenesis. The IGF-1R is overexpressed in many types of cancer (Baserga *et al.* 2003). As IGF-1 is both a promoter of proliferation and an antiapoptotic agent, an uncoupling of the tight balance between these processes is likely to result in an increase in cell growth. This is often the first stage of cancer development. Epidemiological data suggests that increased systemic IGF-1 levels are a major risk factor for developing certain cancers (LeRoith & Roberts 2003). The current literature on GH therapy and the risk of cancer, although extensive, is still inconclusive (Cohen *et al.* 2000; Sklar 2004; Jenkins *et al.* 2006). The overriding consensus is that continued long term surveillance of affected individuals is required. An increase in GH action independent of increased systemic IGF-1 may offer an attractive alternative.

Results from the third results chapter add another tier of complexity to the role of GH on promoting growth. Currently, there are no reported clinical cases in which females have been shown to be more responsive to GH than males. The current results however clearly demonstrate that young female mice are more responsive to GH. This has previously been demonstrated in rats (Rol De Lama *et al.* 2000), and is likely to be an age dependent phenomenon. Future work may help to give an insight into the sexually dimorphic response to GH during the period of rapid pubertal growth. These data also highlights the need to consider the confounding effect of sexual dimorphism when studying growth in rodents.

Aside from GH, SOCS2 levels can be stimulated by a number of other cytokines, including proinflammatory cytokines, which are upregulated during inflammation (Starr *et al.* 1997; MacRae *et al.* 2009; Perse & Cerar 2012). It is therefore possible that SOCS2 may play an important role in mediating bone loss in inflammatory conditions.

Secondary osteoporosis is the most common extra intestinal manifestation associated with IBD, and as a result, is a major financial burden (Ali *et al.* 2009).

Analysis of fracture prevalence varies between studies. Two independent reports using quantitative morphometry of X-rays from CD patients have reported a prevalence of 14% and 22% (Klaus *et al.* 2002; Stockbrugger *et al.* 2002). Although the pathogenesis of IBD associated bone loss is multifactorial, it is clear that it is due to a combination of reduced bone formation and increased bone resorption. Currently, the primary therapy is the anti-resorptive bisphosphonate drugs risedronate and alendronate (Dunn & Goa 2001; Compston 2003). Orally administered bisphosphonates have low absorption levels in healthy people (1-5%). These drugs may therefore not be the most suitable therapy in cases of deteriorated gut health (Compston 2003). There is currently interest in developing anabolic agents to promote bone formation in people with IBD.

GH is already a widely used growth promoting treatment (Allen 2006). As discussed previously, studies have also highlighted the potential use of GH treatment in osteoporosis (Landin-Wilhelmsen *et al.* 2003; Biermasz *et al.* 2004). Clinical studies have also indicated that GH treatment, when giving along with corticosteroids, can be used to treat growth failure in children with CD (Denson *et al.* 2010). GH has not only been shown to improve linear bone growth, but also lean body mass and bone calcium accretion in children with IBD (Mauras 2001). The use of such a commercially available agent for treatment is an attractive prospect. There is however the need for further research into the mechanisms and possible drawbacks of these therapies.

IBD is associated with an increase in the proinflammatory cytokines which contribute to bone loss; either directly or indirectly through GH resistance (Tenore *et al.* 1977; Katsanos *et al.* 2001). The current work has led to the identification of a link between increased proinflammatory cytokine levels and GH resistance at a local level. Increased *Socs2* expression levels in bone from mice with DSS induced colitis were associated with a decrease in bone health. An increase in *Socs2* expression levels in response to TNF-α; a proinflammatory cytokine up regulated during IBD; has been previously reported (Sands & Kaplan 2007; MacRae *et al.* 2009; Perse &

Cerar 2012). Data presented in this thesis indicates that an increase in SOCS2 is likely to inhibit GH action on osteoblasts, and subsequently bone formation. The improved bone health observed in colitic *Socs2*$^{-/-}$ mice confirm SOCS2 as an important regulator of inflammatory driven bone loss.

The protected bone phenotype of *Socs2*$^{-/-}$ mice with colitis has a number of implications in the treatment of skeletal health of IBD patients. As described previously, SOCS2 is a potent regulator of GH action, and in showing that *Socs2*$^{-/-}$ mice are partly protective against bone loss in IBD the present results have given strength to the emerging concept that GH therapy may be used to treat secondary osteoporosis. It has also been suggested that GH may act to improve disease activity index (DIA) in CD patients (Slonim *et al.* 2000). Furthermore, another report has highlighted that although GH improves DAI it does not reduce mucosal inflammation (Denson *et al.* 2010). Analysis of GH transgenic mice highlights that GH overexpression may offer some protection against gut pathology (Williams *et al.* 2001). There was however little evidence in the current studies to suggest that the absence of SOCS2 was beneficial to the mucosal integrity during colitis. The effects of SOCS2 are therefore likely due to the direct effects of inhibited GH action at the osteoblast level, and not an indirect result of improved gut health. This work identifies SOCS2 as a critical regulator through which pro-inflammatory cytokines inhibit GH/IGF-1 signalling and decrease bone health.

Gaining a full understanding on how SOCS2 regulates GH's actions on the skeleton is important because SOCS2 has the potential to be a therapeutic target. A site on the SOCS2 C terminus has been identified as a target for low-molecular-weight inhibitors (Bullock *et al.* 2006). The challenge remains in the development of drugs that can switch off SOCS2 in the organ of interest. Recently, it has also emerged that a patient with increased height and weight, but normal systemic IGF-1 levels, was found to have a heterozygous mutation in the SOCS2 gene (Suda *et al.* 2011). This

confirms that SOCS2 has a critical role in regulating GH signalling in humans necessitating an improved knowledge of its mode of action.

There are limitations to the work presented in this thesis. The next section of this discussion will focus on some of these limitations and possible solutions.

Due to time and money constraints experimental numbers where kept low. In some cases where variation was high this meant that data had to be interpreted with caution. This was evident in the *in vivo* the data presented in chapter 5. It may have been more beneficial to increase sample sizes in certain key experiments so definite conclusions could be drawn.

RNA is a single stranded chain of nucleotides with a ribose, phosphate backbone making it more unstable than DNA and therefore care must be taken in the storage of RNA. There are also a number of endogenous ribonucleases (RNases) present in tissue and cells that can withstand harsh conditions. Although storage of cell pellets and tissue at -80°C in this thesis will have inhibited the actions of some RNases it is likely that there may still have been RNA degradation. Throughout this thesis the utmost care was taken to ensure the highest quality RNA was gained. The quality of the RNA was not however measured. To assess quality, samples would have to be run on a denaturing gel to compare 18S/28S ratios. It is therefore possible that the variation seen in some transcript data in this thesis may be the result of a reduction in quality of RNA due to improper storage. Ideally, RNA would have been stored in a lysis buffer which contains RNase inhibitors.

GH and IGF-1 concentrations used in metatarsal (chapter 3) and osteoblast (chapter 4) cultures were based on previously published research and were not based on the physiological levels of proteins in mice. Caution must therefore be taken when relating these *in vitro* and *ex vivo* experiemnts to the in vivo situation. It would have also been beneficial to complete a dose response curve for GH and IGF-1 action to

gain a full understanding of the effects of these proteins over a range on concentrations.

7.2 Directions for future research

The results presented in this thesis have confirmed a critical role for SOCS2 in regulating endochondral bone growth and bone accrual. Both *ex vivo* and *in vivo* studies have suggested that this role is independent of local IGF-1 production. Further work is however desirable to fully elucidate the importance of IGF-1 in mediating GH action in the *Socs2*$^{-/-}$ mouse model.

Examination of *Socs2;*^{ob}*Igf1r* double knockout mice (Zhang *et al.* 2002) would help confirm that IGF-1/2 signalling are not essential for mediating the *Socs2*$^{-/-}$ skeletal phenotype. Data could be collected to allow assessment with regards to both longitudinal and radial bone growth. In addition, crossing *Socs2*$^{-/-}$ mice to osteoblast or chondrocyte specific *Igf1*$^{-/-}$ mice and examination of their offspring would give further insight into the specific importance of local IGF-1 production in regulating the bone phenotype characteristic of *Socs2*$^{-/-}$ mice. Mice without osteoblast *Igf1* expression could be generated by breeding floxed–*Igf1* mice with mice expressing Cre recombinase, under the control of the 2.3-kb proximal fragment of the α1(I)-collagen promoter; expressed in early osteoblasts and throughout their differentiation (Dacquin *et al.* 2002). Generation of mice using the Cre reombinase-*LoxP* system has been used to knockout IGF-1 in other tissues (Liu *et al.* 2000).

In this thesis, *Socs2*$^{-/-}$ osteoblasts revealed only modestly enhanced *Igf1* expression in response to GH. This was not observed *in vivo*. Identification of alternative genes, preferentially expressed in *Socs2*$^{-/-}$ osteoblasts following GH treatment proved unsuccessful. Due to financial constraints this was confined to a PCR array, focussing only on key genes associated with the JAK/STAT pathway. It would be highly informative to identify the transcriptional signature of *Socs2*$^{-/-}$ osteoblasts in response to GH. This could be completed using Affymetrix gene microarrays, or full

genome sequencing. Data analysis would help identify key genes that are differentially regulated in the absence of SOCS2.

The identification of a sexually dimorphic response of mice to GH in chapter 5 of this thesis is an interesting observation, however further work is required to identify the mechanisms behind this. Initially, work should focus on determining if this is an age dependent effect. Treating older male and female mice with GH would confirm this. As the noted differences in GH sensitivity occurred around the age of sexually dimorphic growth, it would be beneficial to assess the impact of oestrogen in regulating GH action. Serum analysis of oestrogen levels at points before and during the GH responsive phase in females would help determine the serum profile. Furthermore, assessment of the growth rate and bone phenotype of GH treated ovariectomised female mice would address the role of oestrogen as a potential regulator of GH action.

The work carried out in chapter 6 of this thesis was very translational and could potentially lead to the development of new therapeutics to treat bone loss associated with inflammatory disorders such as IBD. It is for this reason that future funding would be best placed further investigating the role SOCS2 in IBD mediated bone loss. The following experiments would continue on nicely from the work presented in this thesis.

Socs2$^{-/-}$ mice are partly protected from IBD associated bone loss. These data are however collected from the end of the experiment, and it is therefore unknown if the absence of SOCS2 expression limits bone loss or accelerated bone mass recovery during colitis progression. Future experiments should look to complete *in vivo* bone scanning; tracking the bone phenotype during the initiation and progression of colitis. Having established the point at which SOCS2 is regulating bone loss, studies could then focus on examining the functional role of SOCS2 in the aetiology of secondary osteoporosis in experimental colitis. It is likely that bone loss in experimental colitis is a result of local GH resistance in bone, due to increased SOCS2. *In vivo* analysis of STAT signalling in response to GH challenge in colitic WT

and *Socs2*$^{-/-}$ mice would help confirm key mechanisms behind IBD induced bone loss.

The use of the *Socs2*$^{-/-}$ model of colitis is highly informative, but it would be essential to establish that a similar course of events occurs in human IBD. This could be investigated by culturing human osteoblasts and treating them with serum from IBD patients and assessing SOCS2 levels.

References

Abad V, Meyers JL, Weise M, Gafni RI, Barnes KM, Nilsson O, Bacher JD & Baron J 2002 The role of the resting zone in growth plate chondrogenesis. *Endocrinology* **143** 1851-1857.

Abreu MT, Geller JL, Vasiliauskas EA, Kam LY, Vora P, Martyak LA, Yang HY, Hu B, Lin YC, Keenan G, Price J, Landers CJ, Adams JS & Targan SR 2006 Treatment with infliximab is associated with increased markers of bone formation in patients with Crohn's disease. *Journal of Clinical Gastroenterology* **40** 55-63.

Adams TE, Epa VC, Garrett TPJ & Ward CW 2000 Structure and function of the type 1 insulin-like growth factor receptor. *Cellular and Molecular Life Sciences* **57** 1050-1093.

Adams TE, Hansen JA, Starr R, Nicola NA, Hilton DJ & Billestrup N 1998 Growth hormone preferentially induces the rapid, transient expression of SOCS-3, a novel inhibitor of cytokine receptor signalling. *Journal of Biological Chemistry* **273** 1285-1287.

Ahmed SF & Farquharson C 2010 The effect of GH and IGF1 on linear growth and skeletal development and their modulation by SOCS proteins. *Journal of Endocrinology.* **206** 249-259.

Akiyama H, Chaboissier MC, Martin JF, Schedl A & de Crombrugghe B 2002 The transcrintion factor Sox9 has essential roles in successive steps of the chondrocyte differentiation pathway and is required for expression of Sox5 and Sox6. *Genes & Development* **16** 2813-2828.

Akune T, Ogata N, Hoshi K, Kubota N, Terauchi Y, Tobe K, Takagi H, Azuma Y, Kadowaki T, Nakamura K & Kawaguchi H 2002 Insulin receptor substrate-2 maintains predominance of anabolic function over catabolic function of osteoblasts. *Journal of Cell Biology* **159** 147-156.

Alex P, Zachos NC, Nguyen T, Gonzales L, Chen TE, Conklin LS, Centola M & Li XH 2009 Distinct Cytokine Patterns Identified from Multiplex Profiles of Murine DSS and TNBS-induced Colitis. *Inflammatory Bowel Diseases* **15** 341-352.

Alexander WS, Starr R, Fenner JE, Scott GL, Handman E, Sprigg NS, Corbin JE, Cornish AL, Darwiche R, Owczarek CM, Kay TWH, Nicola NA, Hertzog PJ, Metcalf D & Hilton DJ 1999 SOCS1 is a critical inhibitor of interferon gamma signalling and prevents the potentially fatal neonatal actions of this cytokine. *Cell* **98** 597-608.

Alexeeva L, Burkhardt P, Christiansen C, Cooper C, Delmas P, Johnell O, Johnston C, Kanis JA, Lips P, Melton LJ, Meunier P, Seeman E, Stepan J & Tosteson A 1994 Assessment of Fracture Risk and Its Application to Screening for Postmenopausal Osteoporosis. *Assessment of Fracture Risk and Its Application to Screening for Postmenopausal Osteoporosis* **843** 1-129.

Ali T, Lam D, Bronze MS & Humphrey MB 2009 Osteoporosis in Inflammatory Bowel Disease. *American Journal of Medicine* **122** 599-604.

Allen DB 2006 Growth hormone therapy for short stature: Is the benefit worth the burden? *Pediatrics* **118** 343-348.

Allen DB 2011 Safety of Growth Hormone Treatment of Children with Idiopathic Short Stature: The US Experience. *Hormone Research in Paediatrics* **76** 45-47.

Almeida M, Iyer S, Martin-Millan M, Bartell SM, Han L, Ambrogini E, Onal M, Xiong JH, Weinstein RS, Jilka RL, O'Brien CA & Manolagas SC 2013 Estrogen receptor-alpha signalling in osteoblast progenitors stimulates cortical bone accrual. *Journal of Clinical Investigation* **123** 394-404.

Andreassen TT, Jorgensen PH, Flyvbjerg A, Orskov H & Oxlund H 1995 Growth-Hormone Stimulates Bone-Formation and Strength of Cortical Bone in Aged Rats. *Journal of Bone and Mineral Research* **10** 1057-1067.

Annunziata M, Granata R & Ghigo E 2011 The IGF system. *Acta Diabetologica* **48** 1-9.

Araki Y, Mukaisyo KI, Sugihara H, Fujiyama Y & Hattori T 2010 Increased apoptosis and decreased proliferation of colonic epithelium in dextran sulfate sodium-induced colitis in mice. *Oncology Reports* **24** 869-874.

Aubin JE 1998 Advances in the osteoblast lineage. *Biochemistry and Cell Biology-Biochimie et Biologie Cellulaire* **76** 899-910.

Aubin JE, Liu F, Malaval L & Gupta AK 1995 Osteoblast and Chondroblast Differentiation. *Bone* **17** S77-S83.

Bagi CM, Brommage R, Deleon L, Adams S, Rosen D & Sommer A 1994 Benefit of Systemically Administered Rhigf-I and Rhigf-I Igfbp-3 on Cancellous Bone in Ovariectomized Rats. *Journal of Bone and Mineral Research* **9** 1301-1312.

Baker AR, Hollingshead PG, Pittsmeek S, Hansen S, Taylor R & Stewart TA 1992 Osteoblast-Specific Expression of Growth-Hormone Stimulates Bone-Growth in Transgenic Mice. *Molecular and Cellular Biology* **12** 5541-5547.

Baker J, Liu JP, Robertson EJ & Efstratiadis A 1993 Role of Insulin-Like Growth-Factors in Embryonic and Postnatal-Growth. *Cell* **75** 73-82.

Baldock PA, Allison S, McDonald MM, Sainsbury A, Enriquez RF, Little DG, Eisman JA, Gardiner EM & Herzog H 2006 Hypothalamic regulation of cortical bone mass: Opposing activity of Y2 receptor and leptin pathways. *Journal of Bone and Mineral Research* **21** 1600-1607.

Ballesteros M, Leung KC, Ross RJM, Iismaa TP & Ho KKY 2000 Distribution and abundance of messenger ribonucleic acid for growth hormone receptor isoforms in human tissues. *Journal of Clinical Endocrinology & Metabolism* **85** 2865-2871.

Ballinger AB, Azooz O, El-Hajh T, Poole S & Farthing MJG 2000 Growth failure occurs through a decrease in insulin-like growth factor 1 which is independent of undernutrition in a rat model of colitis. *Gut* **46** 694-700.

Ballock RT & O'Keefe RJ 2003 The biology of the growth plate. *Journal of Bone and Joint Surgery-American Volume* **85A** 715-726.

Bang P, Ahmed SF, Argente J, Backeljauw P, Bettendorf M, Bona G, Coutant R, Rosenfeld RG, Walenkamp MJ & Savage MO 2012 Identification and management of poor response to growth-promoting therapy in children with short stature. *Clinical Endocrinology* **77** 169-181.

Bang P, Bjerknes R, Dahlgren J, Dunkel L, Gustafsson J, Juul A, Kristrom B, Tapanainen P & Aberg V 2011 A Comparison of Different Definitions of Growth Response in Short Prepubertal Children Treated with Growth Hormone. *Hormone Research in Paediatrics* **75** 335-345.

Bannink EMN, van der Palen RLF, Mulder PGH & Keizer-Schrama SMPF 2009 Long-Term Follow-Up of GH-Treated Girls with Turner Syndrome: Metabolic Consequences. *Hormone Research* **71** 343-349.

Barnard R, Haynes KM, Werther GA & Waters MJ 1988 The Ontogeny of Growth-Hormone Receptors in the Rabbit Tibia. *Endocrinology* **122** 2562-2569.

Barnard R, Ng KW, Martin TJ & Waters MJ 1991 Growth-Hormone (Gh) Receptors in Clonal Osteoblast-Like Cells Mediate A Mitogenic Response to Gh. *Endocrinology* **128** 1459-1464.

Baserga R, Peruzzi F & Reiss K 2003 The igf-1 receptor in cancer biology. *International Journal of Cancer* **107** 873-877.

Baumann G 2001 Growth hormone binding protein 2001. *Journal of Pediatric Endocrinology & Metabolism* **14** 355-375.

Baumann G, Amburn KD & Buchanan TA 1987 The Effect of Circulating Growth Hormone-Binding Protein on Metabolic-Clearance, Distribution, and Degradation of Human Growth-Hormone. *Journal of Clinical Endocrinology & Metabolism* **64** 657-660.

Beauloye V, Willems B, de Coninck V, Frank SJ, Edery M & Thissen JP 2002 Impairment of liver GH receptor signalling by fasting. *Endocrinology* **143** 792-800.

Berg DJ, Davidson N, Kuhn R, Muller W, Menon S, Holland G, ThompsonSnipes L, Leach MW & Rennick D 1996 Enterocolitis and colon cancer in interleukin-10-

deficient mice are associated with aberrant cytokine production and CD4(+) TH1-like responses. *Journal of Clinical Investigation* **98** 1010-1020.

Berg DJ, Zhang J, Weinstock JV, Ismail HF, Earle KA, Alila H, Pamukcu R, Moore S & Lynch RG 2002 Rapid development of colitis in NSAID-treated IL-10-deficient mice. *Gastroenterology* **123** 1527-1542.

Bielohuby M, Schaab M, Kummann M, Sawitzky M, Gebhardt R, Binder G, Frystyk J, Bjerre M, Hoeflich A, Kratzsch J & Bidlingmaier M 2011 Serum IGF-I Is Not a Reliable Pharmacodynamic Marker of Exogenous Growth Hormone Activity in Mice. *Endocrinology* **152** 4764-4776.

Biermasz NR, Hamdy NAT, Pereira AM, Romijn JA & Roelfsema F 2004 Long-term skeletal effects of recombinant human growth hormone (rhGH) alone and rhGH combined with alendronate in GH-deficient adults: a seven-year follow-up study. *Clinical Endocrinology* **60** 568-575.

Bikle D, Majumdar S, Laib A, Powell-Braxton L, Rosen C, Beamer W, Nauman E, Leary C & Halloran B 2001 The skeletal structure of insulin-like growth factor I-deficient mice. *Journal of Bone and Mineral Research* **16** 2320-2329.

Bjarnason I, Macpherson A, Mackintosh C, BuxtonThomas M, Forgacs I & Moniz C 1997 Reduced bone density in patients with inflammatory bowel disease. *Gut* **40** 228-233.

Boisclair YR, Rhoads RP, Ueki I, Wang J & Ooi GT 2001 The acid-labile subunit (ALS) of the 150 kDa IGF-binding protein complex: an important but forgotten component of the circulating IGF system. *Journal of Endocrinology* **170** 63-70.

Boisclair YR, Wang JR, Shi JR, Hurst KR & Ooi GT 2000 Role of the suppressor of cytokine signalling-3 in mediating the inhibitory effects of interleukin-1 beta on the growth hormone-dependent transcription of the acid-labile subunit gene in liver cells. *Journal of Biological Chemistry* **275** 3841-3847.

Boismenu R & Chen YP 2000 Insights from mouse models of colitis. *Journal of Leukocyte Biology* **67** 267-278.

Bolamperti S, Mrak E, Moro G, Sirtori P, Fraschini G, Guidobono F, Rubinacci A & Villa I 2013 17 beta-Estradiol positively modulates growth hormone signalling through the reduction of SOCS2 negative feedback in human osteoblasts. *Bone* **55** 84-92.

Bonewald LF 2007 Osteocytes as dynamic multifunctional cells. *Skeletal Biology and Medicine, Pt A* **1116** 281-290.

Bonewald LF 2011 The Amazing Osteocyte. *Journal of Bone and Mineral Research* **26** 229-238.

Borjesson AE, Lagerquist MK, Liu C, Shao RJ, Windahl SH, Karlsson C, Sjogren K, Moverare-Skrtic S, Antal MC, Krust A, Mohan S, Chambon P, Savendahl L & Ohlsson C 2010 The Role of Estrogen Receptor alpha in Growth Plate Cartilage for Longitudinal Bone Growth. *Journal of Bone and Mineral Research* **25** 2414-2424.

Brooks AJ, Wooh JW, Tunny KA & Waters MJ 2008 Growth hormone receptor; mechanism of action. *Int.J.Biochem.Cell Biol.* **40** 1984-1989.

Buckwalter JA, Mower D, Ungar R, Schaeffer J & Ginsberg B 1986 Morphometric Analysis of Chondrocyte Hypertrophy. *Journal of Bone and Joint Surgery-American Volume* **68A** 243-255.

Bullock AN, Debreczeni JE, Edwards AM, Sundstrom M & Knapp S 2006 Crystal structure of the SOCS2-elongin C-elongin B complex defines a prototypical SOCS box ubiquitin ligase. *Proceedings of the National Academy of Sciences of the United States of America* **103** 7637-7642.

Burdan F, Szumilo J, Korobowicz A, Farooquee R, Patel S, Patel A, Dave A, Szumilo M, Solecki M, Klepacz R & Dudka J 2009 Morphology and physiology of the epiphyseal growth plate. *Folia Histochemica et Cytobiologica* **47** 5-16.

Burman P, Johansson AG, Siegbahn A, Vessby B & Karlsson FA 1997 Growth hormone (GH)-deficient men are more responsive to GH replacement therapy than women. *Journal of Clinical Endocrinology & Metabolism* **82** 550-555.

Bush PG, Hall AC & Macnicol MF 2008 New insights into function of the growth plate: clinical observations, chondrocyte enlargement and a possible role for membrane transporters. *Journal of Bone and Joint Surgery-British Volume* **90B** 1541-1547.

Callewaert F, Venken K, Kopchick JJ, Torcasio A, van Lenthe GH, Boonen S & Vanderschueren D 2010 Sexual Dimorphism in Cortical Bone Size and Strength But Not Density Is Determined by Independent and Time-Specific Actions of Sex Steroids and IGF-1: Evidence From Pubertal Mouse Models. *Journal of Bone and Mineral Research* **25** 617-626.

Callewaert F, Venken K, Ophoff J, De Gendt K, Torcasio A, van Lenthe GH, Van Oosterwyck H, Boonen S, Bouillon R, Verhoeven G & Vanderschueren D 2009 Differential regulation of bone and body composition in male mice with combined inactivation of androgen and estrogen receptor-alpha. *Faseb Journal* **23** 232-240.

Canalis E 1980 Effect of Insulin-Like Growth Factor-I on Dna and Protein-Synthesis in Cultured Rat Calvaria. *Journal of Clinical Investigation* **66** 709-719.

Canalis E, Rydziel S, Delany AM, Varghese S & Jeffrey JJ 1995 Insulin-Like Growth-Factors Inhibit Interstitial Collagenase Synthesis in Bone Cell-Cultures. *Endocrinology* **136** 1348-1354.

Chagin AS, Karimian E, Sundstrom K, Eriksson E & Savendahl L 2010 Catch-up growth after dexamethasone withdrawal occurs in cultured postnatal rat metatarsal bones. *Journal of Endocrinology* **204** 21-29.

Chen LA, Jiang W, Huang JY, He BC, Zuo GW, Zhang WL, Luo Q, Shi QO, Zhang BQ, Wagner ER, Luo JY, Tang M, Wietholt C, Luo XJ, Bi Y, Su YX, Liu B, Kim SH, He CJ, Hu YW, Shen JK, Rastegar F, Huang EY, Gao YH, Gao JL, Zhou JZ, Reid RR, Luu HH, Haydon RC, He TC & Deng ZL 2010 Insulin-like Growth Factor 2 (IGF-2) Potentiates BMP-9-Induced Osteogenic Differentiation and Bone Formation. *Journal of Bone and Mineral Research* **25** 2447-2459.

Chen Y, Sood S, Krishnamurthy VMR, Rotwein P & Rabkin R 2009 Endotoxin-Induced Growth Hormone Resistance in Skeletal Muscle. *Endocrinology* **150** 3620-3626.

Chen Y, Sun DF, Krishnamurthy VMR & Rabkin R 2007 Endotoxin attenuates growth hormone-induced hepatic insulin-like growth factor I expression by inhibiting JAK2/STAT5 signal transduction and STAT5b DNA binding. *American Journal of Physiology-Endocrinology and Metabolism* **292** E1856-E1862.

Cheung WW, Rosengren S, Boyle DL & Mak RH 2008 Modulation of melanocortin signalling ameliorates uremic cachexia. *Kidney International* **74** 180-186.

Chowen JA, Frago LM & Argente J 2004 The regulation of GH secretion by sex steroids. *European Journal of Endocrinology* **151** U95-U100.

Clarke B 2008 Normal Bone Anatomy and Physiology. *Clinical Journal of the American Society of Nephrology* **3** S131-S139.

Clemmons DR 1998 Role of insulin-like growth factor binding proteins in controlling IGF actions. *Molecular and Cellular Endocrinology* **140** 19-24.

Cohen P, Clemmons DR & Rosenfeld RG 2000 Does the GH-IGF axis play a role in cancer pathogenesis? *Growth Hormone & Igf Research* **10** 297-305.

Cohen SL, Moore AM & Ward WE 2004 Interleukin-10 knockout mouse: A model for studying bone metabolism during intestinal inflammation. *Inflammatory Bowel Diseases* **10** 557-563.

Colson A, Le Cam A, Maiter D, Edery M & Thissen JP 2000 Potentiation of growth hormone-induced liver suppressors of cytokine signalling messenger ribonucleic acid by cytokines. *Endocrinology* **141** 3687-3695.

Compston J 2003 Osteoporosis in inflammatory bowel disease. *Gut* **52** 63-64.

Compston JE 2001 Sex steroids and bone. *Physiological Reviews* **81** 419-447.

Compston JE, Judd D, Crawley EO, Evans WD, Evans C, Church HA, Reid EM & Rhodes J 1987 Osteoporosis in Patients with Inflammatory Bowel-Disease. *Gut* **28** 410-415.

Cooper HS, Murthy SNS, Shah RS & Sedergran DJ 1993 Clinicopathological Study of Dextran Sulfate Sodium Experimental Murine Colitis. *Laboratory Investigation* **69** 238-249.

Courtland HW, Sun H, Beth-On M, Wu YJ, Elis S, Rosen CJ & Yakar S 2011 Growth Hormone Mediates Pubertal Skeletal Development Independent of Hepatic IGF-1 Production. *Journal of Bone and Mineral Research* **26** 761-768.

Coxam V, Miller MA, Bowman MB & Miller SC 1996 Ontogenesis of IGF regulation of longitudinal bone growth in rat metatarsal rudiments cultured in serum-free medium. *Archives of Physiology and Biochemistry* **104** 173-179.

Crockett JC, Rogers MJ, Coxon FP, Hocking LJ & Helfrich MH 2011 Bone remodelling at a glance. *Journal of Cell Science* **124** 991-998.

Croker BA, Kiu H & Nicholson SE 2008 SOCS regulation of the JAK/STAT signalling pathway. *Seminars in Cell & Developmental Biology* **19** 414-422.

Czekanska EM, Stoddart MJ, Richards RG & Hayes JS 2012 In Search of An Osteoblast Cell Model for in Vitro Research. *European Cells & Materials* **24** 1-17.

Dacquin R, Starbuck M, Schinke T & Karsenty G 2002 Mouse alpha 1(I)-collagen promoter is the best known promoter to drive efficient Cre recombinase expression in osteoblast. *Developmental Dynamics* **224** 245-251.

Dallas SL & Bonewald LF 2010 Dynamics of the transition from osteoblast to osteocyte. *Skeletal Biology and Medicine* **1192** 437-443.

Datta SR, Dudek H, Tao X, Masters S, Fu HA, Gotoh Y & Greenberg ME 1997 Akt phosphorylation of BAD couples survival signals to the cell-intrinsic death machinery. *Cell* **91** 231-241.

Daughada WH & Reeder C 1966 Synchronous Activation of Dna Synthesis in Hypophysectomized Rat Cartilage by Growth Hormone. *Journal of Laboratory and Clinical Medicine* **68** 357-&.

Daughada WH, Salmon WD, Vandenbr JL, Vanwyk JJ, Raben MS & Hall K 1972 Somatomedin - Proposed Designation for Sulfation Factor. *Nature* **235** 107-&.

Davey HW, McLachlan MJ, Wilkins RJ, Hilton DJ & Adams TE 1999a STAT5b mediates the GH-induced expression of SOCS-2 and SOCS-3 mRNA in the liver. *Molecular and Cellular Endocrinology* **158** 111-116.

Davey HW, Wilkins RJ & Waxman DJ 1999b STAT5 signalling in sexually dimorphic gene expression and growth patterns. *American Journal of Human Genetics* **65** 959-965.

Davey HW, Xie T, McLachlan MJ, Wilkins RJ, Waxman DJ & Grattan DR 2001 STAT5b is required for GH-induced liver Igf-I gene expression. *Endocrinology* **142** 3836-3841.

Davison KS, Siminoski K, Adachi JD, Hanley DA, Goltzman D, Hodsman AB, Josse R, Kaiser S, Olszynski WP, Papaioannou A, Ste-Marie LG, Kendler DL, Tenenhouse A & Brown JP 2006 Bone strength: The whole is greater than the sum of its parts. *Seminars in Arthritis and Rheumatism* **36** 22-31.

Day TF, Guo XZ, Garrett-Beal L & Yang YZ 2005 Wnt/beta-catenin signalling in mesenchymal progenitors controls osteoblast and chondrocyte differentiation during vertebrate skeletogenesis. *Developmental Cell* **8** 739-750.

De Benedetti F, Pignatti P, Vivarelli M, Meazza C, Ciliberto G, Savino R & Martini A 2001 In vivo neutralization of human IL-6 (hIL-6) achieved by immunization of hIL-6-transgenic mice with a hIL-6 receptor antagonist. *Journal of Immunology* **166** 4334-4340.

De Benedetti F, Rucci N, Del Fattore A, Peruzzi B, Paro R, Longo M, Vivarelli M, Muratori F, Berni S, Ballanti P, Ferrari S & Teti A 2006 Impaired skeletal development in interleukin-6-transgenic mice - A model for the impact of chronic inflammation on the growing skeletal system. *Arthritis and Rheumatism* **54** 3551-3563.

DeBenedetti F, Alonzi T, Moretta A, Lazzaro D, Costa P, Poli V, Martini A, Ciliberto G & Fattori E 1997 Interleukin 6 causes growth impairment in transgenic mice through a decrease in insulin-like growth factor-I - A model for stunted growth in children with chronic inflammation. *Journal of Clinical Investigation* **99** 643-650.

Dechiara TM, Efstratiadis A & Robertson EJ 1990 A Growth-Deficiency Phenotype in Heterozygous Mice Carrying An Insulin-Like Growth Factor-Ii Gene Disrupted by Targeting. *Nature* **345** 78-80.

Decker T & Kovarik P 2000 Serine phosphorylation of STATs. *Oncogene* **19** 2628-2637.

Delaisse JM, Andersen TL, Engsig MT, Henriksen K, Troen T & Blavier L 2003 Matrix metalloproteinases (MMP) and cathepsin K contribute differently to osteoclastic activities. *Microscopy Research and Technique* **61** 504-513.

Delise AM & Tuan RS 2002 Alterations in the spatiotemporal expression pattern and function of N-cadherin inhibit cellular condensation and chondrogenesis of limb mesenchymal cells in vitro. *Journal of Cellular Biochemistry* **87** 342-359.

Demellow JSM & Baxter RC 1988 Growth Hormone-Dependent Insulin-Like Growth-Factor (Igf) Binding-Protein Both Inhibits and Potentiates Igf-I-Stimulated Dna-Synthesis in Human-Skin Fibroblasts. *Biochemical and Biophysical Research Communications* **156** 199-204.

Denko CW & Malemud CJ 2004 The serum growth hormone to somatostatin ratio is skewed upward in rheumatoid arthritis patients. *Frontiers in Bioscience* **9** 1660-1664.

Denson LA, Held MA, Menon RK, Frank SJ, Parlow AF & Arnold DL 2003 Interleukin-6 inhibits hepatic growth hormone signalling via upregulation of Cis and Socs-3. *American Journal of Physiology-Gastrointestinal and Liver Physiology* **284** G646-G654.

Denson LA, Kim MO, Bezold R, Carey R, Osuntokun B, Nylund C, Willson T, Bonkowski E, Li DD, Ballard E, Collins M, Moyer MS & Klein DJ 2010 A Randomized Controlled Trial of Growth Hormone in Active Pediatric Crohn Disease. *Journal of Pediatric Gastroenterology and Nutrition* **51** 130-139.

Denson LA, Menon RK, Shaufl A, Bajwa HS, Williams CR & Karpen SJ 2001 TNF-alpha downregulates murine hepatic growth hormone receptor expression by inhibiting Sp1 and Sp3 binding. *Journal of Clinical Investigation* **107** 1451-1458.

Dercole AJ, Stiles AD & Underwood LE 1984 Tissue Concentrations of Somatomedin-C - Further Evidence for Multiple Sites of Synthesis and Paracrine Or Autocrine Mechanisms of Action. *Proceedings of the National Academy of Sciences of the United States of America-Biological Sciences* **81** 935-939.

Dessau W, Vondermark H, Vondermark K & Fischer S 1980 Changes in the Patterns of Collagens and Fibronectin During Limb-Bud Chondrogenesis. *Journal of Embryology and Experimental Morphology* **57** 51-60.

Dey BR, Spence SL, Nissley P & Furlanetto RW 1998 Interaction of Human Suppressor of Cytokine Signalling (SOCS)-2 with the Insulin-like Growth Factor-I Receptor. *Journal of Biological Chemistry* **273** 24095-24101.

Dieleman LA, Palmen MJHJ, Akol H, Bloemena E, Pena AS, Meuwissen SGM & van Rees EP 1998 Chronic experimental colitis induced by dextran sulphate sodium (DSS) is characterized by Th1 and Th2 cytokines. *Clinical and Experimental Immunology* **114** 385-391.

Difedele LM, He JM, Bonkowski EL, Han XN, Held MA, Bohan A, Menon RK & Denson LA 2005 Tumor necrosis factor alpha blockade restores growth hormone signalling in murine colitis. *Gastroenterology* **128** 1278-1291.

DiGirolamo DJ, Mukherjee A, Fulzele K, Gan YJ, Cao XM, Frank SJ & Clemens TL 2007 Mode of growth hormone action in osteoblasts
5. *Journal of Biological Chemistry* **282** 31666-31674.

Dinca M, Fries W, Luisetto G, Peccolo F, Bottega F, Leone L, Naccarato R & Martin A 1999 Evolution of osteopenia in inflammatory bowel disease. *American Journal of Gastroenterology* **94** 1292-1297.

Donahue LR & Beamer WG 1993 Growth-Hormone Deficiency in Little Mice Results in Aberrant Body-Composition, Reduced Insulin-Like Growth Factor-I and Insulin-Like Growth Factor-Binding Protein-3 (Igfbp-3), But Does Not Affect Igfbp-2, Igfbp-1 Or Igfbp-4. *Journal of Endocrinology* **136** 91-104.

Dubner SE, Shults J, Baldassano RN, Zemel BS, Thayu M, Burnham JM, Herskovitz RM, Howard KM & Leonarda MB 2009 Longitudinal Assessment of Bone Density and Structure in an Incident Cohort of Children With Crohn's Disease. *Gastroenterology* **136** 123-130.

Dudley HR & Spiro D 1961 Fine Structure of Bone Cells. *Journal of Biophysical and Biochemical Cytology* **11** 627-&.

Dunn CJ & Goa KL 2001 Risedronate - A review of its pharmacological properties and clinical use in resorptive bone disease. *Drugs* **61** 685-712.

Durbin JE, Hackenmiller R, Simon MC & Levy DE 1996 Targeted disruption of the mouse STAT1 results in compromised innate immunity to viral disease. *Cell* **84** 443-450.

Eckstein F, Weusten A, Schmidt C, Wehr U, Wanke R, Rambeck W, Wolf E & Mohan S 2004 Longitudinal in vivo effects of growth hormone overexpression on bone in transgenic mice. *Journal of Bone and Mineral Research* **19** 802-810.

Eicher EM & Beamer WG 1976 Inherited Ateliotic Dwarfism in Mice - Characteristics of Mutation, Little, on Chromosome-6. *Journal of Heredity* **67** 87-91.

Eivindson M, Gronbaek H, Skogstrand K, Thorsen P, Frystyk J, Flyvbjerg A & Dahlerup JF 2007 The insulin-like growth factor (IGF) system and its relation to infliximab treatment in adult patients with Crohn's disease. *Scandinavian Journal of Gastroenterology* **42** 464-470.

Eleswarapu S, Gu ZL & Jiang HL 2008 Growth hormone regulation of insulin-like growth factor-I gene expression may be mediated by multiple distal signal transducer and activator of transcription 5 binding sites. *Endocrinology* **149** 2230-2240.

Elis S, Courtland HW, Wu YJ, Rosen CJ, Sun H, Jepsen KJ, Majeska RJ & Yakar S 2010 Elevated Serum Levels of IGF-1 Are Sufficient to Establish Normal Body Size

and Skeletal Properties Even in the Absence of Tissue IGF-1. *Journal of Bone and Mineral Research* **25** 1257-1266.

Farnum CE, Lee R, O'Hara K & Urban JPG 2002 Volume increase in growth plate chondrocytes during hypertrophy: The contribution of organic osmolytes. *Bone* **30** 574-581.

Farnum CE & Wilsman NJ 1993 Determination of Proliferative Characteristics of Growth Plate Chondrocytes by Labeling with Bromodeoxyuridine. *Calcified Tissue International* **52** 110-119.

Farquharson C & Jefferies D 2000 Chondrocytes and longitudinal bone growth: The development of tibial dyschondroplasia. *Poultry Science* **79** 994-1004.

Favre H, Benhamou A, Finidori J, Kelly PA & Edery M 1999 Dual effects of suppressor of cytokine signalling (SOCS-2) on growth hormone signal transduction. *Febs Letters* **453** 63-66.

Flores-Morales A, Greenhalgh CJ, Norstedt G & Rico-Bautista E 2006 Negative regulation of growth hormone receptor signalling. *Mol.Endocrinol.* **20** 241-253.

Fox SW, Haque SJ, Lovibond AC & Chambers TJ 2003 The possible role of TGF-beta-induced suppressors of cytokine signalling expression in osteoclast/macrophage lineage commitment in vitro. *Journal of Immunology* **170** 3679-3687.

Frank SJ 2001 Growth hormone signalling and its regulation: Preventing too much of a good thing. *Growth Hormone & Igf Research* **11** 201-212.

Frohman LA, Downs TR & Chomczynski P 1992 Regulation of Growth-Hormone Secretion. *Frontiers in Neuroendocrinology* **13** 344-405.

Fruchtman S, Simmons JG, Michaylira CZ, Miller ME, Greenhalgh CJ, Ney DM & Lund PK 2005 Suppressor of cytokine signalling-2 modulates the fibrogenic actions of GH and IGF-I in intestinal mesenchymal cells. *American Journal of Physiology-Gastrointestinal and Liver Physiology* **289** G342-G350.

Fujimoto M, Naka T, Nakagawa R, Kawazoe Y, Morita Y, Tateishi A, Okumura K, Narazaki M & Kishimoto T 2000 Defective thymocyte development and perturbed homeostasis of T cells in STAT-induced STAT inhibitor-1/suppressors of cytokine signalling-1 transgenic mice. *Journal of Immunology* **165** 1799-1806.

Fukumoto S & Martin TJ 2009 Bone as an endocrine organ. *Trends in Endocrinology and Metabolism* **20** 230-236.

Garcia-Echeverria C, Pearson MA, Marti A, Meyer T, Mestan J, Zimmermann J, Gao JP, Brueggen J, Capraro HG, Cozens R, Evans DB, Fabbro D, Furet P, Porta DG, Liebetanz J, Martiny-Baron G, Ruetz S & Hofmann F 2004 In vivo antitumor activity of NVP-AEW541 - A novel, potent, and selective inhibitor of the IGF-IR kinase. *Cancer Cell* **5** 231-239.

Garland JT, Lottes ME, Kozak S & Daughada WH 1972 Stimulation of Dna-Synthesis in Isolated Chondrocytes by Sulfation Factor. *Endocrinology* **90** 1086-&.

Gevers EF, Loveridge N & Robinson IC 2002a Bone marrow adipocytes: a neglected target tissue for growth hormone. *Endocrinology* **143** 4065-4073.

Gevers EF, Van Der Eerden BCJ, Karperien M, Raap AK, Robinson ICAF & Wit JM 2002b Localization and regulation of the growth hormone receptor and growth hormone-binding protein in the rat growth plate. *Journal of Bone and Mineral Research* **17** 1408-1419.

Gilbert L, He XF, Farmer P, Boden S, Kozlowski M, Rubin J & Nanes MS 2000 Inhibition of osteoblast differentiation by tumor necrosis factor-alpha. *Endocrinology* **141** 3956-3964.

Gilbert SF 2006 Developmental Biology, 8th Edition , in: ISBN 0-87893-250-X

Gillberg P, Mallmin H, Petren-Mallmin M, Ljunghall S & Nilsson AG 2002 Two years of treatment with recombinant human growth hormone increases bone mineral density in men with idiopathic osteoporosis. *Journal of Clinical Endocrinology & Metabolism* **87** 4900-4906.

Girnita A, Girnita L, del Prete F, Bartolazzi A, Larsson O & Axelson M 2004 Cyclolignans as inhibitors of the insulin-like growth factor-1 receptor and malignant cell growth. *Cancer Research* **64** 236-242.

Giustina A, Mazziotti G & Canalis E 2008 Growth hormone, insulin-like growth factors, and the skeleton. *Endocr.Rev.* **29** 535-559.

Giustina A & Veldhuis JD 1998 Pathophysiology of the neuroregulation of growth hormone secretion in experimental animals and the human. *Endocrine Reviews* **19** 717-797.

Gluckman PD & Pinal CS 2003 Regulation of fetal growth by the somatotrophic axis. *Journal of Nutrition* **133** 1741S-1746S.

Goedbloed JF 1980 Embryonic and Postnatal-Growth of the Rat and Mouse .6. Prenatal Growth of Organs and Tissues - Individual Organs - Final Remarks on Parts I-Vi, Phase-Transitions. *Acta Anatomica* **106** 108-128.

Goldring MB, Tsuchimochi K & Ijiri K 2006 The control of chondrogenesis. *Journal of Cellular Biochemistry* **97** 33-44.

Goldshmit Y, Walters CE, Scott HJ, Greenhalgh CJ & Turnley AM 2004 SOCS2 induces neurite outgrowth by regulation of epidermal growth factor receptor activation. *Journal of Biological Chemistry* **279** 16349-16355.

Govoni KE, Lee SK, Chadwick RB, Yu HR, Kasukawa Y, Baylink DJ & Mohan S 2006 Whole genome microarray analysis of growth hormone-induced gene expression in bone: T-box3, a novel transcription factor, regulates osteoblast proliferation. *American Journal of Physiology-Endocrinology and Metabolism* **291** E128-E136.

Govoni KE, Lee SK, Chung YS, Behringer RR, Wergedal JE, Baylink DJ & Mohan S 2007a Disruption of insulin-like growth factor-I expression in type II alpha I collagen-expressing cells reduces bone length and width in mice. *Physiological Genomics* **30** 354-362.

Govoni KE, Wergedal JE, Florin L, Angel P, Baylink DJ & Mohan S 2007b Conditional deletion of insulin-like growth factor-I in collagen type 1 alpha 2-expressing cells results in postnatal lethality and a dramatic reduction in bone accretion. *Endocrinology* **148** 5706-5715.

Green H, Morikawa M & Mxon T 1985 A dual effector theory of growth-hormone action. *Differentiation* **29** 195-198.

Greenhalgh CJ & Alexander WS 2004 Suppressors of cytokine signalling and regulation of growth hormone action. *Growth Horm.IGF Res.* **14** 200-206.

Greenhalgh CJ, Bertolino P, Asa SL, Metcalf D, Corbin JE, Adams TE, Davey HW, Nicola NA, Hilton DJ & Alexander WS 2002 Growth enhancement in suppressor of cytokine signalling 2 (SOCS-2)-deficient mice is dependent on signal transducer and activator of transcription 5b (STAT5b). *Molecular Endocrinology* **16** 1394-1406.

Greenhalgh CJ & Hilton DJ 2001 Negative regulation of cytokine signalling. *Journal of Leukocyte Biology* **70** 348-356.

Greenhalgh CJ, Metcalf D, Thaus AL, Corbin JE, Uren R, Morgan PO, Fabri LJ, Zhang JG, Martin HM, Willson TA, Billestrup N, Nicola NA, Baca M, Alexander WS & Hilton DJ 2002b Biological evidence that SOCS-2 can act either as an enhancer or suppressor of growth hormone signalling. *Journal of Biological Chemistry* **277** 40181-40184.

Greenhalgh CJ, Rico-Bautista E, Lorentzon M, Thaus AL, Morgan PO, Willson TA, Zervoudakis P, Metcalf D, Street I, Nicola NA, Nash AD, Fabri LJ, Norstedt G, Ohlsson C, Flores-Morales A, Alexander WS & Hilton DJ 2005 SOCS2 negatively regulates growth hormone action in vitro and in vivo. *J.Clin.Invest* **115** 397-406.

Guarnieri G, Biolo G, Zanetti M & Barazzoni R 2004 Chronic systemic inflammation in uremia: Potential therapeutic approaches. *Seminars in Nephrology* **24** 441-445.

Guasti L, Ferretti P, Bulstrode B & Dunkel L 2013 FGF21 causes GH resistance in human chondrocytes through activation of SOCS2 and inhibition of IGF1 expression. *Endocrine Abstracts* **33**.

Guicheux J, Heymann D, Rousselle AV, Gouin F, Pilet P, Yamada S & Daculsi G 1998 Growth hormone stimulatory effects on osteoclastic resorption are partly mediated by insulin-like growth factor I: An in vitro study. *Bone* **22** 25-31.

Guntur AR & Rosen CJ 2012 Bone As An Endocrine Organ. *Endocrine Practice* **18** 758-762.

Hadjidakis DJ & Androulakis II 2006 Bone remodeling. *Women'S Health and Disease: Gynecologic, Endocrine, and Reproductive Issues* **1092** 385-396.

Hahn M, Vogel M, Pompesiuskempa M & Delling G 1992 Trabecular Bone Pattern Factor - A New Parameter for Simple Quantification of Bone Microarchitecture. *Bone* **13** 327-330.

Hale LP, Gottfried MR & Swidinski A 2005 Piroxicam treatment of IL-10-deficient mice enhances colonic epithelial apoptosis and mucosal exposure to intestinal bacteria. *Inflammatory Bowel Diseases* **11** 1060-1069.

Hamamura K, Zhang P & Yokota H 2008 IGF2-driven PI3 kinase and TGF beta signalling pathways in chondrogenesis. *Cell Biology International* **32** 1238-1246.

Hamdani G, Gabet Y, Rachmilewitz D, Karmeli F, Bab I & Dresner-Pollak R 2008 Dextran sodium sulfate-induced colitis causes rapid bone loss in mice. *Bone* **43** 945-950.

Han YL, Leaman DW, Watling D, Rogers NC, Groner B, Kerr IM, Wood WI & Stark GR 1996 Participation of JAK and STAT proteins in growth hormone-induced signalling. *Journal of Biological Chemistry* **271** 5947-5952.

Hansen I, Tsalikian E, Beaufrere B, Gerich J, Haymond M & Rizza R 1986 Insulin Resistance in Acromegaly - Defects in Both Hepatic and Extrahepatic Insulin Action. *American Journal of Physiology* **250** E269-E273.

Harmey D, Hessle L, Narisawa S, Johnson KA, Terkeltaub R & Millan JL 2004 Concerted regulation of inorganic pyrophosphate and osteopontin by Akp2, Enpp1, and Ank - An integrated model of the pathogenesis of mineralization disorders. *American Journal of Pathology* **164** 1199-1209.

Harris J, Stanford PM, Sutherland K, Oakes SR, Naylor MJ, Robertson FG, Blazek KD, Kazlauskas M, Hilton HN, Wittlin S, Alexander WS, Lindeman GJ, Visvader JE

& Ormandy CJ 2006 Socs2 and Elf5 mediate prolactin-induced mammary gland development. *Molecular Endocrinology* **20** 1177-1187.

Harris L, Senagore P, Young VB & Mccabe LR 2009 Inflammatory bowel disease causes reversible suppression of osteoblast and chondrocyte function in mice. *American Journal of Physiology-Gastrointestinal and Liver Physiology* **296** G1020-G1029.

He JN, Rosen CJ, Adams DJ & Kream BE 2006 Postnatal growth and bone mass in mice with IGF-I haploinsufficiency. *Bone* **38** 826-835.

Heiman ML, Tinsley FC, Mattison JA, Hauck S, Bartket A 2003 Body composition of prolactin-, growth hormonw-, and thyrotropin-deficinet ames dwarf mice. *Endocrinology* 2003 **20** 149-154

Heinrichs C, Yanovski JA, Roth AH, Yu YM, Domene HM, Yano K, Cutler GB & Baron J 1994 Dexamethasone Increases Growth-Hormone Receptor Messenger-Ribonucleic-Acid Levels in Liver and Growth-Plate. *Endocrinology* **135** 1113-1118.

Herrington J, Smit LS, Schwartz J & Carter-Su C 2000 The role of STAT proteins in growth hormone signalling. *Oncogene* **19** 2585-2597.

Hill PA 1998 Bone remodelling. *Br.J.Orthod.* **25** 101-107.

Hill TP, Spater D, Taketo MM, Birchmeier W & Hartmann C 2005 Canonical Wnt/beta-catenin signalling prevents osteoblasts from differentiating into chondrocytes. *Developmental Cell* **8** 727-738.

Hilton DJ 1999 Negative regulators of cytokine signal transduction. *Cell Mol Life Sci.* **55** 1568-1577.

Holgersen K, Kvist PH, Markholst H, Hansen AK & Holm TL 2014 Characterisation of enterocolitis in the piroxicam-accelerated interleukin-10 knock out mouse - A model mimicking inflammatory bowel disease. *Journal of Crohns & Colitis* **8** 147-160.

Holly J & Perks C 2006 The role of insulin-like growth factor binding proteins. *Neuroendocrinology* **83** 154-160.

Horton WA 2003 Skeletal development: insights from targeting the mouse genome. *Lancet* **362** 560-569.

Horvat S & Medrano JF 1998 A 500-kb YAC and BAC contig encompassing the high-growth deletion in mouse chromosome 10 and identification of the murine Raidd/Cradd gene in the candidate region. *Genomics* **54** 159-164.

Horvat S & Medrano JF 2001 Lack of Socs2 expression causes the high-growth phenotype in mice. *Genomics* **72** 209-212.

Howarth GS, Xian CJ & Read LC 1998 Insulin-like growth factor-1 partially attenuates colonic damage in rats with experimental colitis induced by oral dextran sulphate sodium. *Scandinavian Journal of Gastroenterology* **33** 180-190.

Hughes FJ, Turner W, Belibasakis G & Martuscelli G 2006 Effects of growth factors and cytokines on osteoblast differentiation. *Periodontology 2000* **41** 48-72.

Hunziker EB 1994 Mechanism of Longitudinal Bone-Growth and Its Regulation by Growth-Plate Chondrocytes. *Microscopy Research and Technique* **28** 505-519.

Hunziker EB, Schenk RK & Cruzorive LM 1987 Quantitation of Chondrocyte Performance in Growth-Plate Cartilage During Longitudinal Bone-Growth. *Journal of Bone and Joint Surgery-American Volume* **69A** 162-173.

Hunziker EB, Wagner J & Zapf J 1994 Differential-Effects of Insulin-Like Growth-Factor-I and Growth-Hormone on Developmental Stages of Rat Growth-Plate Chondrocytes In-Vivo. *Journal of Clinical Investigation* **93** 1078-1086.

Iglesias-Gato D, Chuan YC, Wikstrom P, Augsten S, Jiang N, Niu YJ, Seipel A, Danneman D, Vermeij M, Fernandez-Perez L, Jenster G, Egevad L, Norstedt G & Flores-Morales A 2014 SOCS2 mediates the cross talk between androgen and growth hormone signalling in prostate cancer. *Carcinogenesis* **35** 24-33.

Inagaki T, Dutchak P, Zhao GX, Ding XS, Gautron L, Parameswara V, Li Y, Goetz R, Mohammadi M, Esser V, Elmquist JK, Gerard RD, Burgess SC, Hammer RE, Mangelsdorf DJ & Kliewer SA 2007 Endocrine regulation of the fasting response by PPAR alpha-mediated induction of fibroblast growth factor 21. *Cell Metabolism* **5** 415-425.

Inagaki T, Lin VY, Goetz R, Mohammadi M, Mangelsdorf DJ & Kliewer SA 2008 Inhibition of growth hormone signalling by the fasting-induced hormone FGF21. *Cell Metabolism* **8** 77-83.

Isaksson OGP 1982 Role of Somatomedin in Growth-Hormone Action. *Acta Physiologica Scandinavica* 19.

Isaksson OGP, Jansson JO & Gause IAM 1982 Growth-Hormone Stimulates Longitudinal Bone-Growth Directly. *Science* **216** 1237-1239.

Isaksson OGP, Lindahl A, Nilsson A & Isgaard J 1987 Mechanism of the Stimulatory Effect of Growth-Hormone on Longitudinal Bone-Growth. *Endocrine Reviews* **8** 426-438.

Isgaard J, Carlsson L, Isaksson OGP & Jansson JO 1988a Pulsatile Intravenous Growth-Hormone (Gh) Infusion to Hypophysectomized Rats Increases Insulin-Like Growth Factor-I Messenger Ribonucleic-Acid in Skeletal Tissues More Effectively Than Continuous Gh Infusion. *Endocrinology* **123** 2605-2610.

Isgaard J, Moller C, Isaksson OGP, Nilsson A, Mathews LS & Norstedt G 1988b Regulation of Insulin-Like Growth-Factor Messenger Ribonucleic-Acid in Rat Growth Plate by Growth-Hormone. *Endocrinology* **122** 1515-1520.

Isgaard J, Nilsson A, Vikman K & Isaksson OG 1989 Growth hormone regulates the level of insulin-like growth factor-I mRNA in rat skeletal muscle. *Journal of Endocrinology* **120** 107-112.

Jansson JO, Eden S & Isaksson O 1985 Sexual Dimorphism in the Control of Growth-Hormone Secretion. *Endocrine Reviews* **6** 128-150.

Jelinsky SA, Harris HA, Brown EL, Flanagan K, Zhang XC, Tunkey C, Lai KD, Lane MV, Simcoe DK & Evans MJ 2003 Global transcription profiling of estrogen activity: Estrogen receptor a regulates gene expression in the kidney. *Endocrinology* **144** 701-710.

Jenkins PJ, Mukherjee A & Shalet SM 2006 Does growth hormone cause cancer? *Clinical Endocrinology* **64** 115-121.

Jensen T, Klarlund M, Hansen M, Jensen KE, Skjodt H & Hyldstrup L 2004 Connective tissue metabolism in patients with unclassified polyarthritis and early rheumatoid arthritis. Relationship to disease activity, bone mineral density, and radiographic outcome. *Journal of Rheumatology* **31** 1698-1708.

Jones JI & Clemmons DR 1995 Insulin-Like Growth-Factors and Their Binding-Proteins - Biological Actions. *Endocrine Reviews* **16** 3-34.

Kaplan SA & Cohen P 2007 Review: The somatomedin hypothesis 2007 : 50 years later. *Journal of Clinical Endocrinology & Metabolism* **92** 4529-4535.

Kassem M, Blum W, Ristelli J, Mosekilde L & Eriksen EF 1993 Growth hormone stimulates proliferation and differentiation of normal human osteoblast-like cells in vitro 13. *Calcif.Tissue Int.* **52** 222-226.

Katsanos KH, Tsatsoulis A, Christodoulou D, Challa A, Katsaraki A & Tsianos EV 2001 Reduced serum insulin-like growth factor-1 (IGF-1) and IGF-binding protein-3 levels in adults with inflammatory bowel disease. *Growth Hormone & Igf Research* **11** 364-367.

Kazama JJ, Iwasaki Y & Fukagawa M 2013 Uremic osteoporosis. *Kidney International Supplements* **3** 446-450.

Kember NF 1972 Comparative Patterns of Cell-Division in Epiphyseal Cartilage Plates in Rat. *Journal of Anatomy* **111** 137-&.

Kember NF 1985 Comparative Patterns of Cell-Division in Epiphyseal Cartilage Plates in the Rabbit. *Journal of Anatomy* **142** 185-190.

Kember NF & Sissons HA 1976 Quantitative Histology of Human Growth Plate. *Journal of Bone and Joint Surgery-British Volume* **58** 426-435.

Khosla S, Oursler MJ & Monroe DG 2012 Estrogen and the skeleton. *Trends in Endocrinology and Metabolism* **23** 576-581.

Kiepe D, Ciarmatori S, Hoeflich A, Wolf E & Tonshoff B 2005 Insulin-like growth factor (IGF)-I stimulates cell proliferation and induces IGF binding protein (IGFBP)-3 and IGFBP-5 gene expression in cultured growth plate chondrocytes via distinct signalling pathways. *Endocrinology* **146** 3096-3104.

Kim SO, Jiang J, Yi WS, Feng GS & Frank SJ 1998 Involvement of the Src homology 2-containing tyrosine phosphatase SHP-2 in growth hormone signalling. *Journal of Biological Chemistry* **273** 2344-2354.

Kim SW, Her SJ, Park SJ, Kim D, Park KS, Lee HY, Han BH, Kim MS, Shin CS & Kim SY 2005 Ghrelin stimulates proliferation and differentiation and inhibits apoptosis in osteoblastic MC3T3-E1 cells. *Bone* **37** 359-369.

Kirkwood JK, Spratt DMJ, Duignan PJ & Kember NF 1989 Patterns of Cell-Proliferation and Growth-Rate in Limb Bones of the Domestic-Fowl (Gallus-Domesticus). *Research in Veterinary Science* **47** 139-147.

Kishimoto K, Kitazawa R, Kurosaka M, Maeda S & Kitazawa S 2006 Expression profile of genes related to osteoclastogenesis in mouse growth plate and articular cartilage. *Histochemistry and Cell Biology* **125** 593-602.

Kitajima S, Takuma S & Morimoto M 2000 Histological analysis of murine colitis induced by dextran sulfate sodium of different molecular weights. *Experimental Animals* **49** 9-15.

Kitamura H, Kawata H, Takahashi F, Higuchi Y, Furuichi T & Ohkawa H 1995 Bone-Marrow Neutrophilia and Suppressed Bone Turnover in Human Interleukin-6 Transgenic Mice - A Cellular Relationship Among Hematopoietic-Cells, Osteoblasts, and Osteoclasts Mediated by Stromal Cells in Bone-Marrow. *American Journal of Pathology* **147** 1682-1692.

Klapper DG, Svoboda ME & Vanwyk JJ 1983 Sequence-Analysis of Somatomedin-C - Confirmation of Identity with Insulin-Like Growth Factor-I. *Endocrinology* **112** 2215-2217.

Klaus J, Armbrecht G, Steinkamp M, Bruckel J, Rieber A, Adler G, Reinshagen M, Felsenberg D & von Tirpitz C 2002 High prevalence of osteoporotic vertebral fractures in patients with Crohn's disease. *Gut* **51** 654-658.

Klover P & Hennighausen L 2007 Postnatal body growth is dependent on the transcription factors signal transducers and activators of transcription 5a/b in

muscle: A role for autocrine/paracrine insulin-like growth factor I. *Endocrinology* **148** 1489-1497.

Kofoed EM, Hwa V, Little B, Woods KA, Buckway CK, Tsubaki J, Pratt KL, Bezrodnik L, Jasper H, Tepper A, Heinrich JJ & Rosenfeld RG 2003 Growth hormone insensitivity associated with a STAT5b mutation. *New England Journal of Medicine* **349** 1139-1147.

Komori T 2006 Regulation of osteoblast differentiation by transcription factors. *Journal of Cellular Biochemistry* **99** 1233-1239.

Komori T, Yagi H, Nomura S, Yamaguchi A, Sasaki K, Deguchi K, Shimizu Y, Bronson RT, Gao YH, Inada M, Sato M, Okamoto R, Kitamura Y, Yoshiki S & Kishimoto T 1997 Targeted disruption of Cbfa1 results in a complete lack of bone formation owing to maturational arrest of osteoblasts. *Cell* **89** 755-764.

Kopchick JJ, Bellush LL & Coschigano KT 1999 Transgenic models of growth hormone action. *Annual Review of Nutrition* **19** 437-461.

Kornak U 2011 Animal models with pathological mineralization phenotypes. *Joint Bone Spine* **78** 561-567.

Kornfeld JW, Grebien F, Kerenyi MA, Friedbichler K, Kovacic B, Zankl B, Hoelbl A, Nivarti H, Beug H, Sexl V, Muller M, Kenner L, Mullner EW, Gouilleux F & Moriggl R 2008 The different functions of Stat5 and chromatin alteration through Stat5 proteins. *Frontiers in Bioscience* **13** 6237-6254.

Krebs DL & Hilton DJ 2001 SOCS proteins: Negative regulators of cytokine signalling. *Stem Cells* **19** 378-387.

Kronenberg HM 2003 Developmental regulation of the growth plate. *Nature* **423** 332-336.

Kuhn R, Lohler J, Rennick D, Rajewsky K & Muller W 1993 Interleukin-10-Deficient Mice Develop Chronic Enterocolitis. *Cell* **75** 263-274.

Kular J, Tickner J, Chim SM & Xu JK 2012 An overview of the regulation of bone remodelling at the cellular level. *Clinical Biochemistry* **45** 863-873.

Kuroki T, Shingu M, Koshihara Y & Nobunaga M 1994 Effects of Cytokines on Alkaline-Phosphatase and Osteocalcin Production, Calcification and Calcium-Release by Human Osteoblastic Cells. *British Journal of Rheumatology* **33** 224-230.

Laakso S, Valta H, Verkasalo M, Toiviainen-Salo S & Makitie O 2014 Compromised Peak Bone Mass in Patients with Inflammatory Bowel Disease-A Prospective Study. *Journal of Pediatrics* **164** 1436-+.

Laakso S, Valta H, Verkasalo M, Toiviainen-Salo S, Viljakainen H & Makitie O 2012 Impaired Bone Health in Inflammatory Bowel Disease: A Case-Control Study in 80 Pediatric Patients. *Calcified Tissue International* **91** 121-130.

Lai CF, Chaudhary L, Fausto A, Halstead LR, Ory DS, Avioli LV & Cheng SL 2001 Erk is essential for growth, differentiation, integrin expression, and cell function in human osteoblastic cells. *Journal of Biological Chemistry* **276** 14443-14450.

Lakatos PL 2006 Recent trends in the epidemiology of inflammatory bowel diseases: Up or down? *World Journal of Gastroenterology* **12** 6102-6108.

Landin-Wilhelmsen K, Nilsson A, Bosaeus I & Bengtsson BA 2003 Growth hormone increases bone mineral content in postmenopausal osteoporosis: A randomized placebo-controlled trial. *Journal of Bone and Mineral Research* **18** 393-405.

Lang CH, Pollard V, Fan J, Traber LD, Traber DL, Frost RA, Gelato MC & Prough DS 1997 Acute alterations in growth hormone insulin-like growth factor axis in humans injected with endotoxin. *American Journal of Physiology-Regulatory Integrative and Comparative Physiology* **273** R371-R378.

Lang CH, Silvis C, Deshpande N, Nystrom G & Frost RA 2003 Endotoxin stimulates in vivo expression of inflammatory cytokines tumor necrosis factor alpha, interleukin-1 beta,-6, and high-mobility-group protein-1 in skeletal muscle. *Shock* **19** 538-546.

Laron Z 2004 Extensive personal experience - Laron syndrome (primary growth hormone resistance or insensitivity): The personal experience 1958-2003. *Journal of Clinical Endocrinology & Metabolism* **89** 1031-1044.

Laviola L, Natalicchio A & Giorgino F 2007 The IGF-I signalling pathway. *Current Pharmaceutical Design* **13** 663-669.

Le Roith D, Bondy C, Yakar S, Liu JL & Butler A 2001 The Somatomedin Hypothesis: 2001. *Endocrine Reviews* **22** 53-74.

Lee NK, Sowa H, Hinoi E, Ferron M, Ahn JD, Confavreux C, Dacquin R, Mee PJ, Mckee MD, Jung DY, Zhang Z, Kim JK, Mauvais-Jarvis F, Ducy P & Karsenty G 2007 Endocrine regulation of energy metabolism by the skeleton. *Cell* **130** 456-469.

Lefebvre V, Li P & de Crombrugghe B 1998 A new long form of Sox5 (L-Sox5), Sox6 and Sox9 are coexpressed in chondrogenesis and cooperatively activate the type II collagen gene. *Embo Journal* **17** 5718-5733.

Leong GM, Moverare S, Brce J, Doyle N, Sjogren K, Dahlman-Wright K, Gustafsson JA, Ho KKY, Ohlsson C & Leung KC 2004 Estrogen up-regulates hepatic expression of suppressors of cytokine signalling-2 and -3 in vivo and in vitro. *Endocrinology* **145** 5525-5531.

LeRoith D & Roberts CT 2003 The insulin-like growth factor system and cancer. *Cancer Letters* **195** 127-137.

Leung KC, Doyle N, Ballesteros M, Sjogren K, Watts CKW, Low TH, Leong GM, Ross RJM & Ho KKY 2003 Estrogen inhibits GH signalling by suppressing GH-induced JAK2 phosphorylation, an effect mediated by SOCS-2. *Proceedings of the National Academy of Sciences of the United States of America* **100** 1016-1021.

Li XF, Zhang YZ, Kang HS, Liu WZ, Liu P, Zhang JG, Harris SE & Wu DQ 2005 Sclerostin binds to LRP5/6 and antagonizes canonical Wnt signalling. *Journal of Biological Chemistry* **280** 19883-19887.

Lin CL, Moniz C, Chambers TJ & Chow JWM 1996 Colitis causes bone loss in rats through suppression of bone formation. *Gastroenterology* **111** 1263-1271.

Liu JL & LeRoith D 1999 Insulin-like growth factor I is essential for postnatal growth in response to growth hormone. *Endocrinology* **140** 5178-5184.

Liu JP, Baker J, Perkins AS, Robertson EJ & Efstratiadis A 1993 Mice Carrying Null Mutations of the Genes Encoding Insulin-Like Growth Factor-I (Igf-1) and Type-1 Igf Receptor (Igf1R). *Cell* **75** 59-72.

Liu JL, Yakar S & LeRoith D 2000 Conditional Knockout of Mouse Insulin-Like Growth Factor-1 Gene Using the Cre/loxP System. *Proceedings of the Society for Experimental Biology and Medicine* **223** 344-351.

Livak KJ & Schmittgen TD 2001 Analysis of relative gene expression data using real-time quantitative PCR and the 2(T)(-Delta Delta C) method. *Methods* **25** 402-408.

Long FX 2012 Building strong bones: molecular regulation of the osteoblast lineage. *Nature Reviews Molecular Cell Biology* **13** 27-38.

Lorentzon M, Greenhalgh CJ, Mohan S, Alexander WS & Ohlsson C 2005 Reduced bone mineral density in SOCS-2-deficient mice. *Pediatr.Res.* **57** 223-226.

Loqman MY, Bush PG, Farquharson C & Hall AC 2010 A cell shrinkage artefact in growth plate chondrocytes with common fixative solutions: importance of fixative osmolarity for maintaining morphology. *European Cells and Materials* **19** 214-227

Lorenzo J 2000 Interactions between immune and bone cells: new insights with many remaining questions. *Journal of Clinical Investigation* **106** 749-752.

Lowe WL, Lasky SR, LeRoith D & Roberts CT 1988 Distribution and Regulation of Rat Insulin-Like Growth Factor-I Messenger Ribonucleic-Acids Encoding Alternative Carboxyterminal E-Peptides - Evidence for Differential Processing and Regulation in Liver. *Molecular Endocrinology* **2** 528-535.

Ludvigsson JF, Michaelsson K, Ekbom A & Montgomery SM 2007 Coeliac disease and the risk of fractures - a general population-based cohort study. *Alimentary Pharmacology & Therapeutics* **25** 273-285.

Lui JC, Finkielstain GP, Barnes KM & Baron J 2008 An imprinted gene network that controls mammalian somatic growth is down-regulated during postnatal growth deceleration in multiple organs. *American Journal of Physiology-Regulatory Integrative and Comparative Physiology* **295** R189-R196.

Lupu F, Terwilliger JD, Lee K, Segre GV & Efstratiadis A 2001 Roles of growth hormone and insulin-like growth factor 1 in mouse postnatal growth 1. *Dev.Biol.* **229** 141-162.

MacDonald TT 1994 Gastrointestinal Inflammation - Inflammatory Bowel-Disease in Knockout Mice. *Current Biology* **4** 261-263.

Mackie EJ, Tatarczuch L & Mirams M 2011 The skeleton: a multi-functional complex organ. The growth plate chondrocyte and endochondral ossification. *Journal of Endocrinology* **211** 109-121.

Macleod JN, Pampori NA & Shapiro BH 1991 Sex-Differences in the Ultradian Pattern of Plasma Growth-Hormone Concentrations in Mice. *Journal of Endocrinology* **131** 395-399.

MacRae VE, Ahmed SF, Mushtaq T & Farquharson C 2007 IGF-I signalling in bone growth: Inhibitory actions of dexamethasone and IL-1 beta. *Growth Hormone & Igf Research* **17** 435-439.
MacRae VE, Burdon T, Ahmed SF & Farquharson C 2006a Ceramide inhibition of chondrocyte proliferation and bone growth is IGF-I independent. *Journal of Endocrinology* **191** 369-377.

MacRae VE, Farquharson C & Ahmed SF 2006b The restricted potential for recovery of growth plate chondrogenesis and longitudinal bone growth following exposure to pro-inflammatory cytokines. *Journal of Endocrinology* **189** 319-328.

MacRae VE, Horvat S, Pells SC, Dale H, Collinson RS, Pitsillides AA, Ahmed SF & Farquharson C 2009 Increased bone mass, altered trabecular architecture and modified growth plate organization in the growing skeleton of SOCS2 deficient mice. *Journal of Cellular Physiology* **218** 276-284.

Mahler M, Bristol IJ, Leiter EH, Workman AE, Birkenmeier EH, Elson CO & Sundberg JP 1998 Differential susceptibility of inbred mouse strains to dextran sulfate sodium-induced colitis. *American Journal of Physiology-Gastrointestinal and Liver Physiology* **274** G544-G551.

Mak RH & Cheung W 2007 Cachexia in chronic kidney disease: role of inflammation and neuropeptide signalling. *Current Opinion in Nephrology and Hypertension* **16** 27-31.

Mak RH, Cheung W, Cone RD & Marks DL 2006 Mechanisms of Disease: cytokine and adipokine signalling in uremic cachexia. *Nature Clinical Practice Nephrology* **2** 527-534.

Marine JC, Mckay C, Wang DM, Topham DJ, Parganas E, Nakajima H, Pendeville H, Yasukawa H, Sasaki A, Yoshimura A & Ihle JN 1999a SOCS3 is essential in the regulation of fetal liver erythropoiesis. *Cell* **98** 617-627.

Marine JC, Topham DJ, Mckay C, Wang DM, Parganas E, Stravopodis D, Yoshimura A & Ihle JN 1999b SOCS1 deficiency causes a lymphocyte-dependent perinatal lethality. *Cell* **98** 609-616.

Martinez CS, Piazza VG, Ratner LD, Matos MN, Gonzalez L, Rulli SB, Miquet JG & Sotelo AI 2013 Growth hormone STAT5-mediated signalling and its modulation in mice liver during the growth period. *Growth Hormone & Igf Research* **23** 19-28.

Mathews LS, Hammer RE, Brinster RL & Palmiter RD 1988 Expression of Insulin-Like Growth Factor-I in Transgenic Mice with Elevated Levels of Growth-Hormone Is Correlated with Growth. *Endocrinology* **123** 433-437.

Matsumoto A, Seki Y, Kubo M, Ohtsuka S, Suzuki A, Hayashi I, Tsuji K, Nakahata T, Okabe M, Yamada S & Yoshimura A 1999 Suppression of STAT5 functions in liver, mammary glands, and T cells in cytokine-inducible SH2-containing protein 1 transgenic mice. *Molecular and Cellular Biology* **19** 6396-6407.

Mauras N 2001 Growth hormone therapy in the glucocorticosteroid-dependent child: Metabolic and linear growth effects. *Hormone Research* **56** 13-18.

Melgar S, Engstrom K, Jagervall A & Martinez V 2008 Psychological stress reactivates dextran sulfate sodium-induced chronic colitis in mice. *Stress-the International Journal on the Biology of Stress* **11** 348-362.

Melgar S, Karlsson A & Michaelsson EM 2005 Acute colitis induced by dextran sulfate sodium progresses to chronicity in C57BL/6 but not in BALB/c mice: correlation between symptoms and inflammation. *American Journal of Physiology-Gastrointestinal and Liver Physiology* **288** G1328-G1338.

Melmed S 1999 Editorial: Insulin-like growth factor I - A prototypic peripheral-paracrine hormone? *Endocrinology* **140** 3879-3880.

Melrose J, Smith SM, Smith MM & Little CB 2008 The use of Histochoice (TM)(R) for histological examination of articular and growth plate cartilages, intervertebral disc and meniscus. *Biotechnic & Histochemistry* **83** 47-53.

Meraz MA, White JM, Sheehan KCF, Bach EA, Rodig SJ, Dighe AS, Kaplan DH, Riley JK, Greenlund AC, Campbell D, CarverMoore K, Dubois RN, Clark R, Aguet M & Schreiber RD 1996 Targeted disruption of the STAT1 gene in mice reveals unexpected physiologic specificity in the JAK-STAT signalling pathway. *Cell* **84** 431-442.

Metcalf D, Greenhalgh CJ, Viney E, Willson TA, Starr R, Nicola NA, Hilton DJ & Alexander WS 2000 Gigantism in mice lacking suppressor of cytokine signalling-2. *Nature* **405** 1069-1073.

Meton I, Boot EPJ, Sussenbach JS & Steenbergh PH 1999 Growth hormone induces insulin-like growth factor-I gene transcription by a synergistic action of STAT5 and HNF-1 alpha. *Febs Letters* **444** 155-159.

Millan JL 2013 The Role of Phosphatases in the Initiation of Skeletal Mineralization. *Calcified Tissue International* **93** 299-306.

Minamoto S, Ikegame K, Ueno K, Narazaki M, Naka T, Yamamoto H, Matsumoto T, Saito H, Hosoe S & Kishimoto T 1997 Cloning and functional analysis of new members of STAT induced STAT inhibitor (SSI) family: SSI-2 and SSI-3. *Biochemical and Biophysical Research Communications* **237** 79-83.

Mochizuki H, Hakeda Y, Wakatsuki N, Usui N, Akashi S, Sato T, Tanaka K & Kumegawa M 1992 Insulin-Like Growth Factor-I Supports Formation and Activation of Osteoclasts. *Endocrinology* **131** 1075-1080.

Moerth C, Schneider MR, Renner-Mueller I, Blutke A, Elmlinger MW, Erben RG, Camacho-Hubner C, Hoeflich A & Wolf E 2007 Postnatally elevated levels of insulin-like growth factor (IGF)-II fail to rescue the dwarfism of IGF-I-deficient mice except kidney weight. *Endocrinology* **148** 441-451.

Moester MJC, Papapoulos SE, Lowik CWGM & van Bezooijen RL 2010 Sclerostin: Current Knowledge and Future Perspectives. *Calcified Tissue International* **87** 99-107.

Mohammad, Chirgwin & Guise 2008 Assessing New Bone Formation in Neonatal Calvarial Organ Culture. In *Osteoporosis Methods and Protocols*, edn 455, pp 19-35. Ed Jennifer J.Westendorf.

Mohan S & Baylink DJ 2002 IGF-binding proteins are multifunctional and act via IGF-dependent and -independent mechanisms. *Journal of Endocrinology* **175** 19-31.

Mohan S & Baylink DJ 2005 Impaired skeletal growth in mice with haploinsufficiency of IGF-I: genetic evidence that differences in IGF-I expression could contribute to peak bone mineral density differences. *Journal of Endocrinology* **185** 415-420.

Mohan S, Richman C, Guo RQ, Amaar Y, Donahue LR, Wergedal J & Baylink DJ 2003 Insulin-like growth factor regulates peak bone mineral density in mice by both growth hormone-dependent and -independent mechanisms. *Endocrinology* **144** 929-936.

Morel G, Chavassieux P, Barenton B, Dubois PM, Meunier PJ & Boivin G 1993 Evidence for A Direct Effect of Growth-Hormone on Osteoblasts. *Cell and Tissue Research* **273** 279-286.

Morris GP, Beck PL, Herridge MS, Depew WT, Szewczuk MR & Wallace JL 1989 Hapten-Induced Model of Chronic Inflammation and Ulceration in the Rat Colon. *Gastroenterology* **96** 795-803.

Mrak E, Villa I, Lanzi R, Losa M, Guidobono F & Rubinacci A 2007 Growth hormone stimulates osteoprotegerin expression and secretion in human osteoblast-like cells. *Journal of Endocrinology* **192** 689-645

Murphy LJ, Bell GI & Friesen HG 1987 Tissue Distribution of Insulin-Like Growth Factor-I and Factor-Ii Messenger-Ribonucleic-Acid in the Adult-Rat. *Endocrinology* **120** 1279-1282.

Mushtaq T, Bijman P, Ahmed SF & Farquharson C 2004 Insulin-like growth factor-I augments chondrocyte hypertrophy and reverses glucocorticoid-mediated growth retardation in fetal mice metatarsal cultures. *Endocrinology* **145** 2478-2486.

Naka T, Matsumoto T, Narazaki M, Fujimoto M, Morita Y, Ohsawa Y, Saito H, Nagasawa T, Uchiyama Y & Kishimoto T 1998 Accelerated apoptosis of lymphocytes by augmented induction of Bax in SSI-1 (STAT-induced STAT inhibitor-1) deficient mice. *Proceedings of the National Academy of Sciences of the United States of America* **95** 15577-15582.

Nakashima K, Zhou X, Kunkel G, Zhang ZP, Deng JM, Behringer RR & de Crombrugghe B 2002 The novel zinc finger-containing transcription factor Osterix is required for osteoblast differentiation and bone formation. *Cell* **108** 17-29.

Nakashima T, Hayashi M, Fukunaga T, Kurata K, Oh-Hora M, Feng JQ, Bonewald LF, Kodama T, Wutz A, Wagner EF, Penninger JM & Takayanagi H 2011 Evidence for osteocyte regulation of bone homeostasis through RANKL expression. *Nature Medicine* **17** 1231-1234.

Nilsson A, Isgaard J, Lindahl A, Dahlstrom A, Skottner A & Isaksson OGP 1986 Regulation by Growth-Hormone of Number of Chondrocytes Containing Igf-I in Rat Growth Plate. *Science* **233** 571-574.

Nilsson A, Swolin D, Enerback S & Ohlsson C 1995 Expression of functional growth hormone receptors in cultured human osteoblast-like cells. *Journal of Clinical Endocrinology Metabolism* **80** 3483-3488.

Nilsson O, Chrysis D, Pajulo I, Boman A, Holst M, Rubinstein J, Ritzen EM & Savendahl L 2003 Localization of estrogen receptors-alpha and -beta and androgen receptor in the human growth plate at different pubertal stages. *Journal of Endocrinology* **177** 319-326.

Nilsson O, Marino R, De Luca F, Phillip M & Baron J 2005 Endocrine regulation of the growth plate. *Hormone Research* **64** 157-165.

Nilsson O, Parker EA, Hegde A, Chau M, Barnes KM & Baron J 2007 Gradients in bone morphogenetic protein-related gene expression across the growth plate. *Journal of Endocrinology* **193** 75-84.

Nishio Y, Dong YF, Paris M, O'Keefe RJ, Schwarz EM & Drissi H 2006 Runx2-mediated regulation of the zinc finger Osterix/Sp7 gene. *Gene* **372** 62-70.

Nishiyama K, Sugimoto T, Kaji H, Kanatani M, Kobayashi T & Chihara K 1996 Stimulatory effect of growth hormone on bone resorption and osteoclast differentiation. *Endocrinology* **137** 35-41.

Oberbauer AM, Currier TA, Nancarrow CD, Ward KA & Murray JD 1992 Linear Bone-Growth of Omt1A-Ogh Transgenic Male-Mice. *American Journal of Physiology* **262** E936-E942.

Ogata N, Chikazu D, Kubota N, Terauchi Y, Tobe K, Azuma Y, Ohta T, Kadowaki T, Nakamura K & Kawaguchi H 2000 Insulin receptor substrate-1 in osteoblast is indispensible for maintaining bone turnover. *Journal of Clinical Investigation* **105** 935-943.

Oh Y, Muller HL, Pham H & Rosenfeld RG 1993 Demonstration of Receptors for Insulin-Like Growth-Factor Binding Protein-3 on Hs578T Human Breast-Cancer Cells. *Journal of Biological Chemistry* **268** 26045-26048.

Ohlsson C, Bengtsson BA, Isaksson OG, Andreassen TT & Slootweg MC 1998 Growth hormone and bone. *Endocrine Reviews.* **19** 55-79.

Ohlsson C, Nilsson A, Isaksson O & Lindahl A 1992 Growth hormone induces multiplication of the slowly cycling germinal cells of the rat tibial growth plate. *Proceedings of the National Academy of Sciences* **89** 9826-9830.

Okayasu I, Hatakeyama S, Yamada M, Ohkusa T, Inagaki Y & Nakaya R 1990 A Novel Method in the Induction of Reliable Experimental Acute and Chronic Ulcerative-Colitis in Mice. *Gastroenterology* **98** 694-702.

Olsen BR, Reginato AM & Wang WF 2000 Bone development. *Annual Review of Cell and Developmental Biology* **16** 191-220.

Omelon S, Georgiou J, Henneman ZJ, Wise LM, Sukhu B, Hunt T, Wynnyckyj C, Holmyard D, Bielecki R & Grynpas MD 2009 Control of Vertebrate Skeletal Mineralization by Polyphosphates. *Plos One* **4**(5):e5634.

Papadakis KA & Targan SR 2000 Role of cytokines in the pathogenesis of inflammatory bowel disease. *Annual Review of Medicine* **51** 289-298.

Parker EA, Hegde A, Buckley M, Barnes KM, Baron J & Nilsson O 2007 Spatial and temporal regulation of GH-IGF-related gene expression in growth plate cartilage. *Journal of Endocrinology* **194** 31-40.

Pasquali C, Curchod ML, Walchli S, Espanel X, Guerrier M, Arigoni F, Strous G & van Huijsduijnen RH 2003 Identification of protein tyrosine phosphatases with specificity for the ligand-activated growth hormone receptor. *Molecular Endocrinology* **17** 2228-2239.

Pass C, MacRae VE, Ahmed SF & Farquharson C 2009 Inflammatory cytokines and the GH/IGF-I axis: novel actions on bone growth. *Cell Biochem.Funct.* **27** 119-127.

Pass C, MacRae VE, Huesa C, Ahmed SF & Farquharson C 2012 SOCS2 is the critical regulator of GH action in murine growth plate chondrogenesis. *Journal of Bone and Mineral Research.* **27**(5):1055-66

Peng XD, Xu PZ, Chen ML, Hahn-Windgassen A, Skeen J, Jacobs J, Sundararajan D, Chen WS, Crawford SE, Coleman KG & Hay N 2003 Dwarfism, impaired skin development, skeletal muscle atrophy, delayed bone developement, and impeded adipogenesis in mice lacking Akt1 and Akt2. *Genes & Development* **17** 1352-1365.

Perrini S, Laviola L, Carreira MC, Cignarelli A, Natalicchio A & Giorgino F 2010 The GH/IGF1 axis and signalling pathways in the muscle and bone: mechanisms underlying age-related skeletal muscle wasting and osteoporosis. *Journal of Endocrinology* **205** 201-210.

Perse M & Cerar A 2012 Dextran Sodium Sulphate Colitis Mouse Model: Traps and Tricks. *Journal of Biomedicine and Biotechnology*. 718617.

Phornphutkul C, Frick GP, Goodman HM, Berry SA & Gruppuso PA 2000 Hepatic growth hormone signalling in the late gestation fetal rat. *Endocrinology* **141** 3527-3533.

Piessevaux J, Lavens D, Montoye T, Wauman J, Catteeuw D, Vandekerckhove J, Belsham D, Peelman F & Tavernier J 2006 Functional cross-modulation between SOCS proteins can stimulate cytokine signalling. *Journal of Biological Chemistry* **281** 32953-32966.

Proff P & Romer P 2009 The molecular mechanism behind bone remodelling: a review. *Clinical Oral Investigations* **13** 355-362.

Quarles LD, Yohay DA, Lever LW, Caton R & Wenstrup RJ 1992 Distinct Proliferative and Differentiated Stages of Murine Mc3T3-E1 Cells in Culture - An Invitro Model of Osteoblast Development. *Journal of Bone and Mineral Research* **7** 683-692.

Ram PA, Park SH, Choi HK & Waxman DJ 1996 Growth hormone activation of Stat 1, Stat 3, and Stat 5 in rat liver - Differential kinetics of hormone desensitization and growth hormone stimulation of both tyrosine phosphorylation and serine/threonine phosphorylation. *Journal of Biological Chemistry* **271** 5929-5940.

Ram PA & Waxman DJ 1997 Interaction of growth hormone-activated STATs with SH2-containing phosphotyrosine phosphatase SHP-1 and nuclear JAK2 tyrosine kinase. *Journal of Biological Chemistry* **272** 17694-17702.

Ram PA & Waxman DJ 1999 SOCS/CIS Protein Inhibition of Growth Hormone-stimulated STAT5 Signalling by Multiple Mechanisms. *Journal of Biological Chemistry* **274** 35553-35561.

Reinshagen M 2008 Osteoporosis in inflammatory bowel disease. *Journal of Crohns & Colitis* **2** 202-207.

Rennick DM, Fort MM & Davidson NJ 1997 Studies with IL-10(-/-) mice: An overview. *Journal of Leukocyte Biology* **61** 389-396.

Rico-Bautista E, Flores-Morales A & Fernandez-Perez L 2006 Suppressor of cytokine signalling (SOCS) 2, a protein with multiple functions. *Cytokine Growth Factor Rev.* **17** 431-439.

Rico-Bautista E, Greenhalgh CJ, Tollet-Egnell P, Hilton DJ, Alexander WS, Norstedt G & Flores-Morales A 2005 Suppressor of cytokine signalling-2 deficiency induces molecular and metabolic changes that partially overlap with growth hormone-dependent effects. *Molecular Endocrinology* **19** 781-793.

Roberts AW, Robb L, Rakar S, Hartley L, Cluse L, Nicola NA, Metcalf D, Hilton DJ & Alexander WS 2001 Placental defects and embryonic lethality in mice lacking suppressor of cytokine signalling 3. *Proceedings of the National Academy of Sciences of the United States of America* **98** 9324-9329.

Robson H, Siebler T, Shalet SM & Williams GR 2002 Interactions between GH, IGF-I, glucocorticoids, and thyroid hormone during skeletal growth. *Pediatric Research* **52** 137-147

Rogler G & Andus T 1998 Cytokines in inflammatory bowel disease. *World Journal of Surgery* **22** 382-389.

Rol De Lama MA, Perez-Romero A, Tresguerres JAF, Hermanussen M & Ariznavarreta C 2000 Recombinant human growth hormone enhances tibial growth

in peripubertal female rats but not in males. *European Journal of Endocrinology* **142** 517-523.

Sadlack B, Merz H, Schorle H, Schimpl A, Feller AC & Horak I 1993 Ulcerative Colitis-Like Disease in Mice with A Disrupted Interleukin-2 Gene. *Cell* **75** 253-261.

Sanchez-Munoz F, Dominguez-Lopez A & Yamamoto-Furusho JK 2008 Role of cytokines in inflammatory bowel disease. *World Journal of Gastroenterology* **14** 4280-4288.

Sandler RS, Everhart JE, Donowitz M, Adams E, Cronin K, Goodman C, Gemmen E, Shah S, Avdic A & Rubin R 2002 The burden of selected digestive diseases in the United States. *Gastroenterology* **122** 1500-1511.

Sands BE & Kaplan GG 2007 The role of TNF alpha in ulcerative colitis. *Journal of Clinical Pharmacology* **47** 930-941.

Sandstedt J, Tornell J, Norjavaara E, Isaksson OGP & Ohlsson C 1996 Elevated levels of growth hormone increase bone mineral content in normal young mice, but not in ovariectomized mice. *Endocrinology* **137** 3368-3374.

Sartor RB 1997 Pathogenesis and immune mechanisms of chronic inflammatory bowel diseases. *American Journal of Gastroenterology* **92** S5-S11.

Schett G, Redlich K, Hayer S, Zwerina J, Bolon B, Dunstan C, Gortz B, Schulz A, Bergmeister H, Kollias G, Steiner G & Smolen JS 2003 Osteoprotegerin protects against generalized bone loss in tumor necrosis factor-transgenic mice. *Arthritis and Rheumatism* **48** 2042-2051.

Scheven BAA & Hamilton NJ 1991 Longitudinal Bone-Growth Invitro - Effects of Insulin-Like Growth Factor-I and Growth-Hormone. *Acta Endocrinologica* **124** 602-607.

Schmid C, Schlapfer I, Peter M, Bonischnetzler M, Schwander J, Zapf J & Froesch ER 1994 Growth-Hormone and Parathyroid-Hormone Stimulate Igfbp-3 in Rat Osteoblasts. *American Journal of Physiology* **267** E226-E233.

Seeman E 2001 Sexual dimorphism in skeletal size, density, and strength. *Journal of Clinical Endocrinology & Metabolism* **86** 4576-4584.

Seeman E 2008 Bone quality: the material and structural basis of bone strength. *Journal of Bone and Mineral Metabolism* **26** 1-8.

Seriolo B, Paolino S, Sulli A, Ferretti V & Cutolo M 2006 Bone metabolism changes during anti-TNF-alpha therapy in patients with active rheumatoid arthritis. *Basic and Clinical Aspects of Neuroendocrine Immunology in Rheumatic Diseases* **1069** 420-427.

Sheng MHC, Baylink DJ, Beamer WG, Donahue LR, Rosen CJ, Lau KHW & Wergedal JE 1999 Histomorphometric studies show that bone formation and bone mineral apposition rates are greater in C3H/HeJ (high-density) than C57BL/6J (low-density) mice during growth. *Bone* **25** 421-429.

Sims NA, Clement-Lacroix P, Da PF, Bouali Y, Binart N, Moriggl R, Goffin V, Coschigano K, Gaillard-Kelly M, Kopchick J, Baron R & Kelly PA 2000 Bone homeostasis in growth hormone receptor-null mice is restored by IGF-I but independent of Stat5. *Journal of Clinical Investigation* **106** 1095-1103.

Sjogren K, Bohlooly YM, Olsson B, Coschigano K, Tornell J, Mohan S, Isaksson OGP, Baumann G, Kopchick J & Ohlsson C 2000 Disproportional skeletal growth and markedly decreased bone mineral content in growth hormone receptor -/- mice. *Biochemical and Biophysical Research Communications* **267** 603-608.

Sjogren K, Liu JL, Blad K, Skrtic S, Vidal O, Wallenius V, LeRoith D, Tornell J, Isaksson OGP, Jansson JO & Ohlsson C 1999 Liver-derived insulin-like growth factor I (IGF-I) is the principal source of IGF-I in blood but is not required for postnatal body growth in mice. *Proceedings of the National Academy of Sciences of the United States of America* **96** 7088-7092.

Sjogren K, Sheng M, Moverare S, Liu JL, Wallenius K, Tornell J, Isaksson O, Jansson JO, Mohan S & Ohlsson C 2002 Effects of liver-derived insulin-like growth factor I on bone metabolism in mice. *Journal of Bone and Mineral Research* **17** 1977-1987.

Sklar CA 2004 Growth hormone treatment: Cancer risk. *Hormone Research* **62** 30-34.
Slonim AE, Bulone L, Damore MB, Goldberg T, Wingertzahn MA & McKinley MJ 2000 A preliminary study of growth hormone therapy for Crohn's disease. *New England Journal of Medicine* **342** 1633-1637.

Smeets T, van Buul-Offers S, 1983 A morphological study of the development of the tibial proximal epiphysis and growth plate of normal and dwarfed snell mice. *Growth* 47 145-159

Smit LS, Meyer DJ, Billestrup N, Norstedt G, Schwartz J & Carter-Su C 1996 The role of the growth hormone (GH) receptor and JAK1 and JAK2 kinases in the activation of Stats 1, 3, and 5 by GH. *Molecular Endocrinology* **10** 519-533.

Sommer B, Bickel M, Hofstetter W & Wetterwald A 1996 Expression of matrix proteins during the development of mineralized tissues. *Bone* **19** 371-380.

Sommerfeldt DW & Rubin CT 2001 Biology of bone and how it orchestrates the form and function of the skeleton. *European Spine Journal* **10** S86-S95.

Spagnoli A, Torello M, Nagalla SR, Horton WA, Pattee P, Hwa V, Chiarelli F, Roberts CT & Rosenfeld RG 2002 Identification of STAT-1 as a molecular target of IGFBP-3 in the process of chondrogenesis. *Journal of Biological Chemistry* **277** 18860-18867.

Span JPT, Pieters GFFM, Sweep CGJ, Hermus ARMM & Smals AGH 2000 Gender difference in insulin-like growth factor I response to growth hormone (GH) treatment in GH-deficient adults: Role of sex hormone replacement. *Journal of Clinical Endocrinology & Metabolism* **85** 1121-1125.

Stahl N, Farruggella TJ, Boulton TG, Zhong Z, Darnell JE & Yancopoulos GD 1995 Choice of Stats and Other Substrates Specified by Modular Tyrosine-Based Motifs in Cytokine Receptors. *Science* **267** 1349-1353.

Staines KA, Mackenzie NCW, Clarkin CE, Zelenchuk L, Rowe PS, MacRae VE & Farquharson C 2012 MEPE is a novel regulator of growth plate cartilage mineralization. *Bone* **51** 418-430.

Starr R, Metcalf D, Elefanty AG, Brysha M, Willson TA, Nicola NA, Hilton DJ & Alexander WS 1998 Liver degeneration and lymphoid deficiencies in mice lacking suppressor of cytokine signalling-1. *Proceedings of the National Academy of Sciences of the United States of America* **95** 14395-14399.

Starr R, Willson TA, Viney EM, Murray LJL, Rayner JR, Jenkins BJ, Gonda TJ, Alexander WS, Metcalf D, Nicola NA & Hilton DJ 1997 A family of cytokine-inducible inhibitors of signalling. *Nature* **387** 917-921.

Stewart CEH, Bates PC, Calder TA, Woodall SM & Pell JM 1993 Potentiation of Insulin-Like Growth Factor-I (Igf-I) Activity by An Antibody - Supportive Evidence for Enhancement of Igf-I Bioavailability In-Vivo by Igf Binding-Proteins. *Endocrinology* **133** 1462-1465.

Stockbrugger RW, Schoon EJ, Bollani S, Mills PR, Israeli E, Landgraf L, Felsenberg D, Ljunghall S, Nygard G, Persson T, Graffner H, Porro GB & Ferguson A 2002 Discordance between the degree of osteopenia and the prevalence of spontaneous vertebral fractures in Crohn's disease. *Alimentary Pharmacology & Therapeutics* **16** 1519-1527.

Stratikopoulos E, Szabolcs M, Dragatsis I, Klinakis A & Efstratiadis A 2008 The hormonal action of IGF1 in postnatal mouse growth. *Proceedings of the National Academy of Sciences of the United States of America* **105** 19378-19383.

Suda, K., Iguchi, G., Yamamoto, M., Handayaningsih, A. E., Nishizawa, H., Takahashi, M., Okimura, Y., Kaji, H., Chihara, K., and Takahashi, Y. A case of gigantism associated with a missense mutation in the *SOCS2* gene. Endo 2011: The 93rd Annual Meeting & Expo. 2011.

Sun DF, Zheng ZL, Tummala P, Oh J, Schaefer F & Rabkin R 2004 Chronic uremia attenuates growth hormone-induced signal transduction in skeletal muscle. *Journal of the American Society of Nephrology* **15**:2630-6

Taichman RS & Hauschka PV 1992 Effects of Interleukin-1-Beta and Tumor-Necrosis-Factor-Alpha on Osteoblastic Expression of Osteocalcin and Mineralized Extracellular-Matrix Invitro. *Inflammation* **16** 587-601.

Takeda K, Noguchi K, Shi W, Tanaka T, Matsumoto M, Yoshida N, Kishimoto T & Akira S 1997 Targeted disruption of the mouse Stat3 gene leads to early embryonic lethality. *Proceedings of the National Academy of Sciences of the United States of America* **94** 3801-3804.

Tang ZY, Yu R, Lu YR, Parlow AF & Liu JL 2005 Age-dependent onset of liver-specific IGF-I gene deficiency and its persistence in old age: implications for postnatal growth and insulin resistance in LID mice. *American Journal of Physiology-Endocrinology and Metabolism* **289** E288-E295.

Taniguchi N, Yoshida K, Ito T, Tsuda M, Mishima Y, Furumatsu T, Ronfani L, Abeyama K, Kawahara K, Komiya S, Maruyama I, Lotz M, Bianchi ME & Asahara H 2007 Stage-specific secretion of HMGB1 in cartilage regulates endochondral ossification. *Molecular and Cellular Biology* **27** 5650-5663.

Teglund S, Mckay C, Schuetz E, van Deursen JM, Stravopodis D, Wang DM, Brown M, Bodner S, Grosveld G & Ihle JN 1998 Stat5a and Stat5b proteins have essential and nonessential, or redundant, roles in cytokine responses. *Cell* **93** 841-850.

Tenore A, Berman WF, Parks JS & Bongiovanni AM 1977 Basal and Stimulated Serum Growth-Hormone Concentrations in Inflammatory Bowel-Disease. *Journal of Clinical Endocrinology & Metabolism* **44** 622-628.

Thomson BM, Saklatvala J & Chambers TJ 1986 Osteoblasts Mediate Interleukin-1 Stimulation of Bone-Resorption by Rat Osteoclasts. *Journal of Experimental Medicine* **164** 104-112.

Tilg H, Moschen AR, Kaser A, Pines A & Dotan I 2008 Gut, inflammation and osteoporosis: basic and clinical concepts. *Gut* **57** 684-694.

Tlaskalova-Hogenova H, Tuckova L, Stepankova R, Hudcovic T, Palova-Jelinkova L, Kozakova H, Rossmann P, Sanchez D, Cinova J, Hrncir T, Kverka M, Frolova L, Uhlig H, Powrie F & Bland P 2005 Involvement of innate immunity in the development of inflammatory and autoimmune diseases. *Autoimmune Diseases and Treatment: Organ-Specific and Systemic Disorders* **1051** 787-798.

Tollet-Egnell P, Flores-Morales A, Stavreus-Evers A, Sahlin L & Norstedt G 1999 Growth hormone regulation of SOCS-2, SOCS-3, and CIS messenger ribonucleic acid expression in the rat. *Endocrinology* **140** 3693-3704.

Tronche F, Opherk C, Moriggl R, Kellendonk C, Reimann A, Schwake L, Reichardt HM, Stangl K, Gau D, Hoeflich A, Beug H, Schmid W & Schutz G 2004 Glucocorticoid receptor function in hepatocytes is essential to promote postnatal body growth. *Genes & Development* **18** 492-497.

Tsampalieros A, Lam CKL, Spencer JC, Thayu M, Shults J, Zemel BS, Herskovitz RM, Baldassano RN & Leonard MB 2013 Long-Term Inflammation and Glucocorticoid Therapy Impair Skeletal Modeling During Growth in Childhood Crohn Disease. *Journal of Clinical Endocrinology & Metabolism* **98** 3438-3445.

Tseng KF, Bonadio JF, Stewart TA, Baker AR & Goldstein SA 1996 Local expression of human growth hormone in bone results in impaired mechanical integrity in the skeletal tissue of transgenic mice. *Journal of Orthopaedic Research* **14** 598-604.

Turnley AM 2005 Role of SOCS2 in growth hormone actions. *Trends Endocrinol.Metab* **16** 53-58.

Twigg SM & Baxter RC 1998 Insulin-like growth factor (IGF)-binding protein 5 forms an alternative ternary complex with IGFs and the acid-labile subunit. *Journal of Biological Chemistry* **273** 6074-6079.

Udy GB, Towers RP, Snell RG, Wilkins RJ, Park SH, Ram PA, Waxman DJ & Davey HW 1997 Requirement of STAT5b for sexual dimorphism of body growth rates and liver gene expression. *Proceedings of the National Academy of Sciences of the United States of America* **94** 7239-7244.

Uyttendaele I, Lemmens I, Verhee A, De Smet AS, Vandekerckhove J, Lavens D, Peelman F & Tavernier J 2007 Mammalian Protein-Protein Interaction Trap (MAPPIT) Analysis of STAT5, CIS, and SOCS2 Interactions with the Growth Hormone Receptor. *Molecular Endocrinology* **21** 2821-2831.

Vaananen HK & Horton M 1995 The Osteoclast Clear Zone Is A Specialized Cell-Extracellular Matrix Adhesion Structure. *Journal of Cell Science* **108** 2729-2732.

Van Der Eerden BCJ, Gevers EF, Lowik CWGM, Karperien M & Wit JM 2002 Expression of estrogen receptor alpha and beta in the epiphyseal plate of the rat. *Bone* **30** 478-485.

Van Der Eerden BCJ, Karperien M & Wit JM 2003 Systemic and local regulation of the growth plate. *Endocrine Reviews* **24** 782-801.

Vanderschueren D, Gaytant J, Boonen S & Venken K 2008 Androgens and bone. *Current Opinion in Endocrinology Diabetes and Obesity* **15** 250-254.

Venken K, De Gendt K, Boonen S, Ophoff J, Bouillon R, Swinnen JV, Verhoeven G & Vanderschueren D 2006 Relative impact of androgen and estrogen receptor activation in the effects of androgens on trabecular and cortical bone in growing male mice: A study in the androgen receptor knockout mouse model. *Journal of Bone and Mineral Research* **21** 576-585.

Venken K, Moverare-Skrtic S, Kopchick JJ, Coschigano KT, Ohlsson C, Boonen S, Bouillon R & Vanderschueren D 2007 Impact of androgens, growth hormone, and IGF-I on bone and muscle in male mice during puberty. *Journal of Bone and Mineral Research* **22** 72-82.

Vesterlund M, Zadjali F, Persson T, Nielsen ML, Kessler BM, Norstedt G & Flores-Morales A 2011 The SOCS2 Ubiquitin Ligase Complex Regulates Growth Hormone Receptor Levels. *Plos One* **6**.

Vijayakumar A, Novosyadlyy R, Wu YJ, Yakar S & LeRoith D 2010 Biological effects of growth hormone on carbohydrate and lipid metabolism. *Growth Hormone & Igf Research* **20** 1-7.

Villemure I & Stokes I 2009 Growth plate mechanics and mechanobiology. a survey of present understanding. *Journal of Biochemistry* **42**(12) 1793-1803.

von Horn H, Ekstrom C, Ellis E, Olivecrona H, Einarsson C, Tally M & Ekstrom TJ 2002 GH is a regulator of IGF2 promoter-specific transcription in human liver. *Journal of Endocrinology* **172** 457-465.

Wachter NJ, Krischak GD, Mentzel M, Sarkar MR, Ebinger T, Kinzl L, Claes L & Augat P 2002 Correlation of bone mineral density with strength and microstructural parameters of cortical bone in vitro. *Bone* **31** 90-95.

Wajnrajch MP, Gertner JM, Harbison MD, Chua SC & Leibel RL 1996 Nonsense mutation in the human growth hormone-releasing hormone receptor causes growth failure analogous to the little (lit) mouse. *Nature Genetics* **12** 88-90.

Wang J, Zhou J & Bondy CA 1999a Igf1 promotes longitudinal bone growth by insulin-like actions augmenting chondrocyte hypertrophy. *Faseb Journal* **13** 1985-1990.

Wang J, Zhou J, Powell-Braxton L & Bondy C 1999b Effects of Igf1 gene deletion on postnatal growth patterns. *Endocrinology* **140** 3391-3394.

Wang J, Zhou J, Cheng CM, Kopchick JJ & Bondy CA 2004 Evidence supporting dual, IGF-I-independent and IGF-I-dependent, roles for GH in promoting longitudinal bone growth. *Journal of Endocrinology* **180** 247-255.

Wang YM, Cheng ZQ, Elalieh HZ, Nakamura E, Nguyen MT, Mackem S, Clemens TL, Bikle DD & Chang WH 2011 IGF-1R Signalling in Chondrocytes Modulates

Growth Plate Development by Interacting With the PTHrP/Ihh Pathway. *Journal of Bone and Mineral Research* **26** 1437-1446.

Wang YM, Nishida S, Boudignon BM, Burghardt A, Elalieh HZ, Hamilton MM, Majumdar S, Halloran BP, Clernens TL & Bikle DD 2007 IGF-I receptor is required for the anabolic actions of parathyroid hormone on bone. *Journal of Bone and Mineral Research* **22** 1329-1337.

Waters MJ, Hoang HN, Fairlie DP, Pelekanos RA & Brown RJ 2006 New insights into growth hormone action. *Journal of Molecular Endocrinology* **36** 1-7.

Werther GA, Haynes K, Edmondson S, Oakes S, Buchanan CJ, Herington AC & Waters MJ 1993 Identification of Growth-Hormone Receptors on Human Growth-Plate Chondrocytes. *Acta Paediatrica* **82** 50-53.

Williams KL, Fuller CR, Dieleman LA, DaCosta CM, Haldeman KM, Sartor RB & Lund PK 2001 Enhanced survival and mucosal repair after dextran sodium sulfate-induced colitis in transgenic mice that overexpress growth hormone. *Gastroenterology* **120** 925-937.

Wilsman NJ, Farnum CE, Leiferman EM, Fry M & Barreto C 1996 Differential growth by growth plates as a function of multiple parameters of chondrocytic kinetics. *Journal of Orthopaedic Research* **14** 927-936.

Woelfle J, Chia DJ & Rotwein P 2003 Mechanisms of growth hormone (GH) action - Identification of conserved Stat5 binding sites that mediate GH-induced insulin-like growth factor-I gene activation. *Journal of Biological Chemistry* **278** 51261-51266.

Wolf E, Kramer R, Blum WF, Foll J & Brem G 1994 Consequences of Postnatally Elevated Insulin-Like Growth Factor-Ii in Transgenic Mice - Endocrine Changes and Effects on Body and Organ Growth. *Endocrinology* **135** 1877-1886.

Wolf M, Bohm S, Brand M & Kreymann G 1996 Proinflammatory cytokines interleukin 1 beta and tumor necrosis factor a inhibit growth hormone stimulation of insulin-like growth factor I synthesis and growth hormone receptor mRNA levels in cultured rat liver cells. *European Journal of Endocrinology* **135** 729-737.

Wong PKK, Egan PJ, Croker BA, O'Donnell K, Sims NA, Drake S, Kiu H, McManus EJ, Alexander WS, Roberts AW & Wicks IP 2006 SOCS-3 negatively regulates innate and adaptive immune mechanisms in acute IL-1-dependent inflammatory arthritis. *Journal of Clinical Investigation* **116** 1571-1581.

Wong SC, Catto-Smith AGA & Zacharin M 2014 Pathological fractures in paediatric patients with inflammatory bowel disease. *European Journal of Pediatrics* **173** 141-151.

Wong SC, Smyth A, McNeill E, Galloway PJ, Hassan K, McGrogan P & Ahmed SF 2010 The growth hormone insulin-like growth factor 1 axis in children and

adolescents with inflammatory bowel disease and growth retardation. *Clinical Endocrinology* **73** 220-228.

Wu YJ, Sun H, Yakar S & LeRoith D 2009 Elevated Levels of Insulin-Like Growth Factor (IGF)-I in Serum Rescue the Severe Growth Retardation of IGF-I Null Mice. *Endocrinology* **150** 4395-4403.

Xiao GZ, Gopalakrishnan R, Jiang D, Reith E, Benson MD & Franceschi RT 2002 Bone morphogenetic proteins, extracellular matrix, and mitogen-activated protein kinase signalling pathways are required for osteoblast-specific gene expression and differentiation in MC3T3-E1 cells. *Journal of Bone and Mineral Research* **17** 101-110.

Yadav MC, Simao AMS, Narisawa S, Huesa C, Mckee MD, Farquharson C & Millan JL 2011 Loss of Skeletal Mineralization by the Simultaneous Ablation of PHOSPHO1 and Alkaline Phosphatase Function: A Unified Model of the Mechanisms of Initiation of Skeletal Calcification. *Journal of Bone and Mineral Research* **26** 286-297.

Yakar S, Courtland HW & Clemmons D 2010 IGF-1 and Bone: New Discoveries From Mouse Models. *Journal of Bone and Mineral Research* **25** 2267-2276.

Yakar S, Rosen CJ, Beamer WG, Ackert-Bicknell CL, Wu Y, Liu JL, Ooi GT, Setser J, Frystyk J, Boisclair YR & LeRoith D 2002 Circulating levels of IGF-1 directly regulate bone growth and density. *Journal of Clinical Investigation* **110** 771-781.

Yakar S, Rosen CJ, Bouxsein ML, Sun H, Mejia W, Kawashima Y, Wu Y, Emerton K, Williams V, Jepsen K, Schaffler MB, Majeska RJ, Gavrilova O, Gutierrez M, Hwang D, Pennisi P, Frystyk J, Boisclair Y, Pintar J, Jasper H, Domene H, Cohen P, Clemmons D & LeRoith D 2009a Serum complexes of insulin-like growth factor-1 modulate skeletal integrity and carbohydrate metabolism. *FASEB J.* **23** 709-719.

Yakar S, Liu JL, Stannard B, Butler A, Accili D, Sauer B & LeRoith D 1999 Normal growth and development in the absence of hepatic insulin-like growth factor I. *Proceedings of the National Academy of Sciences of the United States of America* **96** 7324-7329.

Yamaguchi A, Komori T & Suda T 2000 Regulation of osteoblast differentiation mediated by bone morphogenetic proteins, hedgehogs, and Cbfa1. *Endocrine Reviews* **21** 393-411.

Yan YT, Kolachala V, Dalmasso G, Nguyen H, Laroui H, Sitaraman SV & Merlin D 2009 Temporal and Spatial Analysis of Clinical and Molecular Parameters in Dextran Sodium Sulfate Induced Colitis. *Plos One* **4**: e6073.

Yuen KCJ, Frystyk J, White DK, Twickler TB, Koppeschaar HPF, Harris PE, Fryklund L, Murgatroyd PR & Dunger DB 2005 Improvement in insulin sensitivity without concomitant changes in body composition and cardiovascular risk markers

following fixed administration of a very low growth hormone (GH) dose in adults with severe GH deficiency. *Clinical Endocrinology* **63** 428-436.

Zadjali F, Santana-Farre R, Vesterlund M, Carow B, Mirecki-Garrido M, Hernandez-Hernandez I, Flodstrom-Tullberg M, Parini P, Rottenberg M, Norstedt G, Fernandez-Perez L & Flores-Morales A 2012 SOCS2 deletion protects against hepatic steatosis but worsens insulin resistance in high-fat-diet-fed mice. *Faseb Journal* **26** 3282-3291.

Zelzer E, McLean W, Ng YS, Fulkai N, Reginato AM, Lovejoy S, D'Amore PA & Olsen BR 2002 Skeletal defects in VEGF(120/120) mice reveal multiple roles for VEGF in skeletogenesis. *Development* **129** 1893-1904.

Zhang JG, Farley A, Nicholson SE, Willson TA, Zugaro LM, Simpson RJ, Moritz RL, Cary D, Richardson R, Hausmann G, Kile BJ, Kent SBH, Alexander WS, Metcalf D, Hilton DJ, Nicola NA & Baca M 1999a The conserved SOCS box motif in suppressors of cytokine signalling binds to elongins B and C and may couple bound proteins to proteasomal degradation. *Proceedings of the National Academy of Sciences of the United States of America* **96** 2071-2076.

Zhang M, Xuan SH, Bouxsein ML, von Stechow D, Akeno N, Faugere MC, Malluche H, Zhao GS, Rosen CJ, Efstratiadis A & Clemens TL 2002 Osteoblast-specific knockout of the insulin-like growth factor (IGF) receptor gene reveals an essential role of IGF signalling in bone matrix mineralization. *Journal of Biological Chemistry* **277** 44005-44012.

Zhang W, Shen X, Wan C, Zhao Q, Zhang LF, Zhou Q & Deng LF 2012 Effects of insulin and insulin-like growth factor 1 on osteoblast proliferation and differentiation: differential signalling via Akt and ERK. *Cell Biochemistry and Function* **30** 297-302.

Zhang XZ, Kalu DN, Erbas B, Hopper JL & Seeman E 1999 The effects of gonadectomy on bone size, mass, and volumetric density in growing rats are gender-, site-, and growth hormone-specific. *Journal of Bone and Mineral Research* **14** 802-809.

Zhang YH, Heulsmann A, Tondravi MM, Mukherjee A & Abu-Amer Y 2001 Tumor necrosis factor-alpha (TNF) stimulates RANKL-induced osteoclastogenesis via coupling of TNF type 1 receptor and RANK signalling pathways. *Journal of Biological Chemistry* **276** 563-568.

Zhao G, Monier-Faugere MC, Langub MC, Geng Z, Nakayama T, Pike JW, Chernausek SD, Rosen CJ, Donahue LR, Malluche HH, Fagin JA & Clemens TL 2000 Targeted Overexpression of Insulin-Like Growth Factor I to Osteoblasts of Transgenic Mice: Increased Trabecular Bone Volume without Increased Osteoblast Proliferation. *Endocrinology* **141** 2674-2682.

Zhou YH, Xu BXC, Maheshwari HG, He L, Reed M, Lozykowski M, Okada S, Cataldo L, Coschigamo K, Wagner TE, Baumann G & Kopchick JJ 1997 A mammalian model for Laron syndrome produced by targeted disruption of the mouse growth hormone receptor/binding protein gene (the Laron mouse). *Proceedings of the National Academy of Sciences of the United States of America* **94** 13215-13220.

Zhu DX, Mackenzie NCW, Millan JL, Farquharson C & MacRae VE 2011 The Appearance and Modulation of Osteocyte Marker Expression during Calcification of Vascular Smooth Muscle Cells. *Plos One* **6**: e19595

Zhu T, Goh ELK, Graichen R, Ling L & Lobie PE 2001 Signal transduction via the growth hormone receptor. *Cellular Signalling* **13** 599-616.

Zoetis T, Tassinari MS, Bagi C, Walthall K & Hurtt ME 2003 Species comparison of postnatal bone growth and development. *Birth Defects Research.* **68** 86-110

Zong CS, Chan J, Levy DE, Horvath C, Sadowski HB & Wang LH 2000 Mechanism of STAT3 activation by insulin-like growth factor I receptor. *Journal of Biological Chemistry* **275** 15099-15105.

Appendix I

Mediums

Osteoblast medium
αMEM medium containing 5% FBS and 0.05% gentamicin

Serum-free osteoblast medium
αMEM medium containing 0.1% BSA (Fraction V) and 0.05% gentamicin

Freezing Medium
60% αMEM, 20% FBS, 20% DMSO

Metatarsal preparation medium
0.8ml αMEM medium (without ribonucleosides), 10.45ml sterile PBS, 22.5mg BSA (Fraction V)

Embryonic metatarsal medium
αMEM medium (without ribonucleosides) containing 0.2% BSA (Fraction V) 5µg/ml L-ascorbic acid phosphate, imM βGP, 0.05mg/ml gentamicin and 1.25µg/ml fungizone

Postnatal metatarsal medium
DMEM /F-12 medium containing 0.2% BSA (Fraction V) 5µg/ml L-ascorbic acid phosphate, 1mM βGP, 0.05mg/ml gentamicin and 1.25µg/ml fungizone

Qiagen kit buffer composition

Maxiprep re-suspension buffer P1
50mM Tris-HCl, pH8.0, 10mM EDTA, 100µg/ml RNase A

Maxiprep bacterial lysis buffer P2
200mM NaOH, 1% SDS

Maxiprep elution buffer ED
10mM Tris-HCl, pH8.5

Maxiprep neutralisation buffer P3
3M potassium acetate pH5.5

Maxiprep equilibration buffer QBT

750mM NaCl, 50mM 3-[N-morpholino] propanesulfonic acid (MOPS), pH7.0, 15% isopropanol (v/v), 0.15% Triton X-100 (v/v)

Maxiprep column wash buffer QC

1M NaCl, 50mM MOPS pH7.0, 15% isopropanol (v/v), 0.15% Triton X-100 (v/v)

Maxiprep elution buffer QN

1.6M NaCl, 50nM MOPS, pH7.0, 15% isopropanol (v/v)

DNA re-suspension buffer TE

10mM Tris HCl, pH8.0, 1mM EDTA

Western Blotting

RIPA buffer

20mM Tris-HCl (pH8), 135mM NaCl, 10% Glycerol, 1% IGEPAL, 0.1% SDS, 0.5% Na Deoxycholate, 2mM EDTA

LDS sample reducing agent

40% glycerol, 4% LDS, 4% Ficoll*-400, 0.8M triethanolamine-Cl pH7.6, 0.025% phenol red, 0.025% coomassie G250, 2mM EDTA disodium

1xTransfer Buffer

100ml 10x transfer buffer, 200ml 98% ethanol, 700ml dH_2O

10x Transfer Buffer

29.3mg/ml glycine, 58mg/ml Tris Base (trimethylamine) 18.8µl/ml 20% SDS in dH_2O

TBS/T

Tris-buffered saline/Tween-20 consisting of 50mM Tris-HCl, 300mM NaCl, 0.1% Tween-20

MOPS running buffer

50mM MOPS pH7.7, 50mM Tris, 0.1% SDS, 1mM EDTA

Tris-acetate running buffer

50mM Tricine pH8.2, 50mM Tris, 0.1% SDS

Histology Stains

Silver Nitrate Stain

1.5% silver nitrate in dH_2O

Paragon Stain

0.6g basic fuchsin, 1.9g toluidine blue, 250mls 30% ethanol; diluted in borax buffer pH7.8 (6g boric solution, 2g sodium tetraborate, 500ml dH_2O)

Aniline Blue Stain

00.1g aniline blue, 3g phosphotungstic acid, 300ml dH_2O

Appendix II

Restriction enzymes used for restriction digest

Plasmid	Restriction Enzyme	Buffer	Expected Band Size
pcDNA3.1(+)	Nhe I	suRE/Cut buffer H	5428bp
	Pst I	suRE/Cut buffer H	1356bp & 4072bp
pEF-FLAG-I	Asc I	NEB buffer 4	5353bp
	EcoRI	suRE/Cut buffer H	4614bp & 739bp
pEF-FLAG-I/mSOCS2	NdeI	NEB buffer 4	5953bp
	EcoRI	suRE/Cut buffer H	1339bp & 4614bp

Nhe I, Pst I, EcoRI, and suRE/Cut Buffer H = Roche, UK. Asc I, Nde I, and NEB buffer 4 = New England Biolabs, Herts, UK

Primary antibodies and their dilutions

Peptide/protein target	Name of Antibody	Species raised in; monoclonal or polyclonal	Dilution used
SOCS1	SOCS1 (ab)	goat polyclonal	1 in 666
SOCS2	SOCS2 (cs)	rabbit polyclonal	1 in 1000
SOCS3	SOCS3 (ab)	rabbit polyclonal	1 in 369
B -Actin (HRP linked)	B -Actin (s)	mouse monoclonal	1 in 25,000
P-STAT1	P-STAT1 (cs)	rabbit polyclonal	1 in 1000
STAT1	STAT1 (cs)	rabbit polyclonal	1 in 1000
P-STAT3	P-STAT3 (cs)	rabbit polyclonal	1 in 1000
STAT3	STAT3 (cs)	rabbit polyclonal	1 in 1000
P-STAT5	P-STAT5 (cs)	rabbit polyclonal	1 in 1000
STAT5	STAT5 (cs)	rabbit polyclonal	1 in 1000
P-STAT5	P-STAT5 (Tyr 694) (C71E5) (cs)	rabbit monoclonal	1 in50
P-AKT	P-AKT (cs)	rabbit polyclonal	1 in 1000
AKT	AKT (cs)	rabbit polyclonal	1 in 1000
P-P44/42	P-p44/42 MAPK (ERK1/2) (cs)	rabbit polyclonal	1 in 1000
P44/42	p44/42 MAPK (ERK1/2) (cs)	rabbit polyclonal	1 in 1000

Cs=Cell Signalling Technology (New England Biolabs, Hitchin, UK); s= Sigma; ab= Abcam (Cambridge, UK)

Secondary antibodies and their dilutions

Antibody	Dilution
HRP linked goat anti rabbit (d)	1 in 5000
HRP linked rabbit anti goat (d)	1 in 5000
Alexa Fluor 594 goat anti rabbit (ab)	1 in 500

d=Dako, Denmark; ab= Abcam (Cambridge, UK)

Primers used for genotyping and qPCR analysis

Source			Sequences (5′-3′)
Genotyping			
SOCS2	MWG Eurofins	F	TGTTTGACTGAGCTCGCGC
	MWG Eurofins	R	CAACTTTAGTGTCTTGGATCT
Neo	MWG Eurofins	F	ACCCTGCACACTCTCGTTTTG
	MWG Eurofins	R	CCTCGACTAAACACATGTAAAGC
qPCR Analysis			
Socs1	MWG Eurofins	F	TCCGATTACCGGCGCATCACG
	MWG Eurofins	R	CTCCAGCAGCTCGAAAAGGCA
Socs2	MWG Eurofins	F	TGGCTGCTCAAGATCAAATG
	MWG Eurofins	R	TGTCCTCCTGGAAATGGAAG
Socs3	MWG Eurofins	F	GAGTACCCCCAAGAGAGCTTACTA
	MWG Eurofins	R	CTCCTTAAAGTGGAGCATCATACTG
Igf1	Invitrogen	F	Not available
	Invitrogen	R	Not available
Igfbp3	Invitrogen	F	Not available
	Invitrogen	R	Not available
Akp2	MWG Eurofins	F	GGGACGAATCTCAGGGTACA
	MWG Eurofins	R	AGTAACTGGGGTCTCTCTCTTT
Spp1	MWG Eurofins	F	ATCGTCATCATCATCGTCATCAT
	MWG Eurofins	R	GAATGGTGTGTCCTCTGGAGGAA
Gapdh	Primer Design	F	Not available
	Primer Design	R	Not available
Atp5b	Primer Design	F	Not available
	Primer Design	R	Not available